



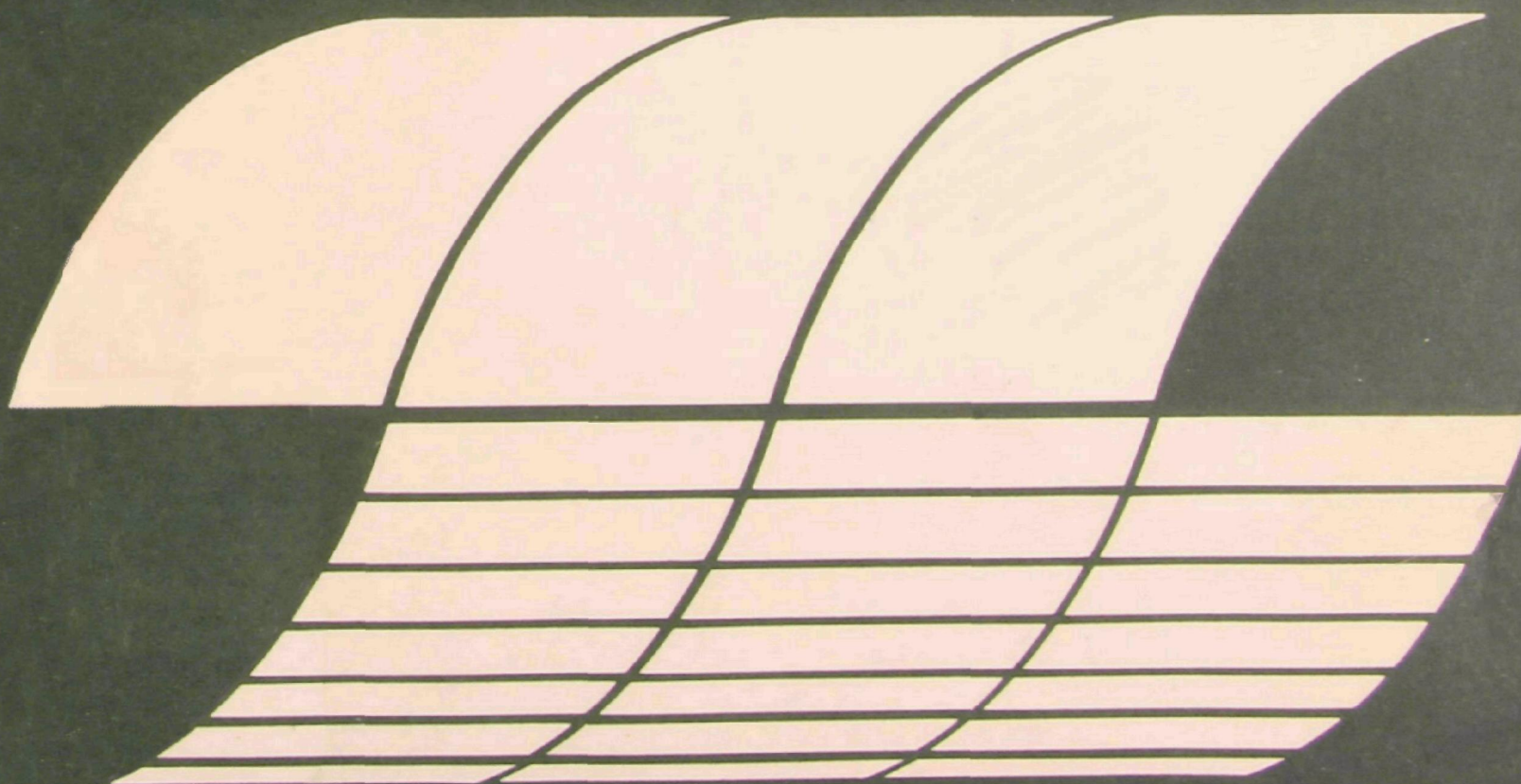
U.S. Environmental Protection Agency  
Office of Research and Development

Industrial Environmental Research  
Laboratory  
Research Triangle Park, North Carolina 27711

**EPA-600/7-77-140**  
**December 1977**

# **PARTICULATE CONTROL WITH CLEANABLE CARTRIDGE FILTERS USING DOUBLE-LAYER MEDIA**

Interagency  
Energy-Environment  
Research and Development  
Program Report



## RESEARCH REPORTING SERIES

Research reports of the Office of Research and Development, U.S. Environmental Protection Agency, have been grouped into seven series. These seven broad categories were established to facilitate further development and application of environmental technology. Elimination of traditional grouping was consciously planned to foster technology transfer and a maximum interface in related fields. The seven series are:

1. Environmental Health Effects Research
2. Environmental Protection Technology
3. Ecological Research
4. Environmental Monitoring
5. Socioeconomic Environmental Studies
6. Scientific and Technical Assessment Reports (STAR)
7. Interagency Energy-Environment Research and Development

This report has been assigned to the INTERAGENCY ENERGY-ENVIRONMENT RESEARCH AND DEVELOPMENT series. Reports in this series result from the effort funded under the 17-agency Federal Energy/Environment Research and Development Program. These studies relate to EPA's mission to protect the public health and welfare from adverse effects of pollutants associated with energy systems. The goal of the Program is to assure the rapid development of domestic energy supplies in an environmentally-compatible manner by providing the necessary environmental data and control technology. Investigations include analyses of the transport of energy-related pollutants and their health and ecological effects; assessments of, and development of, control technologies for energy systems; and integrated assessments of a wide range of energy-related environmental issues.

## REVIEW NOTICE

This report has been reviewed by the participating Federal Agencies, and approved for publication. Approval does not signify that the contents necessarily reflect the views and policies of the Government, nor does mention of trade names or commercial products constitute endorsement or recommendation for use.

This document is available to the public through the National Technical Information Service, Springfield, Virginia 22161.



# **PARTICULATE CONTROL WITH CLEANABLE CARTRIDGE FILTERS USING DOUBLE-LAYER MEDIA**

by

**William J. Krisko and Michael A. Shackleton**

**Donaldson Company, Inc.  
P.O. Box 1299  
Minneapolis, Minnesota 55440**

**Contract No. 68-02-1878  
ROAP No. 77AAU-006  
Program Element No. EHB525**

**EPA Project Officer: Dennis C. Drehmel**

**Industrial Environmental Research Laboratory  
Office of Energy, Minerals, and Industry  
Research Triangle Park, N.C. 27711**

**Prepared for**

**U.S. ENVIRONMENTAL PROTECTION AGENCY  
Office of Research and Development  
Washington, D.C. 20460**

### Disclaimer Statement

This report has been reviewed by Donaldson Company, Inc., the Environmental Protection Agency, and approved for publication. Approval does not signify that the contents necessarily reflect the views and policies of the Environmental Protection Agency, nor does mention of trade names or commercial products constitute endorsement or recommendation for use.



## PREFACE

This report presents results of a study to assess the feasibility of a new concept in fine particle filtration termed Nonwoven Double Mat Filters. The double mat filter consists of a fine fiber filtration layer supported by a porous substrate providing physical strength to the resulting double mat filtration medium. A theoretical basis for fine particle control with this medium is presented. Test results with  $0.3\ \mu\text{m}$  DOP smoke confirmed that the design objective of 90 percent collection efficiency could be obtained. Pressure drop characteristics during pulse-jet cleaning of AC Fine test dust, from flat-sheets, was similar to that of felt baghouse media; while collection efficiency was approximately 99.5 percent for felts, the double mat filter medium achieved a collection efficiency of  $>99.999$  percent for AC Fine. Preliminary economic analysis indicates that the double mat media in a cartridge configuration will provide a less costly filtration system than the standard baghouse. This saving is a result of the system size reduction possible with the pleated cartridge and the potentially higher air-to-cloth ratios with the fine fiber media. These analyses were conducted under Phase I of this contract.

Phase II evaluated the fine particle control characteristics of double mat filtration media in a pulse-jet cleaning cartridge filter configuration. Both laboratory and field tests proved the media to be capable of high dust removal efficiency of fine particles ( $<3\ \mu\text{m}$ ) while achieving good pulse-jet cleaning characteristics.

## TABLE OF CONTENTS

	PREFACE	i
	LIST OF FIGURES	iii
	LIST OF TABLES	vii
	LIST OF ABBREVIATIONS AND SYMBOLS	ix
	ACKNOWLEDGMENTS	x
<u>Sections</u>		
1.0	INTRODUCTION	1
2.0	CONCLUSIONS	3
3.0	RECOMMENDATIONS	7
4.0	THEORETICAL ANALYSIS	9
5.0	PRELIMINARY EXPERIMENTS	23
5.1	DOP Penetration Tests	23
5.2	SEM Analysis	41
5.3	Dust Loading Tests	56
5.4	Pressure Drop Tests	90
6.0	PLEATED CARTRIDGE LABORATORY TESTS	95
6.1	Pleated Cartridge Dust Tests	95
6.2	DOP Penetration Tests	103
7.0	FIELD TESTS	109
7.1	Tests at Cornelius Company	110
7.1.1	Particulate Characterization	110
7.1.2	Performance Tests	125
7.2	Tests at Northern Malleable Iron Company	132
7.2.1	Particulate Characterization	136
7.2.2	Performance Tests	141
8.0	ECONOMIC ANALYSIS	147
8.1	Dust Control from a Vertical Lime Rock Kiln	147
8.2	Particulate Removal from the Exhaust Gas of a Glass-Melting Furnace	165
8.3	Conclusion	165
9.0	GLOSSARY	183
10.0	REFERENCES	185
11.0	CONVERSION FACTORS	187
	TECHNICAL REPORT DATA	189



## LIST OF FIGURES

<u>Figure</u>		<u>Page</u>
4-1	Filter Efficiency as a Function of Basis Weight	10
4-2	G(M) Versus "M" for Torgeson Theory	15
4-3	Basis Weight as Function of Fiber Diameter	18
4-4	Pressure Drop as a Function of Fiber Diameter	20
5-1	DOP Penetration as a Function of Basis Weight	25
5-2	Penetration Tests of Various Media	27
5-3	Penetration as a Function of Basis Weight	31
5-4	Penetration as a Function of Airflow Velocity	32
5-5	Efficiency of Media Samples	34
5-6	Effect of Needle Holes on Efficiency	36
5-7	Penetration as a Function of Basis Weight	39
5-8	Efficiency as a Function of Airflow Velocity	40
5-9	SEM Photomicrograph of Fine Fibers (8/26/75)	42
5-10	Measurement Technique Used to Estimate Average Fiber Diameter	43
5-11	Downstream Side of Media (9/18/75)	45
5-12	Upstream Side of Media (9/18/75)	45
5-13	SEM Photomicrograph of Fiber Bed (1/16/76)	46
5-14	SEM Photomicrograph of Fiber Bed (2/26/76)	47
5-15	SEM Photomicrograph of Gore-Tex Filter Material	49
5-16	5K Photomicrograph of Media Sample (4/10/76)	50
5-17	5K Photomicrograph of Media Sample (5/14/76)	50
5-18	5K Photomicrograph of Media Sample (5/17/76)	51
5-19	1K Photomicrograph of Media Sample (4/10/76)	51
5-20	1K Photomicrograph of Media Sample (5/14/76)	52
5-21	2K Photomicrograph of Media Sample (5/17/76)	52
5-22	200X Photomicrograph of Media Sample (4/10/76)	53
5-23	200X Photomicrograph of Media Sample (5/17/76)	53
5-24	200X Photomicrograph of Media Sample Backing	54
5-25	400X Edge View of Media Sample (5/17/76)	55
5-26	5K Photomicrograph of Media Sample (5/17/76)	55
5-27	Flat Sheet Pulse Jet Test Rig	57
5-28	Flat Sheet Pulse Jet Cleaning Test Rig	58

## LIST OF FIGURES (continued)

<u>Figure</u>		<u>Page</u>
5-29	Particle Size Distribution of AC Fine Test Dust	59
5-30	Media Cleanability Evaluation	71
5-31	Pressure Drop as a Function of Time (Test #16)	72
5-32	Operating Pressure Drop as a Function of Time (Test #18)	77
5-33	Operating Pressure Drop as a Function of Time (Test #23)	79
5-34	Operating Pressure Drop as a Function of Time (Test #24)	81
5-35	Operating Pressure Drop as a Function of Time (Test #25)	83
5-36	Operating Pressure Drop as a Function of Time (Test #26)	85
5-37	Operating Pressure Drop as a Function of Time (Test #27)	86
5-38	Operating Pressure Drop as a Function of Time (Test #28)	88
5-39	Fine Fiber Layer Broken from Felt Backing	89
5-40	Pressure Drop as a Function of Time (Test #29)	91
5-41	Difference Between Actual and Predicted Pressure Drop for Filters Capable of 90% Collection of $0.3\mu\text{m}$ DOP	92
6-1	Pressure Drop Life Characteristics	97
6-2	Pressure Drop Life Characteristics	99
6-3	Pressure Drop Life Characteristics	101
6-4	Pressure Drop Life Characteristics	102
6-5	Particle Size Distribution of Feed & Effluent Dust	104
6-6	Efficiency as a Function of Air-to-Cloth Ratio	105
7-1	Welding Table at Cornelius Company	111
7-2	Installation at Cornelius Company - Welding Fume	112
7-3	Test Setup at Cornelius Company	113
7-4	Pressure Drop Characteristics Field Test Unit at Cornelius Company	114
7-5	820 Magnification of Welding Fume - Stage 4 of Andersen Sampler	117
7-6	10K SEM Micrograph of Ambient Welding Fume	118
7-7	10K SEM Micrograph of Upstream and Downstream Samples of Welding Fume	119



## LIST OF FIGURES (Continued)

<u>Figure</u>		<u>Page</u>
7-8	20K SEM Micrograph of Upstream & Downstream Samples of Welding Fume	120
7-9	SEM Micrographs of Welding Fume - Upstream	121
7-10	SEM Micrographs of Welding Fume - Downstream	122
7-11	10K TEM Micrograph of Upstream & Downstream Samples of Welding Fume	123
7-12	50K TEM Micrograph of Upstream and Downstream Samples of Welding Fume	124
7-13	Operating Pressure Drop as a Function of Time (Cornelius Co.)	128
7-14	Dirty versus Clean Filter Elements - Cornelius Company - Welding Fume	129
7-15	Innoculation Process at Northern Malleable Iron Company	133
7-16	Installation at Northern Malleable Iron Company	134
7-17	Test Setup at Northern Malleable Iron Company	135
7-18	Particle Size Spectrum Analysis Northern Malleable Iron Company	137
7-19	10K TEM Micrograph of Upstream and Downstream Samples of MgO Particulate	138
7-20	SEM Micrographs of MgO Particulate - Upstream	139
7-21	SEM Micrograph of MgO Particulate - Downstream	140
7-22	Dirty versus Clean Filter Cartridges - Northern Malleable - MgO Emission	144
7-23	Failed Filter Cartridge - Light Spot Indicates Hole in Media	145
7-24	Operating Pressure Drop as a Function of Time (Northern Malleable Iron Company)	146
8-1	Capital Costs for Electrostatic Precipitators for Vertical Lime Rock Kilns (High Efficiency)	148
8-2	Annual Costs for Electrostatic Precipitators for Vertical Lime Rock Kilns (High Efficiency)	150
8-3	Capital Costs for Wet Scrubbers for Vertical Lime Rock Kilns (High Efficiency)	152
8-4	Annual Costs for Wet Scrubbers for Vertical Lime Rock Kilns (High Efficiency)	154

## LIST OF FIGURES (Continued)

<u>Figure</u>		<u>Page</u>
8-5	Capital Costs for Fabric Filters for Vertical Lime Rock Kilns	156
8-6	Annual Costs for Fabric Filters for Vertical Lime Rock Kilns	158
8-7	Capital Costs for Cartridge Filters for Vertical Lime Rock Kilns	160
8-8	Annual Costs for Cartridge Filter for Vertical Lime Rock Kilns	162
8-9	Annual Cost Comparison for Electrostatic Precipitators, Wet Scrubbers, Fabric Filters and Cartridge Filters (High Efficiency)	164
8-10	Capital Cost of Electrostatic Precipitators for Glass-Melting Furnace	167
8-11	Annual Cost of Electrostatic Precipitators for Glass-Melting Furnace	169
8-12	Capital Cost of Wet Scrubbers for Glass-Melting Furnace	171
8-13	Annual Cost of Wet Scrubbers for Glass-Melting Furnace	173
8-14	Capital Cost of Fabric Filters for Glass-Melting Furnace	175
8-15	Annual Cost of Fabric Filters for Glass	177
8-16	Capital Cost of Cartridge Filters for Glass-Melting Furnace	179
8-17	Annual Cost of Cartridge Filters for Glass-Melting Furnace	181
8-18	Annual Cost Comparison for Electrostatic Precipitators, Wet Scrubbers, Fabric Filters and Cartridge Filters for Glass-Melting Furnace	182



## LIST OF TABLES

<u>Table</u>		<u>Page</u>
4-1	Langmuir Pressure Drop	19
4-2	Langmuir Pressure Drop with Knudsen Number Correction	21
5-1	Results of Multiple Sheet Testing of Medium (8/26/75)	24
5-2	Physical Data	37
5-3	Physical Data	38
5-4	DOP Efficiency of Medium (4/10/76)	41
5-5	Clean Filter Pressure Drop	90
7-1	Andersen Cascade Impactor Data for Cornelius Company - Upstream Particle Size	115
7-2	DOP Efficiency of Cartridges for Field Test at Cornelius Company	126
7-3	Overall Mass Efficiency for Field Test at Cornelius Company	126
7-4	Fractional Efficiency for Field Test at Cornelius Company	126
7-5	Pulse-Cleaning Durability Tests	130
7-6	Andersen Cascade Impactor Data for Northern Malleable- Upstream Particle Size	131
7-7	DOP Efficiency of Elements for Field Test at Northern Malleable Iron Company	141
7-8	Overall Mass Efficiency for Field Test at Northern Malleable Iron Company	142
7-9	Fractional Efficiency for Field Test at Northern Malleable Iron Company	142
8-1	Estimated Capital Cost Data (Costs in Dollars) for Electrostatic Precipitators for Vertical Lime Rock Kilns	149
8-2	Annual Operating Data (Costs in \$/Yr) for Electrostatic Precip- itators for Vertical Lime Rock Kilns	151
8-3	Estimated Capital Cost Data (Costs in Dollars) for Wet Scrubbers for Vertical Lime Rock Kilns	153
8-4	Annual Operating Cost Data (Costs in \$/Yr) for Wet Scrubbers for Vertical Lime Rock Kilns	155

## LIST OF TABLES (Continued)

<u>Table</u>		<u>Page</u>
8-5	Estimated Capital Cost Data (Costs in Dollars) for Fabric Filters for Vertical Lime Rock Kilns	157
8-6	Annual Operating Cost Data (Cost in \$/Yr) for Fabric Filters for Vertical Lime Rock Kilns	159
8-7	Estimated Capital Cost Data (Costs in Dollars) for Cartridge Filters for Vertical Lime Rock Kilns	161
8-8	Annual Operating Cost Data (Costs in \$/Yr) for Cartridge Filters for Vertical Lime Rock Kilns	163
8-9	Estimated Capital Cost Data (Costs in Dollars) for Electrostatic Precipitators for Glass-Melting Furnace	166
8-10	Annual Operating Cost Data (Costs in \$/Yr) for Electrostatic Precipitators for Glass-Melting Furnace	168
8-11	Estimated Capital Cost Data (Costs in Dollars) for Wet Scrubbers for Glass-Melting Furnace	170
8-12	Annual Operating Cost Data (Costs in \$/Yr) for Wet Scrubbers for Glass-Melting Furnace	172
8-13	Estimated Capital Cost Data (Costs in Dollars) for Fabric Filters for Glass-Melting Furnace	174
8-14	Annual Operating Cost Data (Costs in \$/Yr) for Fabric Filters for Glass-Melting Furnace	176
8-15	Estimated Capital Cost Data (Costs in Dollars) for Cartridge Filters for Glass-Melting Furnace	178
8-16	Annual Operating Cost Data (Costs in \$/Yr) for Cartridge Filters for Glass-Melting Furnace	180

## ABBREVIATIONS AND SYMBOLS

$\text{am}^3/\text{min}$	= actual cubic meters per minute
$C'$	= Cunningham correction factor
$C_D$	= drag coefficient
$d_f$	= fiber diameter
$dp$	= particle diameter
DOP	= dioctylphthalate
$K_I$	= interception parameter
$K_n$	= Knudsen number
$K_p$	= impaction parameter
$\ell$	= length of filter bed measured in direction of gas flow
LA Process Wt	= Los Angeles process weight requirements
$\ln$	= logarithm to base e
$N_{pe}$	= Peclet number
$N_{Ref}$	= Reynold's number, fiber diameter
$P$	= gas pressure
ppsi	= points per square inch
$S$	= solidarity factor, the ratio of the total projected area of fibers to the face area of the filter mat in the direction of gas flow
SEM	= scanning electron micrograph
$\text{sm}^3/\text{min}$	= standard cubic meters per minute
$T$	= gas temperature
$U_o$	= upstream velocity
$w'$	= basis weight
$\eta_D$	= single fiber efficiency for collecting by diffusion
$\eta_{DIP}$	= single fiber efficiency resulting from diffusion, interception and impaction
$\eta_{PI}$	= single fiber efficiency resulting from interception and impaction
$\eta_s$	= effective efficiency of a single fiber
$\lambda$	= mean free path of air molecule
$\mu_g$	= viscosity of gas
$\rho_f$	= fiber density
$\rho_g$	= gas density
$\rho_p$	= particle density

## ACKNOWLEDGMENTS

The work presented in this report was performed by the Protective Systems Department of the CORAD Division of Donaldson Company, Inc. The work was performed as Phase I of Contract 68-02-1878 for the Environmental Protection Agency, Research Triangle Park, North Carolina.

Technical direction from EPA was provided by Dr. Dennis Drehmel, Project Officer.

At Donaldson Company, the Principal Investigator during Phase I and part of Phase II was Michael Shackleton. William Krisko was the Principal Investigator during the field testing portion of this contract. Harry Camplin performed many of the tests and Gene Grassel, Ron Sundberg and Bob Frey provided technical consultation.

Approved for:

Donaldson Company, Inc.

  
John H. Scott  
Contracts Manager

(Date) 20 Oct 1977

## 1.0 INTRODUCTION

Fabric filtration is a historic means of dust control. It has enjoyed wide acceptance in varied applications to remove particles from gas streams. Through tailoring of filter media and proper design application, almost any degree of collection efficiency of any dust distribution can be achieved. Historically, efficiency has been evaluated on the basis of mass removal. Since large particles ( $> 3 \mu\text{m}$ ) are inherently easier to remove than small particles ( $< 3 \mu\text{m}$ ), high efficiency has been obtained even with significant numbers of small particles penetrating the filter.

In recent years, environmental hazards have been associated with the presence of submicrometer and other fine particles. For this reason, the development of economic means of controlling fine particles is desirable.

Improvement in collection efficiency can be achieved by simply making a filter bed thicker, thus increasing the basis weight of the filter (its weight per unit area). However, to achieve high collection efficiency of particles with ordinary filter fibers may lead to excessively thick filter beds which operate at a high pressure drop and are difficult to clean.

Examination of design equations for fabric filters reveals that collection efficiency for a given particle is a function of fiber diameter. This functional relationship is such that collection efficiency is increased as fiber diameter is decreased.

For a given efficiency, the required filter bed thickness is also decreased as fiber diameter is decreased. Analysis indicates that if fiber diameter is made small enough, the filter bed thickness can be reduced to reasonable values, giving a good probability of excellent cleanability as well as satisfactory collection efficiency of submicrometer particles. In order to provide structural strength to a filter bed of a very thin layer of fine fibers, the fine fiber filter is supported upon a backing medium. Ideally, this backing medium is very porous to allow minimum resistance to airflow. The combination of a porous backing medium with a filtration layer of fine fibers is referred to as a double mat filter.



The central purpose of Contract 68-02-1878 was to examine and demonstrate the effectiveness of filters made from fine fibers capable of collecting submicrometer particles in an economic manner.

Our approach to this investigation involved two phases. During Phase I, the theoretical basis for the work was documented and developmental testing to select a suitable media composition for work in Phase II was accomplished. Phase II included testing in a pulse-jet filter unit in both the laboratory and in the field. This report presents the results of work in Phases I and II of this contract.

Examination of design equations for fabric filtration indicate that fabric filters constructed from submicrometer diameter fibers could have significant advantages for fine particle collection. The theoretical relationship between filter performance and fiber diameter is presented in Section 4.0. It is shown theoretically that filters constructed from submicrometer fibers are capable of high efficiency collection (90 percent) of fine particles ( $0.3 \mu\text{m}$ ). Because of the effectiveness of fine fibers, filters constructed from them have basis weights approximately  $10 \text{ gm/m}^2$  ( $0.29 \text{ oz/yd}^2$ ) and is only capable of 10 to 20 percent collection of  $0.3 \mu\text{m}$  particles. The low basis weights possible with fine fibers result in a filtration layer so thin that it is barely perceptible to the naked eye when deposited upon a paper-type filter backing medium. This thin filtration layer encourages surface collection of particles which enhances cleaning.

Results of DOP efficiency testing conducted under the contract show that fine fiber filters with low basis weights are capable of high collection efficiency. Scanning electron micrographs tend to confirm the theoretical relationship between fiber diameter and basis weight of the fine fiber filters.

Dust feeding tests were conducted on various media using AC Fine test dust at 50 mm/sec air-to-cloth ratio in a flat-sheet pulse jet test rig. At this velocity, woven polyester-sateen filter media had a low efficiency and a rapid rate of pressure drop increase. Dacron felt baghouse filter material had better efficiency (99.5 percent) and a slow rate of pressure drop increase with time. These results are similar to those expected for the test conditions and provide confidence that the test rig simulated performance in a full scale filter unit. Tests of fine fiber media indicated that pressure drop performance during dust feeding tests was similar to felt; that is, a relatively low and stable pressure drop was maintained. Overall collection efficiency of AC Fine test dust was much higher for the fine fiber materials than for felt; greater than 99.999 percent by weight was measured for most samples.

Two types of backing materials were evaluated for the fine fiber filters during Phase I. These were felt and synthetic paper filter media. In general, tests involving the felt backing indicated poor adhesion between the fine fiber surface and the backing, resulting in damage to the fine fiber layer. Tests where the fine fiber layer was deposited on a dacron-paper media backing showed good performance. Filter media in this form is also more appropriate for application in a cartridge filter.

Dust tests were conducted in the laboratory on pleated cartridges under Phase II. Cleaning pressures and air-to-cloth ratios were varied. The pressure drop of the cartridges was stabilized at an acceptable level when 689 K Pa of cleaning pressure was used. The test data indicated that collection efficiency for AC Fine test dust is a function of air-to-cloth ratio. (The fine fiber media can achieve the same collection efficiency as standard media, but at higher air-to-cloth ratio.) Fine fiber media can run at air-to-cloth ratio of 8 to 1 at the same efficiency as standard media, at a 2 to 1 air-to-cloth ratio. Cleaning pulse pressure had no effect on collection efficiency.

Field tests at two different sites were conducted under Phase II on pleated cartridge filter units using the fine fiber media and with both sites presenting fine particle emission. One site was a welding fume and the other site consisted of magnesium oxide from a metallurgical process. The particulates were characterized at each site and the overall mass efficiency and fractional efficiency were determined for the systems. The overall mass efficiency was 97.6 percent on the welding fume and 99.95 percent on the magnesium oxide.

Preliminary economic analysis indicated that fine particles can be efficiently removed using the filter cartridge configuration with fine fiber media at costs significantly less than for standard fabric filter application. There are two primary reasons for this cost advantage. These are:

- 1) The cartridge configuration allows a major reduction in the volume of a filter unit for a given through-put flow rate and air-to-cloth ratio. This advantage results from the compactness achieved by pleating the filter medium. Significant cost reduction is achieved with this technique even with standard filter media. When using standard media, as with baghouse fabric filters, high efficiency collection of fine particles is achieved only at very low air-to-cloth ratios (on the order of 5 mm/sec).
- 2) The fine fiber media allows high efficiency collection of fine particles at increased air-to-cloth ratio. This fact results in further reduction in the size of filtration equipment. Our flat-sheet cleaning tests indicate that at an air-to-cloth ratio of 50 mm/sec pressure drop performance of the fine fiber media is similar to standard baghouse felt, while collection efficiency of AC Fine test dust is increased from 99.5 percent for felt to nearly absolute for the fine fiber media.

In a cartridge filter fine fiber air cleaning application, the only component likely to cost more than present systems is the filter medium itself. Even conservative estimates for this cost are overwhelmed by the cost savings resulting from the size reduction obtainable from use of the cartridge configuration and the higher air-to-cloth ratios of the fine fiber medium.

### 3.0

## RECOMMENDATIONS

Based on the encouraging results to date, it is recommended that the fine fiber media be further demonstrated in a pulse-jet cleaned dust collector on a larger scale -- at least 10,000 cfm. The system could be installed at a site that presents an industrial emission of fine particles ( $<3\mu\text{m}$  size). Some of these emissions include: non-ferrous salvage operations, welding fumes, ferroalloy fumes from a cupola or electric furnace, carbon black, solid waste combustion, spray drying operations and asphaltic pavement manufacturing.

The Torit Division of Donaldson Company has a line of dust collectors using pulse-cleaned pleated cartridge filters that could be applied. For example, there is a TD 6120 that uses 32 filter cartridges for an actual total filter area of 6124 sq. ft. Using standard filter media and an air-to-cloth ratio of 1.5, the airflow would be 9186 cfm. However, with the fine fiber cartridges and an air-to-cloth ratio 3 to 1, the airflow could be increased to 18,372 cfm. Since the double mat filter media permits higher inlet velocities and substantially increased air-to-cloth ratios, it may be necessary to modify the dust collector design and to relocate the air inlet. Also, it might be necessary to use baffles between elements which may minimize re-entrainment from the increased velocity.

Collection efficiency for  $0.3 \mu\text{m}$  diameter DOP particles is predicted as a function of filter basis weight with fiber diameter as a parameter.

Particle collection in fibrous beds is influenced primarily by three basic collection mechanisms: Direct interception, inertial impaction and diffusion. Examination of the equations describing the effects of each of these mechanisms reveals that fiber diameter is a parameter in each of them.

The following analysis will result in a prediction of particle collection efficiency for  $0.3 \mu\text{m}$  diameter DOP particles as a function of basis weight for a filter bed composed of  $1.0 \mu\text{m}$  diameter fibers. Figure 4-1 presents the results of this analysis as well as analyses for other fiber diameters determined in the same manner.

Given:

#### Fibers

Fiber diameter  $d_f = 1.0 \mu\text{m} = 0.0001 \text{ cm}$

Fiber density (nylon)  $\rho_f = 1.135 \text{ gm/cm}^3$

#### Particles (DOP)

Particle diameter  $d_p = 0.3 \mu\text{m} = 0.00003 \text{ cm}$

Particle density  $\rho_p = 0.984 \text{ gm/cm}^3$

#### Gas Stream

Upstream velocity  $U_o = 2.54 \text{ cm/sec}$

Viscosity  $\mu_g = 1.8 \times 10^{-4} \text{ gm/cm sec}$

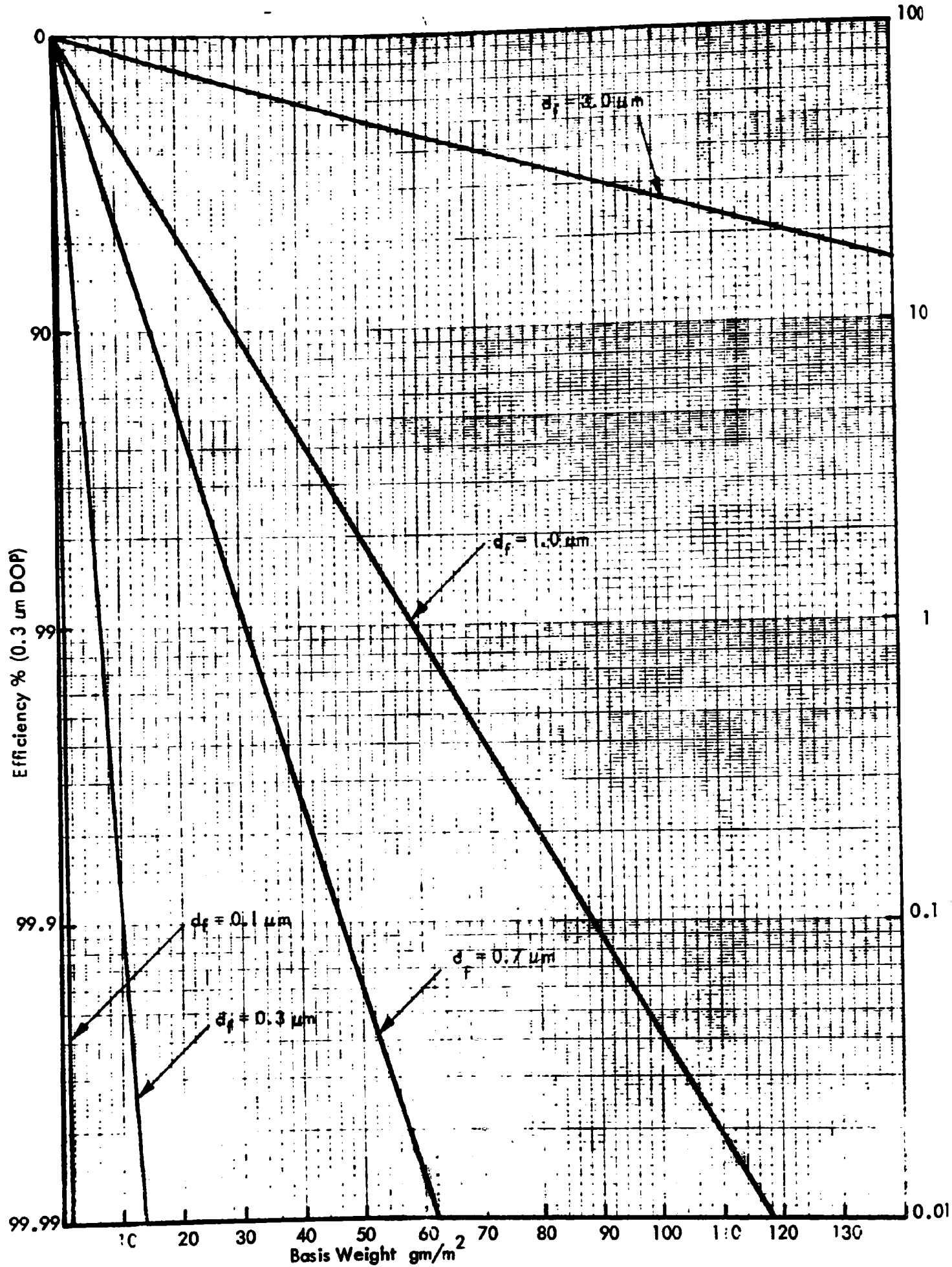


Figure 4-1. Filter Efficiency as a Function of Basis Weight



$$\text{Gas density } \rho_g = 1.2 \times 10^{-3} \text{ gm/cm}^3$$

$$\text{Gas temperature } T = 300^\circ \text{K}$$

$$\text{Gas pressure } P = 76 \text{ cm Hg}$$

Reynolds number is:

$$N_{\text{Ref}} = \frac{U_o \rho_g d_f}{\mu_g}$$

$$N_{\text{Ref}} = \frac{2.54 \text{ cm/sec } 1.2 \times 10^{-3} \text{ gm/cm}^3 0.0001 \text{ cm}}{1.8 \times 10^{-4} \text{ gm/cm sec}}$$

$$N_{\text{Ref}} = \frac{1.69 \times 10^{-3}}{}$$

Since  $N_{\text{Ref}}$  is  $< 1$ , the flow is viscous.

The Cunningham correction factor ( $C'$ ) at 76 cm Hg is given by:

$$C' = \left\{ 1 + \frac{2 T \times 10^{-8}}{dp} \left[ 2.79 + 0.894 \exp \left( \frac{-2.47 \times 10^7 dp}{T} \right) \right] \right\}$$

$$C' = \left\{ 1 + \frac{2 (300) \times 10^{-8}}{0.3 \times 10^{-4}} \left[ 2.79 + 0.894 \exp \left( \frac{-2.47 \times 10^7 (0.3 \times 10^{-4})}{300} \right) \right] \right\}$$

$$C' = 1.573$$

The Peclet number is:

$$N_{\text{pe}} = \frac{U_o d_f}{D_p} = \frac{U_o d_f 3 \pi \mu_g dp}{C' K T}$$

$K$  = Boltzmann's constant

$$N_{pe} = \frac{2.54 \text{ cm/sec} (1 \times 10^{-4} \text{ cm}) 3 \pi (1.8 \times 10^{-4} \text{ gm/cm sec}) 3 \times 10^{-5} \text{ cm}}{1.573 (1.38 \times 10^{-16} \text{ gm cm}^2 \text{ } \rho \text{ K sec}^2) (300^\circ \text{K})}$$

$$\underline{N_{pe} = 198.5}$$

The drag coefficient is calculated from:

$$C_D = \frac{8}{N_{Ref} [2 - \ln(N_{Re})]}$$

$$C_D = \frac{8}{1.69 \times 10^{-3} [2 - \ln(1.69 \times 10^{-3})]}$$

$$\underline{C_D = 1774}$$

Single fiber efficiency for collection by diffusion is then given by Torgeson as:

$$\eta_D = 0.75 \left( \frac{C_D N_{Ref}}{2} \right)^{0.4} (N_{Pe})^{-0.6}$$

$$\eta_D = 0.75 \left( \frac{1774 (1.69 \times 10^{-3})}{2} \right)^{0.4} (198.5)^{-0.6}$$

$$\underline{\eta_D = 0.03686}$$

The interception parameter  $K_I$  is:

$$K_I = \frac{d_p}{d_f} = \frac{0.00003}{0.0001}$$

$$\underline{K_I = 0.3}$$

The impaction parameter  $K_p$  is:

$$K_p = \frac{d_p^2 \rho_p U_o C'}{9 \mu_g d_f}$$

$$K_p = \frac{(3 \times 10^{-5} \text{ cm})^2 (0.984 \text{ gm/cm}^3) (2.54 \text{ cm/sec}) 1.573}{9 (1.8 \times 10^{-4} \text{ gm/sec cm}) (1 \times 10^{-4} \text{ cm})}$$

$$K_p = 0.02184$$

Single fiber efficiency resulting from interception and impaction is given by:

$$\eta_{pi} = 0.0518 \left( \frac{C_D N_{Ref}}{2} \right) K_i^{3/2} + 0.16 \left[ (0.5 + 0.8 K_i) \left( \frac{K_p}{2} \right) - 0.1051 K_i \left( \frac{K_p}{2} \right)^2 \right]$$

$$\eta_{pi} = 0.0518 \left( \frac{(1774) 1.69 \times 10^{-3}}{2} \right) 0.3^{3/2} + 0.16 \left[ (0.5 + 0.8 (.3)) \left( \frac{0.02184}{2} \right) - 0.1052 (.3) \left( \frac{0.02184}{2} \right)^2 \right]$$

$$\eta_{pi} = 0.01405$$

Since the Reynolds number ( $N_{Rep}$ ) is  $< 0.5$ , the Torgeson equation for single fiber efficiency when diffusion, interception and impaction are all operative can be used.

$$\eta_{DIP} = 0.75 \eta_{pi} + F G (M) \eta_D$$

where:

$$F = 1 + 0.025 \left( \frac{C_D N_{Ref}}{2} \right)^{0.6} N_{Pe}^{0.6} \left( \frac{K_p}{2} \right) \left[ 0.5 + 9.48 \left( \frac{C_D N_{Ref}}{2} \right)^{-0.4} N_{Pe}^{-0.4} \right]$$

$$F = 1.01255$$

and:

$$M = \frac{C_D N_{Ref}}{2} K_1^{5/2} N_{Pe}$$

$$M = 14.668$$

$G(M)$  is then determined from the curve, Figure 4-2, as:

$$G(M) = 1.38$$

Substituting:

$$\eta_{DIP} = 0.75 (0.01405) + 1.01255 (1.38) 0.03686$$

$$\eta_{DIP} = 0.06204$$

Kimura and Linoya provide an equation for effective efficiency  $\eta_s$  of a single fiber as follows:

$$\eta_s = \eta_{DIP} \left[ 1 + 10 (N_{Ref})^{1/3} \alpha \right]$$

Effective efficiency provides a measure of the effect of neighboring fibers within a fiber bed.

The factor  $\alpha$  is the volume fraction of a fibrous bed which is solid. For this analysis, assume  $\alpha$  is 0.1. Then:

$$\eta_s = 0.06204 \left[ (1 + 10 (1.69 \times 10^{-3})^{1/3} (0.1)) \right]$$

$$\eta_s = 0.0694$$

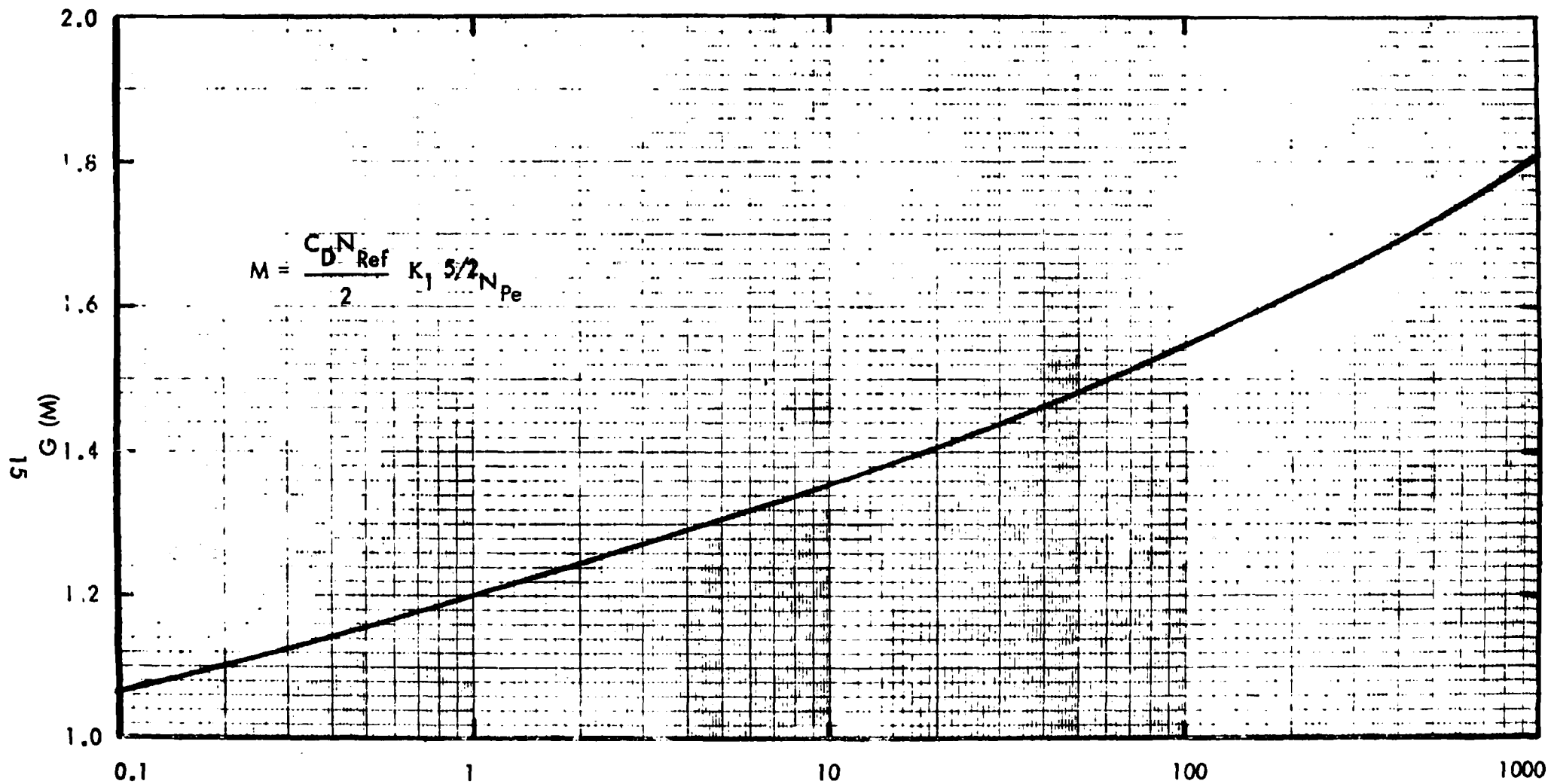


Figure 4-2.  $G(M)$  for Torgeson Theory

Whitby has provided the following equation,

$$E = 1 - \exp(-\eta_s S)$$

to describe the collection efficiency of a bed of clean fibers on particles of a specified size. The term "S" is the solidarity factor which is the ratio of the total projected area of the fibers to the face area of the filter mat in the direction of gas flow.

The solidarity factor is expressed as:

$$S = \frac{4 \ell}{\pi d_f} \quad \alpha = \frac{4 w'}{\pi \rho_f d_f}$$

Where  $\ell$  is the length of filter bed measured in the direction of gas flow and  $w'$  is the basis weight or weight per unit area of the filter bed.

In this analysis, we are trying to achieve 90 percent collection efficiency of 0.3  $\mu$ m DOP particles. Therefore, from:

$$E = 1 - \exp(-\eta_s S)$$

$$e^{-\eta_s S} = 1 - E$$

$$-\eta_s S \ln e = \ln(1 - E)$$

$$S = \frac{-\ln(1-E)}{\eta_s \ln e}$$

$$S = \frac{-\ln(1-0.9)}{0.0694 (1)}$$

$$S = 33.2$$

Therefore, for 1.0  $\mu$ m diameter fibers, 33.2 solidarity factors are required to achieve a filter bed capable of collecting 90 percent of 0.3  $\mu$ m DOP particles.

The basis weight required to achieve this many solidarity factors is determined from:

$$S = \frac{4 w'}{d_f}$$

$$w' = \frac{\pi \rho_f d_f S}{4}$$

$$w' = \pi \frac{1.135 \text{ gm/cm}^3 (0.0001 \text{ cm}) 33.2}{4}$$

$$w' = 0.002959 \text{ gm/cm}^2$$

$$w' = 29.6 \text{ gm/m}^2$$

This result is plotted on Figure 4-1 with the curve extrapolated to show efficiency as a function of basis weight for filter beds of  $1.0 \mu\text{m}$  diameter fibers. The performance of filter beds constructed from other fiber diameters is also shown on Figure 4-1.

Basis weight as a function of fiber diameter for constant efficiency is presented on Figure 4-3.

### Pressure Drop

Longmuir developed an equation to predict pressure drop in a fabric filter as follows:

$$\Delta P = \frac{8 \alpha \mu_g U_o}{(-1/2 \ln \alpha + \alpha - \alpha^2/4 + 3/4) d_f^2} \ell$$

where:

$\alpha$  = fiber volume fraction of the filter = 0.1 for this analysis

$d_f$  = fiber diameter in cm

$\mu_g$  = gas viscosity =  $1.8 \times 10^{-4}$  gm/cm sec

$U_o$  = upstream gas velocity = 2.54 cm/sec

$\ell$  = filter bed thickness in cm (fn  $d_p$ )



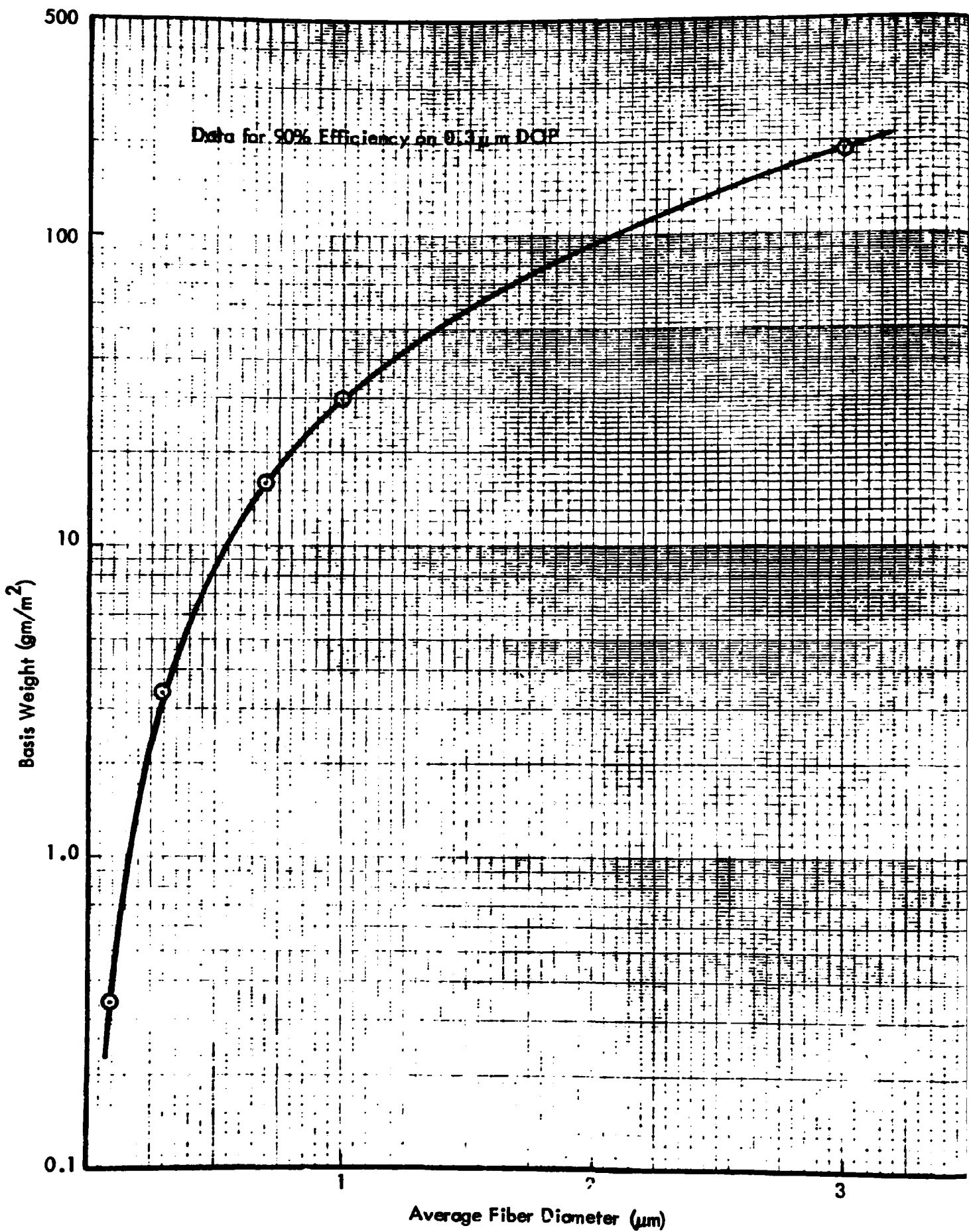


Figure 4-3. Basis Weight as Function of Fiber Diameter

Filter bed thickness is given by,

$$l = \frac{w'}{\alpha \rho_f}$$

For this analysis,

$$\alpha = 0.1$$

$$\rho_f = 1.135 \text{ gm/cm}^3$$

Substituting into the above equation yields pressure drop as a function of fiber diameter for filter beds capable of 90 percent collection efficiency of  $0.3 \text{ } \mu\text{m}$  diameter particles at a filtration velocity of  $2.54 \text{ cm/sec}$ .

Table 4-1 summarizes this analysis. Pressure drop as a function of fiber diameter is plotted as Figure 4-4.

Table 4-1. Langmuir Pressure Drop

Fiber diameter $d_f$ (cm)	Filter bed Thickness $l$ (cm)	Pressure Drop $\Delta P$ (gm/cm <sup>2</sup> )	Pressure Drop $\Delta P$ (mm H <sub>2</sub> O)
$5 \times 10^{-6}$	$5.61 \times 10^{-5}$	1.68	16.8
$1 \times 10^{-5}$	$3.03 \times 10^{-4}$	2.27	22.7
$3 \times 10^{-5}$	$2.97 \times 10^{-3}$	2.47	24.7
$7 \times 10^{-5}$	$1.38 \times 10^{-2}$	2.11	21.1
$1 \times 10^{-4}$	$2.61 \times 10^{-2}$	1.95	19.5
$3 \times 10^{-4}$	$1.633 \times 10^{-1}$	1.36	13.6

Yeh and Liu have developed a correction for slip flow using the Knudsen number ( $K_n$ ). Applying this correction to Langmuir's equation yields:

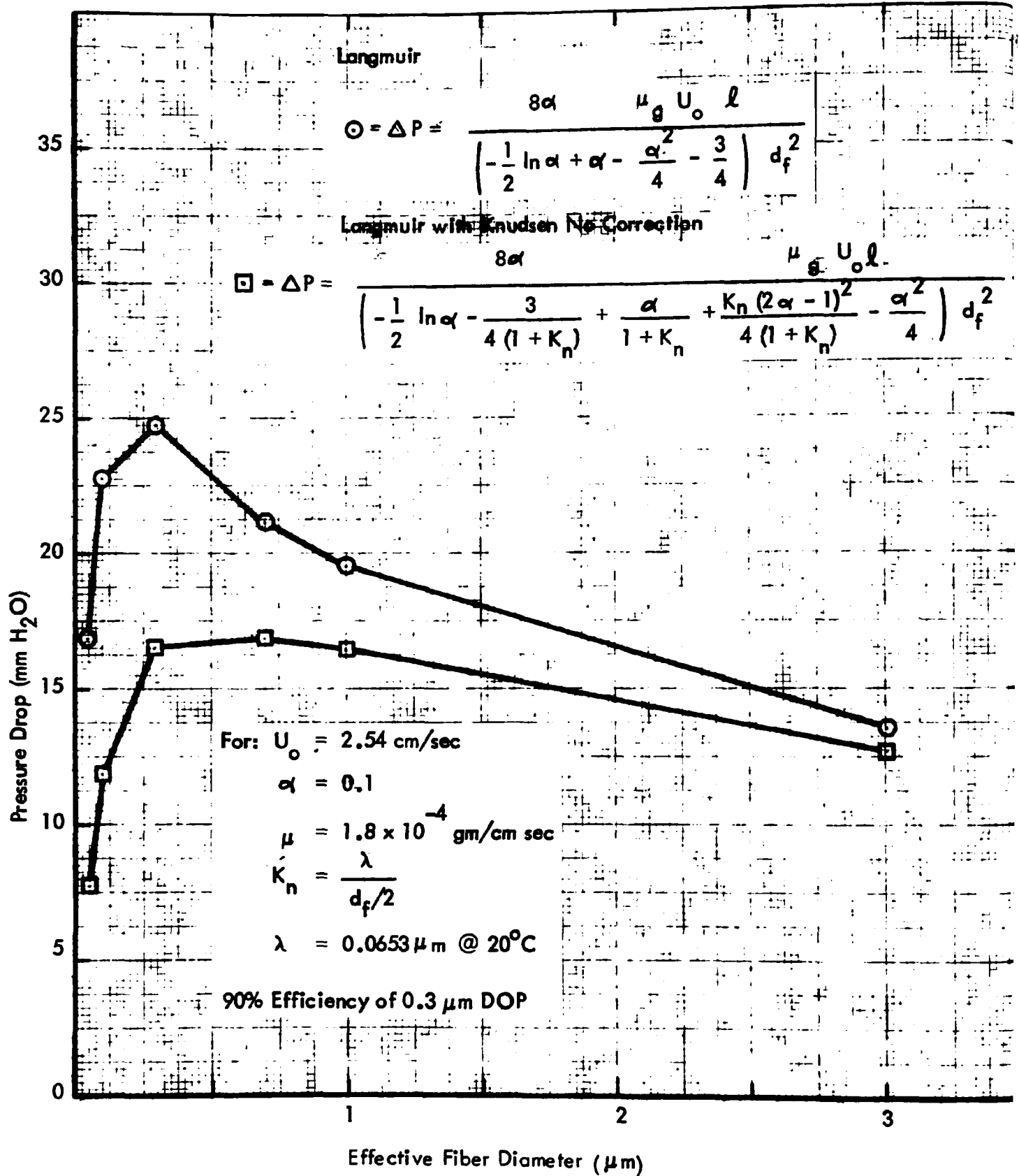


Figure 4-4. Pressure Drop as a Function of Fiber Diameter

$$\Delta P = \frac{8\alpha \mu_g U_o \ell}{\left( -1/2 \ln \alpha - \frac{3}{4(1+K_n)} + \frac{\alpha}{1+K_n} + \frac{K_n(2\alpha-1)^2}{4(1+K_n)} - \frac{\alpha^2}{4} \right) d_f^2}$$

Where:

$$K_n = \frac{\lambda}{d_f/2}, \quad \lambda = 0.0653 \mu\text{m} @ 20^\circ\text{C}$$

= mean free path of gas molecules

Pressure drop using this equation is shown in Table 4-2.

Table 4-2. Langmuir Pressure Drop with Knudsen Number Correction

Fiber diameter $d_f$ (cm)	Knudsen Number $K_n$	Filter Bed Thickness $\ell$ (cm)	Pressure Drop $\Delta P$ (gm/cm <sup>2</sup> )	Pressure Drop $\Delta P$ (mm H <sub>2</sub> O)
$5 \times 10^{-6}$	2.612	$5.61 \times 10^{-5}$	0.77	7.7
$1 \times 10^{-5}$	1.306	$3.03 \times 10^{-4}$	1.18	11.8
$3 \times 10^{-5}$	0.4353	$2.97 \times 10^{-3}$	1.65	16.5
$7 \times 10^{-5}$	0.1866	$1.38 \times 10^{-2}$	1.68	16.8
$1 \times 10^{-4}$	0.1306	$2.61 \times 10^{-2}$	1.64	16.4
$3 \times 10^{-4}$	0.0435	$1.633 \times 10^{-1}$	1.27	12.7

These results are plotted on Figure 4-4. This analysis indicates that there should be no severe pressure drop penalty when employing fabric filters made from fine fibers.

## 5.0

## PRELIMINARY EXPERIMENTS

Preliminary experiments during Phase I were of three types. These were:

- 1) DOP penetration tests to relate basis weight to collection efficiency
- 2) Scanning electron micrograph analysis of fine fibers to relate fiber diameter to basis weight
- 3) Dust loading tests in a flat-sheet pulse-jet test rig to simulate performance in a pulse-jet fabric filter

## 5.1

### DOP Penetration Tests

One of the design objectives of the contract is to produce a cleanable filter media capable of collecting  $0.3\mu\text{m}$  DOP at an efficiency of 90 percent. To meet this objective, DOP penetration tests were used to evaluate various media during Phase I. We have been successful in producing filter media from fine fibers which have high collection efficiency and low basis weight. In general, the theoretical relationship shown on Figure 4-1 was confirmed by the data.

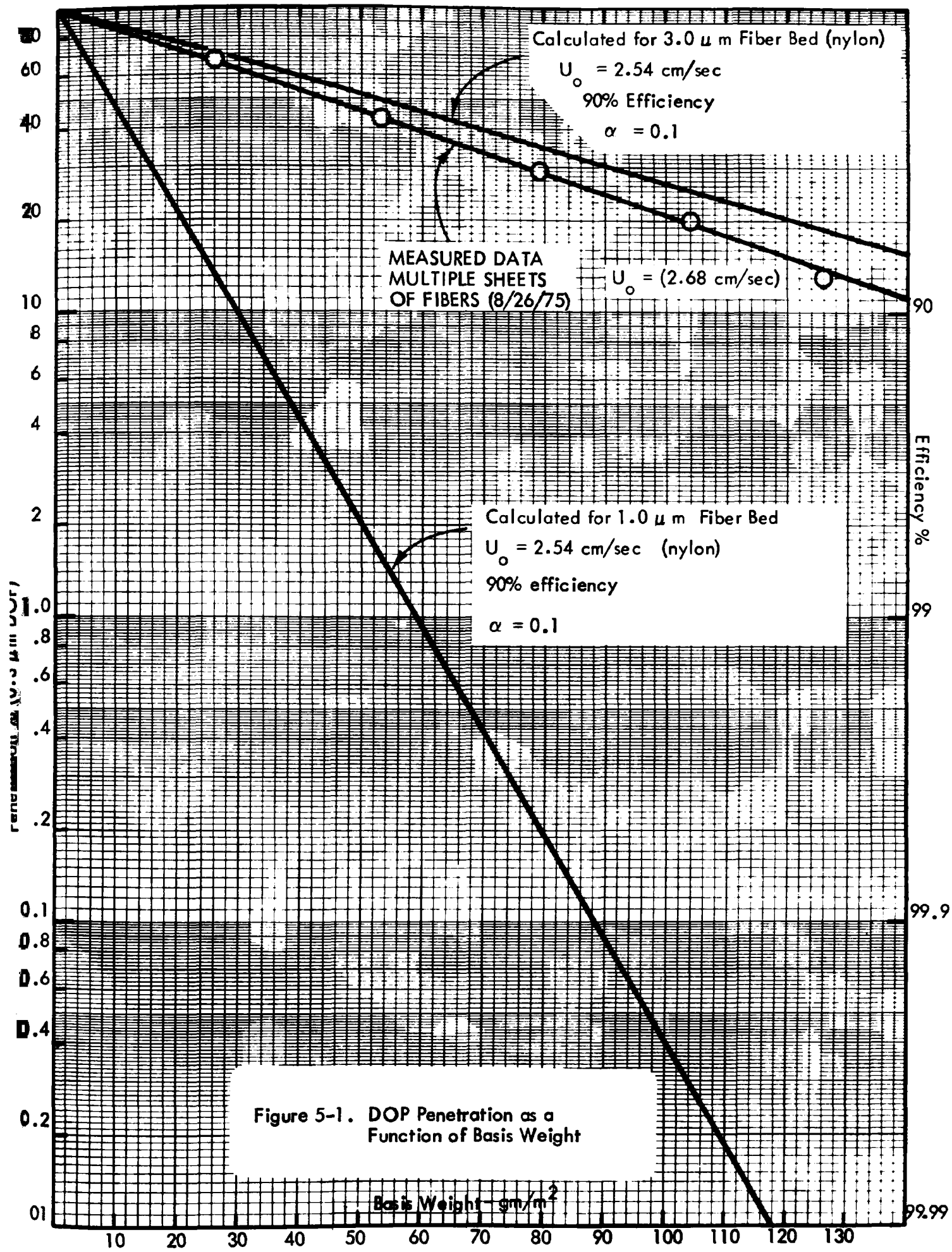
The first sample produced for testing under the contract was a thin layer of fine fibers deposited on a light-weight backing material. The fine fiber sheet was then removed from the backing material and tested alone. Table 5-1 presents the results of testing multiple sheets of this material for basis weight, permeability and penetration. This material is designated medium (8/26/75) because it was made August 26, 1975.

The penetration data is plotted on Figure 5-1 showing a comparison with calculated performance. This first sample had an apparent average fiber diameter of about  $3\mu\text{m}$ .

To obtain the necessary strength in the media, the fine fiber layer must be supported on a backing material. Felt was the first material evaluated as a backing medium. After first determining that the fine fibers could not be separated and handled on a carding machine, the following double mat samples were produced by needle-punching. A #41

Table 5-1. Results of Multiple Sheet Testing of Medium (8/26/75)

Number of Sheets	Basis Weight (gm/m <sup>2</sup> )	Permeability (m <sup>3</sup> /min @ 1.27 cm H <sub>2</sub> O)	Penetration (%)
1	26.16	20.61	66
2	53.28	18.00	43
3	78.47	12.60	29
4	104.14	5.34	20
5	125.94	4.53	13
6	153.55	3.54	9.7



needle was used with about 16 needles per cm (40 needles per inch). The machine was set at 250 punches per minute.

- Sample Number 1:

Two layers of 2 oz ( $68 \text{ gm/m}^2$ ), 3 denier polyester were needled to a 10 x 10 scrim. Then six layers of the fine fibers were placed on top of this backing with the scrim between the fibers and backing. The fine fiber layer was needle-punched into the backing material. This method resulted in poor adhesion of the fine fibers to the backing. The needles also left obvious holes in the fine fiber layer.

- Sample Number 2:

Six layers of fine fibers were needled to the same backing material with the needles passing first through the backing material. This carried some of the felt fibers through the hole in the fine fiber layer and seemed to result in good adhesion.

- Sample Number 3:

Six layers of fine fibers were placed over the same backing, as in Samples 1 and 2 with the scrim between the fibers and back. Then a 2 oz ( $68 \text{ gm/m}^2$ ) polyester sheet was placed over the fine fiber layer. The sample was then needle punched. This method resulted in good adhesion but the layer of felt over the fine fiber layer was considered likely to interfere with cleaning of the fine fiber layer.

In order to illustrate the relative performance of the fine fiber filter, penetration tests using  $0.3 \mu\text{m}$  DOP smoke were made on a variety of materials. Figure 5-2 shows the results of this testing as a function of airflow velocity. This data illustrates the effectiveness of the fine fibers for collection of fine particles. Even a single layer with a basis weight of  $26 \text{ gm/m}^2$  was more effective than standard baghouse filter media. Also illustrated is the degradation caused by the needle punching. Note the difference in collection efficiency between six layers of the fine fibers (Sample M) and media Sample No. 2 which contained six layers of fine fibers with needle holes.



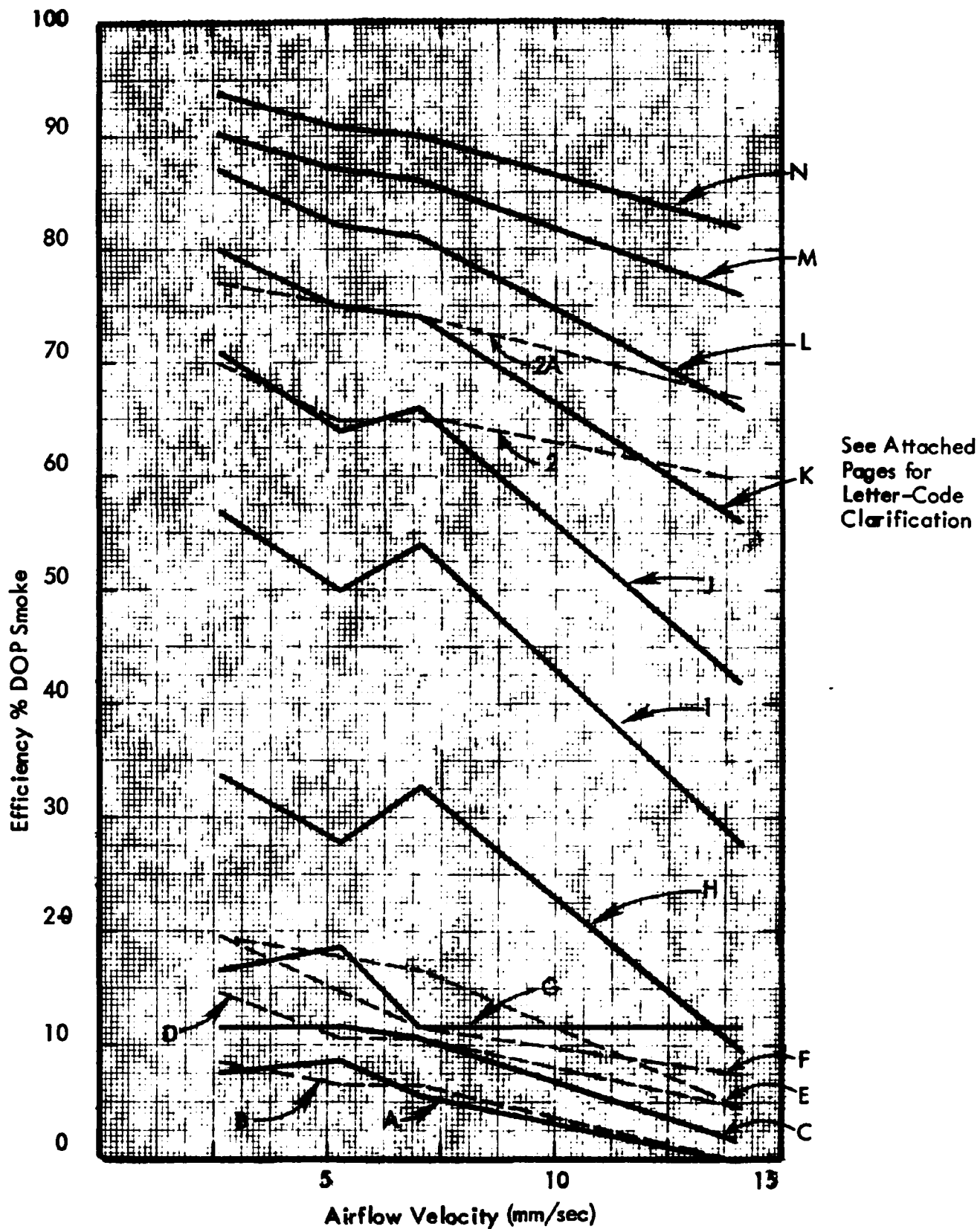


Figure 5-2. Penetration Tests of Various Media

Code Number Identification for Figure 5-2.

Code No.

A	Woven Polyester Felt Perm = $4.38 \text{ m}^3/\text{min}/\text{m}^2$ @ 1.27 cm H <sub>2</sub> O
B	Polyester Twill Perm = $5.06 \text{ m}^3/\text{min}/\text{m}^2$ @ 1.27 cm H <sub>2</sub> O
C	Polyester Sateen Perm = $3.78 \text{ m}^3/\text{min}/\text{m}^2$ @ 1.27 cm H <sub>2</sub> O
D	Polypropylene Felt Perm = $8.53 \text{ m}^3/\text{min}/\text{m}^2$ @ 1.27 cm H <sub>2</sub> O
E	Cotton Sateen Perm = $4.10 \text{ m}^3/\text{min}/\text{m}^2$ @ 1.27 cm H <sub>2</sub> O
F	Felted Dacron Perm = $25.45 \text{ m}^3/\text{min}/\text{m}^2$ @ 1.27 cm H <sub>2</sub> O
G	DURALIFE® II (Commercial Filter Paper) Perm = $6.40 \text{ m}^3/\text{min}/\text{m}^2$ @ 1.27 cm H <sub>2</sub> O
H	1 Layer Fine Fibers (8/26/75) Perm = $20.61 \text{ m}^3/\text{min}/\text{m}^2$ @ 1.27 cm H <sub>2</sub> O Basis Weight = $26.16 \text{ gm}/\text{m}^2$
I	2 Layer Fine Fibers (8/26/75) Perm = $18.00 \text{ m}^3/\text{min}/\text{m}^2$ @ 1.27 cm H <sub>2</sub> O Basis Weight = $53.28 \text{ gm}/\text{m}^2$
J	3 Layers Fine Fibers (8/26/75) Perm = $12.60 \text{ m}^3/\text{min}/\text{m}^2$ @ 1.27 cm H <sub>2</sub> O Basis Weight = $78.47 \text{ gm}/\text{m}^2$
K	4 Layers Fine Fibers (8/26/75) Perm = $5.34 \text{ m}^3/\text{min}/\text{m}^2$ @ 1.27 cm H <sub>2</sub> O Basis Weight = $104.14 \text{ gm}/\text{m}^2$
L	5 Layers Fine Fibers (8/26/75) Perm = $4.53 \text{ m}^3/\text{min}/\text{m}^2$ @ 1.27 cm H <sub>2</sub> O Basis Weight = $125.94 \text{ gm}/\text{m}^2$
M	6 Layers Fine Fibers (8/26/75) Perm = $3.54 \text{ m}^3/\text{min}/\text{m}^2$ @ 1.27 cm H <sub>2</sub> O Basis Weight = $153.55 \text{ gm}/\text{m}^2$

---

® DURALIFE is a registered trademark of Donaldson Company, Inc., Minneapolis, MN. 55435

Code Number Identification for Figure 5-2 (continued)

Code No.

- N      7 Layers Fine Fibers (8/26/75)  
Perm =  $3.07 \text{ m}^3/\text{min}/\text{m}^2$  @  $1.27 \text{ cm H}_2\text{O}$   
Basis Weight =  $182.37 \text{ gm}/\text{m}^2$
- 2      2 Layers 2 Oz., 3 Denier Polyester Needled (#41)  
to Scrim then Needled into 6 Layers of Fine Fibers (8/26/75)  
Perm =  $3.66 \text{ m}^3/\text{min}/\text{m}^2$  @  $1.27 \text{ cm H}_2\text{O}$
- 2A      Same as 2 but with One Additional Layer of Fine  
Fibers (8/26/75) Cemented Over Needle Holes  
Perm =  $3.35 \text{ m}^3/\text{min}/\text{m}^2$  @  $1.27 \text{ cm H}_2\text{O}$

A second run of fine fiber media was produced in an attempt to reduce the average fiber diameter. This medium was produced on 9/18/75 and is referred to as medium (9/18/75). Figure 5-3 shows that a reduction in average fiber diameter was accomplished. Multiple layers of medium (9/18/75) were tested for DOP efficiency as a function of airflow velocity. This data is plotted in Figure 5-4. Because of the smaller average fiber diameter, 100 gm/m<sup>2</sup> of medium (9/18/75) could achieve an efficiency of 90 percent on 0.3 μm DOP; while over 150 gm/m<sup>2</sup> of medium (8/26/75) was required to achieve the same efficiency.

Using medium (9/18/75), additional double mat filter samples were produced. As in Sample No. 2 above, a scrim was needed to a felt backing; then the fine fibers were needed to the scrim/felt by needling through the felt into the fine fibers.

The following samples were obtained:

- Sample Number 4:  
Single layer fine fiber 9/18/75  
6 denier felt - 22 x 18 scrim  
Laminated at 300 points per square inch (ppsi)  
Re-neededled at 250 ppsi
- Sample Number 5:  
Same as No. 4 but re-neededled at 200 ppsi
- Sample Number 6:  
Double layer of fine fibers  
6 denier felt - 22 x 18 scrim  
Laminated at 300 ppsi  
Re-neededled at 200 ppsi
- Sample Number 7:  
Single layer of fine fiber  
6 denier felt - 10 x 10 scrim  
Laminated at 300 ppsi  
Re-neededled at 200 ppsi

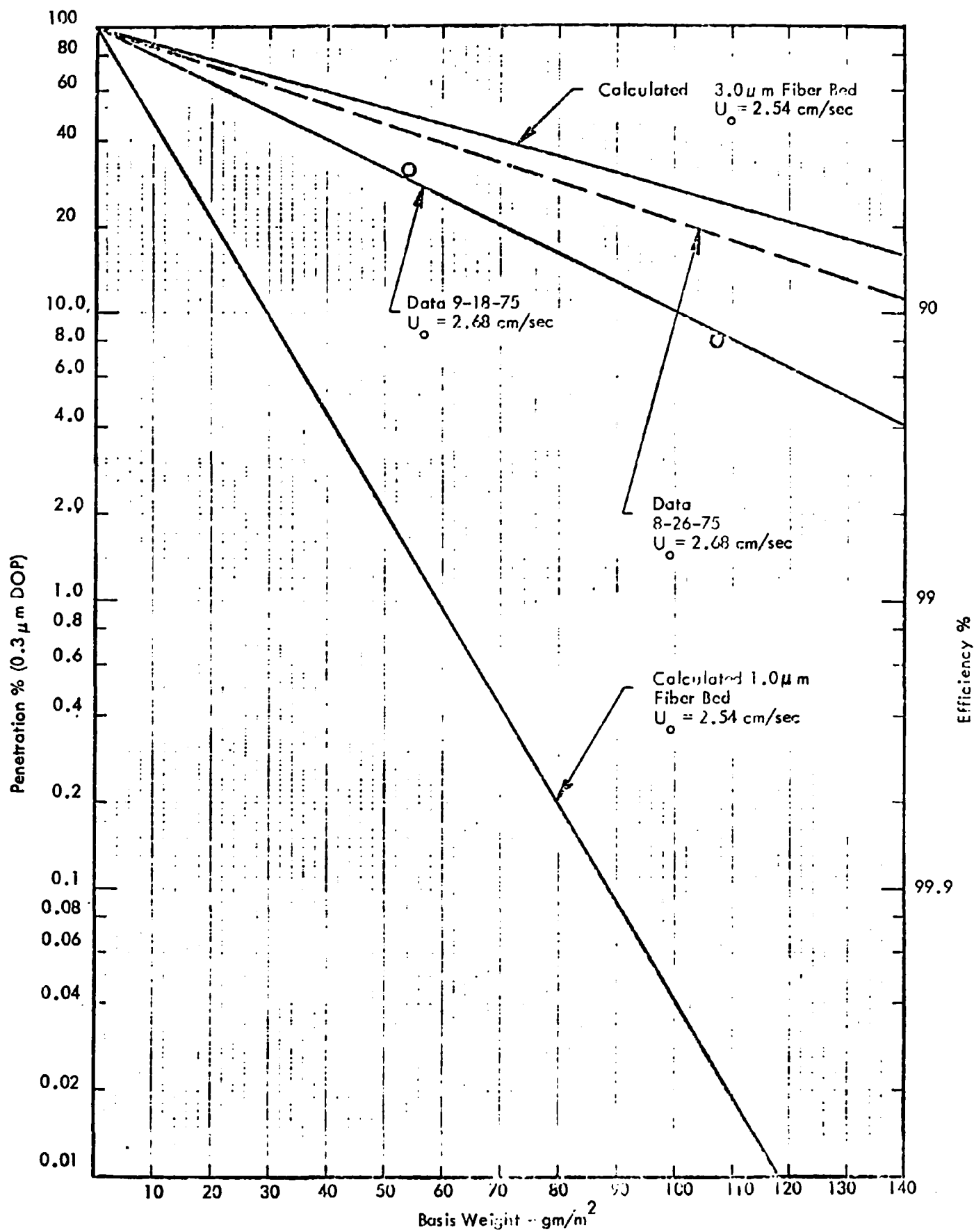


Figure 5-3. Penetration as a Function of Basis Weight

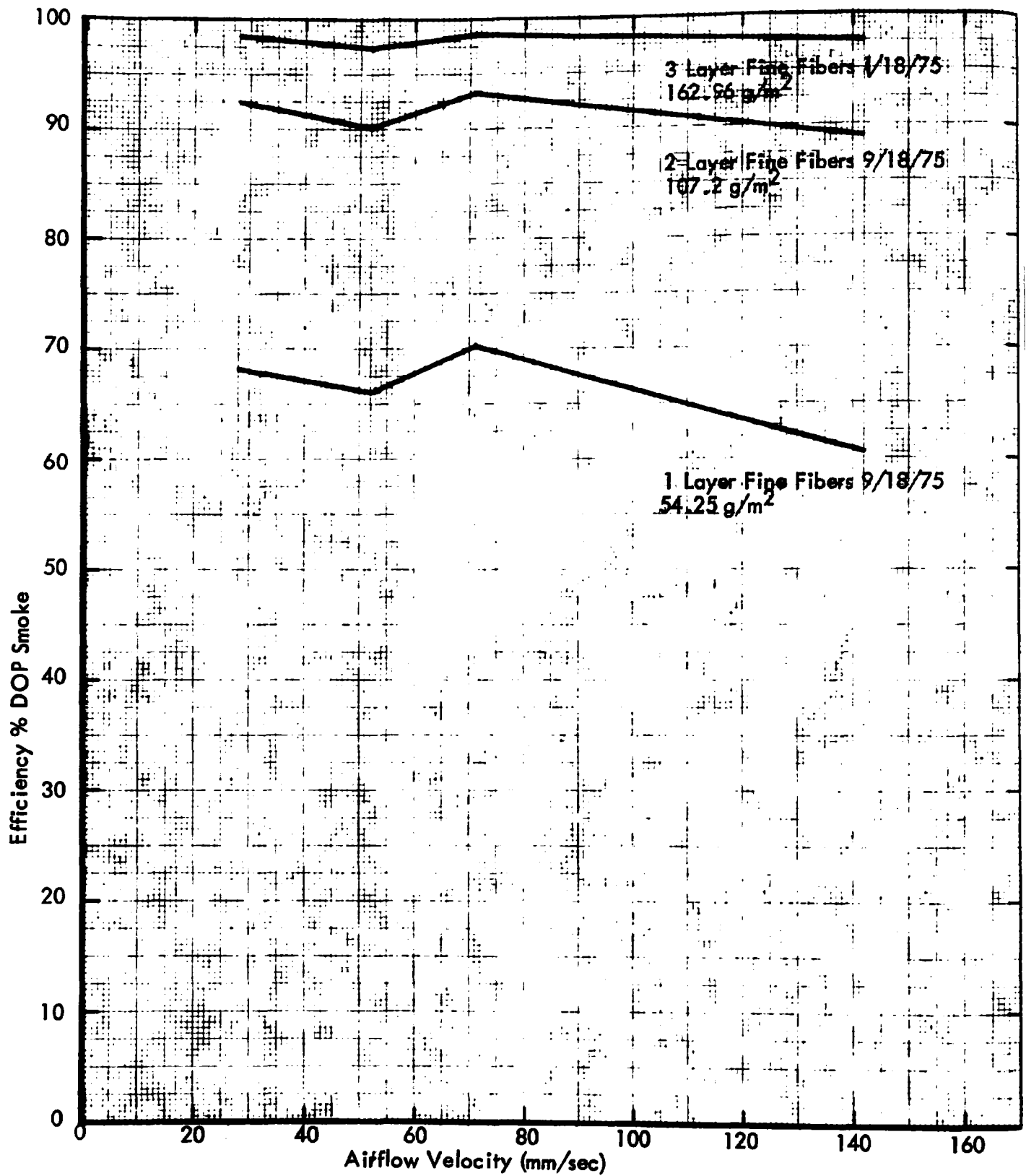


Figure 5-4. Penetration as a Function of Airflow Velocity

- **Sample Number 8:**  
Double layer of fine fiber  
6 denier felt – 10 x 10 scrim  
Laminated at 300 ppsi  
Re-neededled at 200 ppsi
  
- **Sample Number 9:**  
Single layer of fine fibers  
3 denier felt – 10 x 10 scrim  
Laminated at 300 ppsi  
Re-neededled at 200 ppsi
  
- **Sample Number 10:**  
Double layer of fine fibers  
3 denier felt – 10 x 10 scrim  
Laminated at 300 ppsi  
Re-neededled at 200 ppsi
  
- One additional sample was produced by fastening two layers of fine fibers to a backing of 3 denier felt with a 10 x 10 scrim. The adhesion was accomplished by sonic welding on a 2.5 cm square grid pattern. Visually, this method seemed to result in a strong bond between the materials.

The felt and scrims used in these samples were dacron.

DOP penetration tests using  $0.3\ \mu\text{m}$  DOP smoke were made on the media samples. Figure 5-5 shows collection efficiency for the samples. This figure shows the degradation in performance by the needle holes. The performance of one and two layers of these fibers alone are also presented. Media Samples 4 through 10 are shown in the range of 30 to 60 percent efficiency. These samples consisted of one or two layers of fibers needle-punched to a backing material. In general, the samples fabricated from one layer of fiber had slightly lower efficiency than those with two layers of fibers. Samples designated 4A through 10A had an additional layer of fibers placed over the needle holes. Significant recovery of efficiency was achieved from this additional layer of fibers. Note

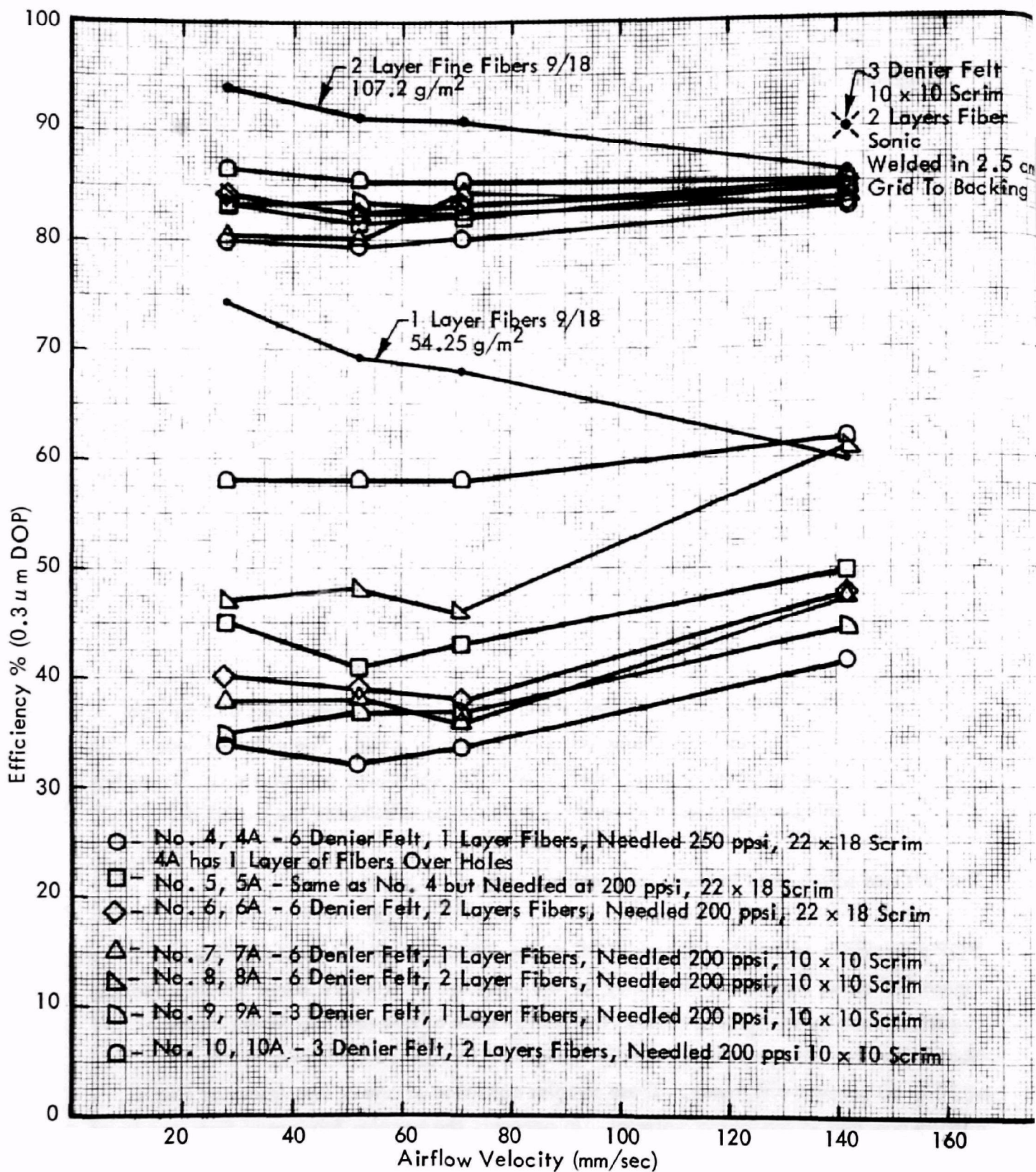


Figure 5-5. Efficiency of Media Samples



also that samples with either one or two layers of fine fibers achieved about the same performance with an additional layer of fibers placed over the needle-holed surface.

Also shown is one data point for a sonic welded sample. Two layers of fibers were placed over a backing of 3 denier felt with a 10 x 10 scrim and welded to the backing in a 2.54 cm grid pattern. This data point shows that the sonic welding method of adhesion does not degrade efficiency.

In order to further examine the effect of the needle holes, we counted the number of holes per square inch ( $6.45 \text{ cm}^2$ ) in Samples 4 and 5. These two samples were produced with the needle punch machine set at 250 points per square inch and 200 points per square inch (ppsi) nominal. Efficiency was then plotted as a function of the number of needle holes to produce the data shown on Figure 5-6. This data shows a clear functional relationship between the number of holes and the loss in efficiency.

Other physical data for the samples are tabulated in Tables 5-2 and 5-3. The average thickness of a single layer of fine fibers (9/18/75) was 0.0335 cm.

Continuing efforts to reduce fiber diameter resulted in medium (1/26/76). Figure 5-7 presents penetration by  $0.3 \mu\text{m}$  DOP as a function of basis weight for this material. Also presented are calculated results for 1 to  $3 \mu\text{m}$  fiber beds and results of testing earlier samples of double mat filters. These results show that the medium (1/26/76) has an average fiber diameter of less than  $1.0 \mu\text{m}$ . Only the basis weight of the fine fiber layer is presented. Collection efficiency of the backing material on DOP particles is essentially zero. The data presented was produced by testing multiple thicknesses of two runs. The first run ( $-\odot-$ ) had a basis weight of  $8.4 \text{ gm/m}^2$ . The second run ( $-\square-$ ) had a basis weight of  $11.1 \text{ gm/m}^2$ . Figure 5-8 presents collection efficiency for  $0.3 \mu\text{m}$  DOP as a function of airflow velocity for a Gore-Tex ( $-\diamond-$ ) medium. It is apparent from this data that greater than 90 percent collection efficiency of  $0.3 \mu\text{m}$  particles can be achieved for these materials from fiber beds of only 10 to  $12 \text{ gm/m}^2$  basis weight.

An attempt to produce a fine fiber media sample with the capability of collecting  $0.3 \mu\text{m}$  DOP at an efficiency of 90 percent in a single sheet resulted in medium 4/10/76. This material had a basis weight of  $20.67 \text{ gm/m}^2$  on a felt backing. Efficiency of collection for  $0.3 \mu\text{m}$  DOP as a function of airflow velocity is as follows:

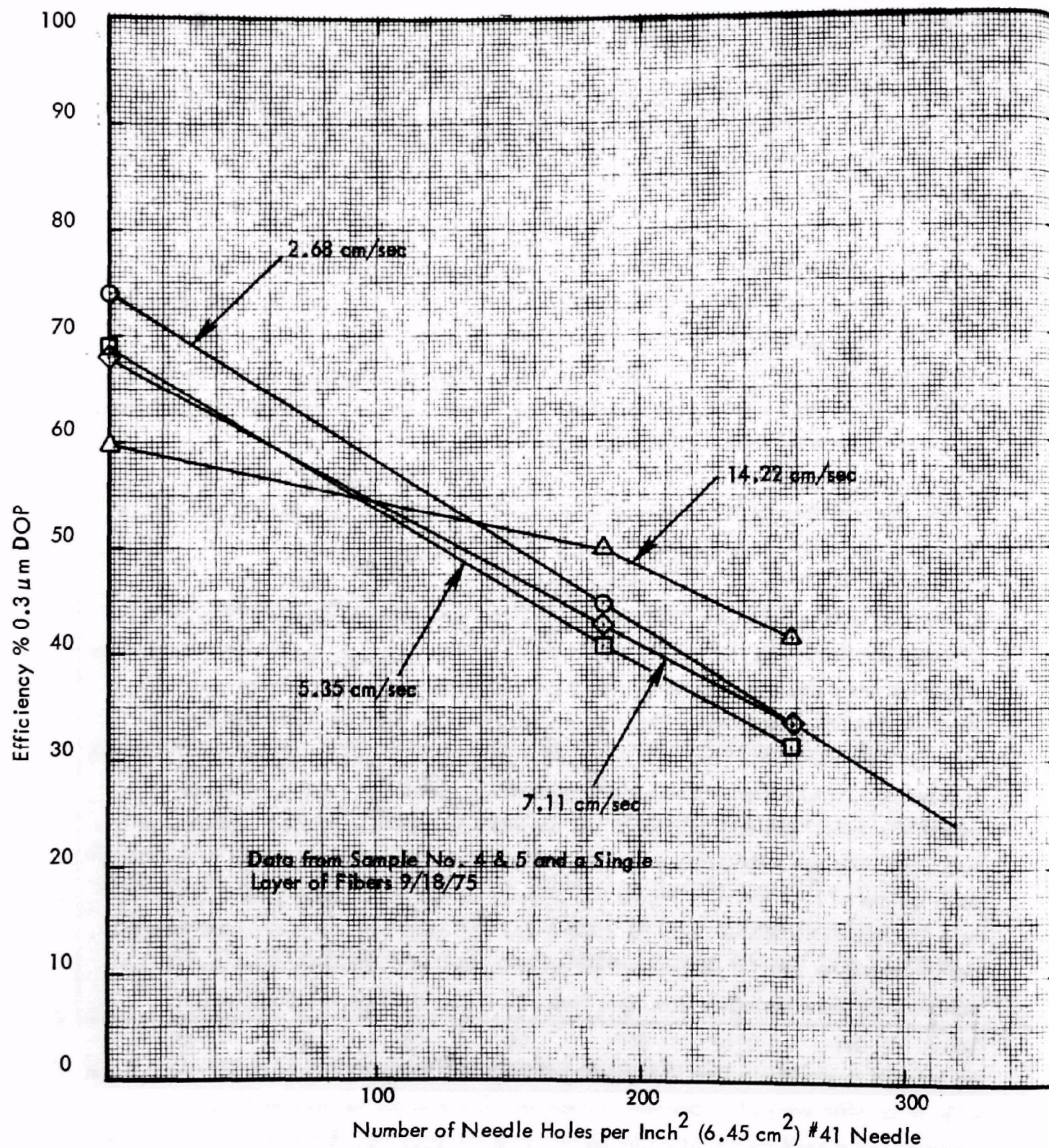


Figure 5-6. Effect of Needle Holes on Efficiency

Table 5-2. Physical Data

Sample	Permeability $\text{m}^3/\text{min}/\text{m}^2$ @ 1.27 cm $\text{H}_2\text{O}$	Pore Size (micrometer average)	Basis weight ( $\text{gm}/\text{m}^2$ )
1 (9/18)	6.64	-	-
1 + 2	3.17	-	-
1 + 2 + 3	1.93	-	-
1 + 2 + 3 + 4	1.51	-	-
Sub 4, 5, 6	130.36	-	-
Sub 7, 8	116.71	-	-
Sub 9, 10	99.95	346.4	-
4	7.76	225	306,125
4A	4.10	-	-
5	12.10	268	285.87
5A	4.65	-	-
6	5.05	202	332.71
6A	3.14	-	-
7	20.11	262	270.89
7A	5.68	-	-
8	5.35	204	310
8A	2.98	-	-
9	12.41	223	280.96
9A	4.44	-	-
10	6.95	146	311.65
10A	3.32	-	-

Table 5-3. Physical Data

Sample	Strength Dry (Newton/5 cm strip)		Mullen Burst (Pascal)	Thickness (Average cm)
4	154	wire	$1.37 \times 10^6$	0.332
		felt	$1.37 \times 10^6$	0.317
5	147	wire	$1.37 \times 10^6$	0.317
		felt	$1.37 \times 10^6$	
6	183	wire	$1.37 \times 10^6$	0.341
		felt	$1.37 \times 10^6$	
7	167	wire	$9.85 \times 10^5$	0.299
		felt	$1.15 \times 10^6$	
8	168	wire	$1.05 \times 10^6$	0.309
		felt	$1.02 \times 10^6$	
9	137	wire	$1.02 \times 10^6$	0.265
		felt	$1.08 \times 10^6$	0.265
10	137	wire	$1.21 \times 10^6$	0.298
		felt	$1.06 \times 10^6$	
9 & 10	-	wire	$9.81 \times 10^5$	0.258
Backing	-	felt	$9.58 \times 10^5$	0.258



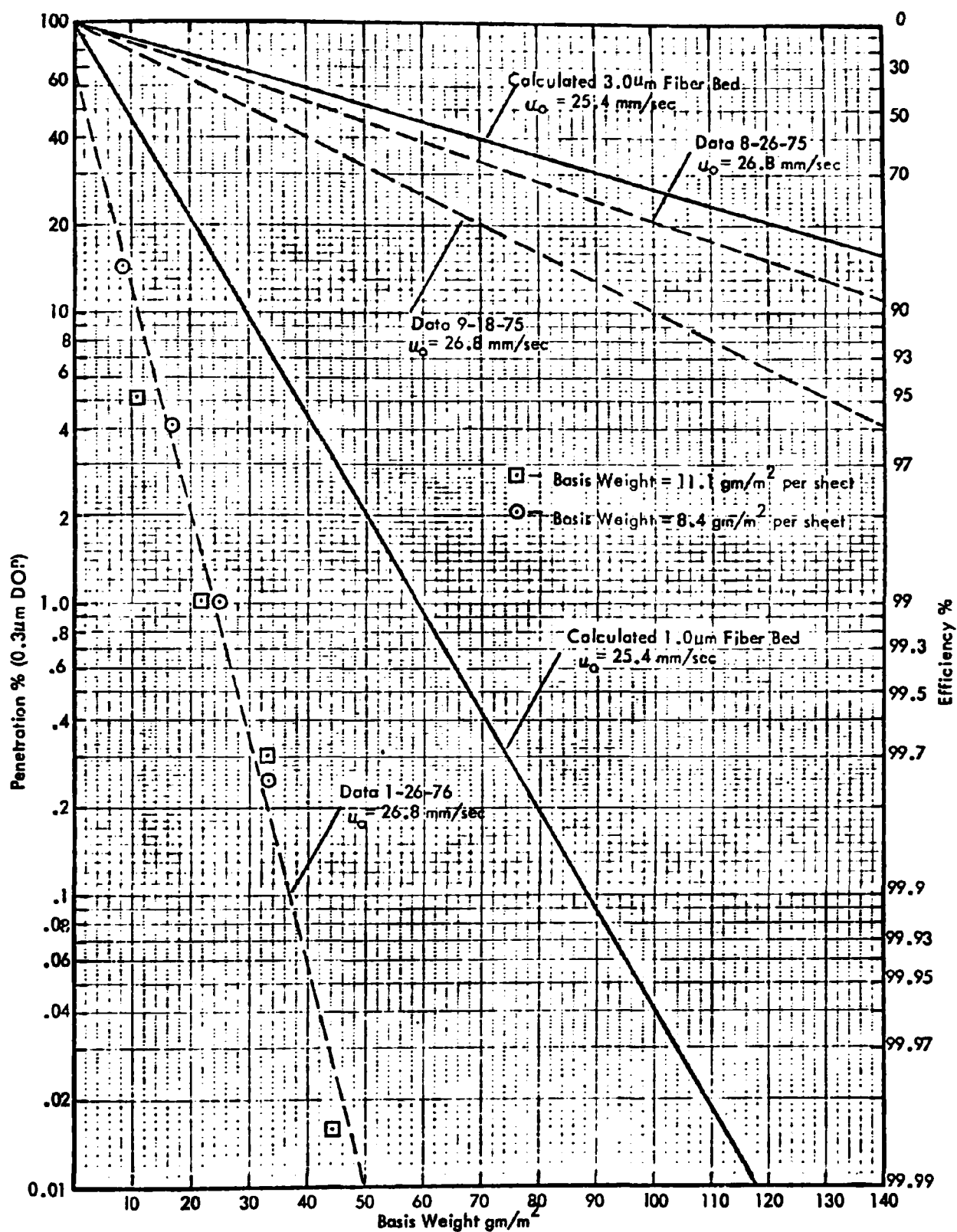


Figure 5-7. Penetration as a Function of Basis Weight

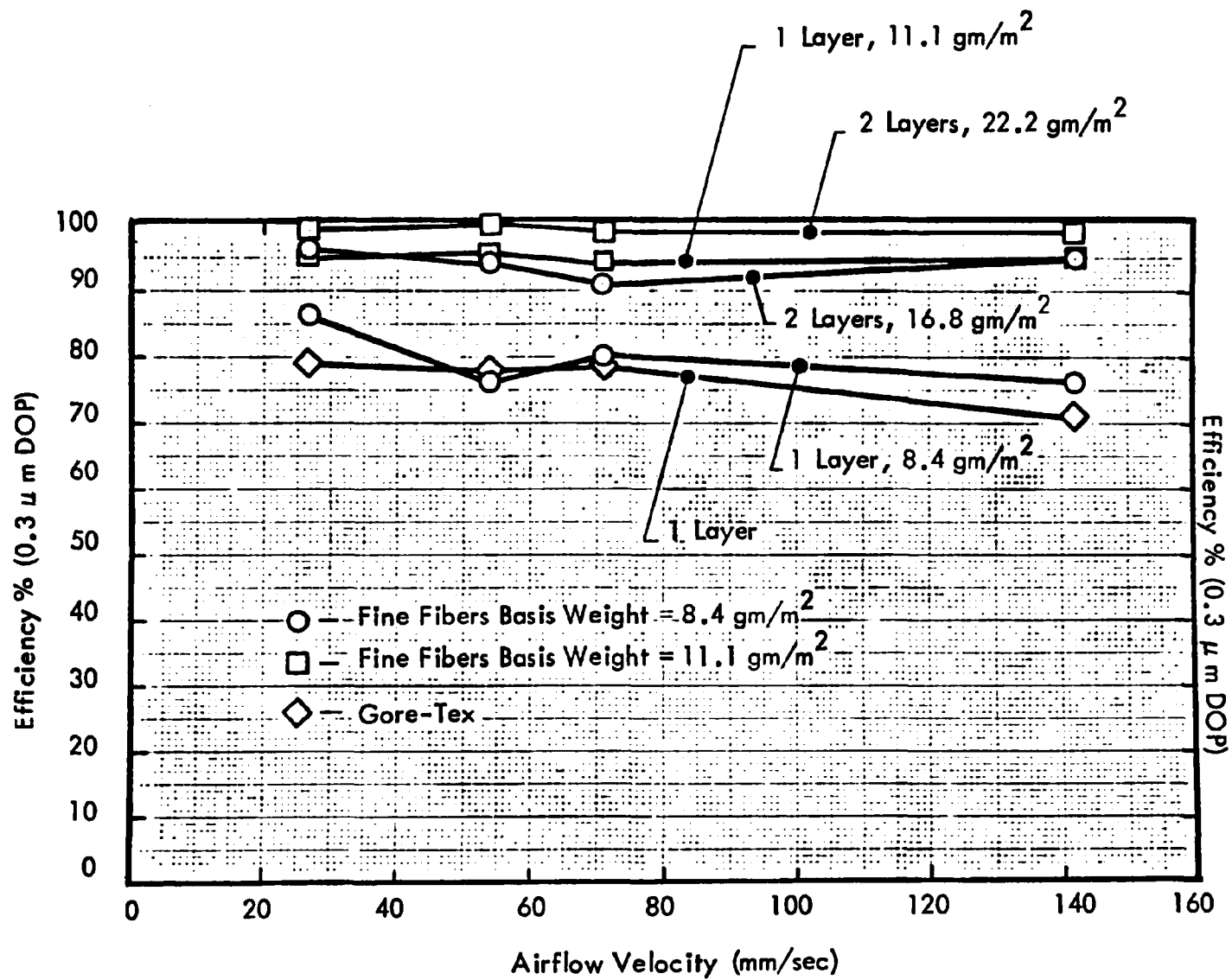


Table 5-4. DOP Efficiency of Medium (4/10/76)

Airflow Velocity mm/sec	Paper Backing DOP Efficiency %	Felt Backing DOP Efficiency %
26.8	92	90
53.5	88	82
71.1	92.7	88
142.2	90	85

This fine fiber material had an apparent fiber diameter larger than medium sample (1/26/76), as indicated by the basis weight of about  $20 \text{ gm/m}^2$  with a DOP efficiency of approximately 90 percent. The earlier results indicated that the basis weight should have been about  $10 \text{ gm/m}^2$ .

Two additional samples were produced to have a target DOP efficiency of 90 percent. One of these, medium sample 5/14/76, had a basis weight of  $3.9 \text{ gm/m}^2$  and a DOP efficiency of 91.8 percent. The other, medium sample 5/17/76, had a basis weight of  $0.5 \text{ gm/m}^2$  and a DOP efficiency of 90 percent.

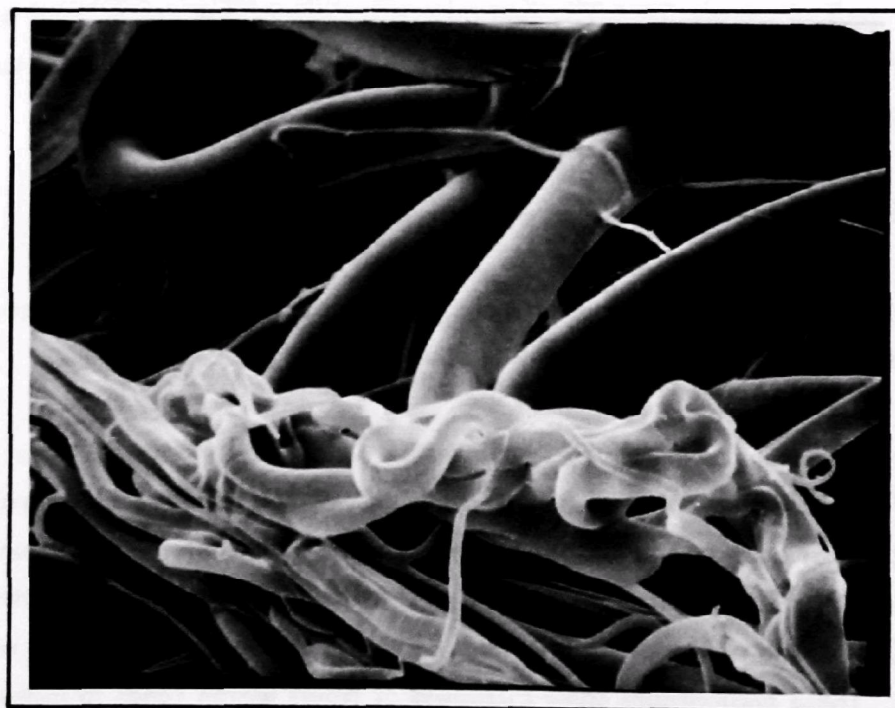
## 5.2 SEM Analysis

During Phase I, scanning electron micrographs (SEM) were made of various fine fiber samples to assist in relating basis weight to fiber diameter.

Scanning electron photomicrographs of the fine fibers produced for the first run of media samples (8/26/75) were made at 3K magnification. Two samples were photographed with five pictures taken of each at random locations. The fiber diameter varied from about  $0.1 \mu\text{m}$  to about  $10 \mu\text{m}$ . Our analysis indicated that the average fiber diameter of one sample was  $2.02 \mu\text{m}$  and of the other sample  $1.82 \mu\text{m}$ . Figure 5-9 shows two of the pictures taken. These photographs show clumping of fibers which tends to make the fibers behave as though they were larger in diameter. Fiber diameters were measured with a scale in lines (3) as shown on the sketch on Figure 5-10. Each fiber intersecting a line was measured and the results averaged.



0.3 cm = 1  $\mu$ m



Basis Weight = 150 gm/m<sup>2</sup> @ 90 % DOP Efficiency

Figure 5-9. SEM Photomicrograph of Fine Fibers (#8/26/75)



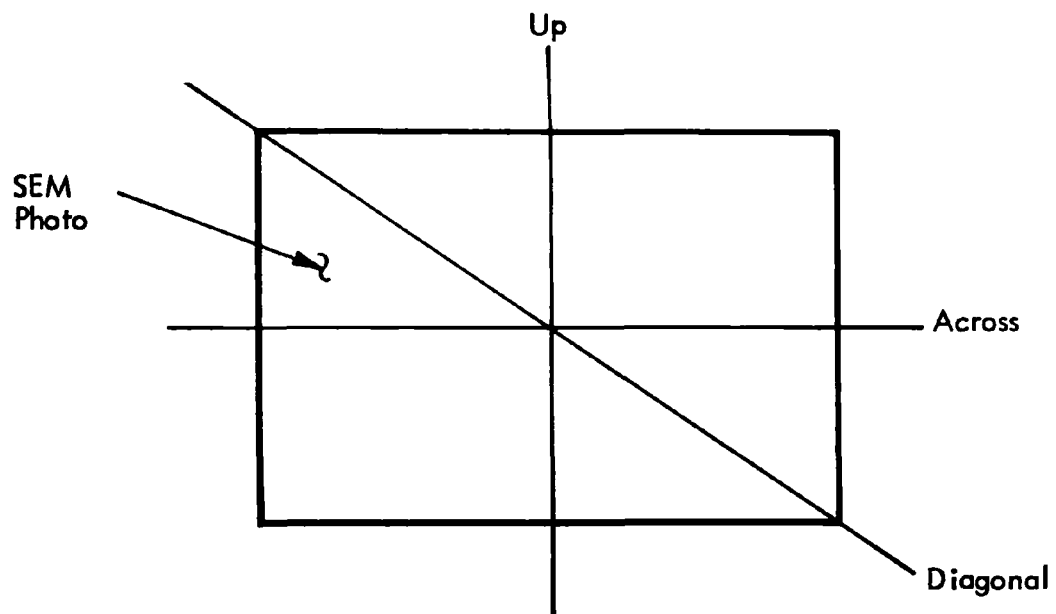


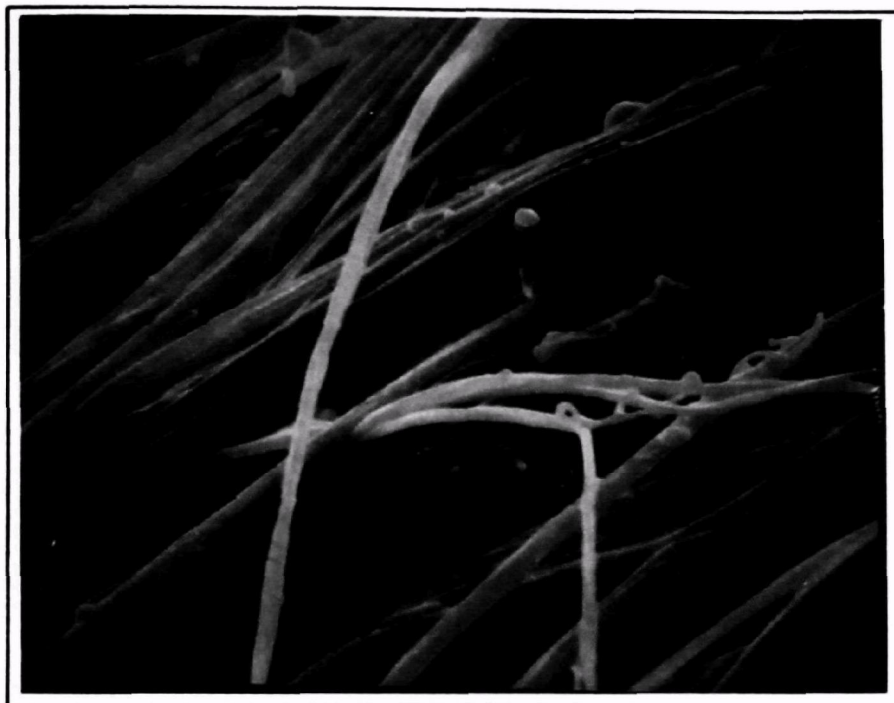
**Figure 5-10. Measurement Technique Used to Estimate Average Fiber Diameter**

Results from this measurement differ from the DOP tests and theoretical analysis. The DOP efficiency as a function of basis weight curve (Figure 5-1) indicated an average diameter close to  $3\text{ }\mu\text{m}$ ; while the analysis from photographs indicated an average diameter closer to  $2\text{ }\mu\text{m}$ . Calculations predict a fiber diameter of about  $2.5\text{ }\mu\text{m}$  for 90 percent DOP efficiency. (See Figure 4-3.) This difference may be attributed to the difficulty of determining the effective diameter of clumps of fiber and to the filtration effects caused by the range from  $0.1\text{ }\mu\text{m}$  to  $10\text{ }\mu\text{m}$  of the actual fiber diameter. Considering the range of fiber diameters seen in the photographs, a difference of only one micrometer is good agreement.

Scanning electron micrographs (SEM) were made of both sides of a piece of fine fiber medium (9/18/75). Figure 5-11 shows a typical picture taken on one side of this material and Figure 5-12 shows the other side. The average diameter of fibers from Figure 5-11 was determined to be  $1.24\text{ }\mu\text{m}$ . The average fiber diameter of the side shown on Figure 5-12 was  $0.98\text{ }\mu\text{m}$ . The fibers shown in Figure 5-11 appear to lie essentially in one direction while those in Figure 5-12 seem more randomly oriented. This results from the way in which the fibers are laid down. Fibers from Figure 5-12 are on the upstream side during fabrication and contain more fiber ends. This may also explain the apparent smaller average fiber diameter seen in Figure 5-12. This medium would achieve an efficiency of 90 percent collection of DOP with a basis weight of  $100\text{ gm/m}^2$ . Theoretical analysis indicates that a uniform bed of  $2.0\text{ }\mu\text{m}$  fibers would achieve a collection efficiency for  $0.3\text{ }\mu\text{m}$  DOP of 90 percent with a basis weight of  $100\text{ gm/m}^2$ . Once again, considering the difficulties of measuring clumped fibers and the range of fiber size present, this is good agreement with theory.

Fine fiber media samples designated (1/26/76) were produced in two runs. One of the samples had a basis weight of  $8.4\text{ gm/m}^2$  and a DOP efficiency of 85.5 percent. The other had a basis weight of  $11.1\text{ gm/m}^2$  and a DOP efficiency of 95.8 percent. Figure 5-7 shows efficiency as a function of basis weight for this material. As seen from the curve on Figure 5-7, this material should exhibit 90 percent DOP efficiency with a basis weight of  $11\text{ gm/m}^2$ .

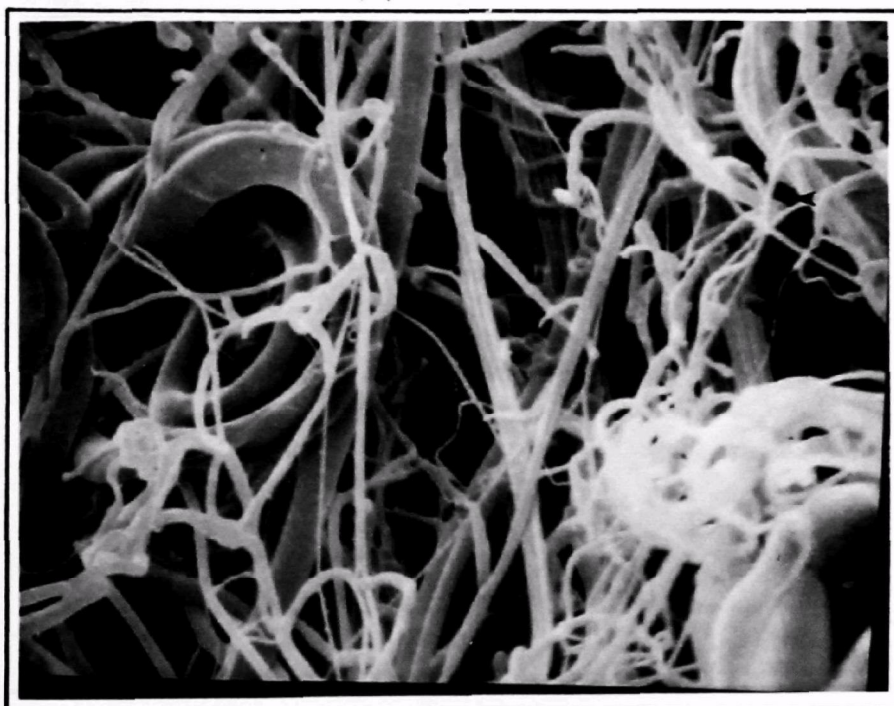
Scanning electron photomicrographs were made for these materials. Figure 5-13 presents two photographs of the  $8.4\text{ gm/m}^2$  basis weight material magnified 5,000 times. Figure 5-14 presents a similar photograph of the  $11.1\text{ gm/m}^2$  basis weight material. Gore-Tex filter



Basis Weight =  $100 \text{ gm/m}^2$  @ 90% DOP Efficiency

Figure 5-11. Downstream Side of Media (9/18/75)

→ | | ← 0.3 cm =  $1.0 \mu\text{m}$



Basis Weight =  $100 \text{ gm/m}^2$  @ 90% DOP Efficiency

Figure 5-12. Upstream Side of Media (9/18/75)



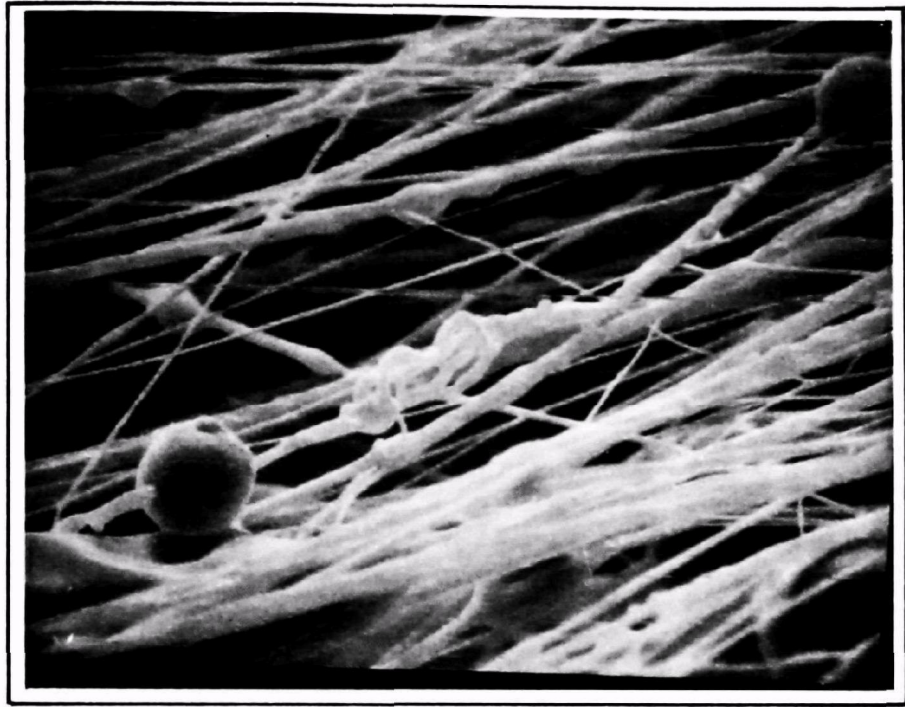
Magnification 5 K

5 mm = 1  $\mu$  m



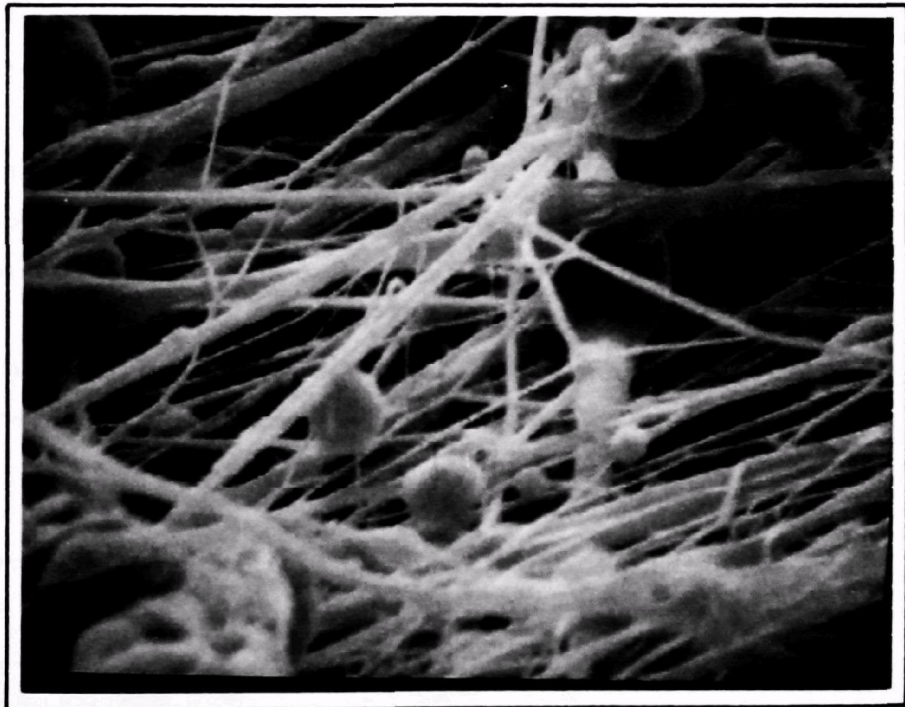
Basis Weight = 11 gm/m<sup>2</sup> for 90% DOP Efficiency

Figure 5-13. SEM Photomicrograph of Fiber Bed (1/16/76)  
(8.4 gm/m<sup>2</sup> Basis Weight)



Magnification 5 K

→ | ← 5 mm = 1  $\mu$ m



Basis Weight = 11 gm/m<sup>2</sup> for 90% DOP Efficiency

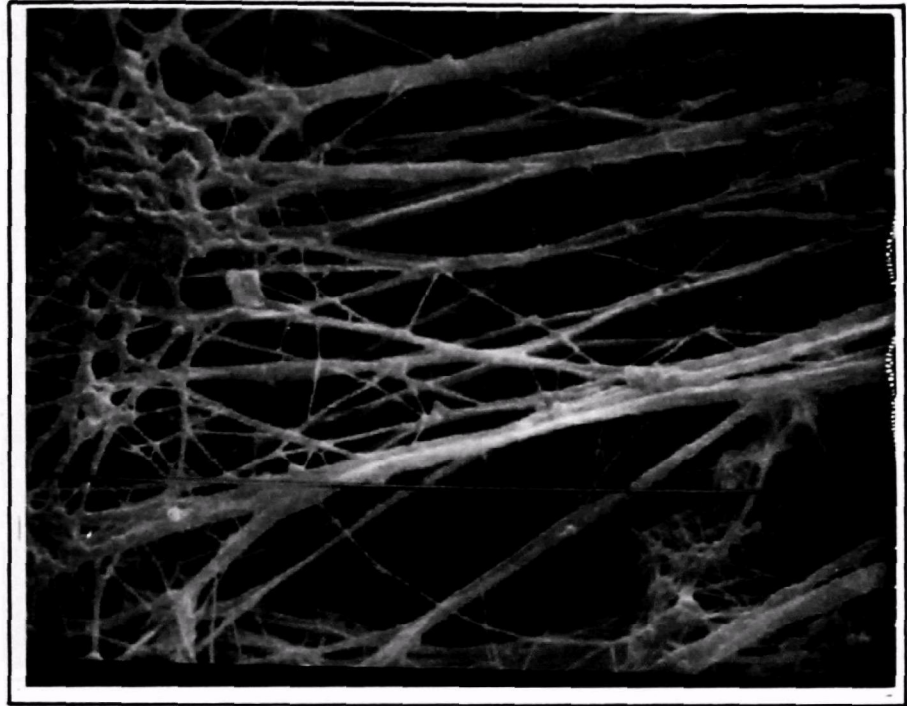
Figure 5-14. SEM Photomicrograph of Fiber Bed (1/26/76) (11.1 gm/m<sup>2</sup> Basis Weight)



material is shown in Figure 5-15 at the same magnification. These photographs reveal the extremely fine fibers present in all three materials. They also confirm the results predicted from theory for fine fiber collection. The average fiber size is  $< 1.0 \mu\text{m}$  and, as shown on Figure 5-7, filtration performance as a function of basis weight is in agreement with theory for fiber size  $< 1.0 \mu\text{m}$ . Theory predicts a fiber diameter of  $0.57 \mu\text{m}$  for a uniform bed of fibers achieving 90 percent DOP efficiency with a basis weight of  $11 \text{ gm/m}^2$ . (See Figure 4-3.)

The following media samples all had efficiencies of approximately 90 percent collection of  $0.3 \mu\text{m}$  DOP. Medium (4/10/76) had a basis weight of  $20.6 \text{ gm/m}^2$ . Medium (5/14/76) had a basis weight of  $3.9 \text{ gm/m}^2$ . Medium 5/17/76 had a basis weight of  $0.5 \text{ gm/m}^2$ . All three of these samples, produced from the same basic material, perform approximately the same (90 percent DOP efficiency). A likely explanation for their different basis weights is that there is a difference in their average fiber diameter. A series of SEM photomicrographs were made to illustrate this difference in fiber diameter. Figure 5-16, 5-17 and 5-18 were taken at 5K magnification and show the three samples in descending order of basis weight. (This should also be their descending order of average fiber diameter.) This change in fiber diameter can be seen in the photograph even though its effect is masked by the presence of some filming of material in sample (4/10/76) and the nodules seen in all the pictures. The Figures 5-19 and 5-20 were taken at 1K magnification and the difference in fiber diameter is readily apparent. Figure 5-20 shows a piece of exposed backing fiber through a small opening in the fine fiber face. Figure 5-21 was taken at 2K because the fibers were not easily seen at 1K. Figures 5-22 and 5-23 provide the best illustration of the difference. They show the largest (4/10/76) and smallest (5/17/76) basis weight (fiber diameter) material at 200X magnification. Figure 5-24 illustrates the backing material at 200X.

Figure 5-25 shows a view of the cut edge of sample (5/17/76) taken at 400X magnification. In this picture, the bottom surface is the fine fiber layer. Figure 5-26 shows the back side (inside surface) of the fine fiber layer at 5K magnification. The picture was taken through an opening in the cut edge of the sample. The calculations shown on Figure 4-3 were used to determine the average diameters shown on the SEM photomicrographs.



Magnification 5 K

→ | ← 5 mm = 1  $\mu$ m

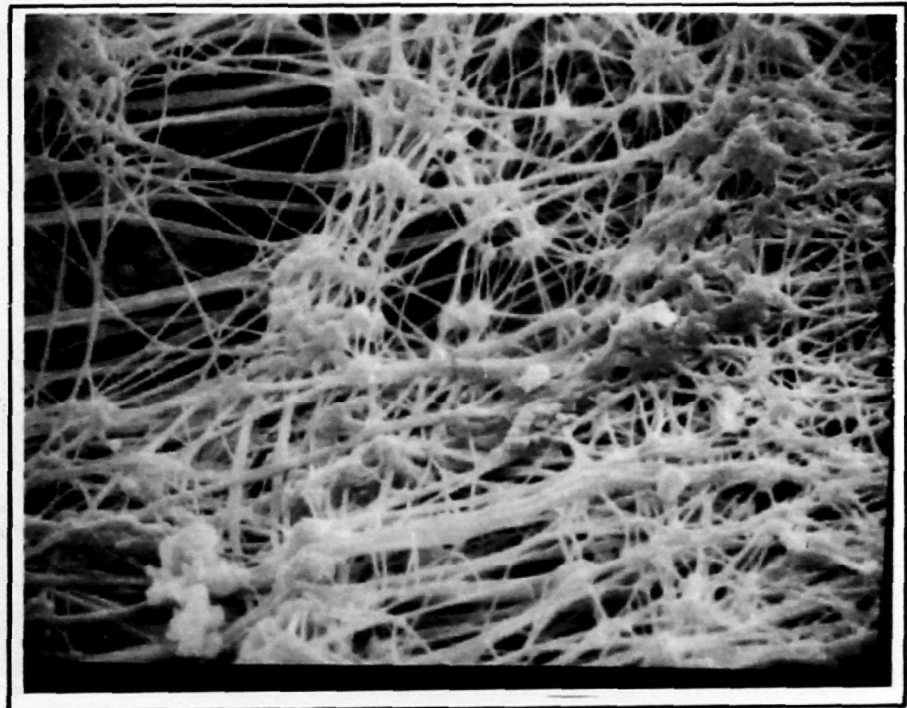


Figure 5-15. SEM Photomicrograph of Gore-Tex Filter Material

5 mm =  $1\mu$  m



Figure 5-16. 5K Photomicrograph of Media Sample (4/10/76)  
Basis Weight =  $20.6\text{ g/m}^2$   
Calculated Average Fiber Diameter =  $0.85\text{ }\mu\text{m}$

5 mm =  $1\mu$  m

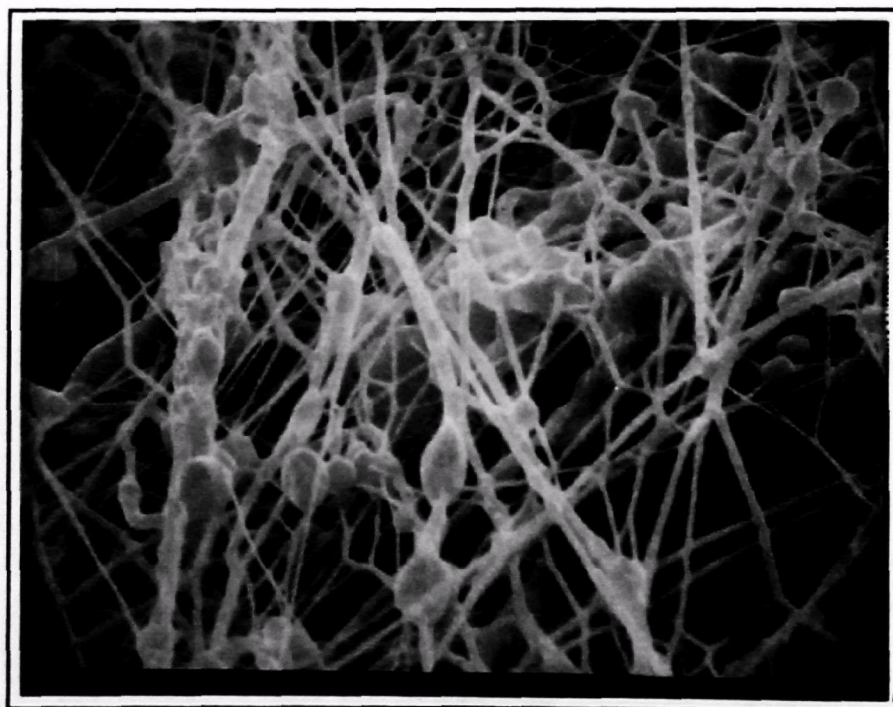


Figure 5-17. 5K Photomicrograph of Media Sample (5/14/76)  
Basis Weight =  $3.9\text{ gm/m}^2$   
Calculated Average Fiber Diameter =  $0.3\text{ }\mu\text{m}$



$\begin{array}{c} \rightarrow | | \leftarrow \\ 5 \text{ mm} = 1 \mu \text{ m} \end{array}$

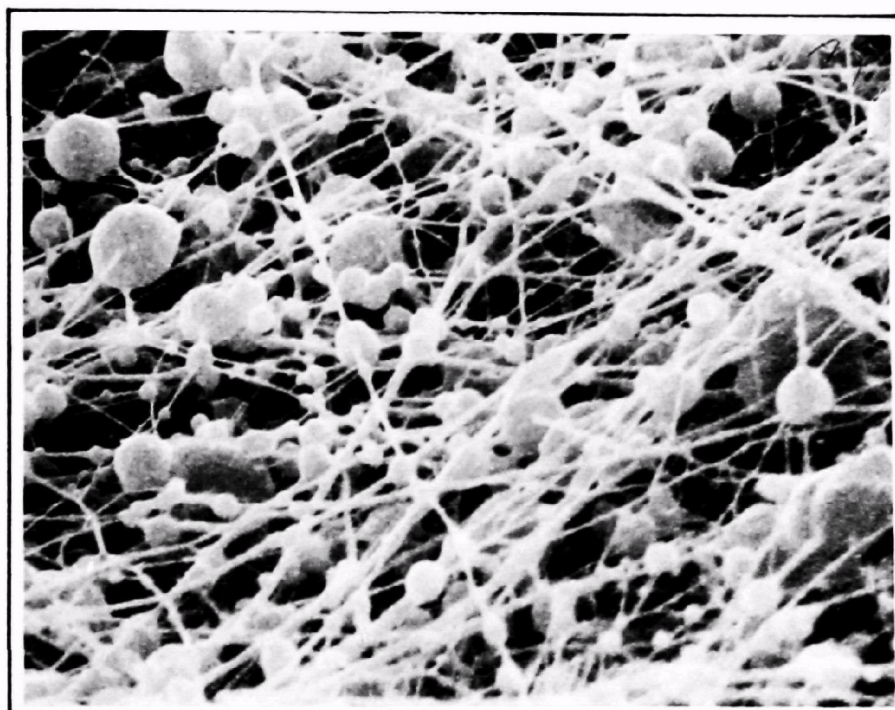


Figure 5-18. 5K Photomicrograph of Media Sample (5/17/76)  
 Basis Weight =  $0.5 \text{ gm/m}^2$   
 Calculated Average Fiber Diameter =  $0.11 \mu \text{ m}$

$1 \text{ mm} = 1 \mu \text{ m}$

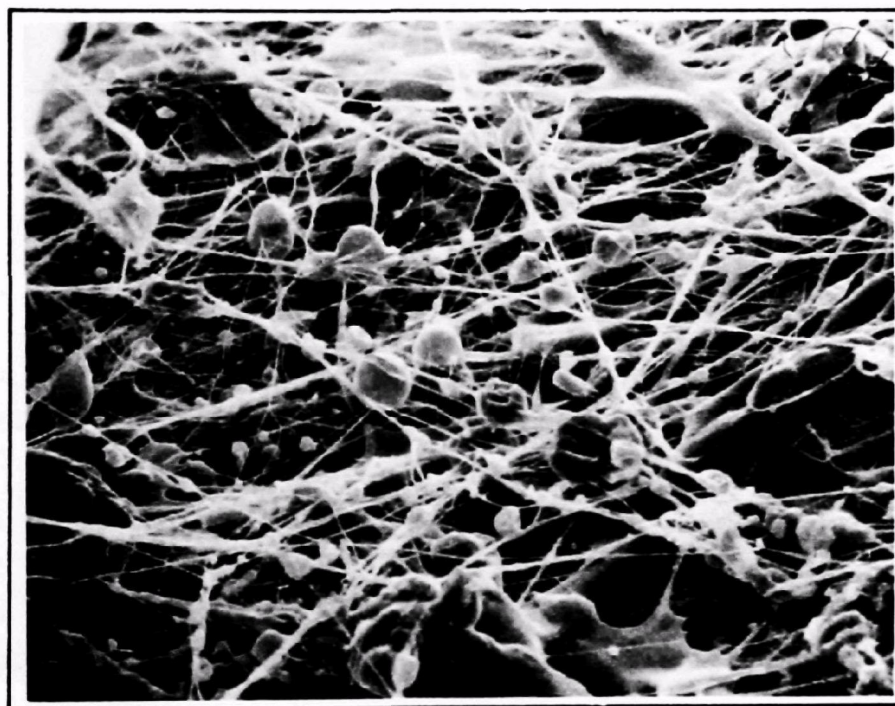


Figure 5-19. 1K Photomicrograph of Media Sample (4/10/76)  
 Basis Weight =  $20.6 \text{ gm/m}^2$   
 Calculated Average Fiber Diameter =  $0.85 \mu \text{ m}$

1 mm = 1  $\mu$  m

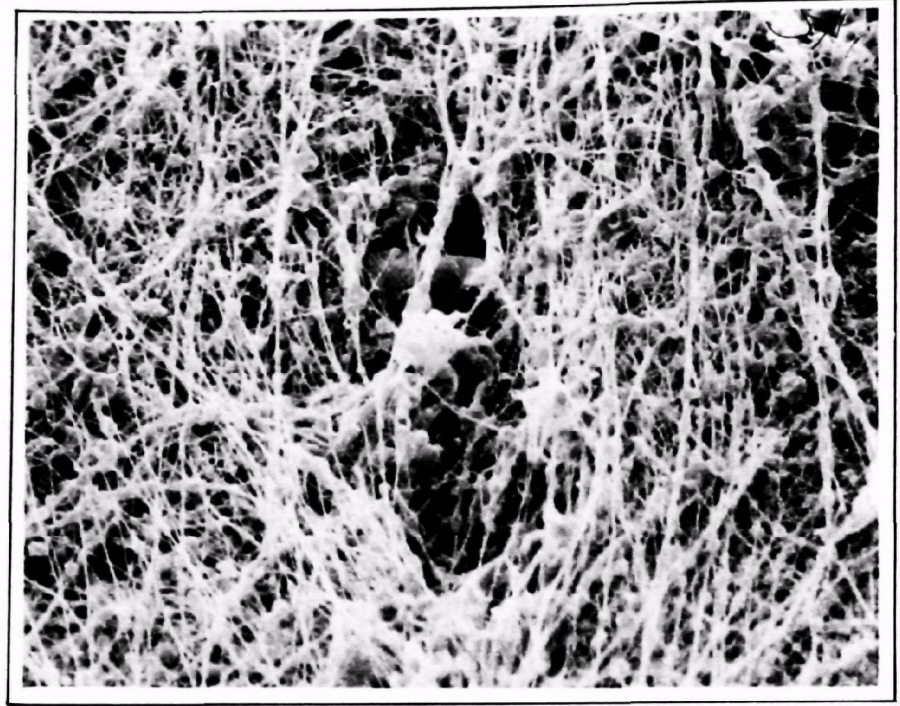


Figure 5-20. 1K Photomicrograph of Media Sample (5/14/76)  
Basis Weight = 3.9 gm/m<sup>2</sup>  
Calculated Average Fiber Diameter = 0.35  $\mu$  m

2 mm = 1  $\mu$  m



Figure 5-21. 2K Photomicrograph of Media Sample (5/17/76)  
Basis Weight = 0.5 gm/m<sup>2</sup>  
Calculated Average Fiber Diameter = 0.11  $\mu$  m



4 mm = 20  $\mu$  m

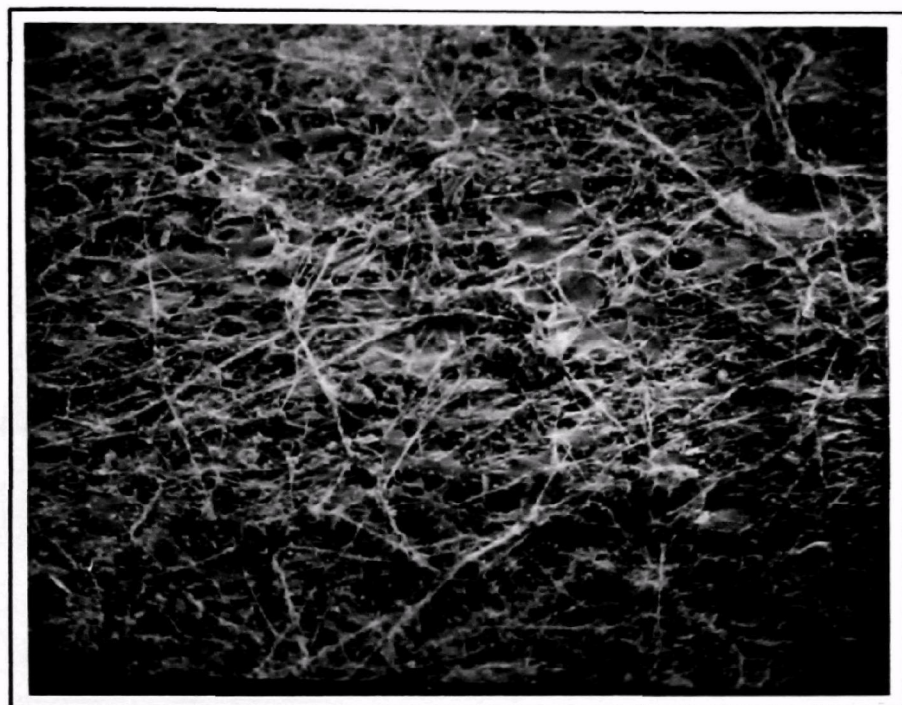


Figure 5-22 200X Photomicrograph of Media Sample  
Basis Weight = 20.6 g/m<sup>2</sup>  
Calculated Average Fiber Diameter = 0.85  $\mu$  m

4 mm = 20  $\mu$  m



Figure 5-23. 200X Photomicrograph of Media Sample  
Basis Weight = 0.5 g/m<sup>2</sup>  
Calculated Average Fiber Diameter = 0.11  $\mu$  m

4 mm = 20  $\mu\text{m}$

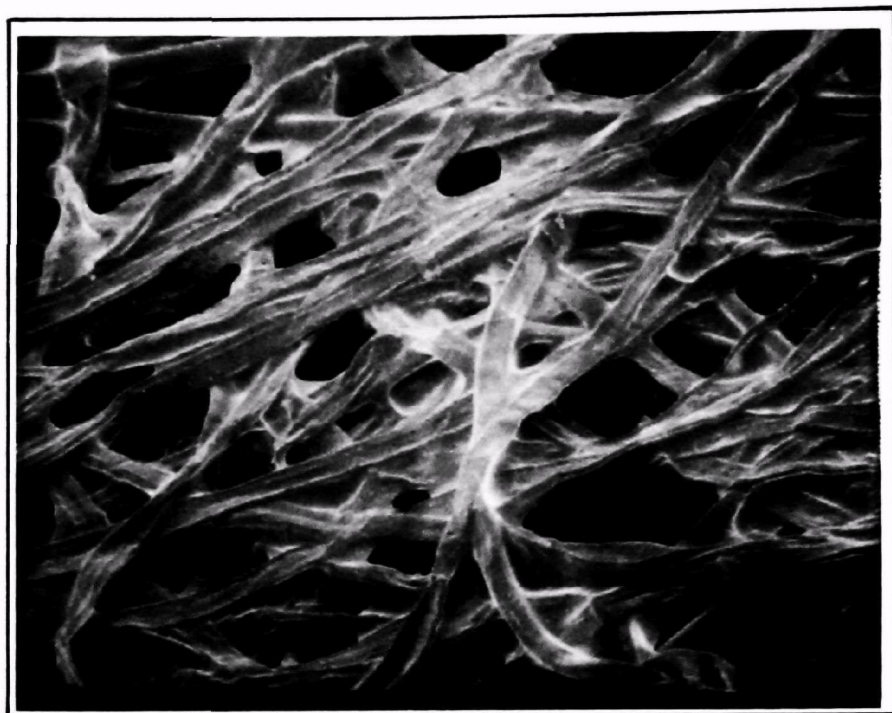


Figure 5-24. 200X Photomicrograph of Media Sample Backing

4 mm = 10  $\mu$  m

Backing Media Surface

Total Media  
Thickness  
0.14 mm

Fine Fiber Surface

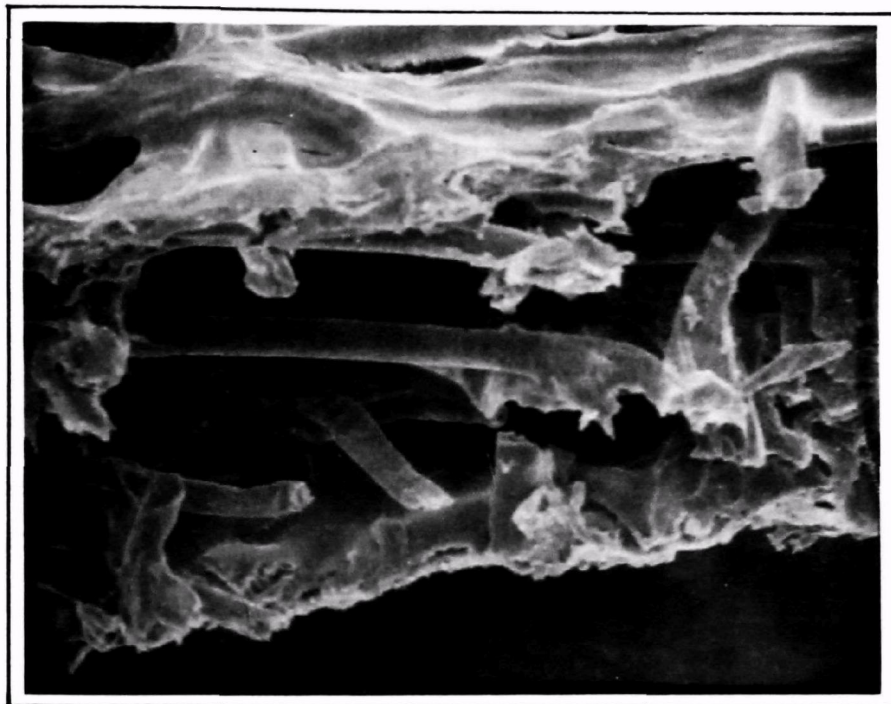


Figure 5-25. 400X Edge View of Media Sample (5/17/76)

5 mm = 1  $\mu$  m

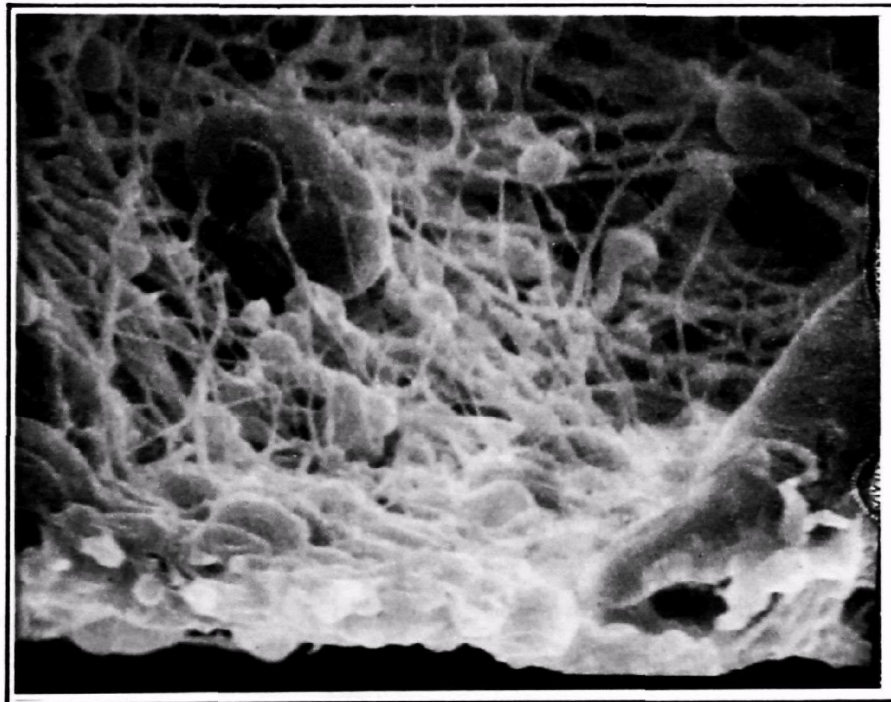


Figure 5-26. 5K Photomicrograph of Media Sample (5/17/76)  
(View of lower edge in Figure 5-25)

### 5.3 Dust Loading Tests

The third major category of Phase I tests was designed to evaluate the cleanability of various filter media by simulating pulse-jet performance. This testing was accomplished in a flat-sheet pulse jet test rig. Figure 5-27 is a simplified sketch of the apparatus. A photograph of the test set-up is shown in Figure 5-28. These dust loading tests allowed us to generate curves of pressure drop as a function of time for comparative evaluation of various media.

Initial tests were designed to establish baseline performance of standard baghouse media. These early tests were attempted at high air-to-cloth ratios in order to accelerate the tests. After the first few tests, we reduced the air-to-cloth ratio from 101.6 mm/sec to 50.8 mm/sec.

Standard AC Fine test dust was used in these tests. A particle size distribution showing the tolerance band for AC Fine test dust is included on Figure 5-29.

The following is a short description of each test conducted in the flat-sheet test rig.

#### Test No. 1

A polyester sateen medium sample was tested under the following conditions:

Air-to-Cloth Ratio	= 101.6 mm/sec
Dust Feed Concentration (AC Fine)	= 67.2 mg/m <sup>3</sup>
Cleaning Pulse Pressure	= 413.4 K Pa
Cleaning Pulse Duration	= 120 ms
Cleaning Pulse Interval	= 57 sec

Initial pressure drop across the medium was 25.4 mm H<sub>2</sub>O. The test was terminated when the pressure drop reached 254 mm H<sub>2</sub>O. Total time of the test was 21.61 minutes. Residual dust loading, the weight per unit area of dust remaining on the media sample, was 6.952 gm/m<sup>2</sup>. Overall dust loading is the weight of dust collected on the sample, plus the

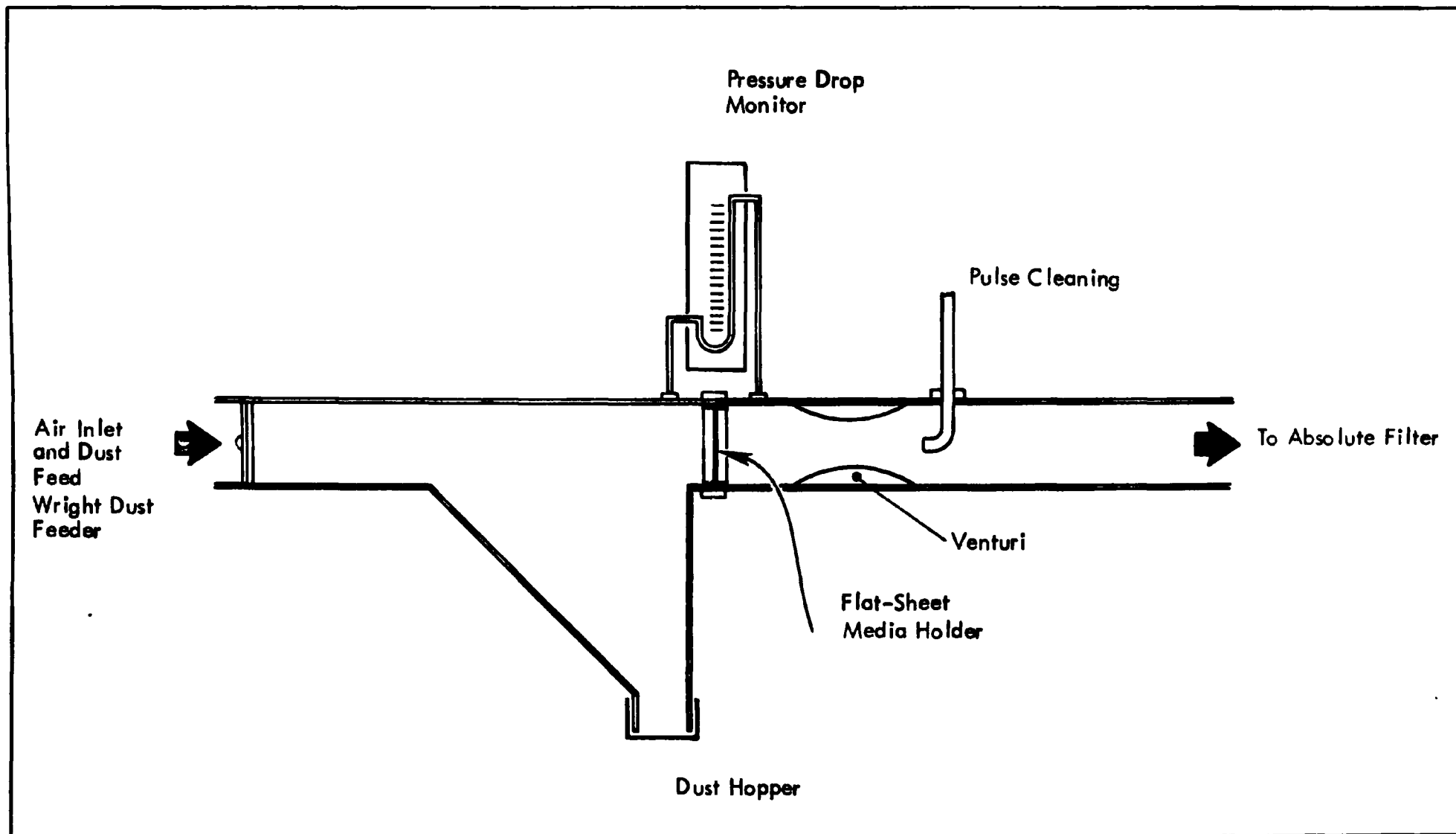


Figure 5-27. Flat Sheet Pulse Jet Test Rig



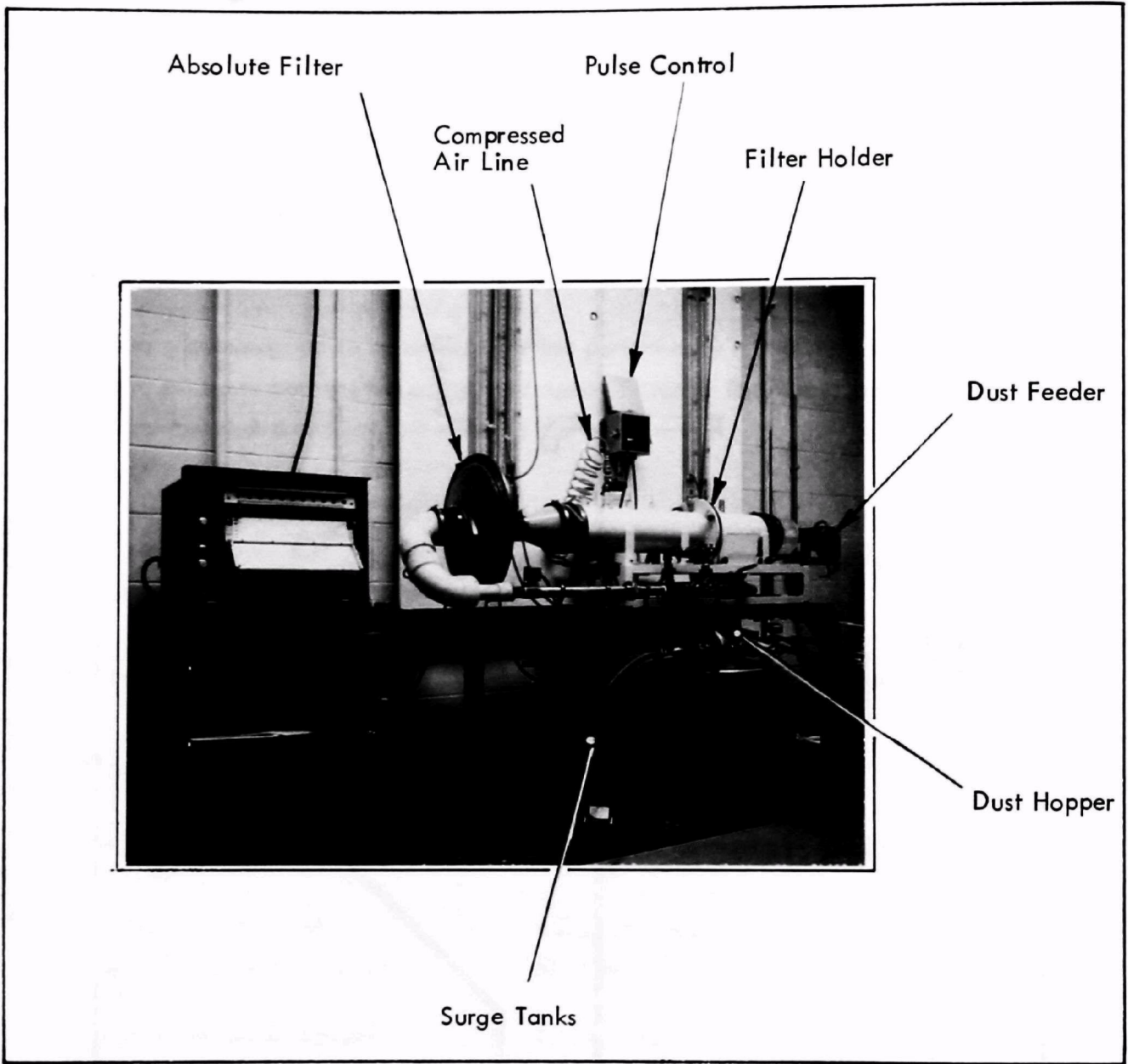


Figure 5-28. Flat-Sheet Pulse-Jet Cleaning Test Rig



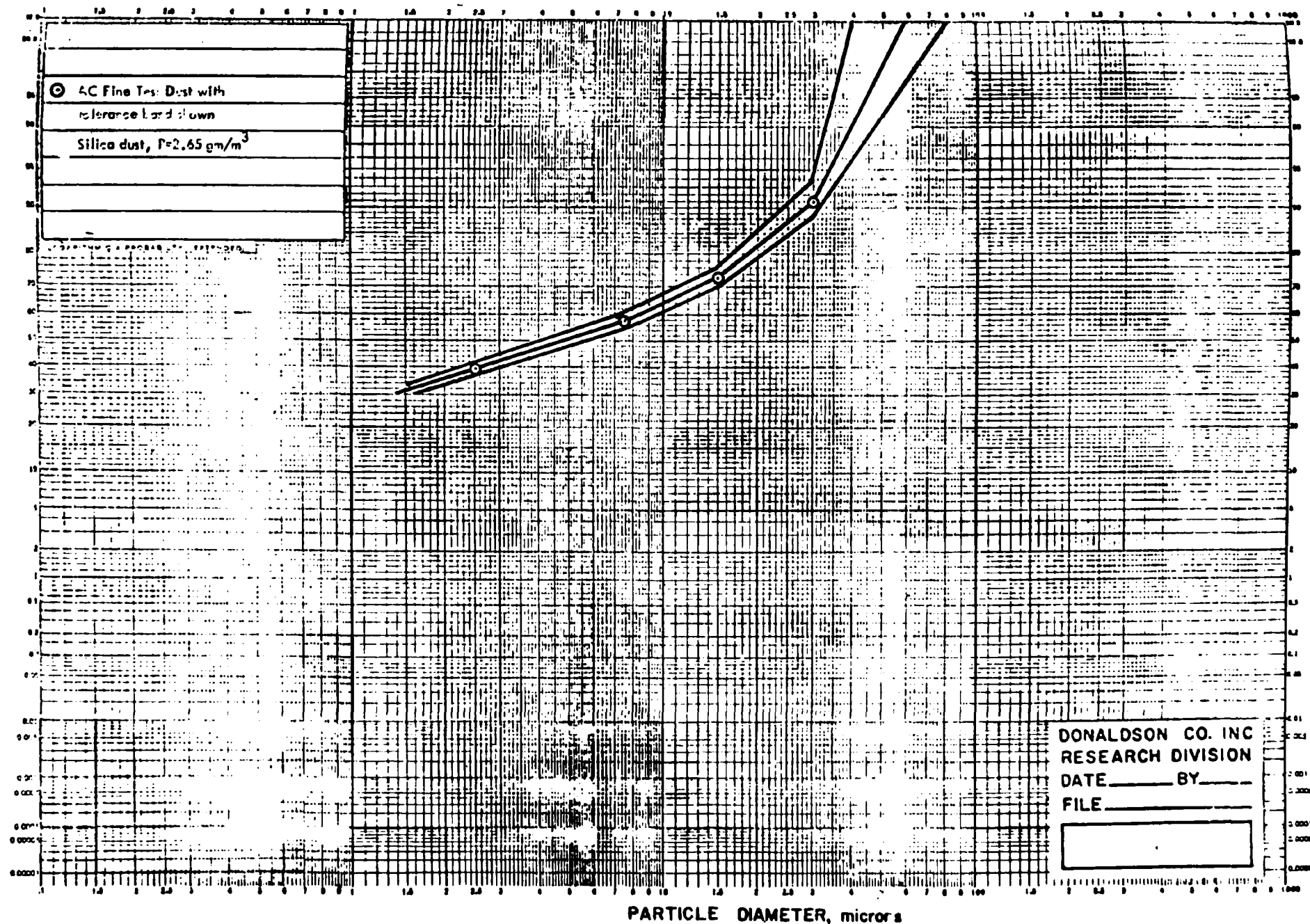


Figure 5-29. Particle Size Distribution of AC Fine Test Dust

weight of dust collected upstream of the sample. In this test, overall dust loading was  $7.856 \text{ gm/m}^2$ . Efficiency is calculated by dividing the weight of dust collected upstream (on media sample, in the hopper and upstream air ducts) by the weight collected upstream plus the weight collected on the downstream absolute (dust that passed through the test medium). For this test, efficiency was 71.1 percent. Only a small amount of dust was removed by the cleaning pulse.

### Test No. 2

Test No. 2 was intended to duplicate Test No. 1. A second polyester sateen medium sample was tested to the following;

Air-to-Cloth Ratio	=	101.6 mm/sec
Dust Feed Concentration (AC Fine)	=	$86.4 \text{ mg/m}^3$
Cleaning Pulse Pressure	=	413.4 K Pa
Cleaning Pulse Duration	=	120 ms
Cleaning Pulse Interval	=	57 sec

Initial pressure drop was 28 mm  $\text{H}_2\text{O}$ . The test was terminated when pressure drop reached 254 mm  $\text{H}_2\text{O}$ . Total time to reach this pressure drop was 21.5 minutes.

Residual Dust Loading	=	$7.029 \text{ gm/m}^2$
Overall Dust Loading	=	$8.524 \text{ gm/m}^2$
Efficiency	=	70.4 percent

Again, overall dust loading is only slightly larger than residual dust loading, indicating that most of the dust stayed on the filter medium. This test essentially repeated the performance of Test No. 1.

### Test No. 3

Donaldson Company standard medium DURALIFE<sup>®</sup> II was selected for this test under the following parameters:

---

<sup>®</sup> DURALIFE is a registered trademark of Donaldson Company, Inc., Mpls., MN 55440

Air-to-Cloth Ratio	= 101.6 mm/sec
Dust Feed Concentration (AC Fine)	= 115.2 gm/m <sup>3</sup>
Cleaning Pulse Pressure	= 413.4 K Pa
Cleaning Pulse Duration	= 120 ms
Cleaning Pulse Interval	= 57 sec

The initial pressure drop was 13 mm H<sub>2</sub>O and the test was terminated when pressure drop reached 254 mm H<sub>2</sub>O. Total time to reach this value was 107 min. During this test, cleaning pulse pressure dropped to 206.7 K Pa because the building compressed air system was not on. This caused an increase in the rate of pressure drop rise. Adjusting the cleaning pulse pressure to 519 K Pa resulted in a reduction of pressure drop of about 75 mm H<sub>2</sub>O. Returning the cleaning pulse pressure to 413 K Pa resulted in a return to the original trend line for pressure drop as a function of time. For this test:

Residual Dust Loading	= 48.8 gm/m <sup>2</sup>
Overall Dust Loading	= 63.3 gm/m <sup>2</sup>
Efficiency	= 81.7 percent

As in the earlier tests, more than half of the dust remained on the filter medium indicating poor cleaning performance.

#### Test No. 4

DURALIFE II medium was used in this test to attempt to duplicate Test No. 3. Test rig settings were:

Air-to-Cloth Ratio	= 101.6 mm/sec
Dust Feed Concentration (AC Fine)	= 67.2 gm/m <sup>3</sup>
Cleaning Pulse Pressure	= 413.4 K Pa
Cleaning Pulse Duration	= 120 ms
Cleaning Pulse Interval	= 57 sec

Initial pressure drop was about 10 mm H<sub>2</sub>O. The test was terminated after 104 minutes when pressure drop reached 254 mm H<sub>2</sub>O. During the first half of the test, the dust feeder was malfunctioning causing a low dust feed rate. After this was corrected, the pressure drop increased with time at approximately a linear rate until the end of the test.

Residual Dust Loading	= 6.34 gm/m <sup>2</sup>
Overall Dust Loading	= 45.0 gm/m <sup>2</sup>
Efficiency	= 94.37 percent

Two differences between Test No. 4 and No. 3 are the increased efficiency in Test No. 4 and the lower residual dust loading, indicating that a relatively large weight fraction of the dust fed was removed from the medium by the cleaning pulses. A reasonable explanation for these differences is that the fine dust fraction remained on the medium. This could cause both the high pressure drop for a small residual dust loading and the increased efficiency.

#### Test No. 5

Polyester sateen was used in this test at higher dust feeding rates. Test rig parameters were:

Air-to-Cloth Ratio	= 101.6 mm/sec
Dust Feed Concentration (AC Fine)	= 273.5 mg/m <sup>3</sup>
Cleaning Pulse Pressure	= 413.4 K Pa
Cleaning Pulse Duration	= 120 ms
Cleaning Pulse Interval	= 55 sec

Initial pressure drop was 25 mm H<sub>2</sub>O. A pressure drop of 254 mm H<sub>2</sub>O was reached after 6.0 minutes. With pressure drop at 254 mm H<sub>2</sub>O, the dust screw was shut off so no additional dust was fed. Two cleaning pulses did not reduce the pressure drop significantly. A solenoid-operated relief valve downstream of the absolute filter was turned on, to open when the cleaning pulse valve operated. This also had little effect on the pressure drop. Cleaning pulse pressure was then set at 551 K Pa. Pulsing at this pressure reduced the medium pressure drop by 56 mm H<sub>2</sub>O. The dust feeder injection air which had been on

during these tests without dust feed was shut off and the system pulsed at 551 K Pa. This reduced pressure drop an additional 114 mm H<sub>2</sub>O to a value of 89 mm H<sub>2</sub>O. At these settings the dust feed was started again. After 4.58 additional minutes of operation, pressure drop reached 254 mm H<sub>2</sub>O and the test was terminated. Total dust feeding time was 10.50 minutes.

Residual Dust Loading	= 10.16 gm/m <sup>3</sup>
Overall Dust Loading	= 15.82 gm/m <sup>3</sup>
Efficiency	= 89.87 percent

#### Test No. 6

A polyester sateen medium sample was installed in the test rig at the following settings:

Air-to-Cloth Ratio	= 101.6 mm/sec
Dust Feed Concentration (AC Fine)	= 247.6 mg/m <sup>3</sup>
Cleaning Pulse Pressure	= 551.2 K Pa
Cleaning Pulse Duration	= 120 ms
Cleaning Pulse Interval	= 55 sec

The downstream solenoid-operated relief valve was connected to operate with the cleaning pulse solenoid for this test. Full scale pressure drop of 254 mm H<sub>2</sub>O was reached in 5.5 minutes. At this time the dust feed and dust feeder air were shut off and the cleaning pulses allowed to continue. After 10 pulses, the medium pressure drop was reduced only 16 mm H<sub>2</sub>O. In order to examine the effects of different cleaning pulse pressure settings, only the filter medium was removed for the next test. Residual dust loading from Test No. 6 was 7.82 gm/m<sup>2</sup>. The efficiency and overall dust loading were not determined.

#### Test No. 7

Test conditions for Test No. 7 were the same as for No. 6 except that the cleaning pulse pressure was cut in half to 275.6 K Pa. Test rig settings for the polyester sateen medium were:

Air-to-Cloth Ratio	= 101.6 mm/sec
Dust Feed Concentration (AC Fine)	= 247.6 mg/m <sup>3</sup>
Cleaning Pulse Pressure	= 275.6 K Pa
Cleaning Pulse Duration	= 120 ms
Cleaning Pulse Interval	= 55 sec

With the solenoid relief valve in operation, it took 4.0 minutes to reach 254 mm H<sub>2</sub>O pressure drop. Dust feed and dust feeder air were shut off and the 275.6 K Pa pulse allowed to continue. This did not reduce the pressure drop. Increasing the cleaning pressure to 413.4 K Pa had little effect on the pressure drop. When the cleaning pressure was increased to 551.2 K Pa, the pressure drop across the media was reduced by 86 mm H<sub>2</sub>O. Residual dust loading was 6.12 gm/m<sup>2</sup>.

#### Test No. 8

A new sheet of polyester sateen was installed with the test rig settings as follows:

Air-to-Cloth Ratio	= 101.6 mm/sec
Dust Feed Concentration (AC Fine)	= 247.6 mg/m <sup>3</sup>
Cleaning Pulse Pressure	= 413.4 K Pa
Cleaning Pulse Duration	= 120 ms
Cleaning Pulse Interval	= 25 sec

Pressure drop was allowed to rise to 254 mm H<sub>2</sub>O without pulsing. This occurred after 7.25 minutes. Dust feed and dust feeder air were turned off for pulsing. Pulsing at 413.4 K Pa reduced pressure drop to 226 mm H<sub>2</sub>O. Pulsing at 551.2 K Pa further reduced pressure drop to 74 mm H<sub>2</sub>O. Pulse pressure was increased to 620 K Pa and additional pulsing at this pressure lowered pressure drop to 47 mm H<sub>2</sub>O. Dust was fed again with no pulsing until a pressure drop of 254 mm H<sub>2</sub>O was reached. This took 4.55 min. Pulsing without dust feed at 620 K Pa lowered pressure drop to 57 mm H<sub>2</sub>O. This sequence of feeding dust and then cleaning was continued to the end of the test. Cleaning-down pressure drop as a function of time is shown in the following chart:

Cumulative Dust Feeding Time (min)	Cleaned Down Pressure Drop (mm H <sub>2</sub> O)
7.25	47
11.80	57
15.71	76
18.71	89
21.99	127
24.0	162
25.76	185
27.56	188
28.67	198
29.67	203
30.35	215
30.7	227
*	235

\* The last clean-down sequence was performed with the pulse interval shortened to one pulse every 5 seconds rather than one every 25 seconds. This did not result in any apparent improvement.

The time presented is the cumulative total dust feeding time. Between each cleaning cycle the pressure drop was allowed to rise to 254 mm H<sub>2</sub>O. Residual dust loading was 16.5 gm/m<sup>2</sup>.

The same absolute filters were used for Tests 6, 7 and 8, so no efficiency data was collected. Dust concentration was averaged for all three tests.

#### Test No. 9

For Test No. 9, the air-to-cloth ratio of the polyester sateen medium was reduced. The following test rig settings were used:

Air-to-Cloth Ratio	= 50.8 mm/sec
Dust Feed Concentration (AC Fine)	= 513.5 mg/m <sup>3</sup>
Cleaning Pulse Pressure	= 551.2 K Pa
Cleaning Pulse Duration	= 120 ms
Cleaning Pulse Interval	= 54 sec

The solenoid-operated relief valve was not used in this test. Pulsing took place at intervals while dust feeding. Maximum pressure drop of 254 mm H<sub>2</sub>O was reached after 108.16 minutes.

Residual Dust Loading	= 59.2 gm/m <sup>2</sup>
Overall Dust Loading	= 167.2 gm/m <sup>2</sup>
Efficiency	= 98.66 percent

At this lower air-to-cloth ratio some improvement in both efficiency and cleaning was noted.

#### Test No. 10

Dust feed concentration was reduced to the polyester sateen medium for Test No. 10. The test rig settings were as follows:

Air-to-Cloth Ratio	= 50.8 mm/sec
Dust Feed Concentration (AC Fine)	= 259.1 mg/m <sup>3</sup>
Cleaning Pulse Pressure	= 551.2 K Pa
Cleaning Pulse Duration	= 120 ms
Cleaning Pulse Interval	= 54 sec

A total of 288 minutes was required to reach a pressure drop of 254 mm H<sub>2</sub>O across the medium.

Residual Dust Loading	= 61.1 gm/m <sup>2</sup>
Overall Dust Loading	= 223.3 gm/m <sup>2</sup>
Efficiency	= 98.13 percent



This test produced expected results based on performance from Test No. 9.

#### Test No. 11

This test was intended to duplicate Test No. 10; however, the dust feeder malfunctioned during the test and the test was abandoned.

#### Test No. 12

A polyester sateen medium was tested with test rig settings as follows:

Air-to-Cloth Ratio	= 50.8 mm/sec
Dust Feed Concentration (AC Fine)	= 327.2 mg/m <sup>3</sup>
Cleaning Pulse Pressure	= 551.2 K Pa
Cleaning Pulse Duration	= 120 ms
Cleaning Pulse Interval	= 53 sec

Maximum pressure drop of 254 mm H<sub>2</sub>O was reached after 317.25 minutes.

Residual Dust Loading	= 65.4 gm/m <sup>2</sup>
Overall Dust Loading	= 311.8 gm/m <sup>2</sup>
Efficiency	= 98.52 percent

Overall dust loading included dust that was lying in the ducts upstream of the filter media holder. This had not been included in previous tests. This additional dust plus the increased time required to reach 254 mm H<sub>2</sub>O pressure drop contributed to the increased overall dust loading from this test.

#### Test No. 13

Polyester sateen was tested again at the following test rig settings:

Air-to-Cloth Ratio	= 50.8 mm/sec
Dust Feed Concentration (AC Fine)	= 484.7 mg/m <sup>3</sup>

Cleaning Pulse Pressure	= 551.2 K Pa
Cleaning Pulse Duration	= 120 ms
Cleaning Pulse Interval	= 53 sec

Maximum pressure drop of 254 mm H<sub>2</sub>O was reached after 435.16 minutes of dust feeding.

Residual Dust Loading	= 82.1 gm/m <sup>2</sup>
Overall Dust Loading	= 642.2 gm/m <sup>2</sup>
Efficiency	= 99.75 percent

Several leaks in the test rig were discovered and repaired during the course of this test. These repairs are possibly the reason for improved performance.

#### Test No. 14

The pulse duration was shortened for this test. A polyester sateen medium sample was used with test rig settings as follows:

Air-to-Cloth Ratio	= 45 mm/sec
Dust Feed Concentration (AC Fine)	= 389.7 mg/m <sup>3</sup>
Cleaning Pulse Pressure	= 551.2 K Pa
Cleaning Pulse Duration	= 40 ms
Cleaning Pulse Interval	= 53.5 sec

Full scale pressure drop of 254 mm H<sub>2</sub>O was reached after 40.43 minutes of operation.

Residual Dust Loading	= 35.2 gm/m <sup>2</sup>
Overall Dust Loading	= 46.3 gm/m <sup>2</sup>
Efficiency	= 96.39 percent

Reducing the pulse duration lowered efficiency as well as life.

### Test No. 15

This test was abandoned because the dust feeder introduced a slug of dust which caused a jump in pressure drop and settled out in the feeder tube.

### Test No. 16

Prior to running this test, additional small leaks in the test rig were discovered and eliminated. Also, the compressed airline delivering cleaning air to the solenoid valve was replaced with a larger tube to ensure that maximum cleaning flow is delivered during the cleaning pulse. A polyester sateen sample was installed and tested with the following test rig settings:

Air-to-Cloth Ratio	= 45 mm/sec
Dust Feed Concentration (AC Fine)	= 604.6 mg/m <sup>3</sup>
Cleaning Pulse Pressure	= 551.2 K Pa
Cleaning Pulse Duration	= 120 ms
Cleaning Pulse Interval	= 53.5 sec

The test was terminated when pressure drop reached 254 mm H<sub>2</sub>O after 751 minutes.

During the test, dust was deposited in various parts of the system. For this test:

5.12952	gm collected in 25 mm dia feed tube
<u>8.03000</u>	gm collected in 150 mm dia tube
13.15952	gm total drop-out
9.509	gm collected from the upstream hopper
0.76023	gm collected on test medium
<u>2.00596</u>	gm collected on downstream absolute
12.27519	gm dust fed out including drop-out dust

Ignoring the drop-out dust:

Residual Dust Loading	= 45.4 gm/m <sup>2</sup>
Overall Dust Loading	= 613 gm/m <sup>2</sup>
Efficiency	= 83.65 percent
Dust Feed Concentration (AC Fine)	= 1165.4 mg/m <sup>3</sup>

Including the drop-out dust:

Residual Dust Loading	= 45.4 gm/m <sup>2</sup>
Overall Dust Loading	= 1398.7 gm/m <sup>2</sup>
Efficiency	= 92.11 percent
Dust Feed Concentration (AC Fine)	= 2224.8 mg/m <sup>3</sup>
Test filter media area is	= 0.01675 m <sup>2</sup>

Previous test calculations have included the drop-out dust.

It is likely that the dust we have termed drop-out dust has settled in the tubes because of the low air velocity there. However, there is a possibility that some of it has been blown back by the cleaning pulse. A Coulter Counter analysis of samples taken from the 25 mm dia feed tube, from the 150 mm dia tube and from the hopper is presented in Figure 5-30. This analysis shows that the drop-out dust tends to be a larger size fraction than that which is collected in the hopper. In any case, the dust being collected by the test filter media has a particle size distribution finer than AC Fine.

A plot of pressure drop across the test filter medium as a function of time is shown in Figure 5-31. This curve shows the large difference between maximum pressure drop and cleaned-down pressure drop. We have concluded the test when maximum pressure drop reaches 254 mm H<sub>2</sub>O. Using this definition for filter life, the length of the test is a function of the dust feed rate since if the dust feed rate were reduced, the spread between cleaned-down pressure drop and maximum pressure drop would also be reduced because of the fixed time between these two extremes with each cleaning pulse.

% LESS THAN STATED SIZE

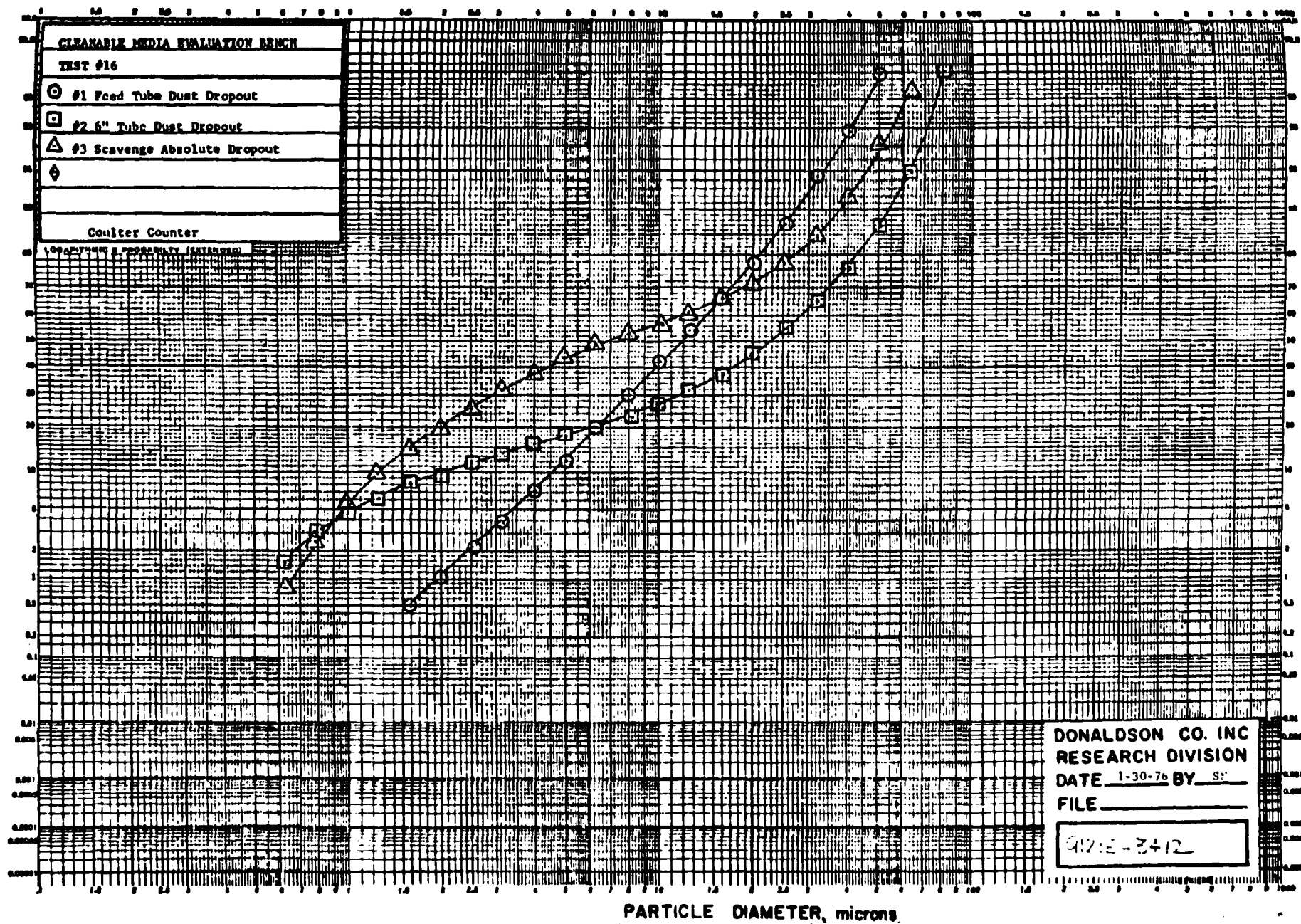


Figure 5-30. Media Cleanability Evaluation

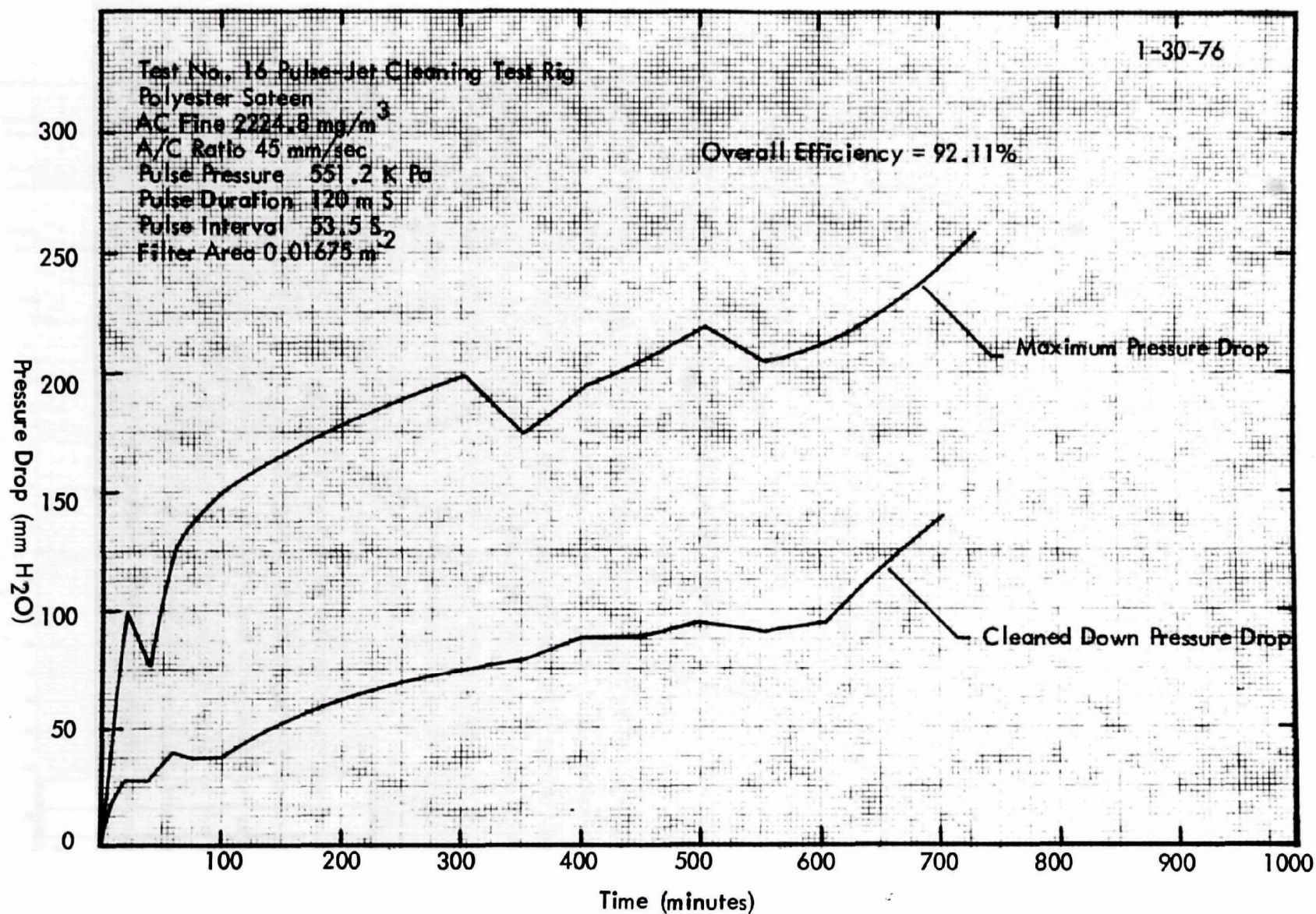


Figure 5-31. Pressure Drop as a Function of Time

### Test No. 17

A polyester sateen medium was tested under the following conditions:

Air-to-Cloth Ratio	= 50.8 mm/sec
Dust Feed Concentration (AC Fine)	= 716 mg/m <sup>3</sup>
Cleaning Pulse Pressure	= 551 K Pa
Cleaning Pulse Duration	= 120 ms
Cleaning Pulse Interval	= 55 sec

Initial pressure drop was 19 mm H<sub>2</sub>O. The test was terminated when pressure drop reached 254 mm H<sub>2</sub>O. Total time to reach this pressure drop was 188.58 minutes. Residual dust loading, the weight per unit area of dust remaining on the media sample, was 29.8 gm/m<sup>2</sup>. Overall dust loading is the weight of dust collected on the sample, plus the weight of dust collected upstream of the sample. In this test, overall dust loading was 391.4 gm/m<sup>2</sup>. Efficiency is calculated by dividing the weight of dust collected upstream (on media sample, in the hopper and upstream air ducts) by the weight collected on the downstream absolute (dust that passed through the test medium). For this test, efficiency was 95.1 percent.

### Test No. 18

A polyester sateen medium sample was tested with the following test rig settings:

Air-to-Cloth Ratio	= 50.8 mm/sec
Dust Feed Concentration (AC Fine)	= 710.6 mg/m <sup>3</sup>
Cleaning Pulse Pressure	= 551.2 K Pa
Cleaning Pulse Duration	= 120 ms
Cleaning Pulse Interval	= 55 sec

Initial pressure drop was 13 mm H<sub>2</sub>O. Maximum pressure drop of 254 mm H<sub>2</sub>O was reached after 366.25 minutes of operation.

Residual Dust Loading	= 44.0 gm/m <sup>2</sup>
Overall Dust Loading	= 741.0 gm/m <sup>2</sup>
Efficiency	= 93.42 percent

#### Test No. 19

A polyester sateen medium was tested at the following test rig settings:

Air-to-Cloth Ratio	= 50.8 mm/sec
Dust Feed Concentration (AC Fine)	= 741.3 mg/m <sup>3</sup>
Cleaning Pulse Pressure	= 551.2 K Pa
Cleaning Pulse Duration	= 120 ms
Cleaning Pulse Interval	= 55 sec

Initial pressure drop was 19 mm H<sub>2</sub>O. Maximum pressure drop of 254 mm H<sub>2</sub>O was reached after 289 minutes.

Residual Dust Loading	= 34.9 gm/m <sup>2</sup>
Overall Dust Loading	= 592.7 gm/m <sup>2</sup>
Efficiency	= 94.05 percent

#### Test No. 20

For this test, a felted dacron medium sample was used in the test rig with the following test settings:

Air-to-Cloth Ratio	= 50.8 mm/sec
Dust Feed Concentration (AC Fine)	= 734.5 mg/m <sup>3</sup>
Cleaning Pulse Pressure	= 551.2 K Pa
Cleaning Pulse Duration	= 120 ms
Cleaning Pulse Interval	= 55 sec



Initial pressure drop was 2.5 mm H<sub>2</sub>O. The test was terminated after 2117 minutes (35.28 hours) because it appeared that the test could last for many more hours without adding to our knowledge of its loading characteristics. Final pressure drop, just prior to a cleaning pulse, was 123 mm H<sub>2</sub>O.

Residual Dust Loading	= 94.9 gm/m <sup>2</sup>
Overall Dust Loading	= 4732 gm/m <sup>3</sup>
Efficiency	= 99.85 percent

As expected, this test shows that felt at these relatively high air-to-cloth ratios and in the pulse-jet cleaning mode performs better than polyester sateen.

#### Test No. 21

A felted dacron medium sample was again used in the test rig with the following test rig settings:

Air-to-Cloth Ratio	= 50.8 mm/sec
Dust Feed Concentration (AC Fine)	= 475.4 mg/m <sup>3</sup>
Cleaning Pulse Pressure	= 551.2 K Pa
Cleaning Pulse Duration	= 120 ms
Cleaning Pulse Interval	= 55 sec

Initial pressure drop was 3.8 mm H<sub>2</sub>O. The test was terminated after 2271.6 minutes (37.86 hours). Final pressure drop was 66 mm H<sub>2</sub>O.

Residual Dust Loading	= 115.4 gm/m <sup>2</sup>
Overall Dust Loading	= 3278 gm/m <sup>2</sup>
Efficiency	= 99.59 percent

Tests No. 20 and No. 21 produced similar results except that the lower dust feeding rate in Test No. 21 resulted in lower operating pressure drop.

## Test No. 22

This was the first test in which a sample of the experimental media was used. A fine fiber having a basis weight of  $11.1 \text{ gm/m}^2$  was tested. The following test rig settings were used.

Air-to-Cloth Ratio	=	50.8 mm/sec
Dust Feed Concentration (AC Fine)	=	$429.0 \text{ mg/m}^3$
Cleaning Pulse Pressure	=	551.2 K Pa
Cleaning Pulse Duration	=	120 ms
Cleaning Pulse Interval	=	55 sec

This medium has a collection efficiency of 95 percent when tested with DOP particles. The initial pressure drop was  $87.6 \text{ mm H}_2\text{O}$ . Pressure drop reached  $254 \text{ mm H}_2\text{O}$  after 1972.2 minutes (32.87 hours), at which time the test was terminated.

Residual Dust Loading	=	$12.74 \text{ gm/m}^2$
Overall Dust Loading	=	$2578.6 \text{ gm/m}^2$
Efficiency	=	99.9997 percent

We feel the relatively high initial pressure drop was caused by the low permeability of this medium; however, other factors may have been involved. After this test, there was a 10 mm wide band across the medium sample which appeared cleaner than the rest of the sample. If this strip was not passing air, this could have contributed to the pressure drop. The low residual dust loading indicates that cleaning was good. The downstream absolute filter gained only 0.00011 gm of dust which resulted in the very high efficiency shown above.

## Operating Pressure Drop Curve

Figure 5-32 shows operating pressure drop as a function of time for polyester sateen (Test No. 18), felted dacron (Test No. 21), and for the fine fiber sample (1/26/76) with basis weight  $11.1 \text{ gm/m}^2$  (Test No. 22). Operating pressure drop in this curve is the pressure drop just prior to a cleaning pulse.

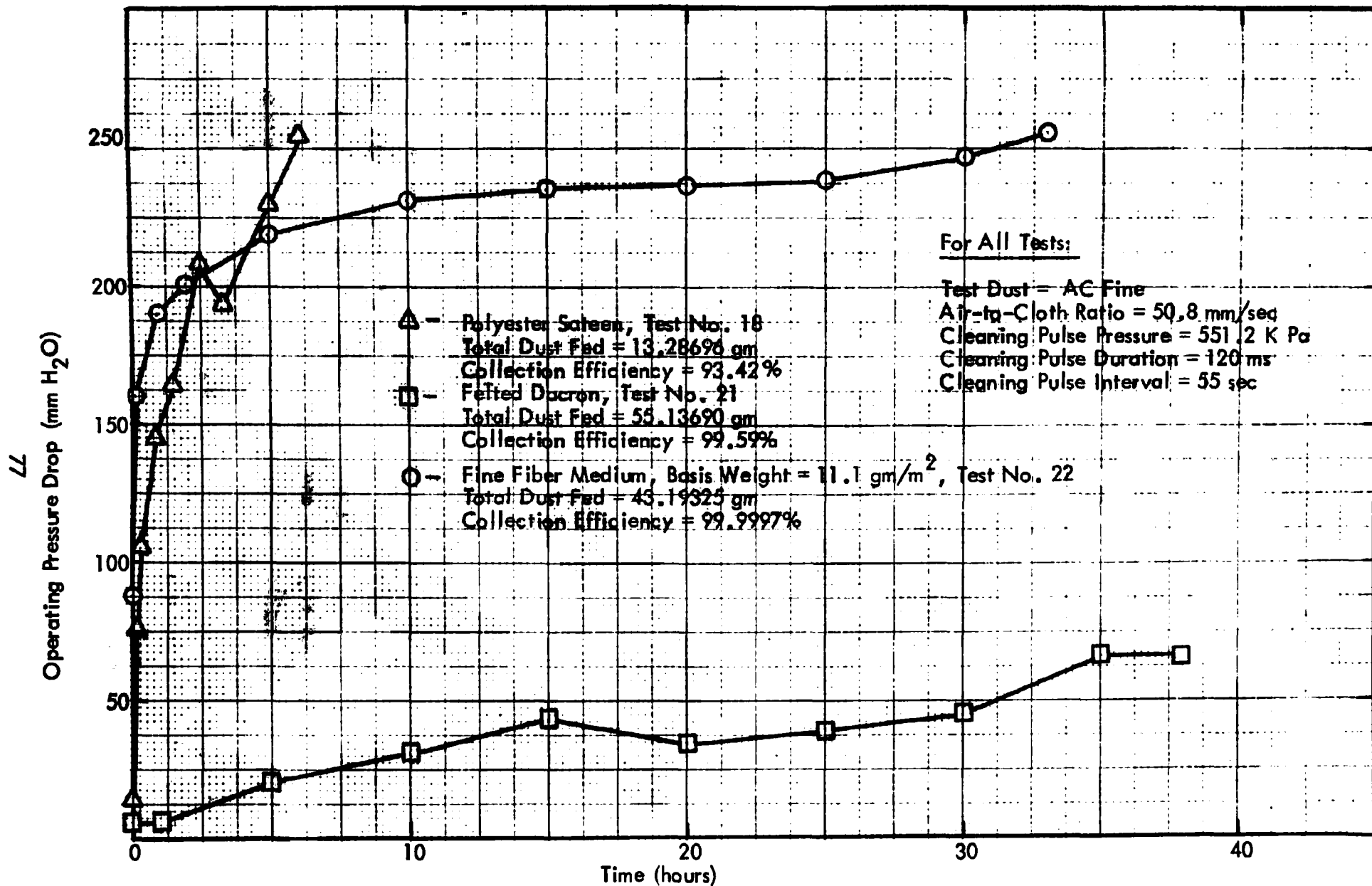


Figure 5-32. Operating Pressure Drop As a Function of Time

### Test No. 23

An experimental fine fiber medium (type 1/26/76) was tested. It had a basis weight of fine fibers of  $8.4 \text{ gm/m}^2$ . The following flat-sheet pulse-jet cleaning test rig settings were used:

Air-to-Cloth Ratio	= 50.8 mm/sec
Dust Feed Concentration (AC Fine)	= $706.5 \text{ mg/m}^3$
Cleaning Pulse Pressure	= 551.2 K Pa
Cleaning Pulse Duration	= 120 ms
Cleaning Pulse Interval	= 55 sec

The test was terminated after 51.43 hours. Pressure drop was  $72.4 \text{ mm H}_2\text{O}$  at the end of the test.

Residual Dust Loading	= $17.72 \text{ gm/m}^2$
Overall Dust Loading	= $6644.8 \text{ gm/m}^2$
Efficiency	= 99.9948 percent

DOP efficiency for this material was 75 percent at the test airflow velocity. Figure 5-33 shows a plot of pressure drop as a function of time for this test.

### Test No. 24

An experimental media was tested. The backing for this medium consisted of a 3 denier felt needle punched to a  $10 \times 10$  scrim. Two layers of fine fibers produced (9/18/75) were attached to the backing by sonic welding in a 2.5 cm square grid pattern. This sample was tested for DOP efficiency and was 90 percent efficient in the collection of DOP smoke. The following flat-sheet pulse jet cleaning test rig settings were used:

Air-to-Cloth Ratio	= 50.8 mm/sec
Dust Feed Concentration (AC Fine)	= $610.6 \text{ mg/m}^3$
Cleaning Pulse Pressure	= 551.2 K Pa

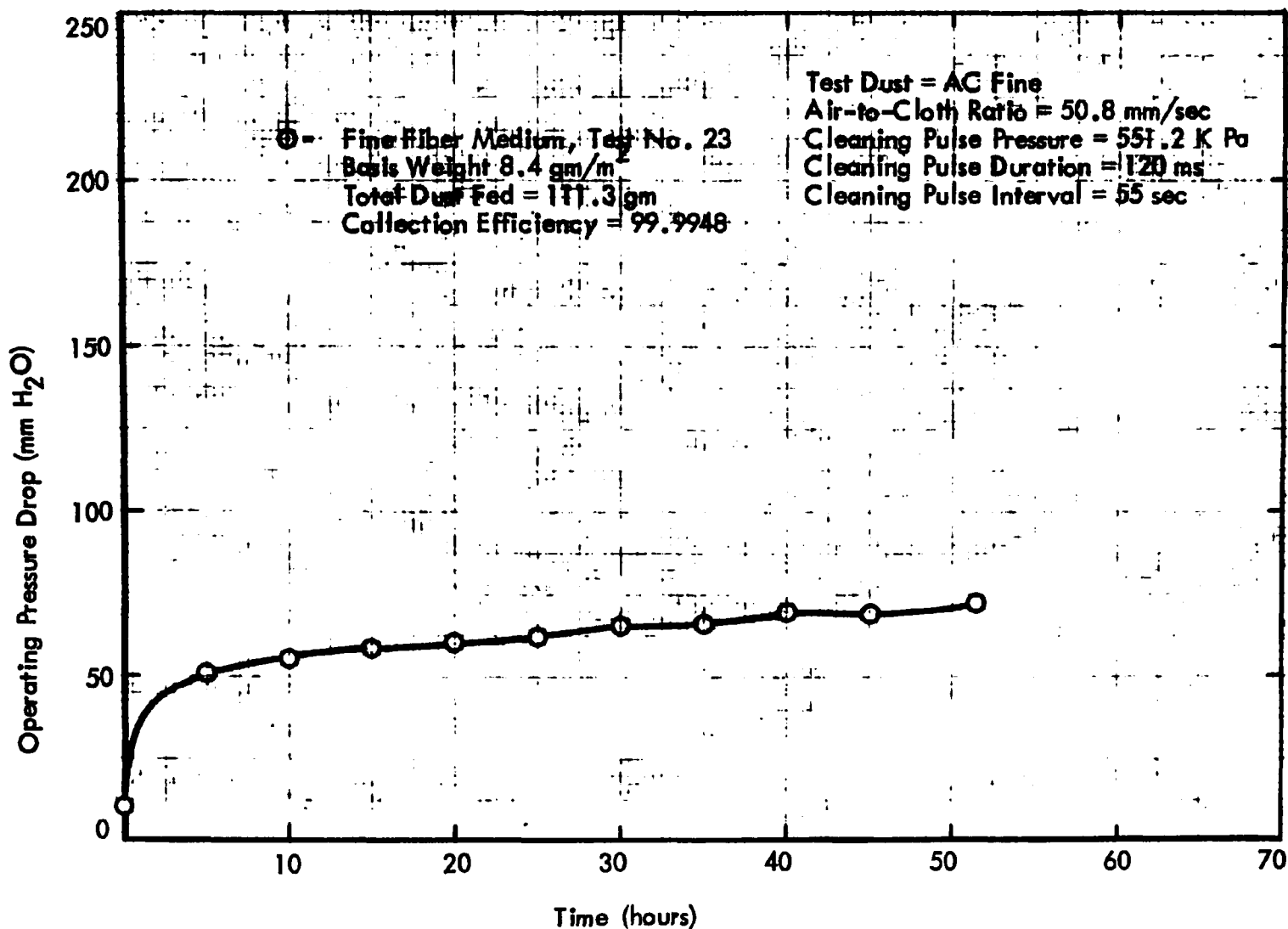


Figure 5-33. Operating Pressure Drop As A Function of Time

Cleaning Pulse Duration	= 120 ms
Cleaning Pulse Interval	= 55 sec

The test was terminated after 44.77 hours. Pressure drop was 124.5 mm H<sub>2</sub>O at the end of the test.

Residual Dust Loading*	= 251.6 gm/m <sup>2</sup>
Overall Dust Loading	= 4998.3 gm/m <sup>2</sup>
Efficiency	= 99.9998 percent

\*Note that the residual dust loading is higher than in previous tests. This was caused by an error in mounting the test sample in the test rig. The sample was installed backwards resulting in the fine fiber side being downstream. Figure 5-34 presents a plot of pressure drop as a function of time. The more rapid pressure drop rate of rise was probably caused by loading of the exposed felt side.

#### Test No. 25

An experimental medium designated as No. 9A was tested. It consisted of a 3 denier felt with one layer of fine fibers (9/18/75) needled to the felt at 200 ppsi. Between these two layers was a 10 x 10 scrim. One additional layer of fine fibers (9/18/75) was placed over the needled fine fiber layer and secured to it with Scotch SPRA-Mount artist adhesive (Cat. No. 6065). The following flat-sheet pulse-jet cleaning test rig settings were used:

Air-to-Cloth Ratio	= 50.8 mm/sec
Dust Feed Concentration (AC Fine)	= 593.3 mg/m <sup>3</sup>
Cleaning Pulse Pressure	= 551.2 K Pa
Cleaning Pulse Duration	= 120 ms
Cleaning Pulse Interval	= 55 sec

This test was terminated after 37.45 hours when pressure drop was 68.6 mm H<sub>2</sub>O.

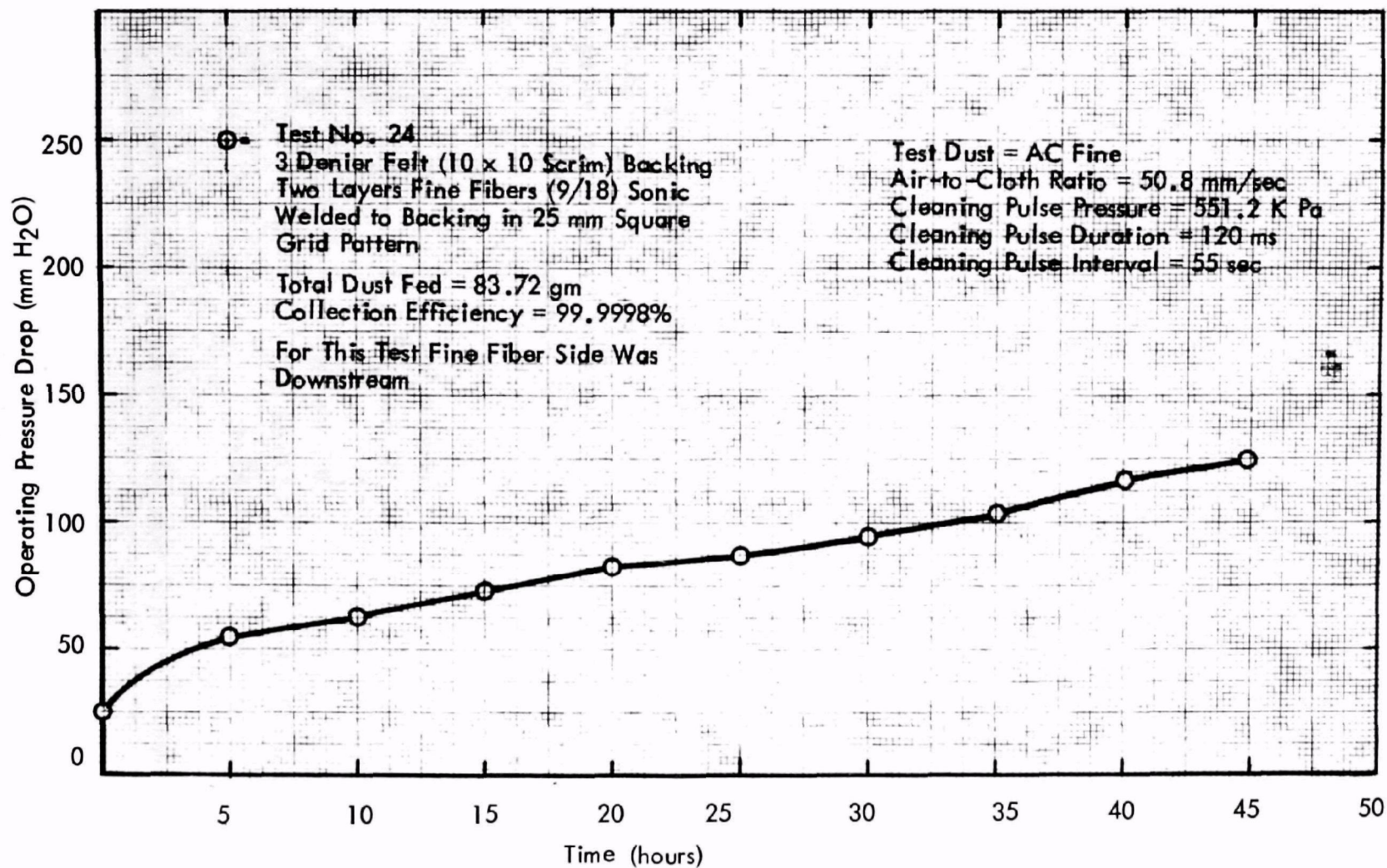


Figure 5-34. Operating Pressure Drop As a Function of Time

At the end of the test:

Residual Dust Loading	= 34.6 gm/m <sup>2</sup>
Overall Dust Loading	= 4077.9 gm/m <sup>2</sup>
Efficiency	= 99.9999 percent

Media Sample No. 9A had a DOP efficiency of 83.5 percent at the test velocity.

Figure 5-35 shows a plot of pressure drop as a function of time for this test. Dust was fed to the fine fiber side of this sample.

Following the test, the fine fiber layer appeared to have loosened from the backing but had not developed any holes or come loose in the fixture clamping area.

#### Test No. 26

An experimental medium designated as No. 10A was tested.

It consisted of a 3 denier felt with two layers of fine fibers (9/18/75) needled to the felt at 200 ppsi. Between the felt and the fine layer was a 10 x 10 scrim. One additional layer of fine fibers (9/18/75) was placed over the needled fine fiber layer and secured to it with Scotch SPRA-Mount Artist adhesive (Cat. No. 6065). The following flat-sheet pulse-jet cleaning test rig settings were used.

Air-to-Cloth Ratio	= 50.8 mm/sec
Dust Feed Concentration (AC Fine)	= 656.5 m <sup>2</sup> /m <sup>3</sup>
Cleaning Pulse Pressure	= 551.2 K Pa
Cleaning Pulse Duration	= 120 ms
Cleaning Pulse Interval	= 55 sec

The test was terminated after 36.87 hours, when the pressure drop had reached 92.7 mm H<sub>2</sub>O.

Residual Dust Loading	= 51.05 gm/m <sup>2</sup>
Overall Dust Loading	= 4426.5 gm/m <sup>2</sup>
Efficiency	= 99.9836 percent



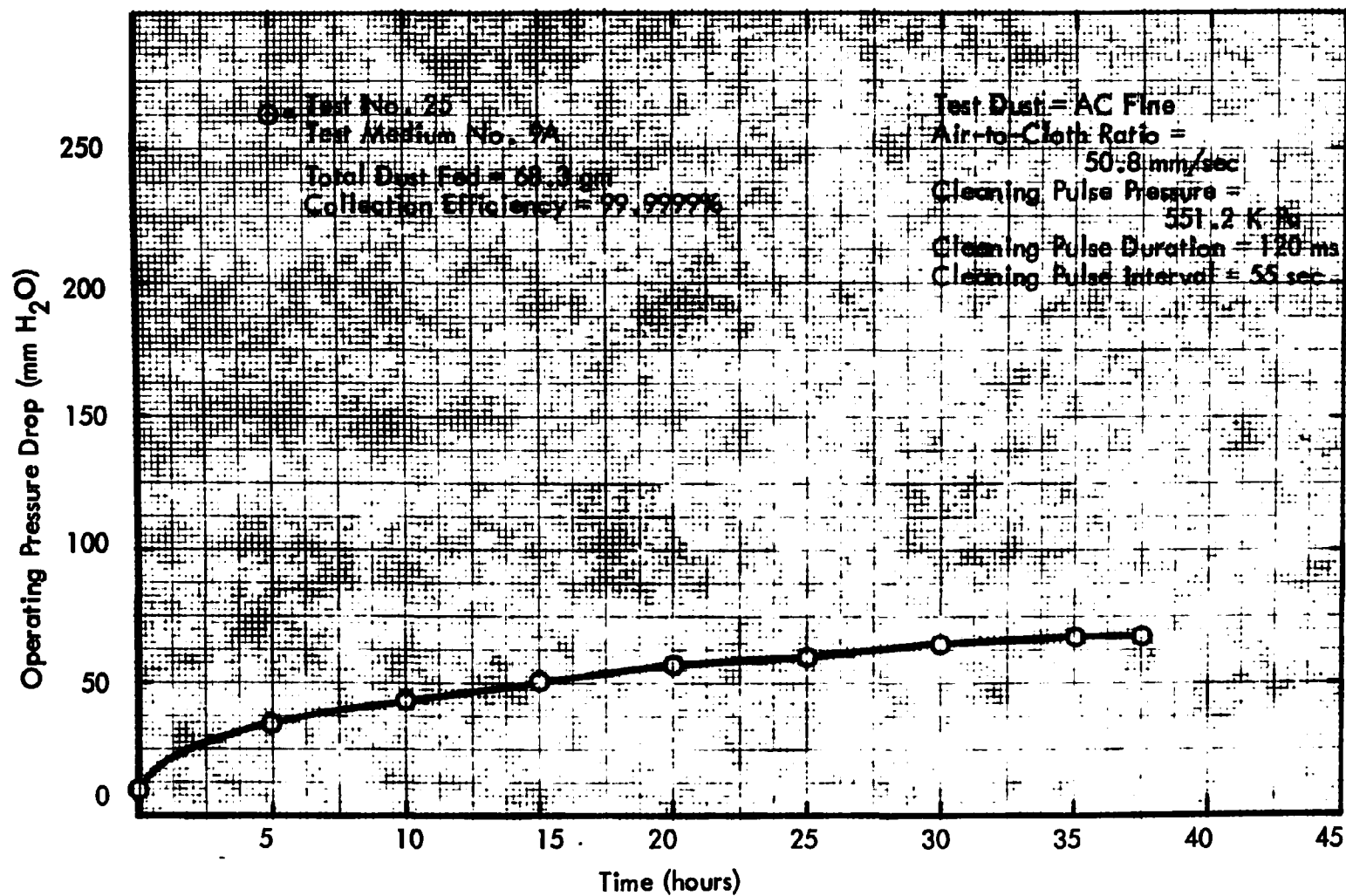


Figure 5-35. Operating Pressure Drop As a Function of Time

Media Sample 10A had a DOP efficiency of 85 percent at the test velocity. Figure 5-36 shows a plot of pressure drop as a function of time for this test.

Following the test, it was noted that the adhesive bonded fine fiber layer had ruptured in several places.

#### Test No. 27

An experimental media (4/10/76) with dacron paper backing was tested. The fine fiber layer had a basis weight of  $20.67 \text{ gm/m}^2$  and a DOP efficiency at the test velocity of 88 percent. The following flat-sheet pulse-jet cleaning test rig settings were used:

Air-to-Cloth Ratio	= 50.8 mm/sec
Dust Feed Concentration (AC Fine)	= $671 \text{ m}^2/\text{m}^3$
Cleaning Pulse Pressure	= 551.2 K Pa
Cleaning Pulse Duration	= 120 ms
Cleaning Pulse Interval	= 55 sec

The test was terminated after 35.17 hours when pressure drop had reached 81.3 mm H<sub>2</sub>O.

Residual Dust Loading	= $16.1 \text{ gm/m}^2$
Overall Dust Loading	= $4316.8 \text{ gm/m}^2$
Efficiency	= 99.9999 percent

This medium produced very good efficiency with excellent cleanability as evidenced by low residual dust loading. Figure 5-37 presents a plot of operating pressure drop as a function of time for the test.

#### Test No. 28

The experimental medium (4/10/76) with felt backing was tested. The fine fiber layer had a basis weight of  $22.57 \text{ gm/m}^2$  and a DOP efficiency at the test velocity of 82 percent. The following flat-sheet pulse-jet cleaning test rig settings were used:

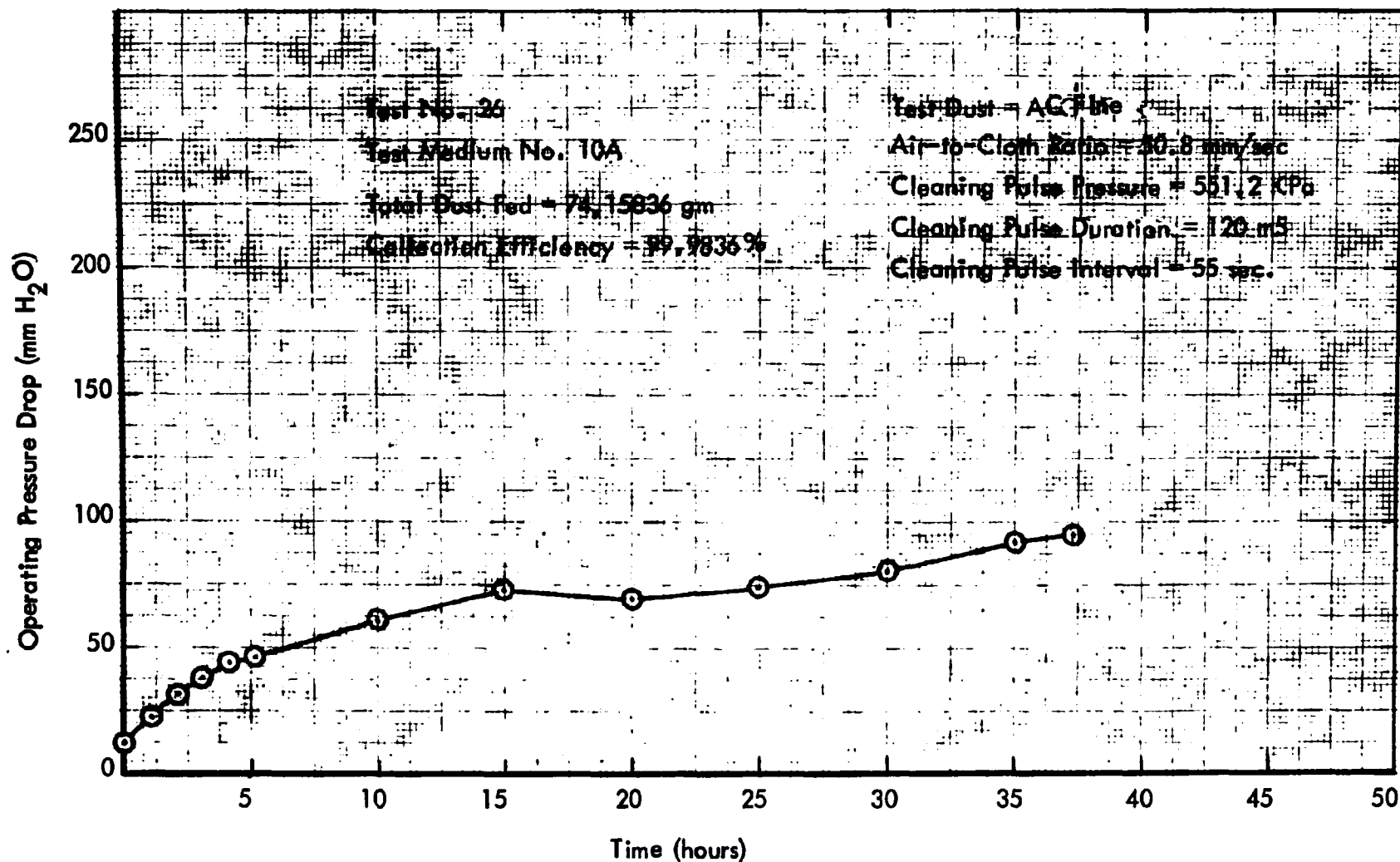


Figure 5-36. Operating Pressure Drop as a Function of Time

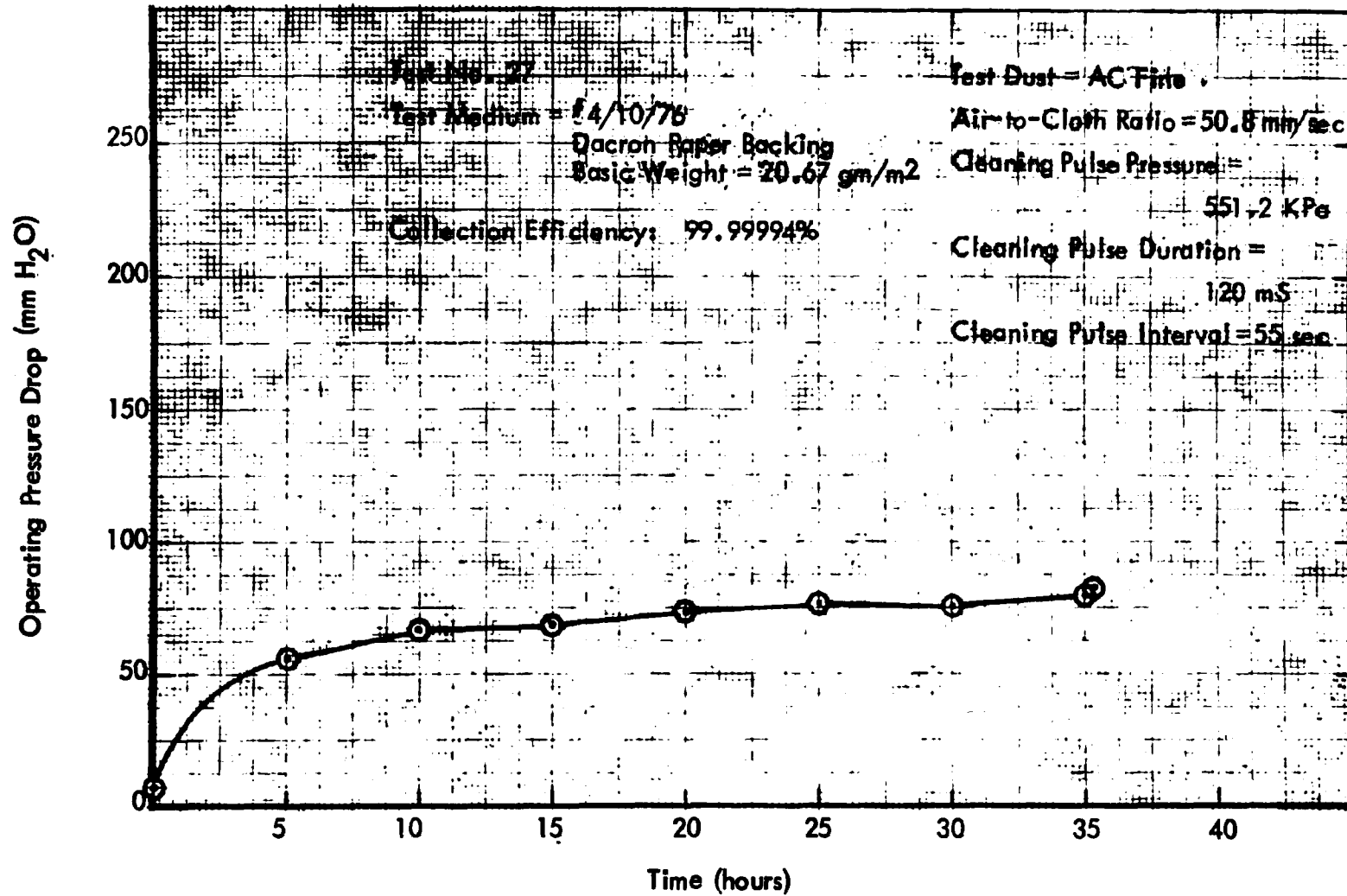


Figure 5-37. Operating Pressure Drop as a Function of Time

Air-to-Cloth Ratio	= 50.8 mm/sec
Dust Feed Concentration (AC Fine)	= 662.9 m <sup>2</sup> /m <sup>3</sup>
Cleaning Pulse Pressure	= 551.2 K Pa
Cleaning Pulse Duration	= 120 ms
Cleaning Pulse Interval	= 55 sec

The test was terminated after 36.02 hours. Pressure drop was 78.7 mm H<sub>2</sub>O at the end of the test.

Residual Dust Loading	= 63.2 gm/m <sup>2</sup>
Overall Dust Loading	= 4363.4 gm/m <sup>2</sup>
Efficiency	= 99.9015 percent

Pressure drop as a function of time for this test is plotted as Figure 5-38.

During this test, large pieces of the fine fiber layer were broken off from the test sheet. Figure 5-39 shows a photograph of the test sheet after the test. Because of the loss of some of the fine fiber layer, the residual dust loading value is incorrect.

#### Test No. 29

A sample of the lowest basis weight material (5/17/76) was installed in the flat-sheet test rig. As in previous tests, standard AC Fine test dust was used. The following flat-sheet pulse-jet test rig settings were used:

Air-to-Cloth Ratio	= 50.8 mm/sec
Dust Feed Concentration (AC Fine)	= 626.8 mg/m <sup>3</sup>
Cleaning Pulse Pressure	= 551.2 K Pa
Cleaning Pulse Duration	= 120 ms
Cleaning Pulse Interval	= 55 sec

The test was terminated after 75.2 hours. Pressure drop was 59.7 mm H<sub>2</sub>O at the end of the test.

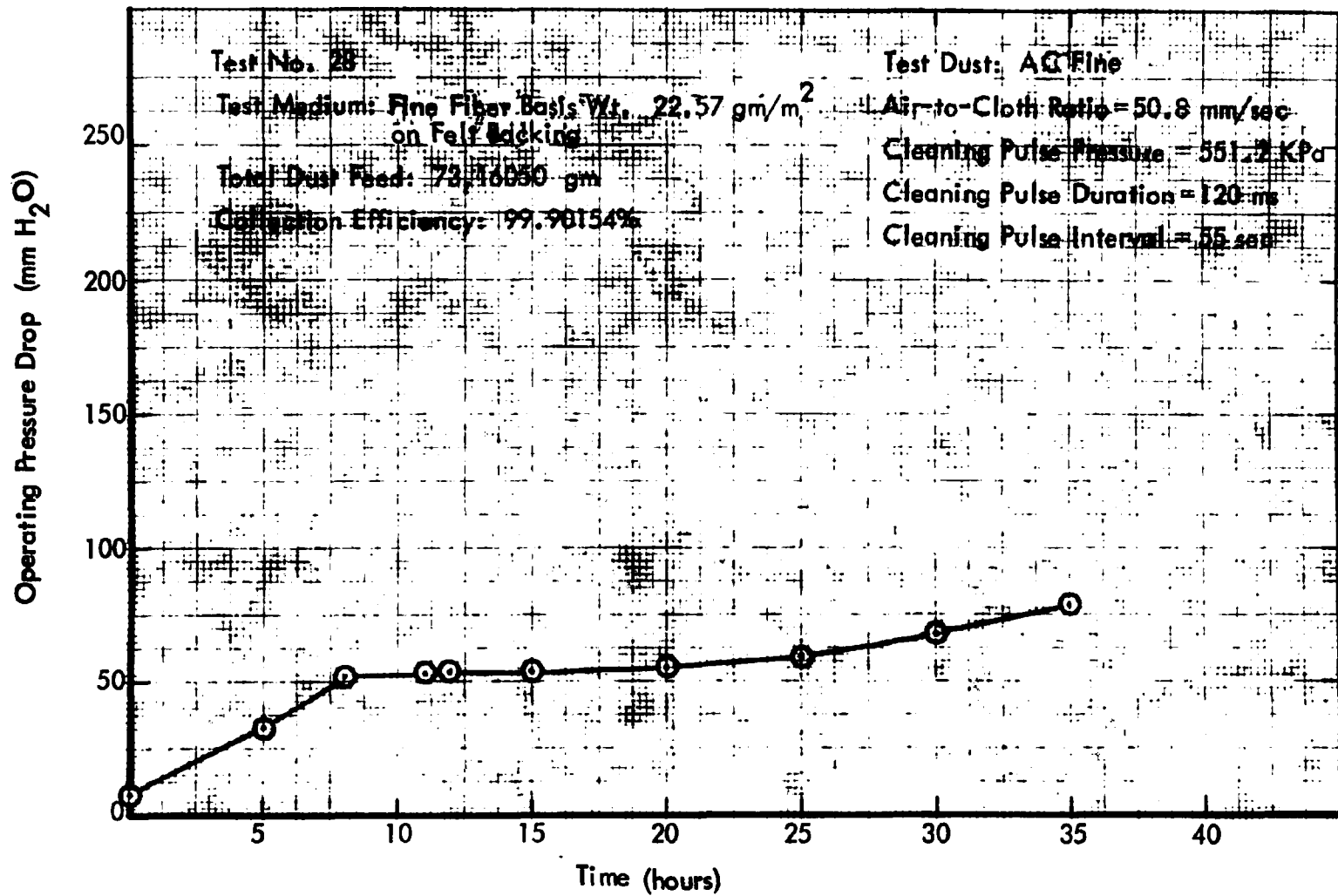


Figure 5-38. Operating Pressure Drop as a Function of Time



Test Sample from Test No. 28  
Fine Fiber Medium (4/10/76) on Felt Backing

Figure 5-39. Fine Fiber Layer Broken from Felt Backing

At the end of the test:

Residual Dust Loading	= 11.1 gm/m <sup>2</sup>
Overall Dust Loading	= 8621 gm/m <sup>2</sup>
Efficiency	= 99.9984 percent

This media sample had a DOP efficiency of 90 percent at the test velocity.

Figure 5-40 shows a plot of pressure drop as a function of time for this test.

#### 5.4 Pressure Drop Tests

Pressure drop was measured for several fine fiber filter media samples. These samples all had DOP efficiency values of approximately 90 percent. Using their measured basis weights, their effective fiber diameter was determined from the curve on Figure 4-3. This data is presented in Table 5-5 below and plotted on Figure 5-41.

Table 5-5. Clean Filter Pressure Drop

Test No. Identification	DOP Efficiency %	Basis Weight gm/m <sup>2</sup>	Effective Fiber dia $\mu$ m	Pressure Drop mm H <sub>2</sub> O
22	95	11.1	0.58	24.5
24	90	107.2	2.15	4.1
26	85	162	2.87	2.8
27	88	20.67	0.82	1.9
29	90	0.5	0.12	3.5
--	90	6.85	0.45	3.35
--	85	6.70	0.44	3.99
--	89	20.15	0.80	6.60
--	85	3.46	0.30	3.94

As can be seen on Figure 5-41, this data does not agree with the value predicted by Langmuir's pressure drop equation. Langmuir's equation does predict pressure drop values as low as the data for 20  $\mu$ m fibers. Data from Test No. 22 was higher than the predicted



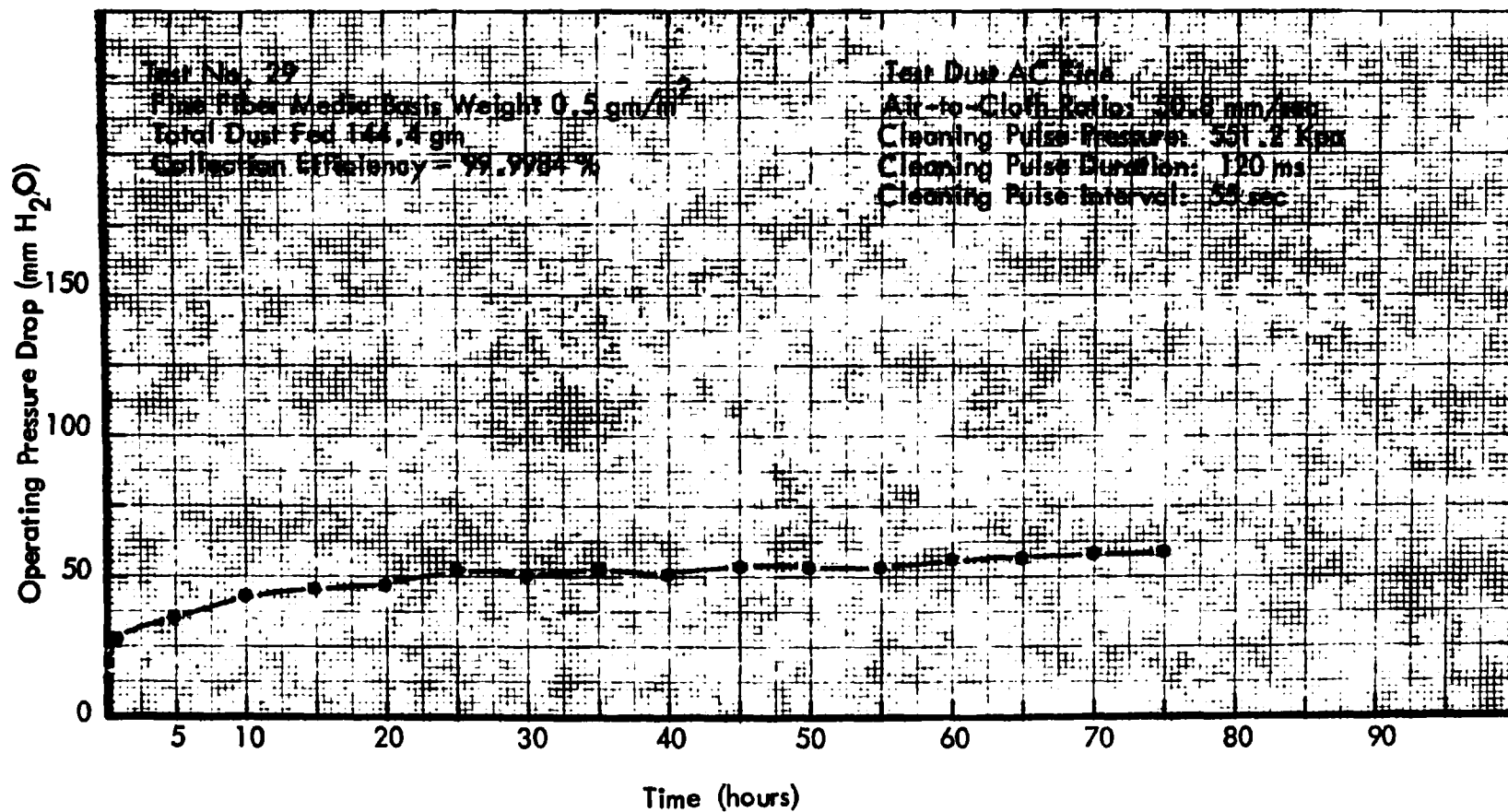


Figure 5-40. Pressure Drop as a Function of Time

Langmuir

$$\odot = \Delta P = \frac{8\alpha}{\left(-\frac{1}{2} \ln \alpha + \alpha - \frac{\alpha^2}{4} - \frac{3}{4}\right)} \frac{\mu_G U_o l}{d_f^2}$$

Langmuir with Knudsen No. Correction

$$\square = \Delta P = \frac{8\alpha}{\left(-\frac{1}{2} \ln \alpha - \frac{3}{4(1+K_n)} + \frac{\alpha}{1+K_n} + \frac{K_n(2\alpha-1)^2}{4(1+K_n)} - \frac{\alpha^2}{4}\right)} \frac{\mu_G U_o l}{d_f^2}$$

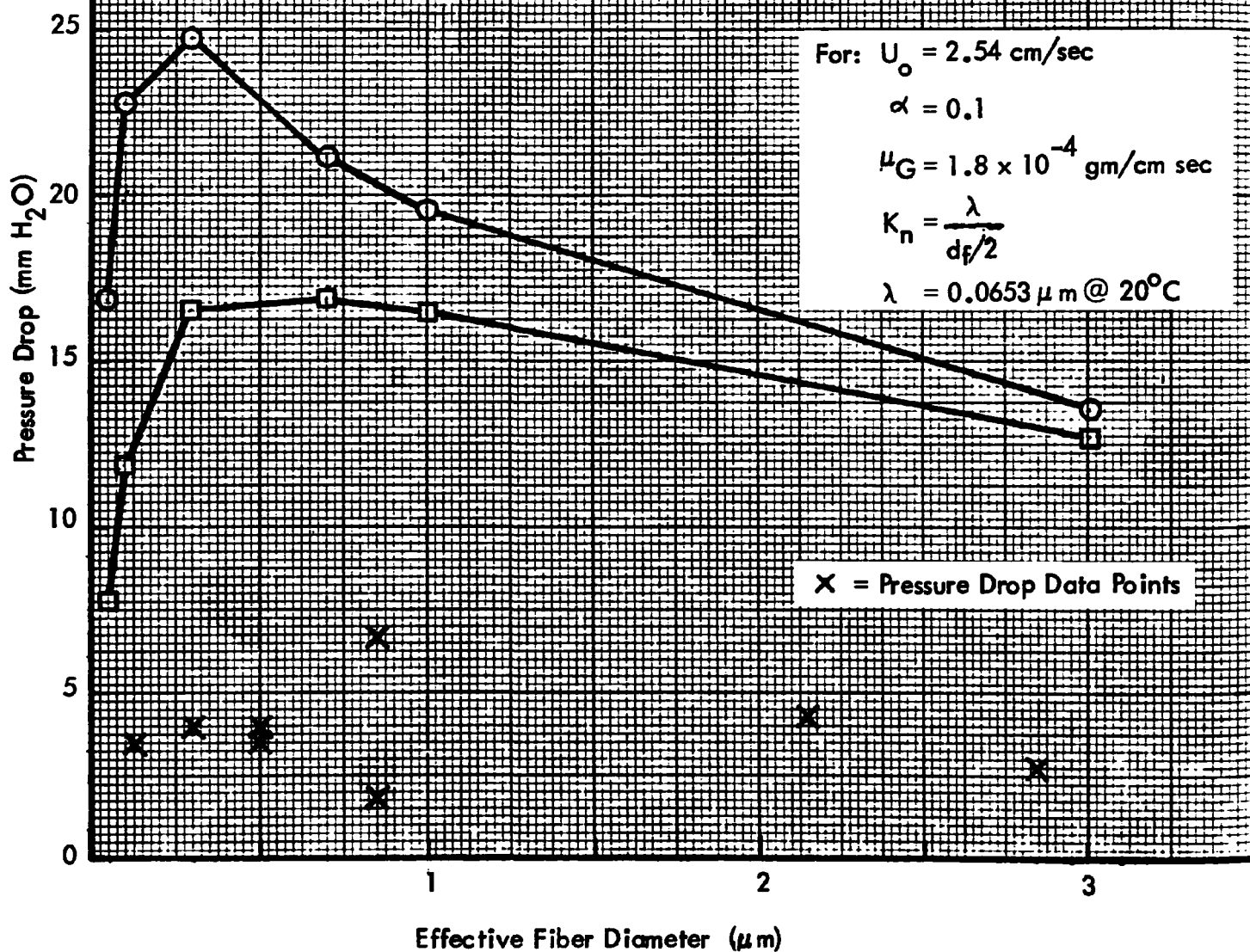


Figure 5-41. Difference Between Actual and Predicted Pressure Drop for Filters Capable of 90% Collection of  $0.3 \mu\text{m}$  DOP

value. Test No. 22 also indicated anomalously high pressure drop during dust feeding. The theoretical curve is for a DOP efficiency of 90 percent and for filter beds of uniform size fibers with solidity ( $\alpha$ ) of 0.1. Several of these parameters are different in the actual filter beds tested. These differences may explain the difference between theoretical and actual  $\Delta P$ ; however, it seems unlikely because of the relatively large differences seen. Fortunately, the actual pressure drop measured is less than the predicted value; consequently, it does not present a problem in the sense of interfering with performance as a practical filter system. For this reason and because the contract is not funded to pursue an explanation for such differences, we cannot at this time attempt to seek an explanation. We will, however, continue to collect this pressure drop data as opportunities arise with new filter media samples.

## 6.0

### PLEATED CARTRIDGE LABORATORY TESTS

Laboratory testing was performed on pleated cartridges using fine fiber media in Phase II. The tests consisted of dust loading in a Torit model pulse-jet air cleaner and DOP penetration tests on individual cartridges before and after the dust tests.

The dust tests indicated high collection efficiencies on AC Fine test dust. Also, it was found that 689 K Pa of cleaning pressure is desirable in order to attain stabilized pressure drop during dust loading.

The DOP penetration tests were performed at air-to-cloth ratios from 10 mm/sec up to 50 mm/sec both before and after the dust tests. The efficiencies were high and there was no degradation in performance due to dust loading and pulse cleaning.

The following paragraphs describe these tests in detail.

## 6.1

### Pleated Cartridge Dust Tests

Dust tests were performed using fine fiber media in a cylindrical pleated cartridge configuration. Three pleated cartridge filters were installed into a Torit model TD pulse-jet air cleaner. The objective of these tests was to determine pressure drop as a function of air-to-cloth ratio and cleaning pulse pressure. Pulse duration was fixed at 120 milliseconds. Pulse interval was nominally 60 seconds so that one of the three elements was pulsed once every 20 seconds. AC Fine test dust was also used for this series of tests. The three element filter unit has a nominal airflow capacity of 28.3 m<sup>3</sup>/min and was operated at rated flow for this test sequence. Air-to-cloth ratio was varied by changing the element configuration in terms of the pleat spacing and the axial length of the cylindrical element. Pleat depth was 5 cm for all the tested elements. The following table describes the element configuration.

	Air-to-Cloth Ratio (mm/sec)			
	10	20	35	50
Element Active Length (cm)	53.3	53.3	28.7	26.9
Number of Pleats	286	143	151	113
Filter Area (m <sup>2</sup> )	15.48	7.74	4.42	3.09

In order to obtain a baseline for comparison, three standard production elements were tested. Air-to-cloth ratio for the standard element tests was 9.25 mm/sec. Cleaning pulse pressure was 413 K Pa with pulse duration of 120 ms. Cleaning pulse interval was once every 58.2 seconds for each element or once every 19.4 seconds in the three element system. Pressure drop as a function of time for this test is shown on Figure 6.1. This test was terminated after 35.32 hours. During the test, 52,992 grams of dust were fed to the air cleaner. The dust collected on the absolute filter weighed 27.63 grams. This yielded an overall efficiency of 99.95 percent.

Three fine fiber elements were installed for testing at an air-to-cloth ratio of 10 mm/sec. Cleaning pulse pressure was held at 413 K Pa with pulse duration of 120 ms. The cleaning pulse interval was set so that each of the three elements were pulsed once every 58.2 seconds. This resulted in the three element system pulsing once every 19.4 seconds.

Pressure drop as a function of time for a dust feed rate of 812.2 mg/m<sup>3</sup>, is shown on Figure 6.1. During the 39.15 hours of this test, 54,194 grams of dust were fed to the system. Only 0.05 grams of dust penetrated the system and were collected on the absolute filter. This resulted in an overall efficiency of 99.9999 percent. As can be seen from the curve at this pulse pressure and air-to-cloth ratio pressure drop, equilibrium was not obtained.

Three new fine fiber elements were installed for tests at air-to-cloth ratio of 20 mm/sec. Using AC Fine test dust at a concentration of 883 mg/m<sup>3</sup>, the elements were allowed

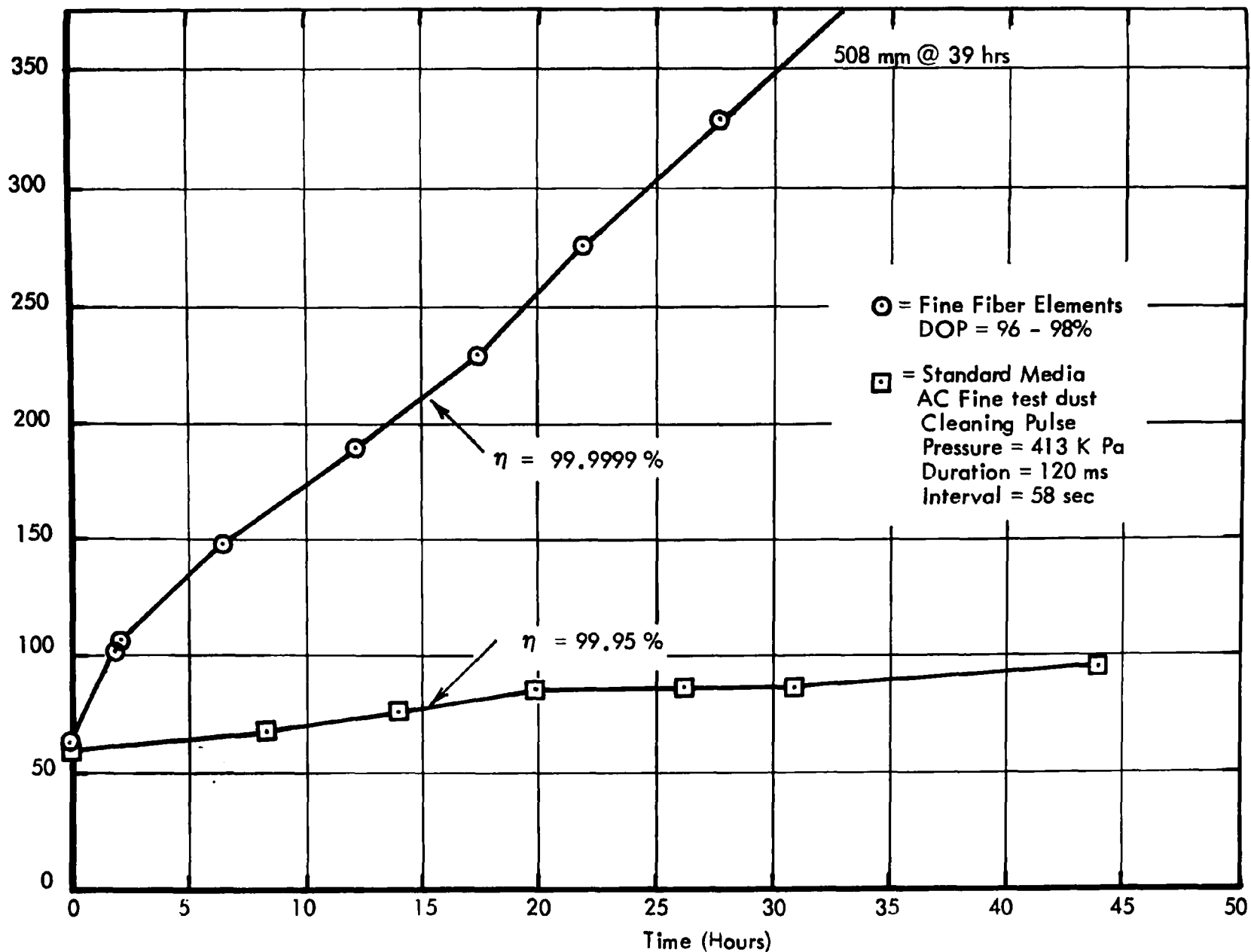


Figure 6-1. Pressure Drop Life Characteristics

to reach a pressure drop of 726 mm H<sub>2</sub>O at a cleaning pulse pressure of 413 K Pa. This occurred after 23.5 hours of operation. Pulse duration was 120 ms and pulse interval was 58 seconds or one pulse every 19 seconds for the three elements.

After completing this test at 413 K Pa, primary flow was reduced to a value resulting in 25 mm H<sub>2</sub>O pressure drop.

Cleaning pressure was set to 689 K Pa and the elements were cleaned without dust feeding. Following this, the primary flow was increased to 28.3 m<sup>3</sup>/min (rated flow) and the unit was operated at a pulse pressure of 551 K Pa for 20 minutes without dust feeding. Pressure drop was then 178 mm H<sub>2</sub>O. Dust feeding was started and continued for one hour. At the end of the hour, pressure drop had risen to 193 mm H<sub>2</sub>O. Cleaning pulse pressure was then increased to 689 K Pa and the unit was operated for one more hour. At the end of this hour, pressure drop was reduced to 170 mm H<sub>2</sub>O. These results indicated that by proper selection of cleaning pulse pressure, one can control pressure drop while feeding dust. To obtain an indication of long term effects, operation was continued with cleaning pulse pressure set at 551 at K Pa. The test was terminated after 46.4 additional hours of operation. Pressure drop had risen to 229 mm H<sub>2</sub>O. This entire test sequence is plotted on Figure 6-2.

During the first 23.5 hours of the test with cleaning pulse pressure set at 413 K Pa, 35,252 grams of dust were fed to the system. The absolute filter collected 0.74 grams which penetrated the elements. This resulted in an efficiency of 99.9979 percent.

During the final 46.4 hours of the test with cleaning pulse pressure set at 551 K Pa, 69,652 grams of dust were fed to the system. The absolute filter gained 0.39 grams resulting in 99.9994 percent collection efficiency.

New fine fiber elements were installed for both tests at air-to-cloth ratios of 35 to 50 mm/sec. For these tests AC Fine test dust was fed to the elements at a concentration of 883 mg/m<sup>3</sup>. Pulse duration (120 ms) and interval (58 seconds or one pulse every





19 seconds for the three elements) were the same as previous tests at air-to-cloth ratios of 10 and 20 mm/sec. Both tests were initially run with a cleaning pulse pressure of 413 K Pa which was later increased to 551 K Pa, then 689 K Pa for the second and third portion of the test.

Figure 6.3 shows operating pressure drop as a function of time for the initial test at 413 K Pa as well as the following test at 551 K Pa and the final test at 689 K Pa. At the end of the 551 K Pa test, pressure drop was reduced by cleaning at 689 K Pa with primary flow reduced to a level resulting in about 25 mm H<sub>2</sub>O without dust feeding. This procedure reduced operating pressure drop to 254 mm H<sub>2</sub>O at rated flow. The test was then continued at 689 K Pa. After 56.08 additional hours of operation, pressure drop had risen to 330 mm H<sub>2</sub>O. At this point the test was stopped. During the test at 689 K Pa 84,120 grams of dust were fed to the system with 5.58 grams penetrating the elements. This resulted in an overall efficiency for this portion of the test of 99.9934 percent.

New elements were installed in a second test unit for tests at an air-to-cloth ratio of 50 mm/sec. Figure 6-4 shows operating pressure drop as a function of time for the initial test at 413 K Pa as well as the following test at 551 K Pa, and the final test at 689 K Pa.

At the end of the 551 K Pa test pressure drop was reduced by cleaning at 689 K Pa with primary flow reduced to a level resulting in about 25 mm H<sub>2</sub>O without dust feeding. This procedure reduced operating pressure drop to 157 mm H<sub>2</sub>O at rated flow. The test was then continued at 689 K Pa. After 19.7 additional hours of operation pressure drop had risen to 256.5 mm H<sub>2</sub>O. At this point the test was stopped. During this test at 689 K Pa, 29,618 grams of dust was fed to the system with 76.47 grams penetrating the elements. This resulted in an overall efficiency of 99.7418 percent.

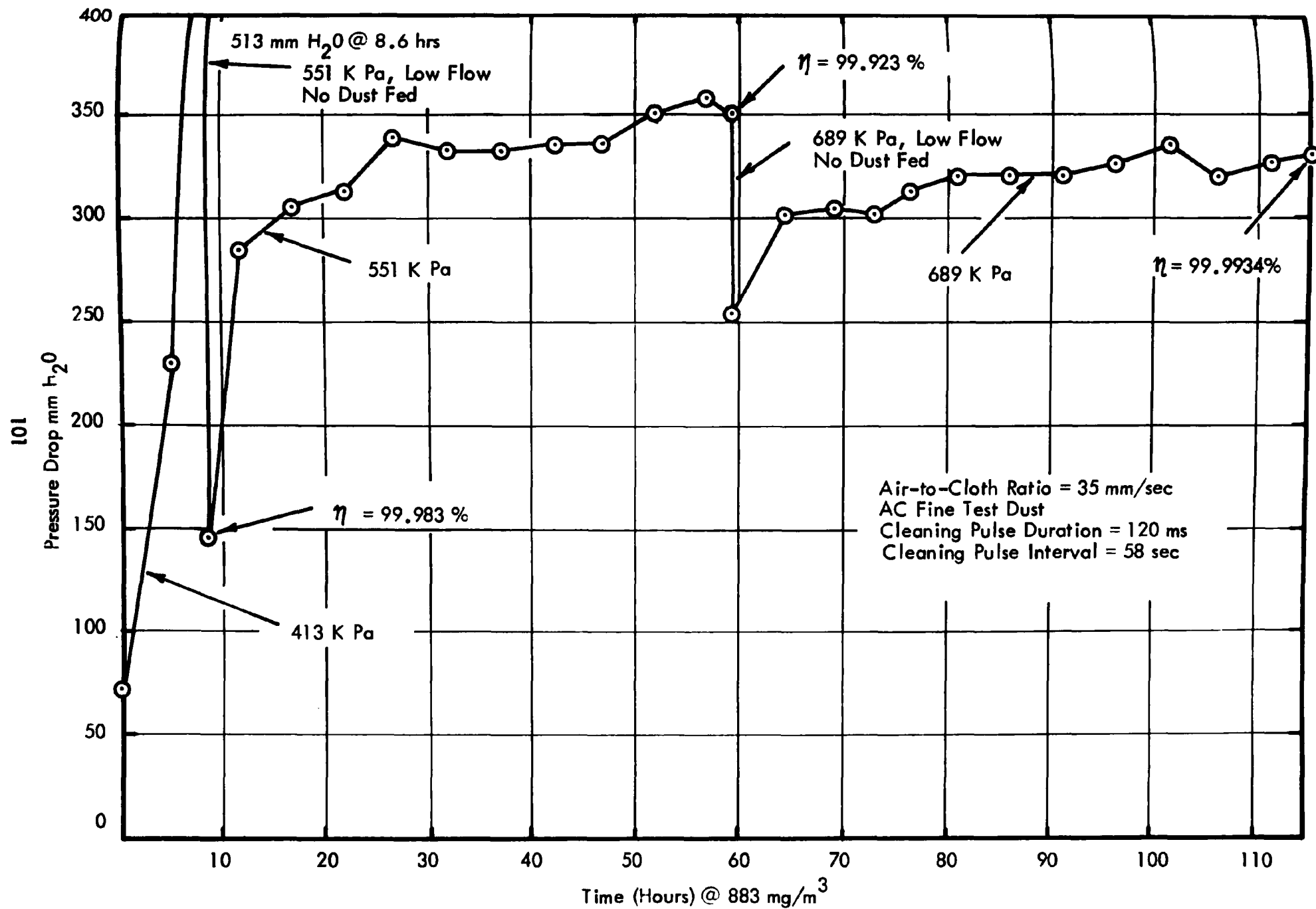


Figure 6-3. Pressure Drop Life Characteristics

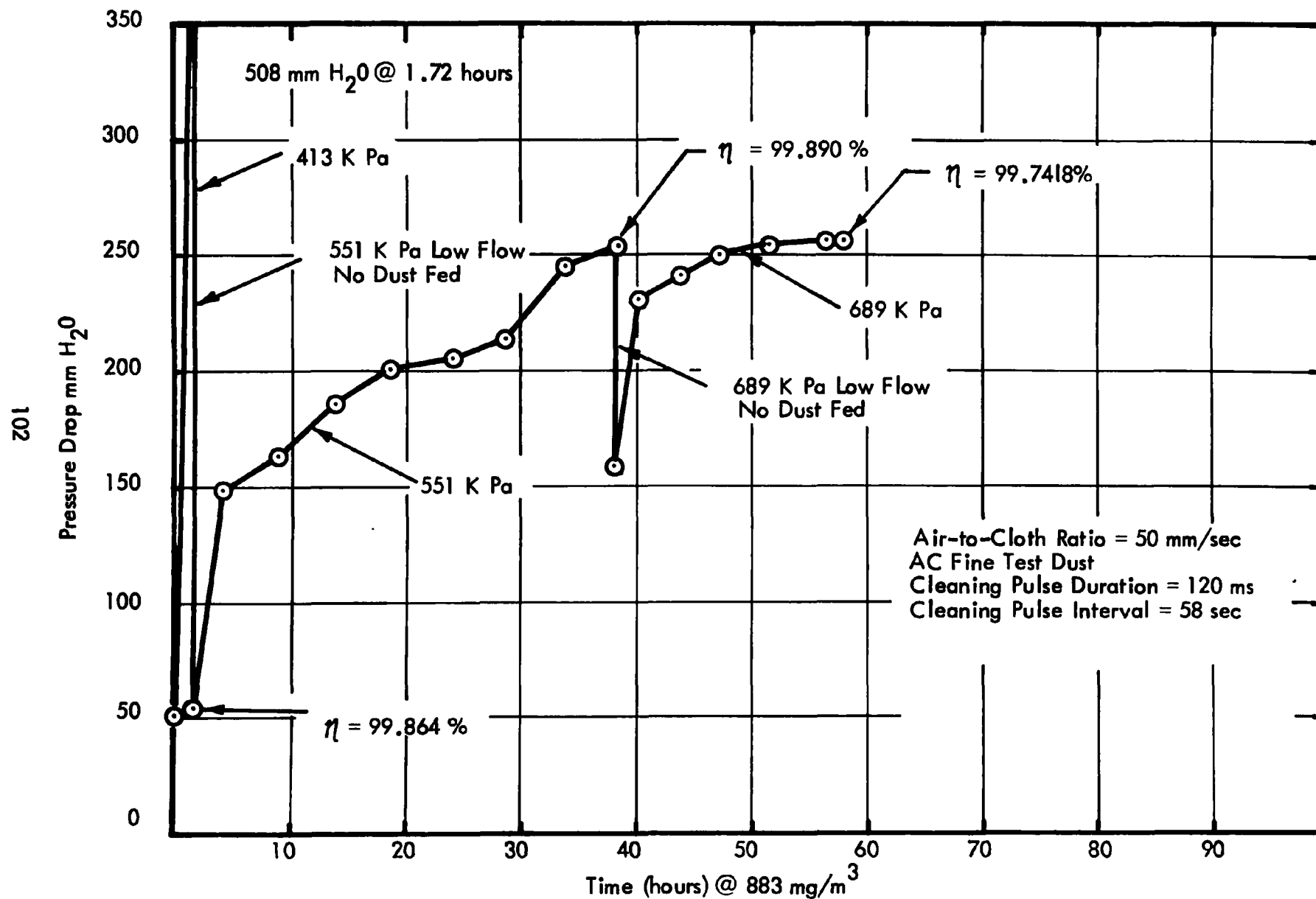


Figure 6-4. Pressure Drop Life Characteristics

During these tests the dust which passed the test elements was collected on an absolute filter located downstream of the pulse jet unit. For both the tests at 35 mm/sec and at 50 mm/sec air-to-cloth ratio, the dust collected in the absolute filter was washed out and analyzed by Coulter Counter. The resulting particle size distribution is plotted on Figure 6-5. The AC Fine feed dust particle size distribution is also shown. Note that while the averaged particle size has been reduced, there are still some relatively large particles present in the dust which passed the fine fiber filter. This is an expected result for a barrier filter. Even though the mass removal efficiency is very high, a few large particles can still penetrate the filter. This is because a filter is a "probability" device and not a screen.

Tests at higher air-to-cloth ratios have shown a decrease in overall efficiency for AC Fine test dust. Collection efficiency for AC Fine test dust is plotted on Figure 6-6 as a function of air-to-cloth ratio, with cleaning pulse pressure as a parameter. This data indicates that collection efficiency for AC Fine test dust is a function of air-to-cloth ratio. It further indicates that the fine fiber media can achieve the same collection efficiency as standard media, but at a higher air-to-cloth ratio. In these tests, fine fiber media can operate at 8 to 1 at the same efficiency as standard media at 2 to 1 air-to-cloth ratio.

Also note that there appears to be little difference between efficiency obtained from tests at different cleaning pulse pressure. This indicates that the changes in efficiency are related to the primary flow velocity.

## 6.2 DOP Penetration Tests

Efficiency for collection of  $0.3 \mu m$  DOP was measured before and after the dust tests of the pleated elements. The following table presents the results of these tests:

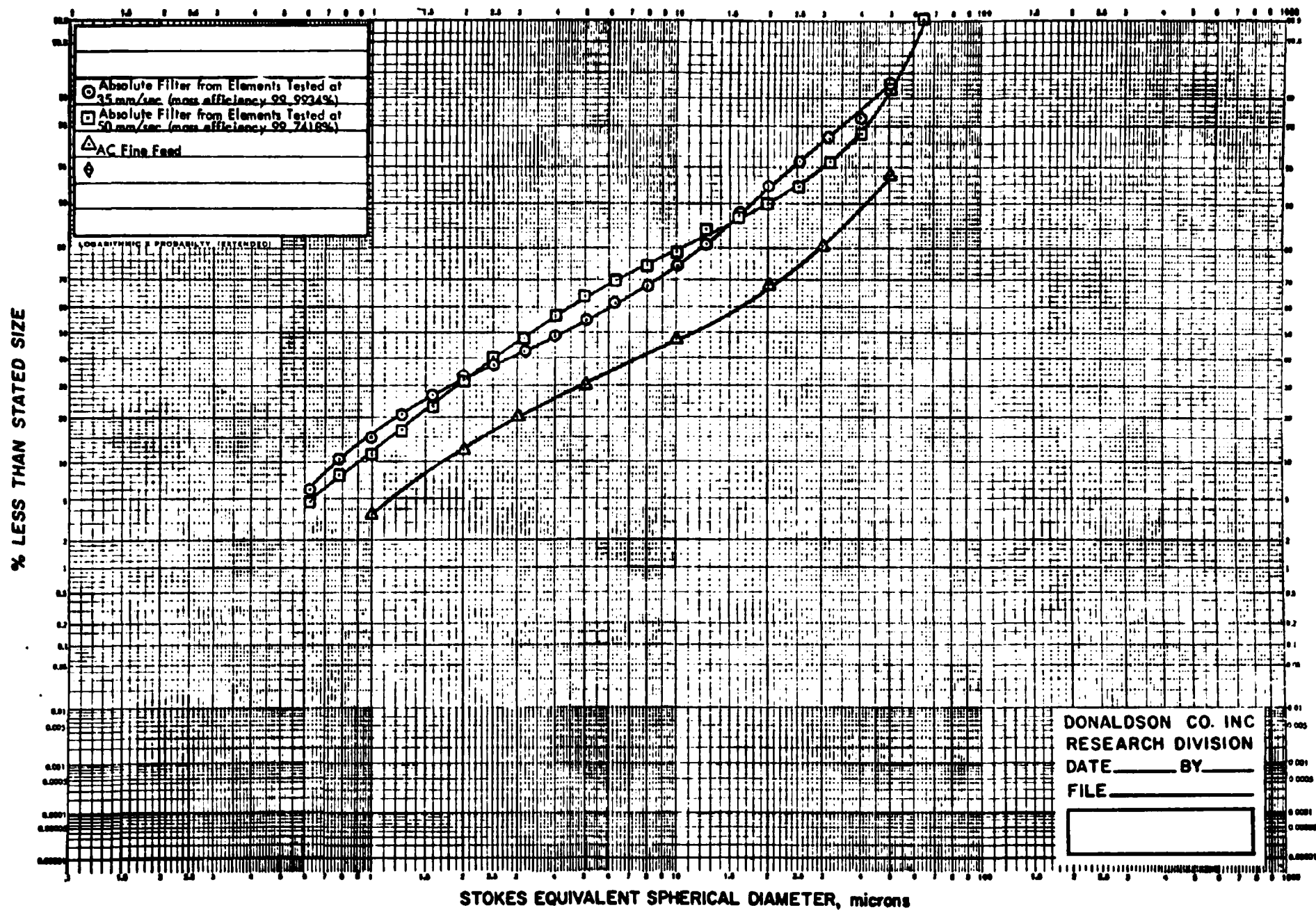


Figure 6-5. Particle Size Distribution of Feed and Effluent Dust

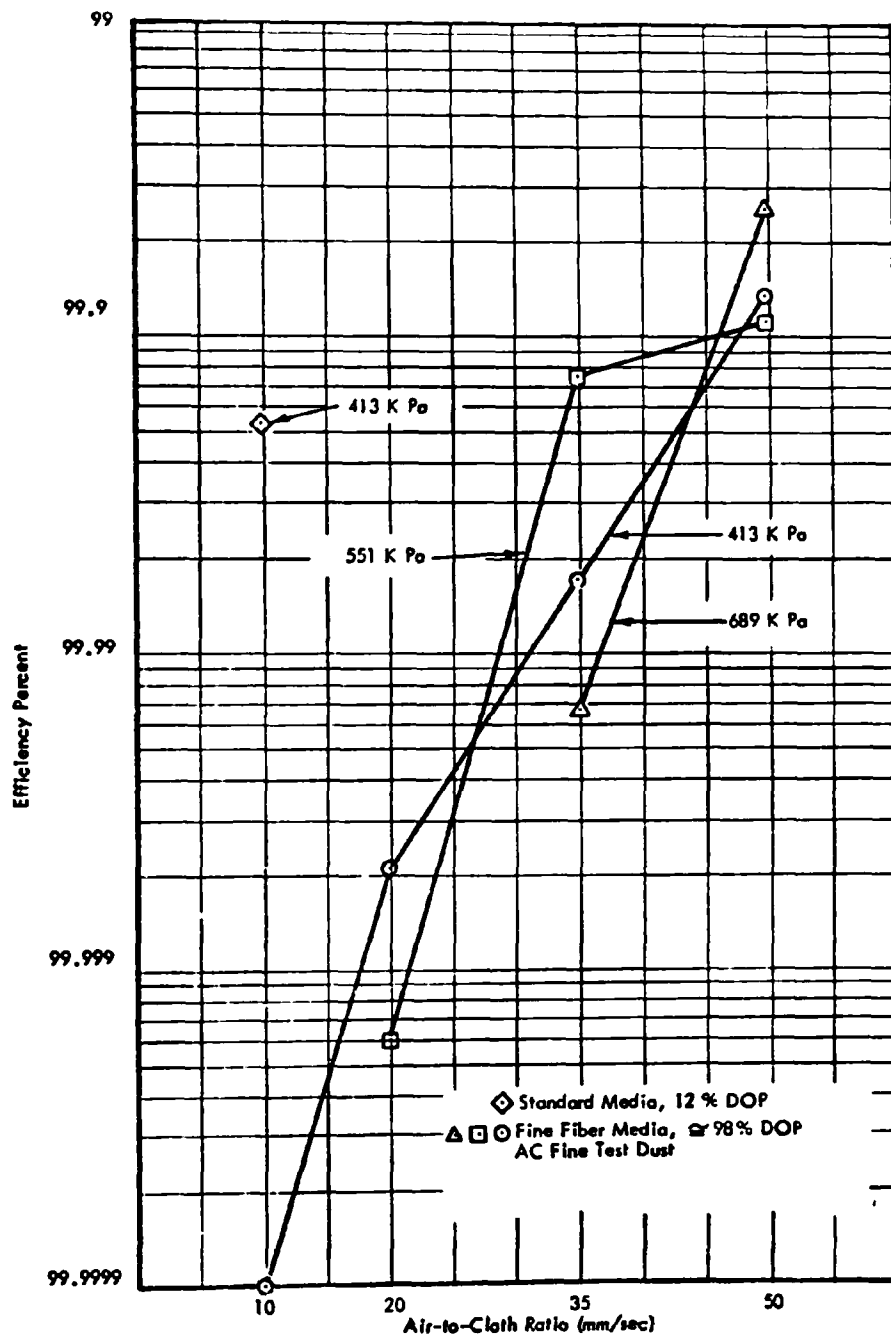


Figure 6-6. Efficiency as a Function of Air-to-Cloth Ratio

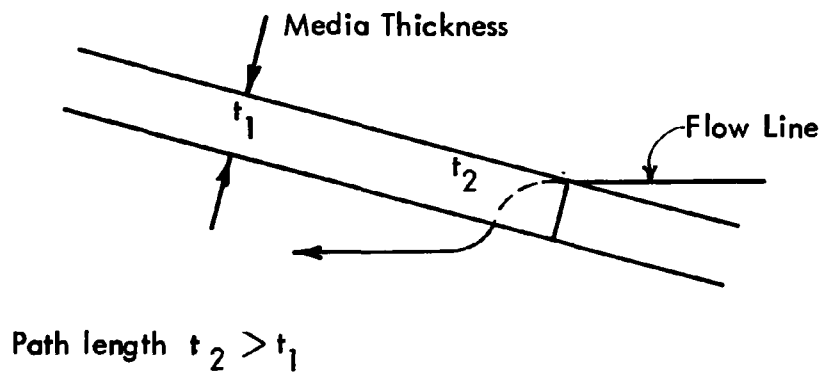
Air-to-Cloth Ratio (mm/sec)	Initial (Clean) DOP Efficiency (%)	Post Dust Test DOP Efficiency (%)
--	98.0	99.2
10	96.0	98.5
--	96.0	98.5
--	98.0	99.8
20	98.5	99.9
--	98.5	99.85
--	99.8	98.5
35	99.9	99.3
--	98.0	99.0
--	93.0	99.8
50	99.0	99.8
--	99.5	99.8

One element tested at air-to-cloth ratio of 50 mm/sec, when clean, had an anomalously low DOP efficiency (93%). If the result for this element is ignored, the remainder of the data suggests that DOP efficiency is only weakly influenced by air-to-cloth ratio. As expected, DOP efficiency from a dirty filter is higher than from a clean filter because the dust cake is providing some filtration.

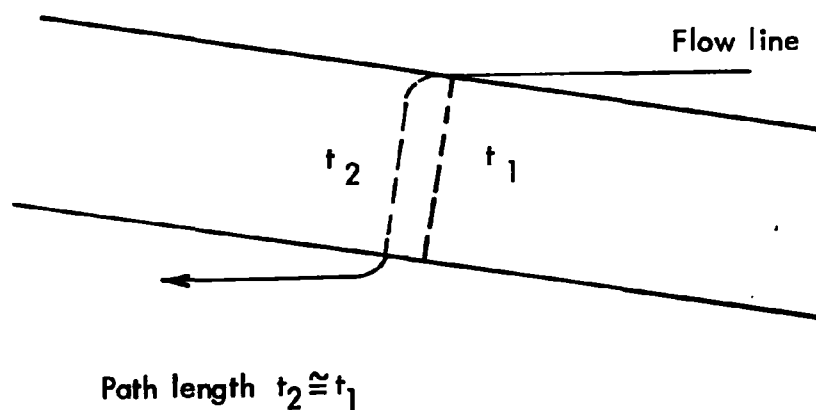
The filter medium from which these elements were fabricated collected 85 to 90 percent of DOP smoke in a flat sheet test, while pleated cartridge DOP results were > 98 percent. Our tests to determine if the DOP machine was giving erroneous results indicate that this difference is real.

A possible explanation for this improved efficiency is that in the pleated configuration, a DOP particle approaches the medium at a shallow angle. This then requires

that the particle alter direction within the medium to follow a given flow line. This curved path is longer than a path straight through the medium. The longer curved path effectively increases the thickness of the medium. See the sketch below.



The reason this phenomenon is not more pronounced in standard media is that standard media is considerably thicker than the fine fiber media and a curved path length through it is proportionally closer to the path length straight through the medium. See the sketch below.





The purpose of the field tests was to demonstrate the performance of filter cartridges made from fine fiber media on actual industrial emissions, which have a high percentage of submicrometer particles. Two sites were selected: Cornelius Company (welding fume emissions), and the Northern Malleable Iron Company (magnesium oxide emissions). These tests were aimed at characterizing the particles and determining the efficiency and life of the fine fiber filter cartridges. The particulate characterization tests consisted of Coulter Counter analysis, Andersen Cascade Impactor sampling, scanning electron micrographs, transmission electron micrographs, solubility tests and x-ray dispersive radiation analysis. The performance tests were directed at determining overall mass efficiency by means of gravimetric sampling, fractional efficiency using an Andersen Cascade Impactor, and filter loading and durability evaluations.

Tests results indicated that the particle size spectrum at both sites contained a high percentage of submicrometer particles. According to the Andersen Cascade Impactor data, particles below  $2\mu\text{m}$  were measured at over 65 percent for the welding fume and over 53 percent for the magnesium oxide emission. The overall mass efficiency of the fine fiber filters on each emission was high; 97.6 percent average for the welding fume and 99.95 percent for the magnesium oxide fume.

A media failure occurred at the Northern Malleable site. The substrate media fatigued and allowed dust to pass sometime between 408.6 hours and 539.6 hours of operation. It is felt, however, that a stronger substrate media will solve this durability problem. Subsequent to this failure, one of the filter units was run in the laboratory at an accelerated cleaning pulse interval to determine if pulse cleaning affected the durability of the media. DOP penetration tests indicated no media failure after 112,626 pulses per element. This is equivalent to 1877.1 hours of operating time at the normal pulse interval.

The following paragraphs describe results of the field tests.

## 7.1 Tests at Cornelius Company (Welding Fume Emission)

Field tests were started at Cornelius Company in March 1977. The emissions at this site were from welding operations at individual welding tables.

Figure 7-1 illustrates an individual welding table. Air is drawn through rectangular openings in the table and is routed through a duct to a large dust collector. The fine fiber filter unit was fitted to one of the individual welding tables as shown in Figure 7-2.

Figure 7-3 is a schematic illustration of the test setup. This filter unit was run at an air-to-cloth ratio of 35 mm/sec and an airflow of  $28.3 \text{ m}^3/\text{min}$ . Figure 7-4 shows the pressure drop of this unit with clean filter elements. The pressure drop for this system was monitored throughout the test program to obtain the projected life or pressure drop versus time.

### 7.1.1 Particulate Characterization - Welding Fume

The following analyses were performed to characterize the welding fume: Coulter Counter, Andersen Cascade Impactor sampling, scanning electron microscopy, transmission electron microscopy, solubility tests, and x-ray analysis.

The Coulter Counter analysis on this particulate material was inconclusive. One analysis indicated a D50 of about  $4 \mu\text{m}$ , whereas, the other indicated about 99 percent of the sample below  $4 \mu\text{m}$ .

Solubility tests were conducted on samples to determine the percentage of oil in the emission. Both benzene and petroleum ether were used as solvents. It was felt that a high percentage of the emission was organic or carbon based because the steel was not degreased prior to welding. The results indicated that oil represented 20 to 50 percent of the sample, which explains the discrepancies in the Coulter Counter analysis.

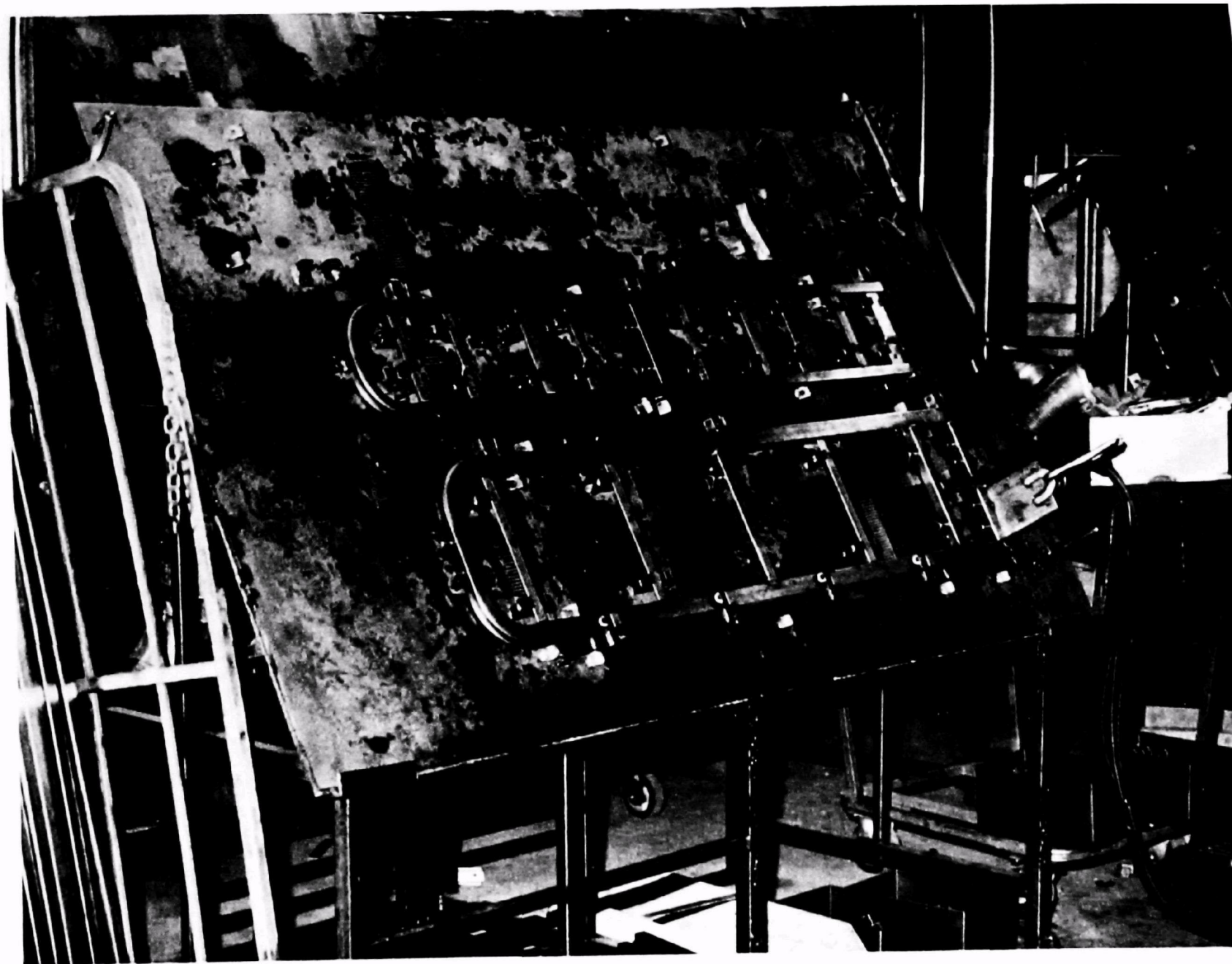


Figure 7-1. Welding Table at Cornelius Company

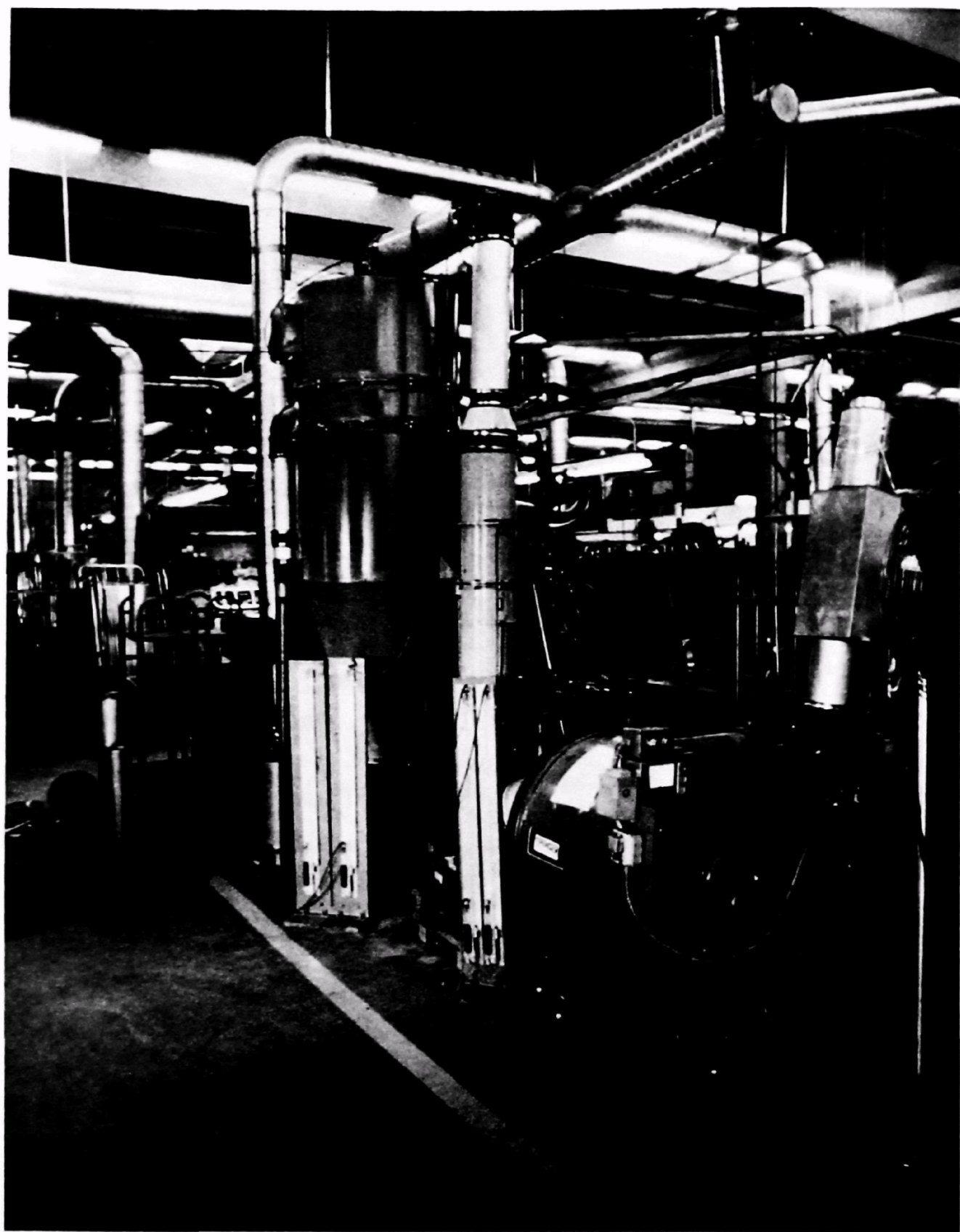


Figure 7-2. Installation at Cornelius Company - Welding Fume

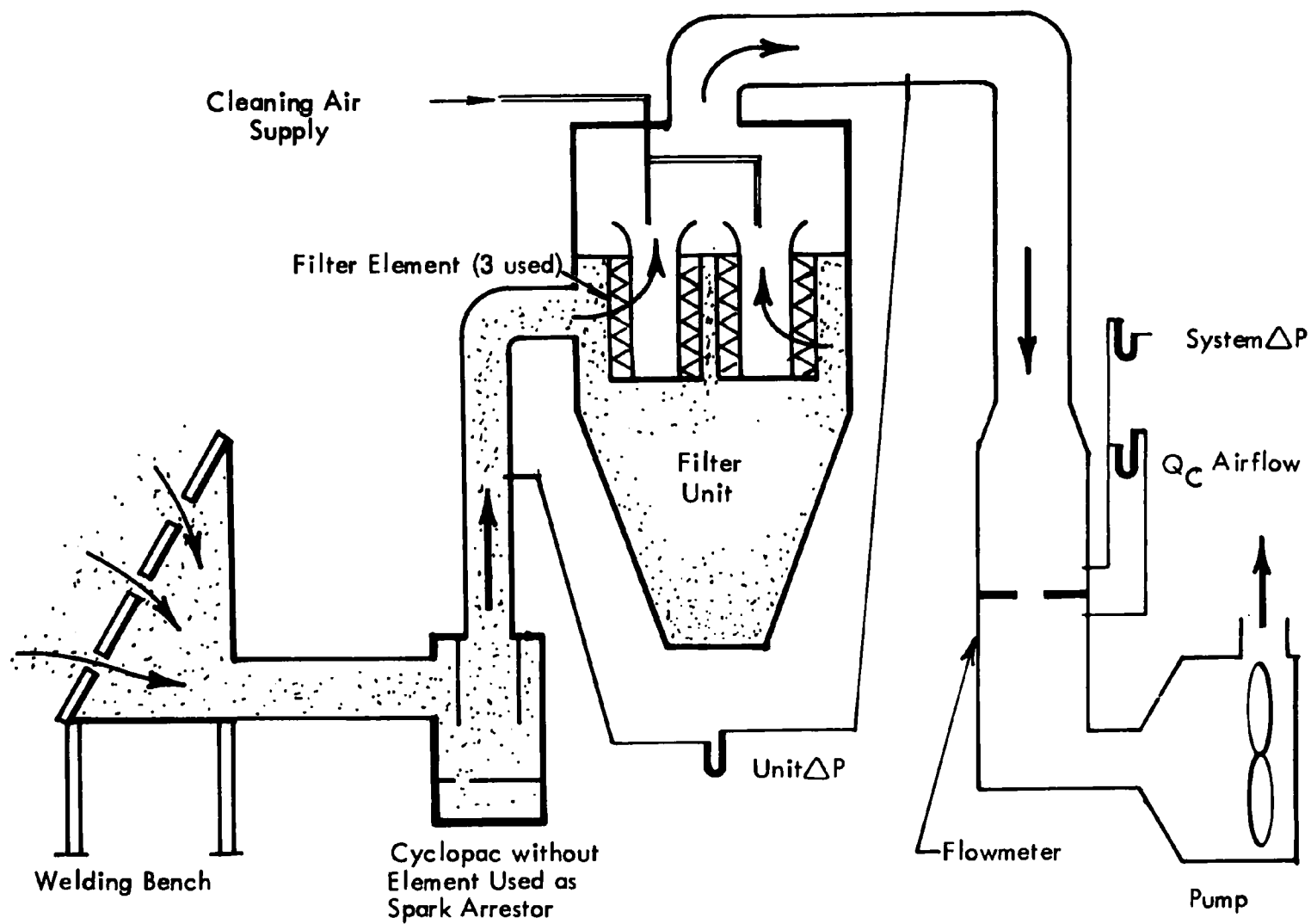


Figure 7-3. Test Setup at Cornelius Company

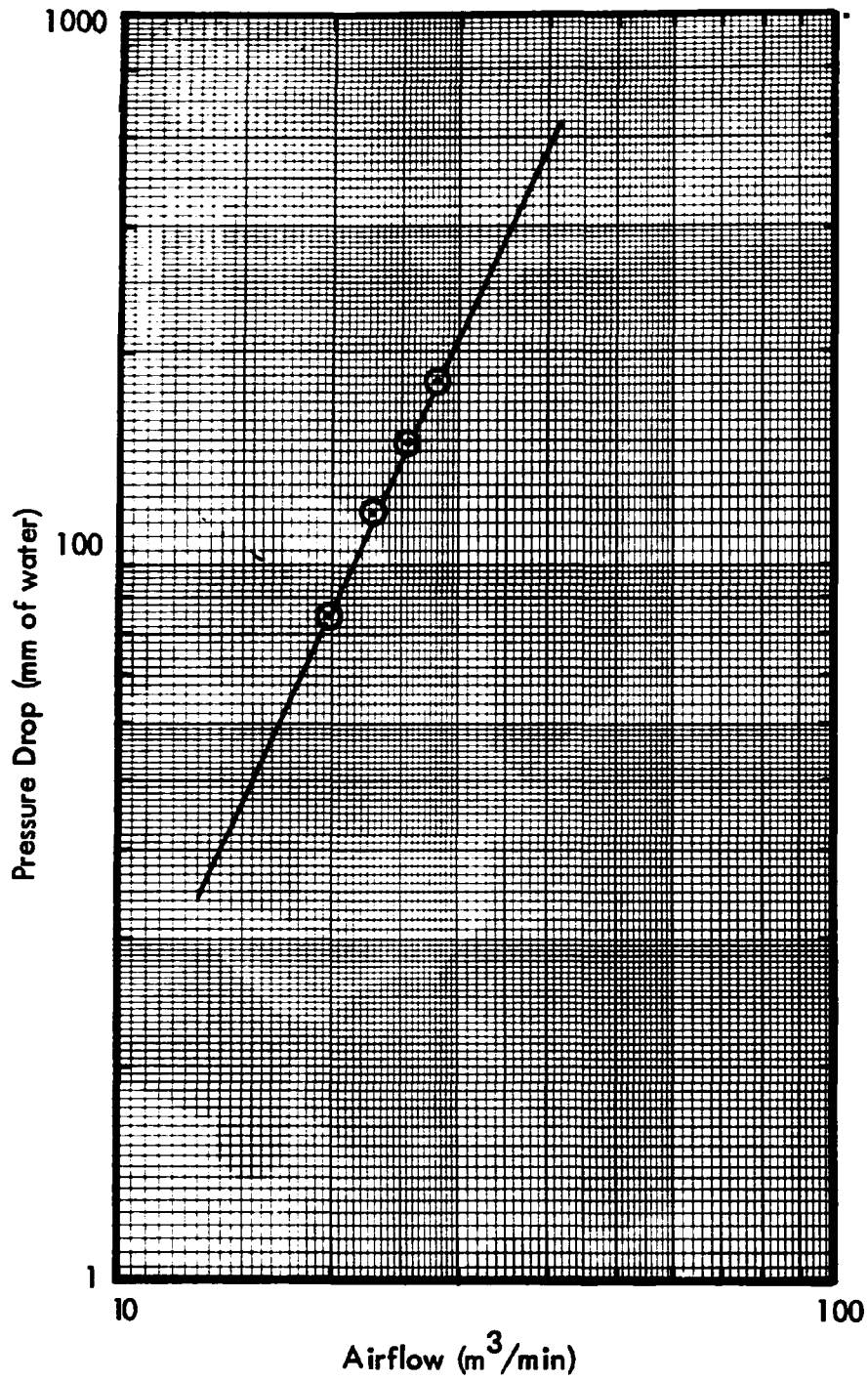


Figure 7-4. Pressure Drop Characteristics Field Test Unit at Cornelius Company

An upstream duct sample was scanned with an x-ray dispersive radiation technique. This scan indicated a low iron content in relation to bulk signal; consequently, it was estimated that approximately 80 percent of the welding fume could be organic or carbon base.

Samples of particulate material were viewed under an optical microscope. The majority of upstream particles appeared to be under  $1\text{ }\mu\text{m}$  in diameter. There also were some larger (up to  $20\text{ }\mu\text{m}$  in diameter) spherical-shaped particles that were apparently metallic. This shape indicated that these particles were generated with a welding torch. The large number of small organic particles was a result of oil contamination on the welded steel.

A six-stage Andersen dust sampler was used to sample the upstream duct. Table 7-1 presents the percent of emission in a given size range (Note: 56.1 percent of the particles are below  $0.3\text{ }\mu\text{m}$ ).

Table 7-1. Andersen Cascade Impactor Data for Cornelius Company - Upstream Particle Size

Particle Size Range (micrometer)	Upstream % Per Size Range	Upstream % Less Than Size
< 0.3	56.10	56.10
0.3 - 1.0	4.53	60.63
1.0 - 2.0	4.64	65.27
2.0 - 3.3	2.51	67.78
3.3 - 5.5	4.68	72.46
5.5 - 9.2	9.71	82.17
9.2 - 20.0	17.83	100.00

Figure 7-5 presents photographs of the particulate material, both upstream and downstream of the filter unit, collected on the fourth stage of the Andersen Cascade impactor. The fourth stage of the Andersen Cascade impactor collects particles ranging from 2.0 to 3.3  $\mu\text{m}$ . For the downstream sample, three stages were removed to obtain weighable samples in a reasonable amount of time. Consequently, the downstream fourth stage collected particles from 2.0 to 5.5  $\mu\text{m}$ . As expected, the upstream sample indicated the presence of some oil particles.

Both scanning electron micrographs and transmission electron micrographs confirmed the existence of a high number of submicrometer particles in the welding fume.

Figure 7-6 presents an SEM micrograph, at 10K magnification, of the ambient sample at the welding table. The 2.5  $\mu\text{m}$  spherical particle in the center of the photomicrograph is undoubtedly a metal particle formed during the welding operation.

Figure 7-7 shows SEM micrographs of both upstream and downstream samples, at 10K magnification.

Figure 7-8 is the same as Figure 7-7 except at 20K magnification.

Figure 7-9 presents SEM micrographs of the upstream sample of welding fume at 10K and 50K.

Figure 7-10 shows downstream samples at the same magnification. The space between the white bars is 0.5  $\mu\text{m}$ . One can readily see from these micrographs that there are many particles around 0.05  $\mu\text{m}$  in diameter. The dark and rather uniform circles in the Nuclepore membrane are holes which are all close to 0.4  $\mu\text{m}$  in diameter.

Transmission electron micrographs were also taken and are presented on Figures 7-11 and 7-12, at 10K and 50K, respectively. These micrographs indicate chains



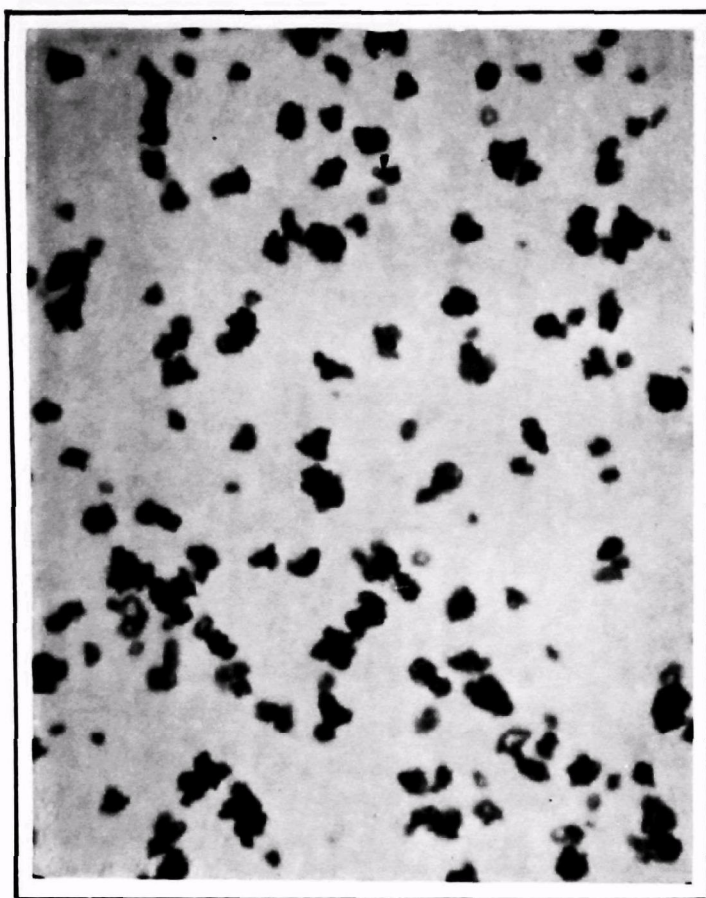
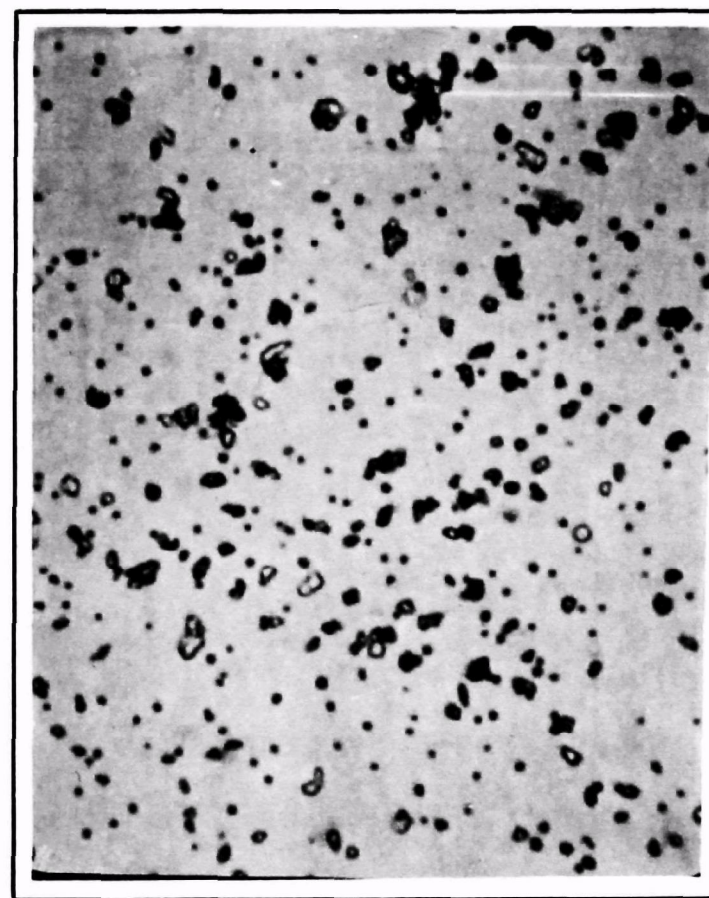
 $5 \mu\text{m}$ Downstream (2.0 - 5.5  $\mu\text{m}$ ) $5 \mu\text{m}$ Upstream (2.0 - 3.3  $\mu\text{m}$ )

Figure 7-5. 820 Magnification of Welding Fume - Stage 4 of Andersen Sampler (Downstream Sample Taken with 3 Stages Removed)

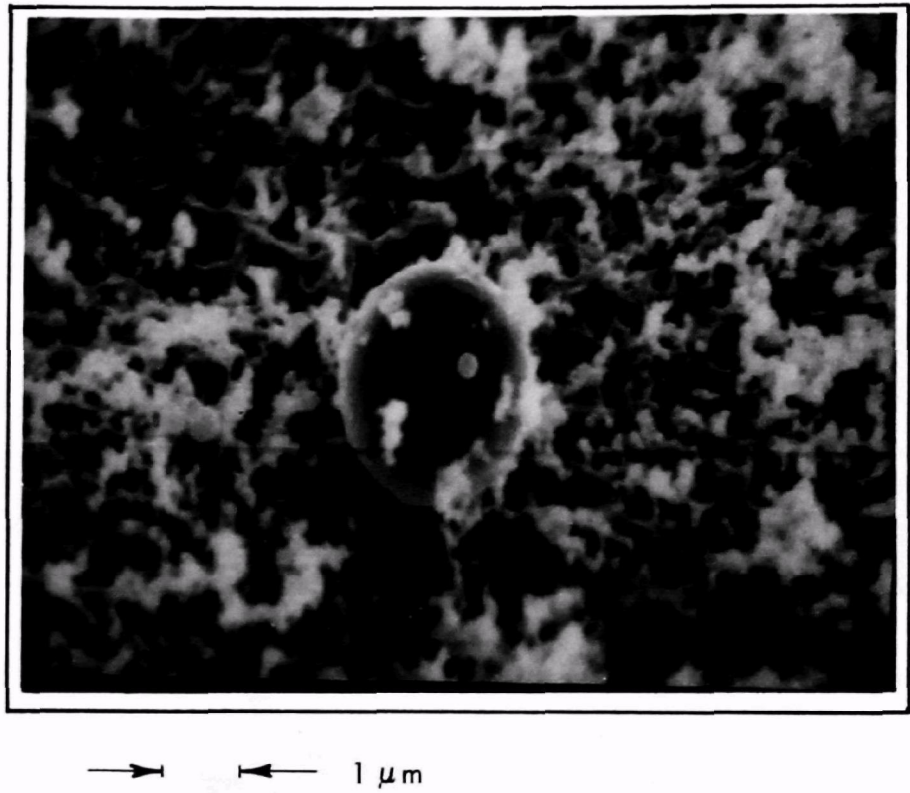
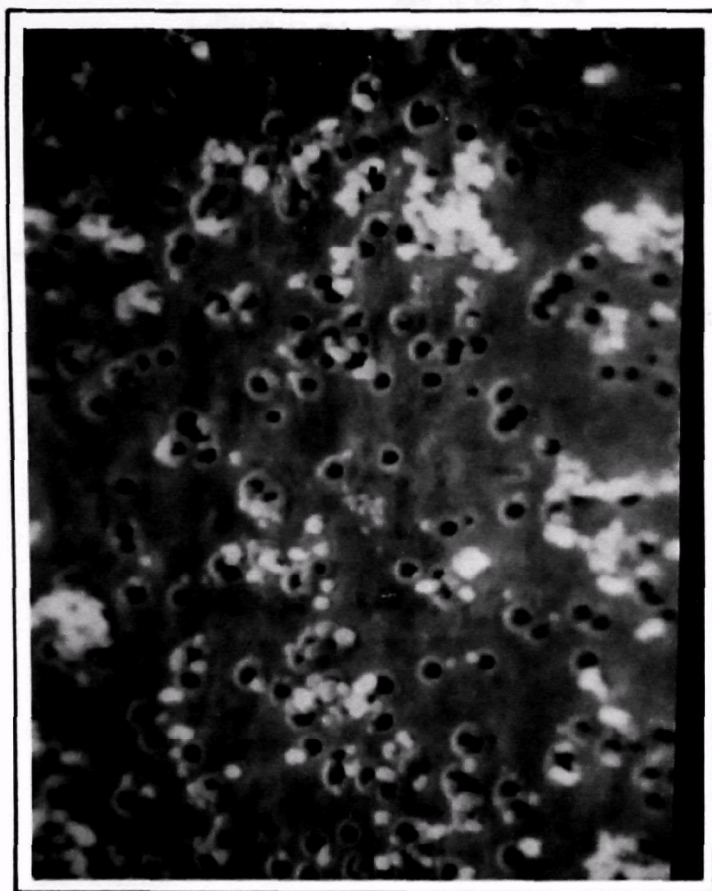
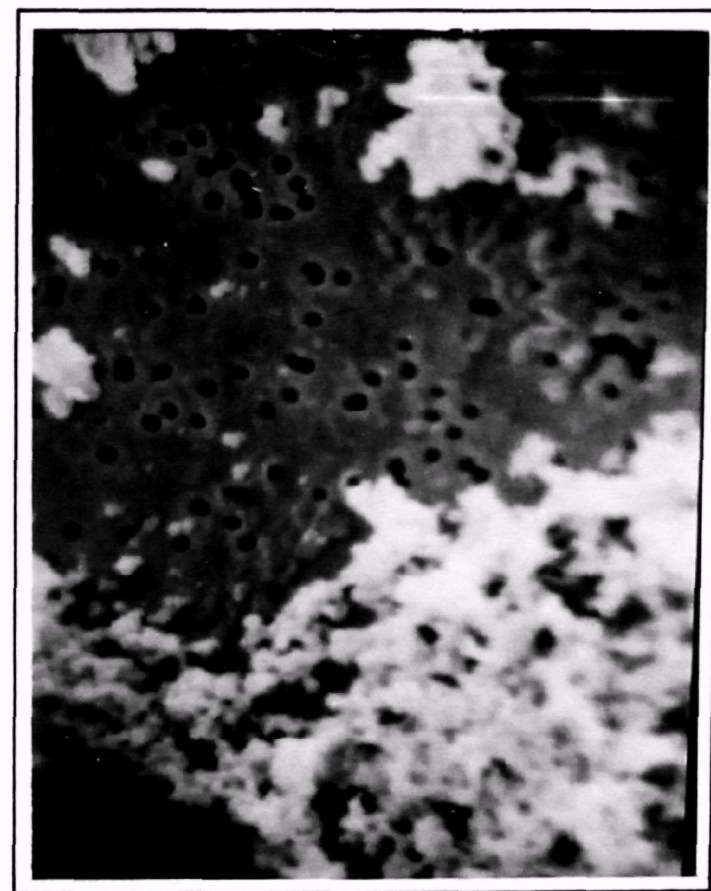


Figure 7-6. 10K SEM Micrograph of Ambient Welding Fume



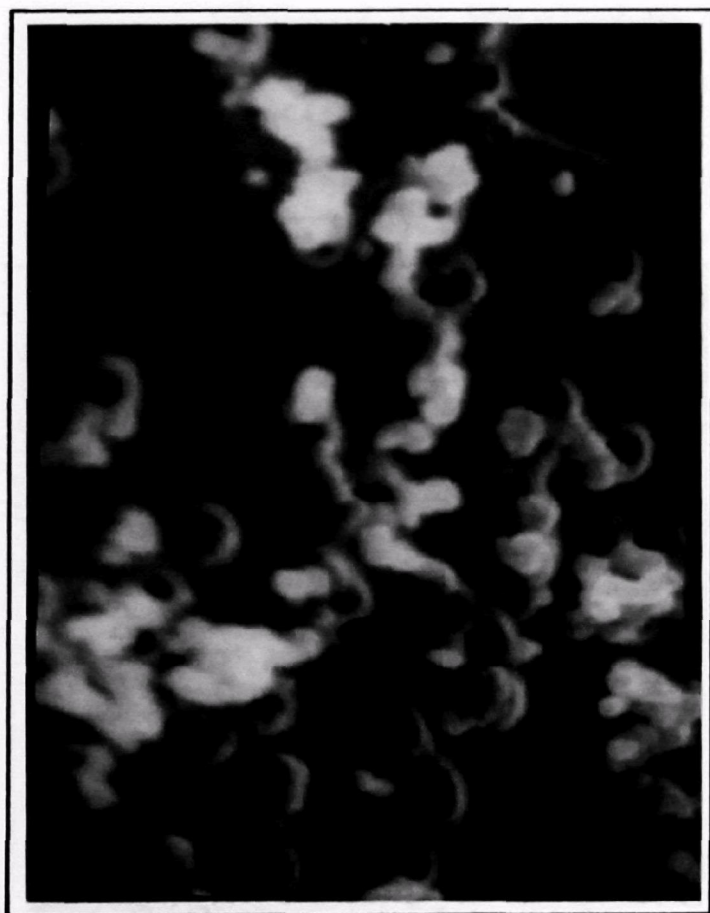
→ |← 1  $\mu$  m  
Downstream



→ |← 1  $\mu$  m  
Upstream

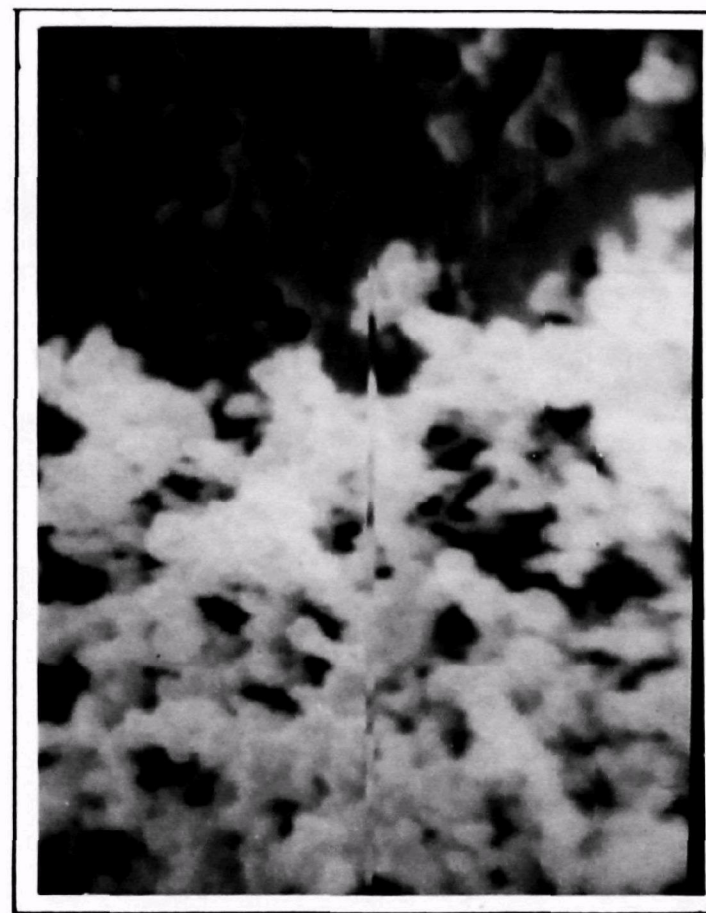
Figure 7-7. 10K SEM Micrograph of Upstream and Downstream Samples of Welding Fume





—→ ←— 1  $\mu$  m

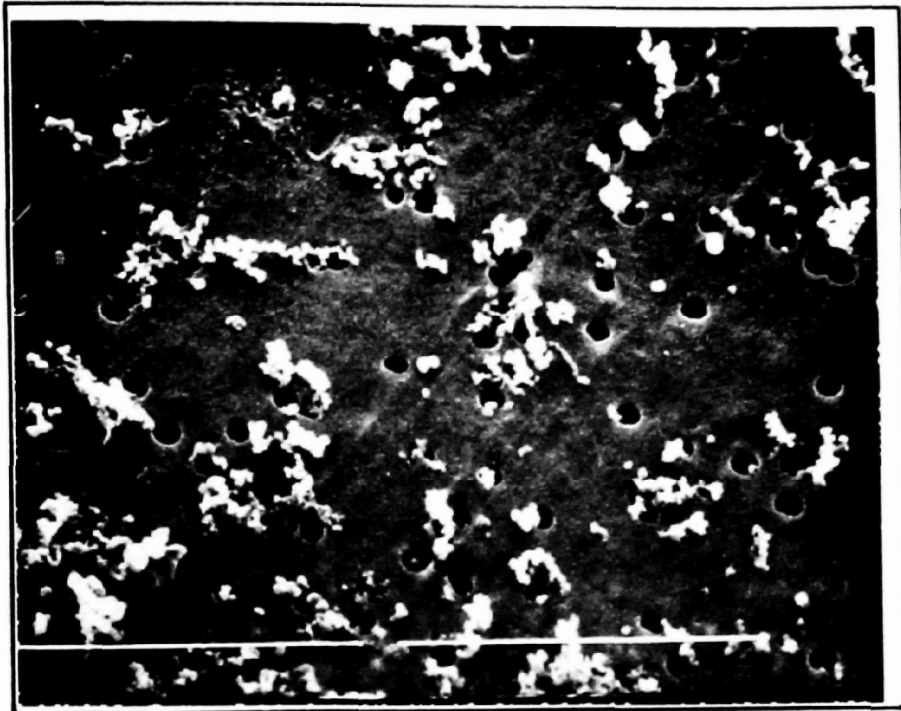
Downstream



—→ ←— 1  $\mu$  m

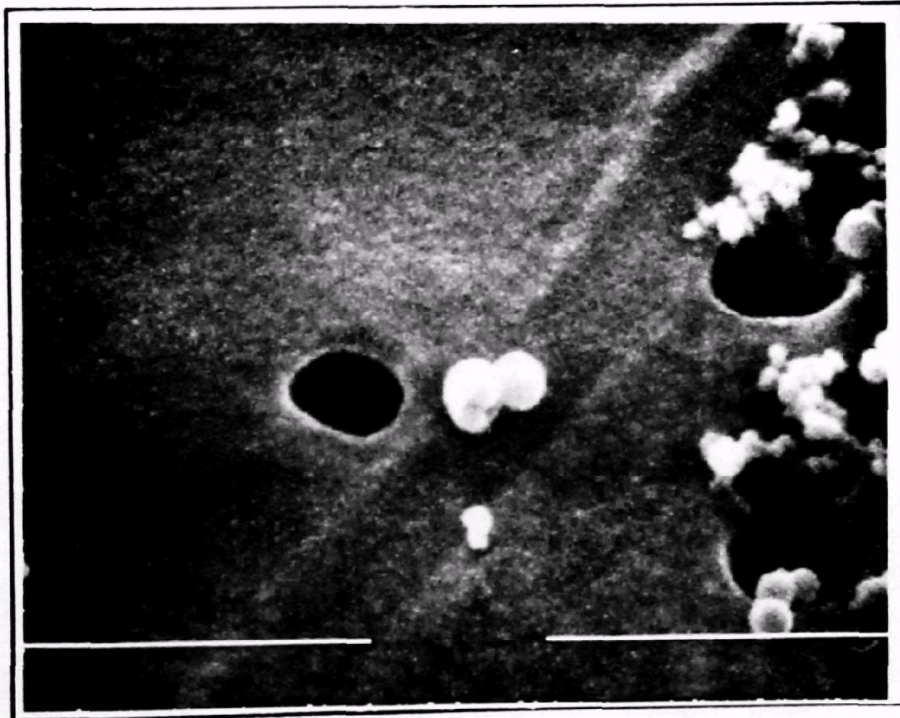
Upstream

Figure 7-8. 20K SEM Micrograph of Upstream and Downstream Samples of Welding Fume



Cornelius Upstream

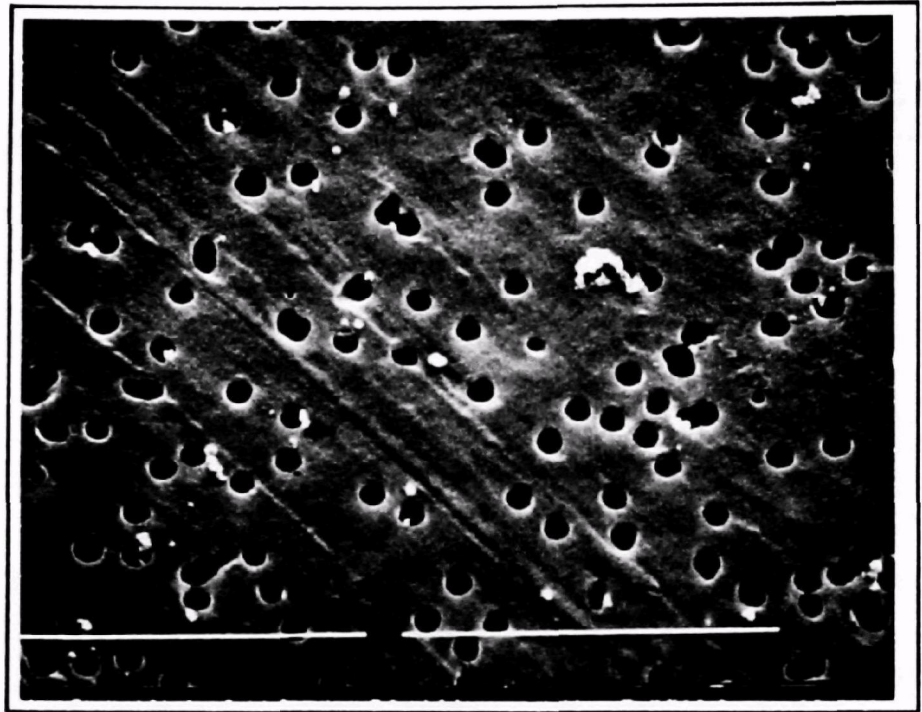
10,000X



Cornelius Upstream

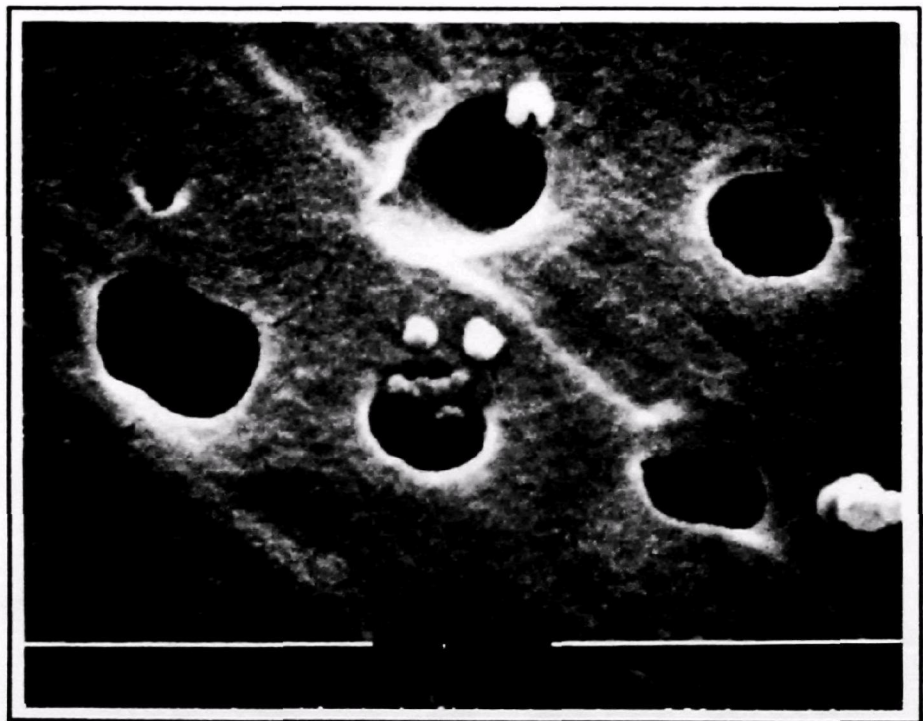
50,000X

Figure 7-9. SEM Micrographs of Welding Fume - Upstream



Cornelius Downstream

10,000X

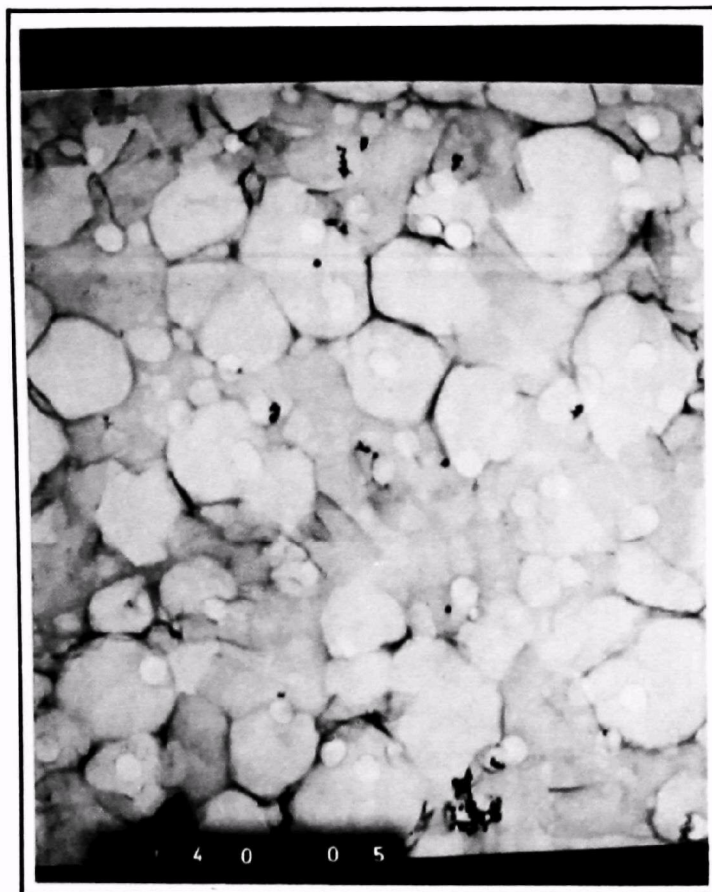


Cornelius Downstream

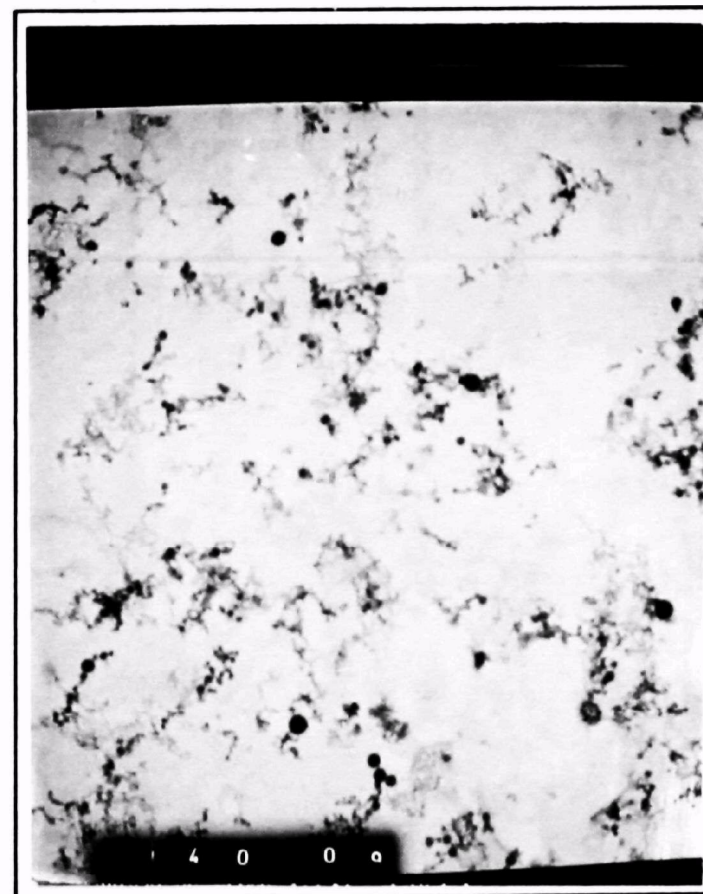
50,000X

Figure 7-10. SEM Micrographs of Welding Fume - Downstream



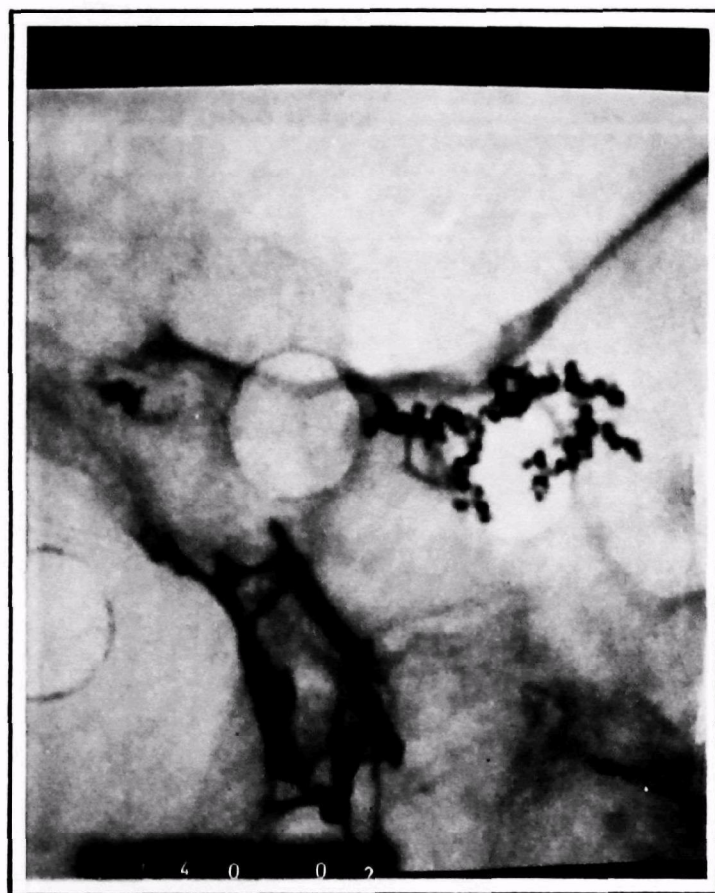


→ ← 1  $\mu$ m  
Downstream

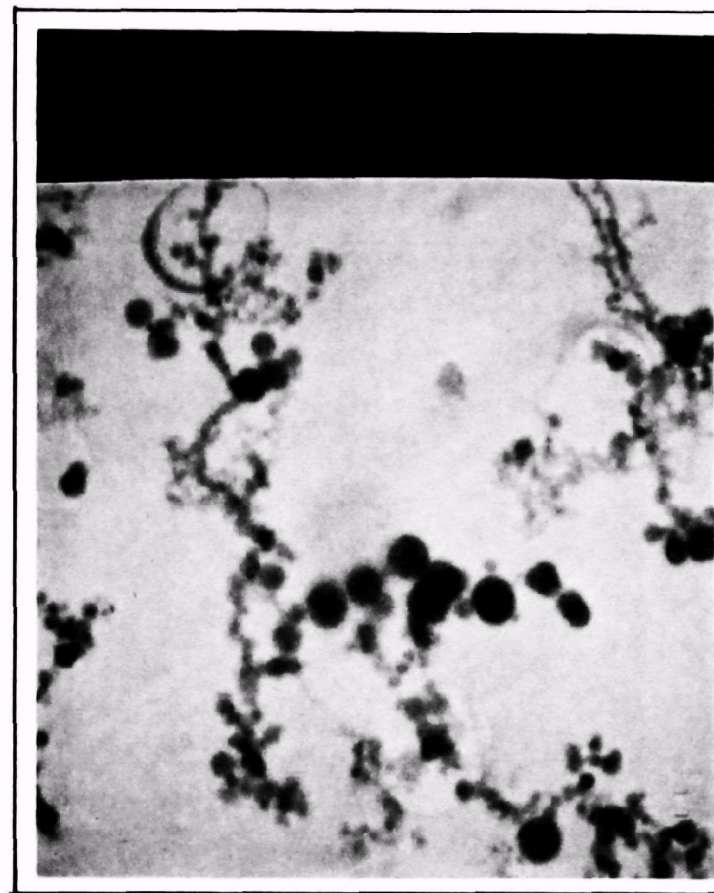


→ ← 1  $\mu$ m  
Upstream

Figure 7-11. 10K TEM Micrograph of Upstream and Downstream Samples of Welding Fume



→ ← 0.1 μm  
Downstream



→ ← 0.1 μm  
Upstream

Figure 7-12. 50K TEM Micrograph of Upstream and Downstream Samples of Welding Fume



of particulates or flocculates in both upstream and downstream samples. Again, many submicrometer particles are present in the samples.

#### 7.1.2 Performance Tests - Cornelius Company

The performance tests of the fine fiber cartridge filter unit of Cornelius Company involved the following: DOP penetration tests of clean cartridges, overall mass efficiency, fractional efficiency, filter dust loading and durability tests. The filter unit at Cornelius Company was operated at an air-to-cloth ratio of 35 mm/sec for all field performance tests.

The filter cartridges were tested for DOP efficiency prior to field tests. Table 7-2 presents the efficiency on  $0.3 \mu m$  diameter DOP particles. The tests were run at an air-to-cloth ratio of 50 mm/sec.

Gravimetric samples were taken simultaneously, upstream and downstream of the filter unit, to determine the overall mass efficiency which is presented in Table 7-3. (The average of five different efficiencies is 97.6 percent.) Also presented in this table is the upstream concentration. The concentration of particles at this site was relatively low (less than  $1.0 \text{ mg/m}^3$ ).

Fractional efficiency data was obtained using an Andersen Cascade impactor. Because of the low downstream concentrations, only three of the six stages were used so that weighable samples could be obtained. Only one Andersen dust sampler was used for these tests so the upstream and downstream samples were not concurrent. Table 7-4 presents the fractional efficiency data obtained at Cornelius Company.

**Table 7-2. DOP Efficiency of Cartridges for Field Test at Cornelius Company**

Element No.	Efficiency on 0.3 $\mu$ m dia. DOP	Air-to-Cloth Ratio	
		DOP Test	Field Test
F1	85%	50 mm/sec	35 mm/sec
F3	95	50	35
F5	80	50	35

**Table 7-3. Overall Mass Efficiency for Field Test at Cornelius Company**

Upstream Concentration (mg/m <sup>3</sup> )	Overall Mass Efficiency (%)
0.666	97.6%
0.715	99.3
0.599	97.0
0.600	95.7
0.916	98.4
	<u>97.6% average</u>

**Table 7-4. Fractional Efficiency for Field Test at Cornelius Company**

Particle Size Range (micrometers)	Efficiency (%)
<0.3	91.7%
0.3 - 2.0	87.1
2.0 - 5.5	79.8
5.5 - 20.0	95.0

The pressure drop and media durability of the filter unit were monitored throughout the field tests. The pressure drop of the unit rose from 182.5 mm H<sub>2</sub>O to 342.9 mm H<sub>2</sub>O and remained stable. The filter media maintained its integrity throughout the test. Figure 7-13 presents a curve of operating pressure drop versus time.

These field tests were terminated on 15 July 1977 after 87.2 hours of operation at the request of Cornelius Company. The request was prompted by their need for the floor space that the filter unit occupied. Both the accumulated operating time and the dust loading were quite low during the test period because of infrequent use of the welding table. Consequently, the premature removal of this unit did not pose any problem, and the sampling tests at this site were accomplished. A photograph of a dirty element from the test side next to a clean element is shown on Figure 7-14. The contaminant is similar in appearance to soot.

Laboratory tests were conducted on the filter unit which was removed from Cornelius Company to determine the durability of the filter medium with regard to cleaning pressure. These tests consisted of operating the unit at an accelerated cleaning pulse interval; and periodically measuring the DOP penetration across the unit. The inlet temperature was ambient and no dust was fed. The unit was run at an air-to-cloth ratio of 35 mm/sec and a cleaning pressure of 689 K Pa. To accelerate the test, each element was pulsed at a rate of one element every five seconds, instead of 20 seconds. DOP penetration tests indicated no media failure after 112,626 cleaning pulses per element (equivalent to 1877.1 hours of operation time for a filter unit with each element being cleaned every 20 seconds).

Table 7-5 presents the DOP penetration data taken during the tests. Initially, DOP penetration was at 0.50 percent, with 5,706 pulses per element, which includes the number of pulses accumulated from tests at Cornelius Company. On 30 August 1977, DOP penetration was 1.9 percent after 112,623 pulses per element. The filter unit pressure drop decreased from 312.42 mm H<sub>2</sub>O to 279.40 mm H<sub>2</sub>O. The increase in DOP penetration and the decrease in pressure drop can both be attributed

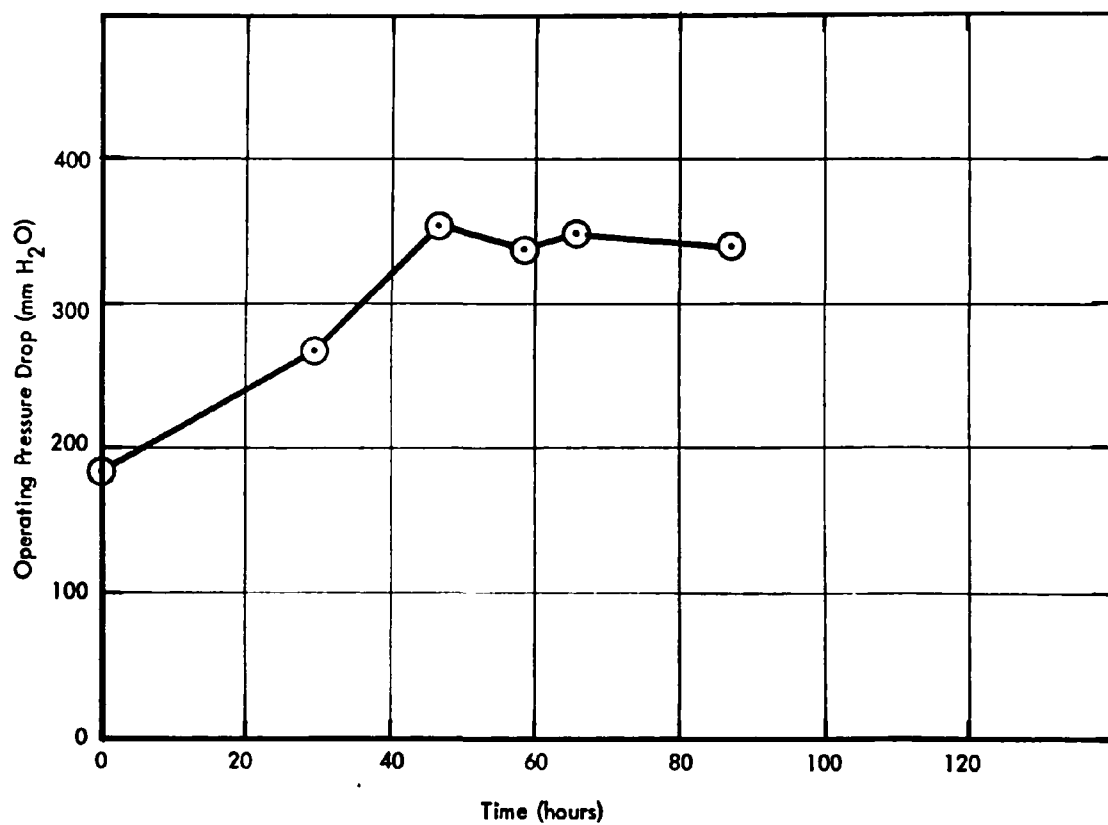


Figure 7-13.: Operating Pressure Drop as a Function of Time (Cornelius Company)

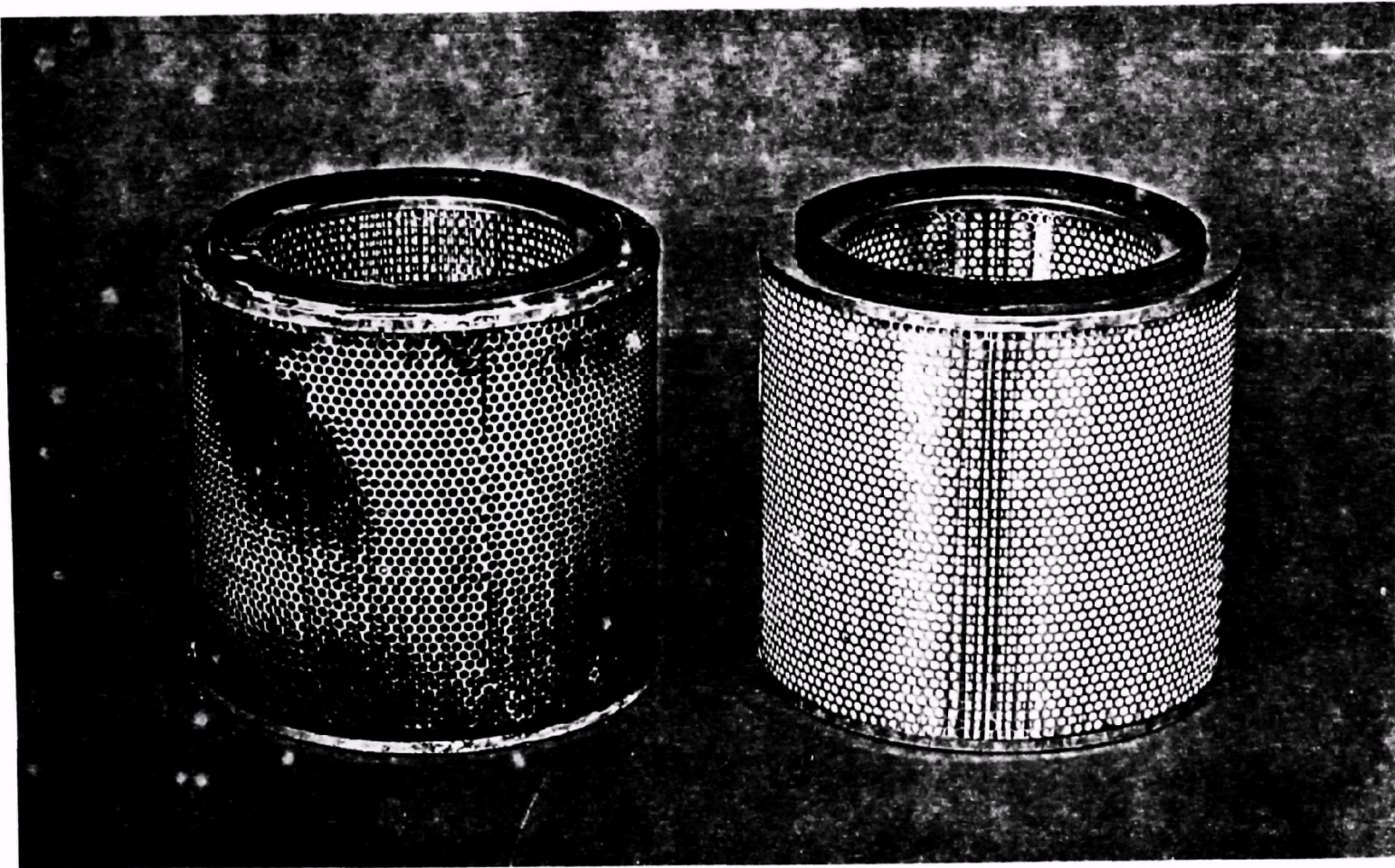


Figure 7-14. Dirty versus Clean Filter Elements -  
Cornelius Company - Welding Fume

**Table 7-5. Pulse-Cleaning Durability Tests**

<b>Date</b>	<b>Accumulated Pulses per Element</b>	<b>Equivalent Operating Time (hrs)</b>	<b>Unit Pressure Drop (mm H<sub>2</sub>O)</b>	<b>DOP Penetration (%)</b>
8/5/77	5,706	95.1	312.42	0.50
8/8/77	6,186	103.1	299.72	0.30
8/9/77	6,690	111.5	322.58	0.30
8/10/77	7,194	119.9	317.50	0.32
8/11/77	8,634	143.9	309.88	0.46
*8/12/77	9,954	165.9	--	--
8/12/77	10,410	173.5	304.80	0.64
8/15/77	27,714	461.9	284.48	1.20
8/16/77	32,274	537.9	287.02	1.50
8/18/77	43,602	726.7	287.02	1.50
8/21/77	66,642	1110.7	287.02	1.60
8/23/77	84,042	1400.7	287.02	1.50
8/30/77	112,626	1877.1	279.40	1.90

\*Increased pulse interval from once every 20 seconds to once every 5 seconds.

**Table 7-6. Andersen Cascade Impactor Data for  
Northern Malleable - Upstream Particle Size**

<b>Particle Size Range (micrometers)</b>	<b>Upstream % Per Size Range</b>	<b>Upstream % Less Than Size</b>
< 0.3	13.80	13.80
0.3 - 1.0	11.06	24.86
1.0 - 2.0	28.83	53.69
2.0 - 3.3	19.92	73.61
3.3 - 5.5	12.03	85.64
5.5 - 9.2	8.40	94.03
9.2 - 20.0	5.97	100.00

to the cleaning of the dust cake from the elements that accumulated during the tests at Cornelius Company.

These tests were prompted by an element failure at an air-to-cloth ratio of 25 mm/sec, at Northern Malleable Iron Company. However, the damaged elements were not only subjected to the cleaning pulses but also to dust loading and an inlet temperature of 150°F. These elements had a greater pressure drop across the media due to the dust loading, resulting in greater deflection and stresses in the media during pulsing.

## 7.2 Tests at Northern Malleable Iron Company (Magnesium Oxide Emission)

The field tests began at Northern Malleable Iron Company in April 1977. The emissions at this site are from a manganese inoculation process in the making of malleable iron. (A high percentage of magnesium oxide emanates from this process.) Figure 7-15 illustrates these emissions. Immediately behind the cupola, next to the person in this photograph, is a vertical ventilation hood. Air is drawn through this hood and is routed through ducting to a baghouse dust collector located on the outside of the building. The fine fiber filter unit was located next to the baghouse. A portion of the air going to the baghouse was routed to the fine fiber filter unit.

Figure 7-16 depicts the installation at Northern Malleable.

Figure 7-17 is a schematic illustration of the test setup. The unit was run at three different air-to-cloth ratios during the testing: 35 mm/sec, 25 mm/sec, and 12 mm/sec. The pressure drop was monitored throughout the testing. The pressure drop did not stabilize while operating at an air-to-cloth ratio of 35 mm/sec. The elements were subsequently replaced and the test run at 25 mm/sec. Again, the pressure drop did not stabilize and again a media failure occurred between 408.6 hours and 539.6 hours of operation. The elements were again replaced and the unit was run at an air-to-cloth ratio of 12 mm/sec until 30 August 77. The unit accumulated 443.2 hours of operation without failure and the pressure drop was stabilized.



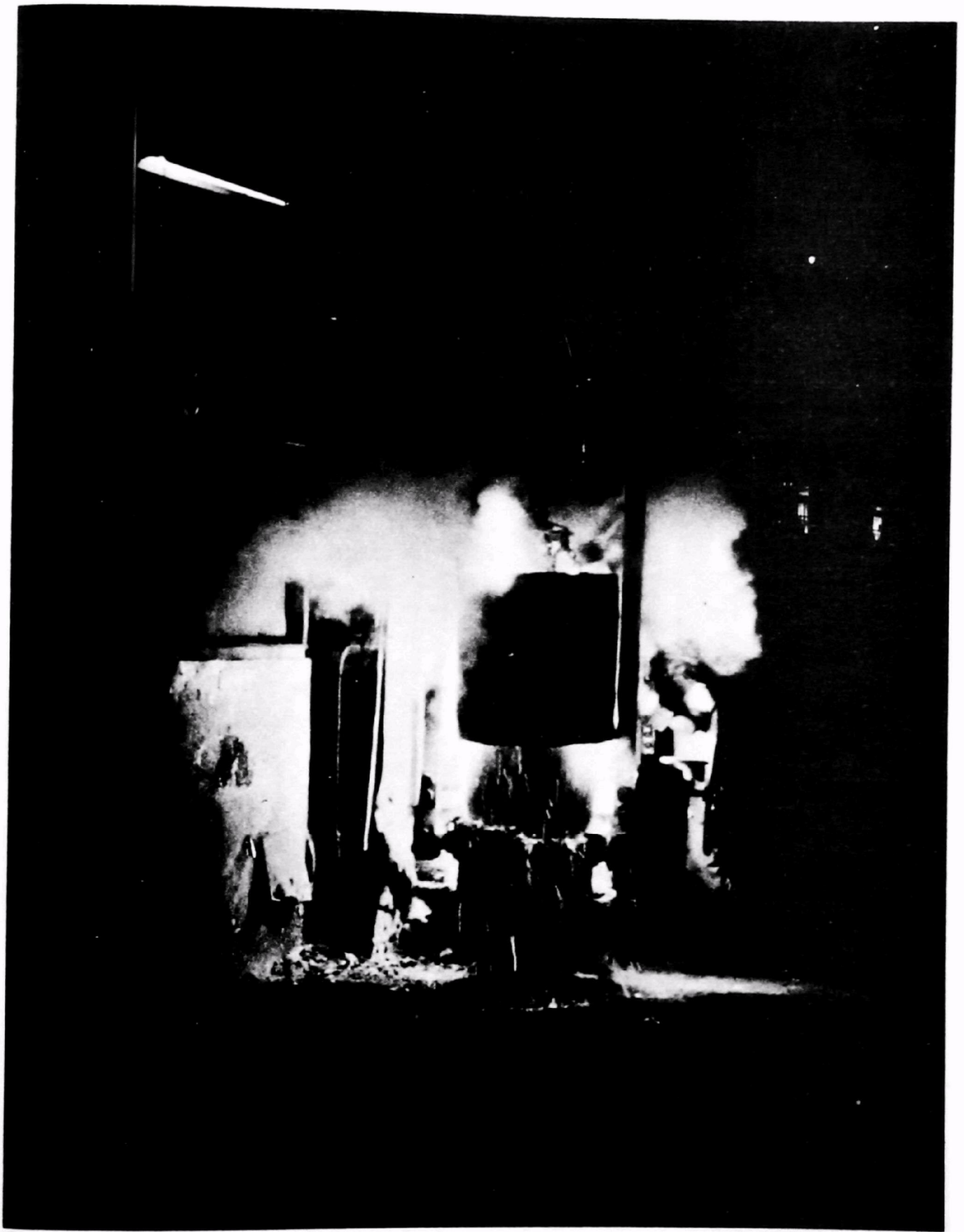


Figure 7-15. Inoculation Process at Northern Malleable Iron Company

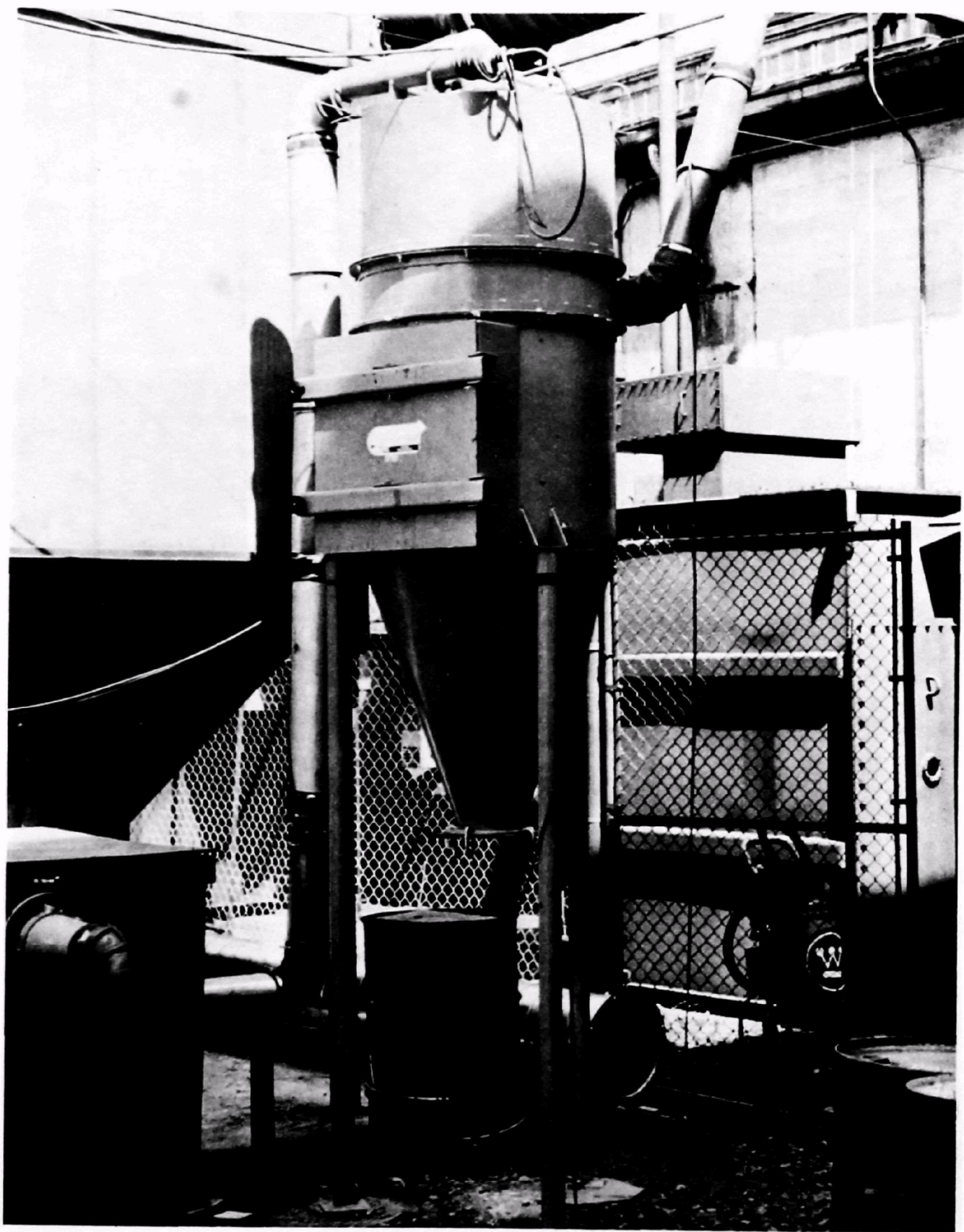


Figure 7-16. Installation at Northern Malleable Iron Company

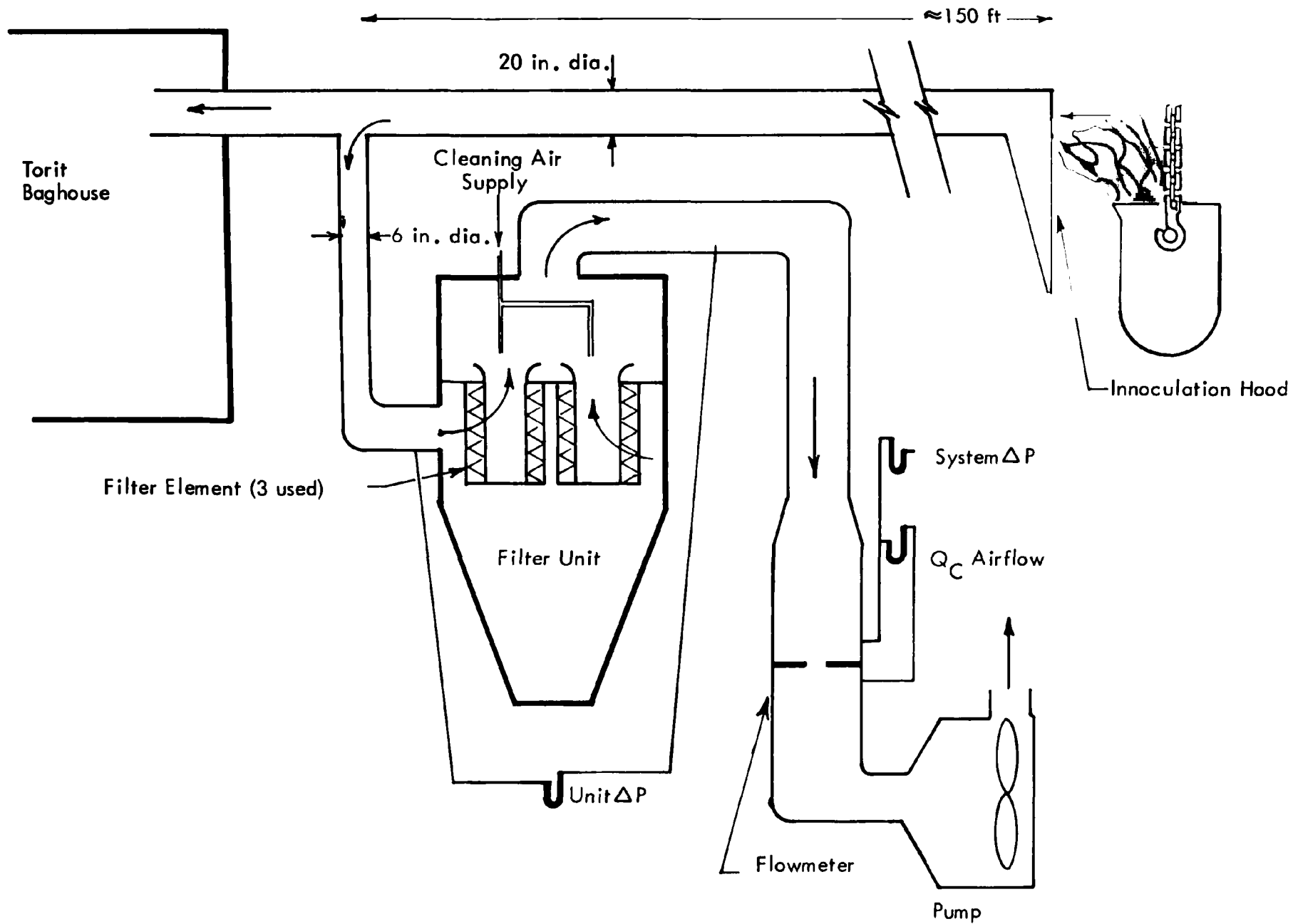


Figure 7-17. Test Setup at Northern Malleable Iron Company

### 7.2.1 Particulate Characterization (Magnesium Oxide Emission)

In order to characterize the magnesium oxide emission, the following analyses were performed: Coulter Counter, Andersen Cascade Impactor sampling, scanning electron microscopy, transmission electron microscopy and x-ray analysis.

Coulter Counter analysis was performed on samples of the emission taken at a point 2.4 meters above the inoculating process and from the collected particles in the bin of the baghouse. Figure 7-18 presents the particle size spectrums. (Note: the D50 of the sample in the baghouse bin is less than  $2.4\text{ }\mu\text{m}$ ).

An x-ray dispersive radiation technique was used to scan particles on both upstream and downstream samples. Analysis of a large cubic particle on a downstream sample revealed that it was high in magnesium. Magnesium oxide has a typical cubic shape. A spherical particle from the upstream sample was found to be comprised mostly of manganese and iron. A relatively high content of silica was also present.

A six-stage Andersen dust sampler was used to sample the upstream duct. Table 7-6 presents the percent of emission in a given size range. Over 53 percent of the particles are below  $2.0\text{ }\mu\text{m}$ .

Scanning electron micrographs and transmission electron micrographs both confirmed the existence of a high number of submicrometer particles in the magnesium oxide emission.

Figure 7-19 depicts transmission electron micrographs of the MgO particulate from upstream and downstream samples at 10K magnification. One can readily see the cubic shape of the MgO particles and a large number of submicrometer particles.

Scanning electron micrographs are shown on Figures 7-20 and 7-21 at 2K and 10K magnification. Figure 7-20 is the upstream sample and Figure 7-21 presents the downstream sample. (The space between the white lines is  $0.5\text{ }\mu\text{m}$ ). These micrographs also show the characteristic cubic shape of the magnesium oxide particulate.



% LESS THAN STATED SIZE

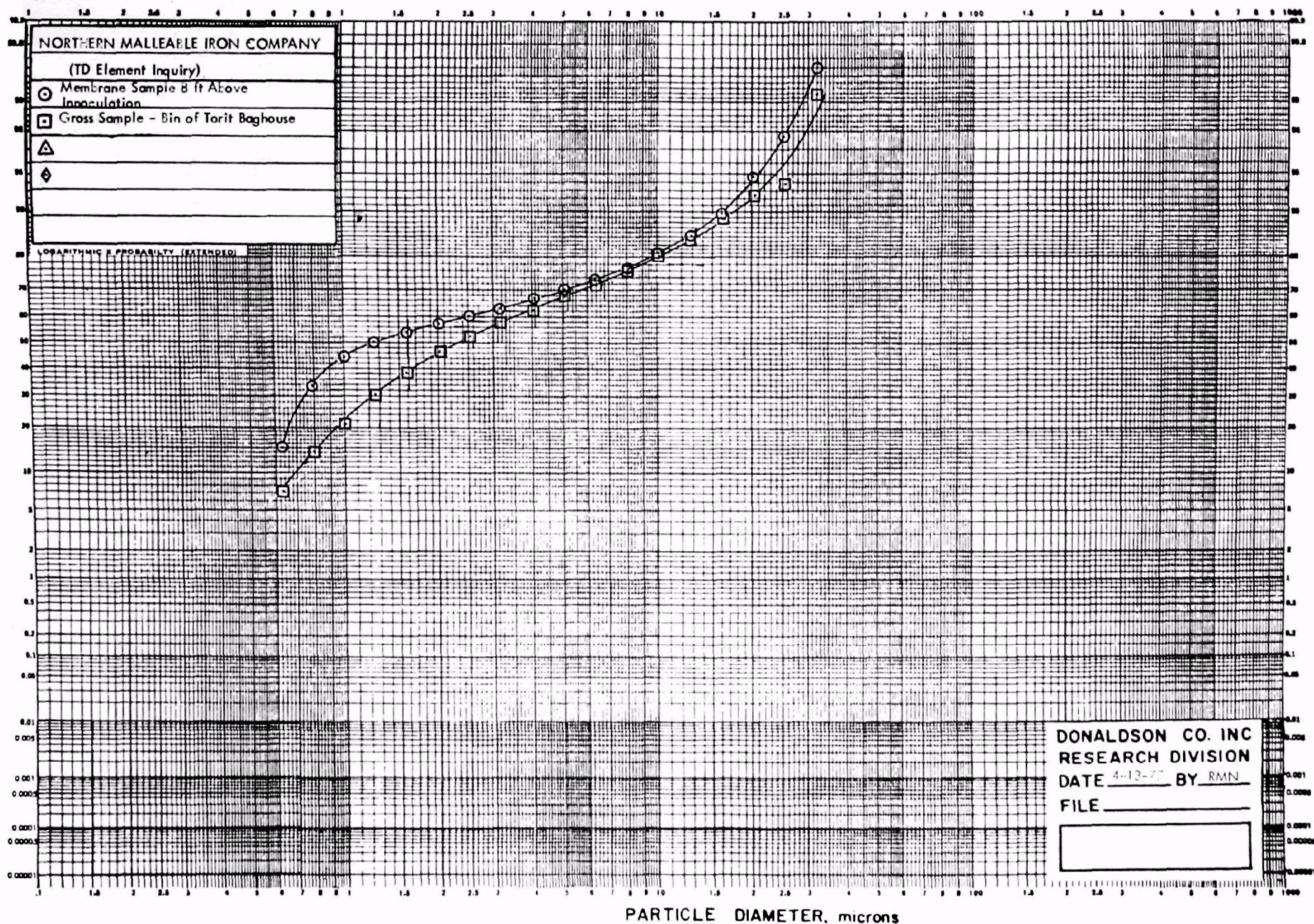
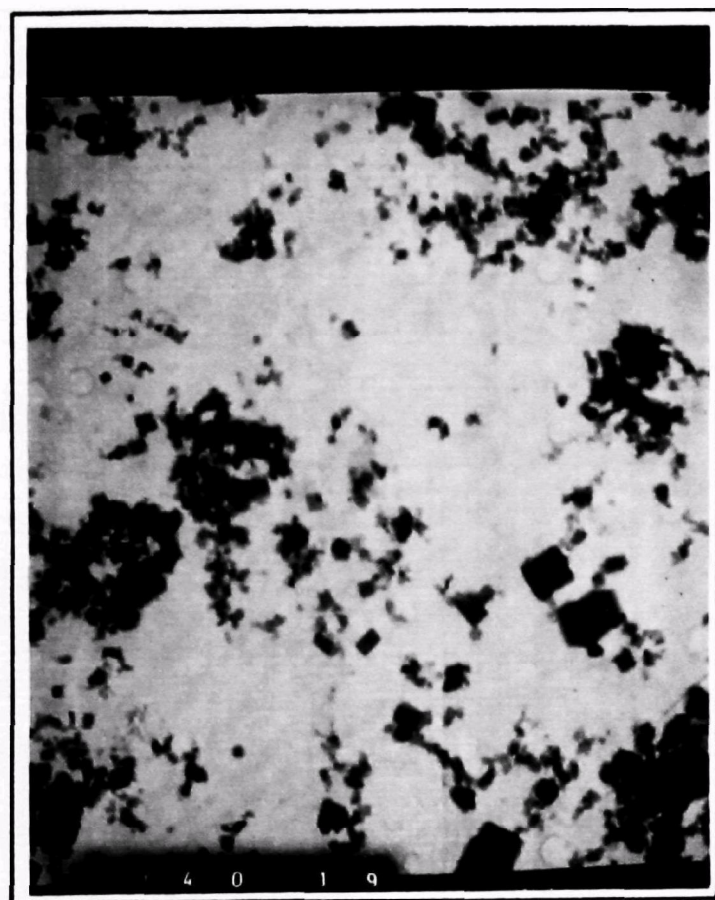
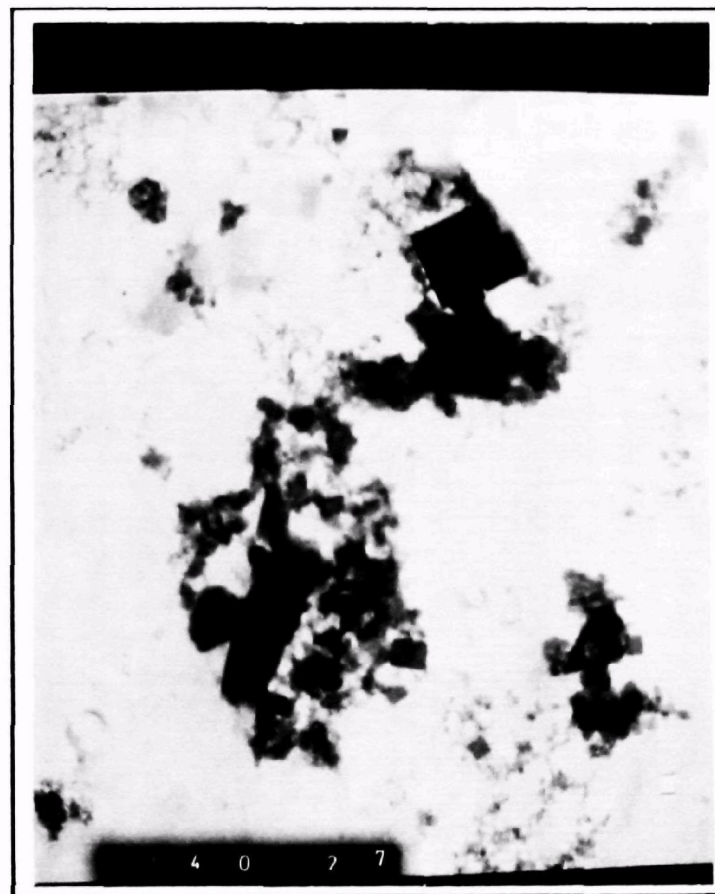


Figure 7-18. Particle Size Spectrum Analysis Northern Malleable Iron Company



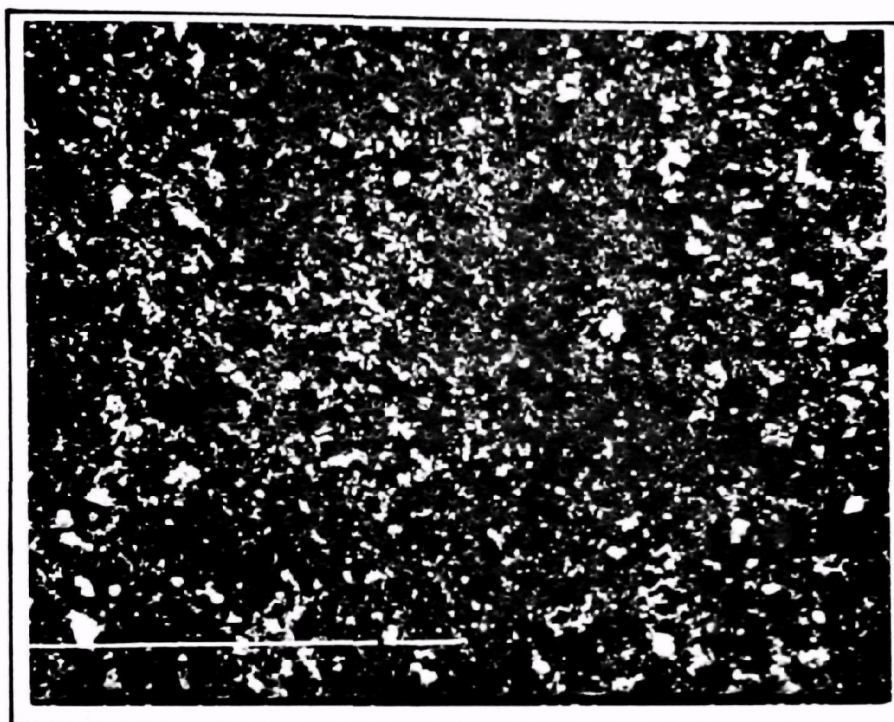


→ ← 1 μm  
Downstream



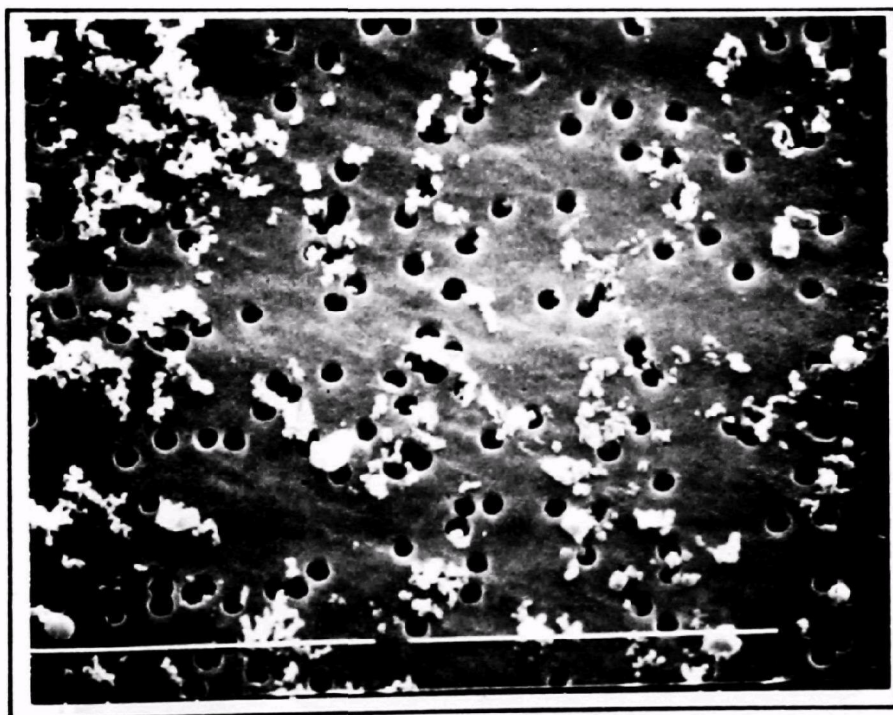
→ ← 1 μm  
Upstream

Figure 7-19. 10K TEM Micrograph of Upstream and Downstream Samples of MgO Particulate



Northern Upstream

2,000X

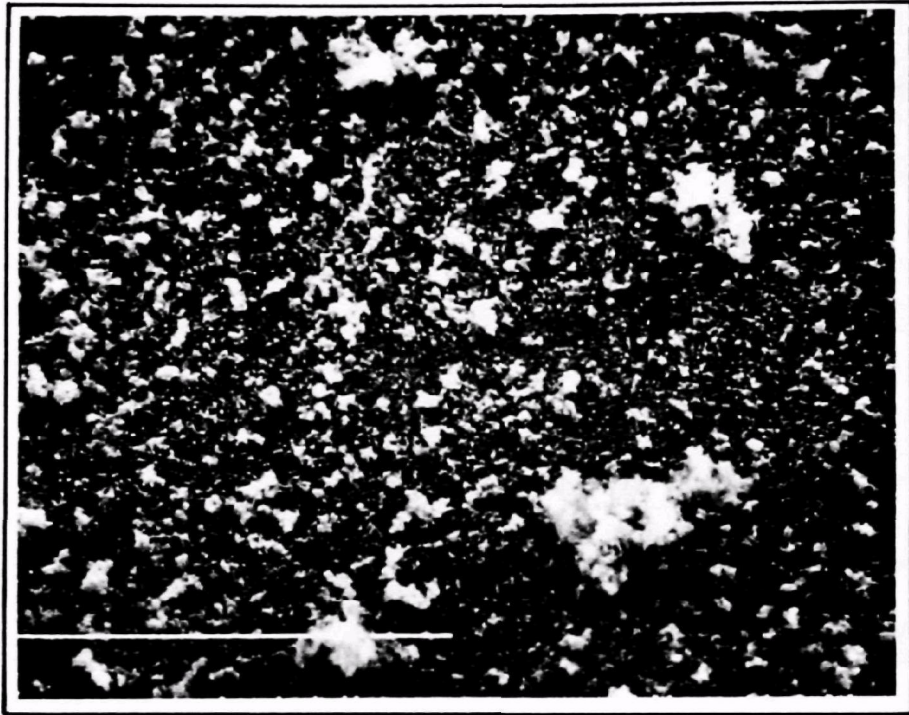


Northern Upstream

10,000X

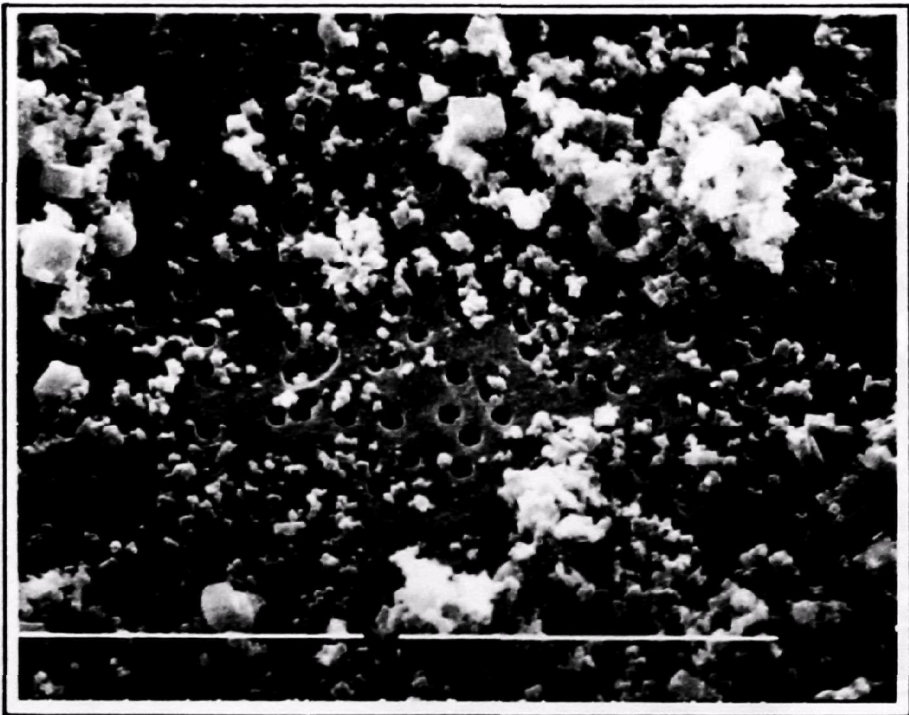
Figure 7-20. SEM Microaraphs of Mg O Particulate - Upstream





Northern Downstream

2,000X



Northern Downstream

10,000X

Figure 7-21 . SEM Micrograph of Mg O Particulate - Downstream



The dark and rather uniform circles are the holes in the Nuclepore membrane. A greater number of large particles is apparent in the downstream sample than the upstream sample showing that some solubility penetration is occurring. (Magnesium oxide is slightly soluble in water and also in acids and ammonium salts).

## 7.2.2 Performance Tests - Norther Malleable Iron Company

The performance tests of the fine fiber cartridge filter unit at Northern Malleable Iron Company involved the following: DOP penetration tests of clean cartridges, overall mass efficiency, fractional efficiency, filter dust loading and durability. The filter unit at Northern Malleable was operated at air-to-cloth ratios of 35 mm/sec, 25 mm/sec, and 12 mm/sec.

The filter elements were tests for DOP efficiency prior to field tests. Table 7-7 presents the efficiency on 0.3  $\mu\text{m}$  diameter DOP particles. These tests were run at an air-to-cloth ratio of 50 mm/sec.

Table 7-7. DOP Efficiency of Elements for Field Test at Northern Malleable Iron Co.

Element No.	Efficiency on 0.3 $\mu\text{m}$ dia. DOP	Air-to-Cloth Ratio	
		DOP Test	Field Test
F2	91%	50 mm/sec	35 mm/sec
F4	90	50	35
F6	90	50	35
F7	95	50	25
F8	97	50	25
F9	94	50	25
F10	Not available	--	12
F11	Not available	--	12
F12	Not available	--	12

Gravimetric samples were taken simultaneously upstream and downstream of the filter unit to determine overall mass efficiency. Table 7-8 presents the overall mass efficiency data. The average of two different efficiency tests is 99.95 percent. Also presented in this table is the upstream concentration. The concentration of particulate material at this site was many times higher than at Cornelius Company ( $185.4 \text{ mg/m}^3$  average for Northern Malleable versus  $0.7 \text{ mg/m}^3$  average at Cornelius).

Table 7-8. Overall Mass Efficiency for Field Test at Northern Malleable Iron Co.

Upstream Concentration ( $\text{mg/m}^3$ )	Overall Mass Efficiency (%)
179.0	99.96%
191.7	<u>99.93</u>
	99.95% average

Fractional efficiency data was obtained using an Andersen Cascade Impactor. Because the downstream concentrations are very low, only three of the six stages were used so that weighable samples could be obtained. Only one Andersen dust sampler was used so the upstream and downstream samples were not concurrent. Table 7-9 presents the fractional efficiency data.

Table 7-9. Fractional Efficiency for Field Test at Northern Malleable Iron Co.

Particle Size Range (micrometers)	Efficiency (%)
<0.3	96.63
0.3 - 2.0	99.04
2.0 - 5.5	97.92
5.5 - 20.0	98.53

The pressure drop and media durability of the system were monitored throughout the field tests. Initially, the filter unit was run at an air-to-cloth ratio of 35 mm/sec. After 160 hours of operation at this air-to-cloth ratio, the system pressure drop had increased from 182.88 mm H<sub>2</sub>O to 571.5 mm H<sub>2</sub>O. The cartridges were subsequently replaced and the air-to-cloth ratio adjusted to 20 mm/sec. Testing was continued until 539.6 hours had accumulated, at which time the filter unit restriction had risen to 546.1 mm H<sub>2</sub>O and dust was visibly passing through the filter unit. This failure occurred sometime between 408.6 hours and 539.6 hours. The filter elements were inspected and it was found that the substrate media had fatigued and there were holes in the media.

Figure 7-22 shows a filter element loaded with the white magnesium oxide compared to a clean filter element.

Figure 7-23 shows one of the holes that developed in the filter medium during the tests at an air-to-cloth ratio of 25 mm/sec. (It appears as a very light area because the element is illuminated from inside with a lightbulb). It is felt that, as the pressure drop across the medium increased due to dust loading, there was greater deflection and stress in the medium during pulse cleaning. Also, the inlet temperature of the gas at this site is 150°F. A stronger substrate medium would probably alleviate this problem. Tests were resumed at Northern Malleable with clean filter cartridges and were run at an air-to-cloth ratio of 12 mm/sec. No failures occurred after 443.2 hours of operation. The pressure drop appeared stable at approximately 290 mm H<sub>2</sub>O.

Figure 7-24 presents the operating pressure drop as a function of time for the three air-to-cloth ratios 35 mm/sec, 25 mm/sec, and 12 mm/sec. The tests at 12 mm/sec concluded the field testing to be performed under this contract as of 30 August 1977.

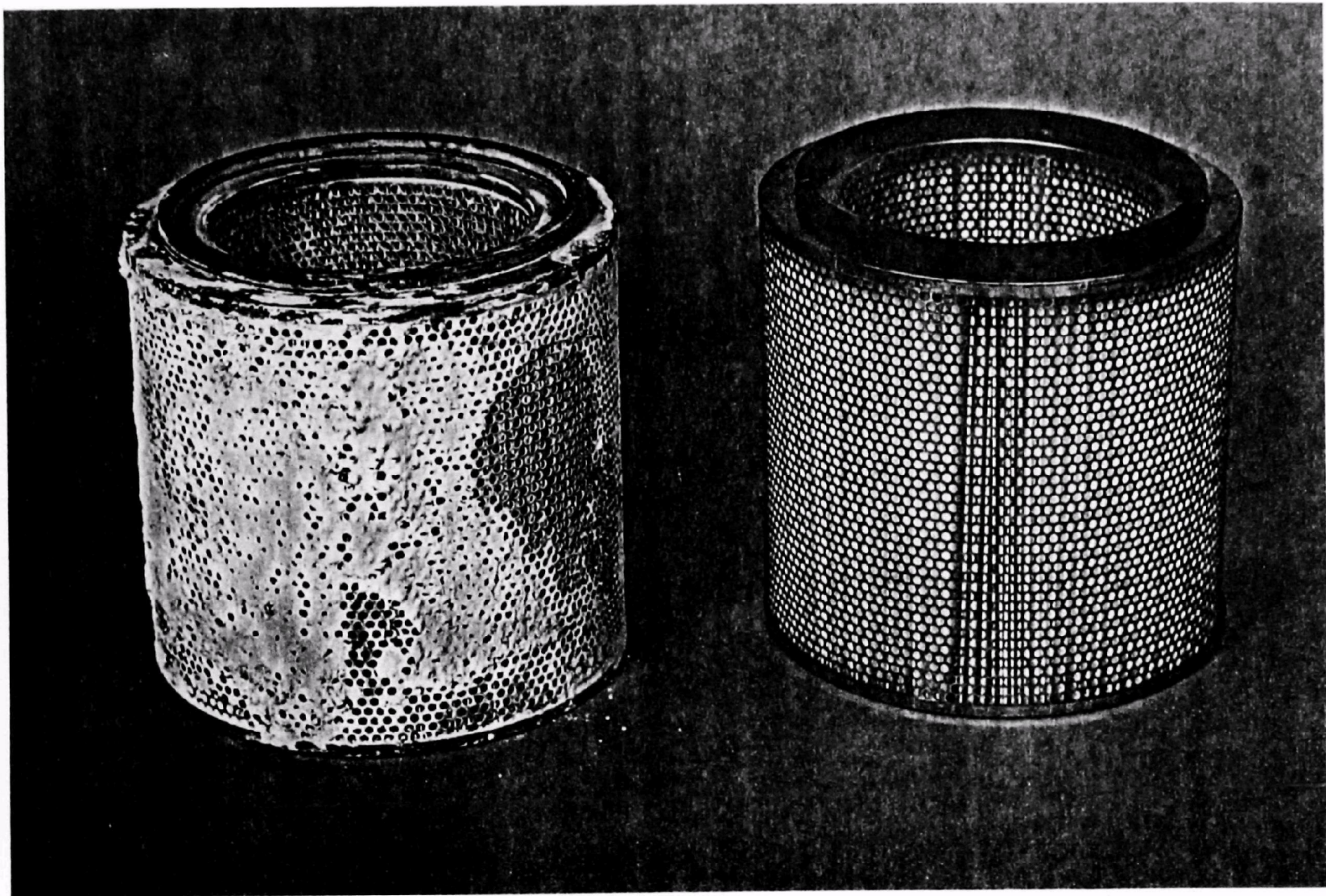


Figure 7-22. Dirty versus Clean Filter Cartridges -  
Northern Malleable -MgO Emission



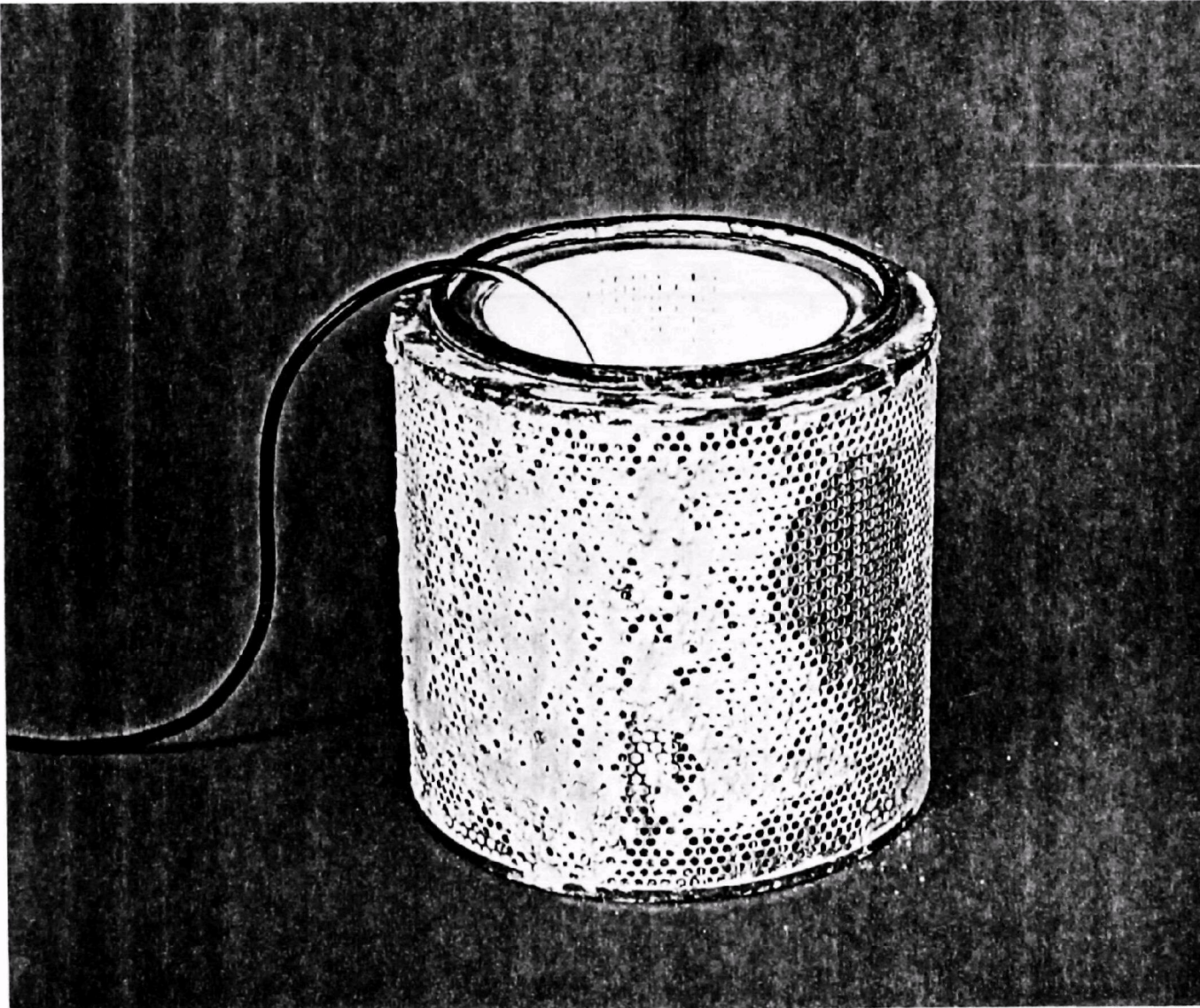


Figure 7-23. Failed Filter Cartridge - Light Spot Indicates Hole in Media

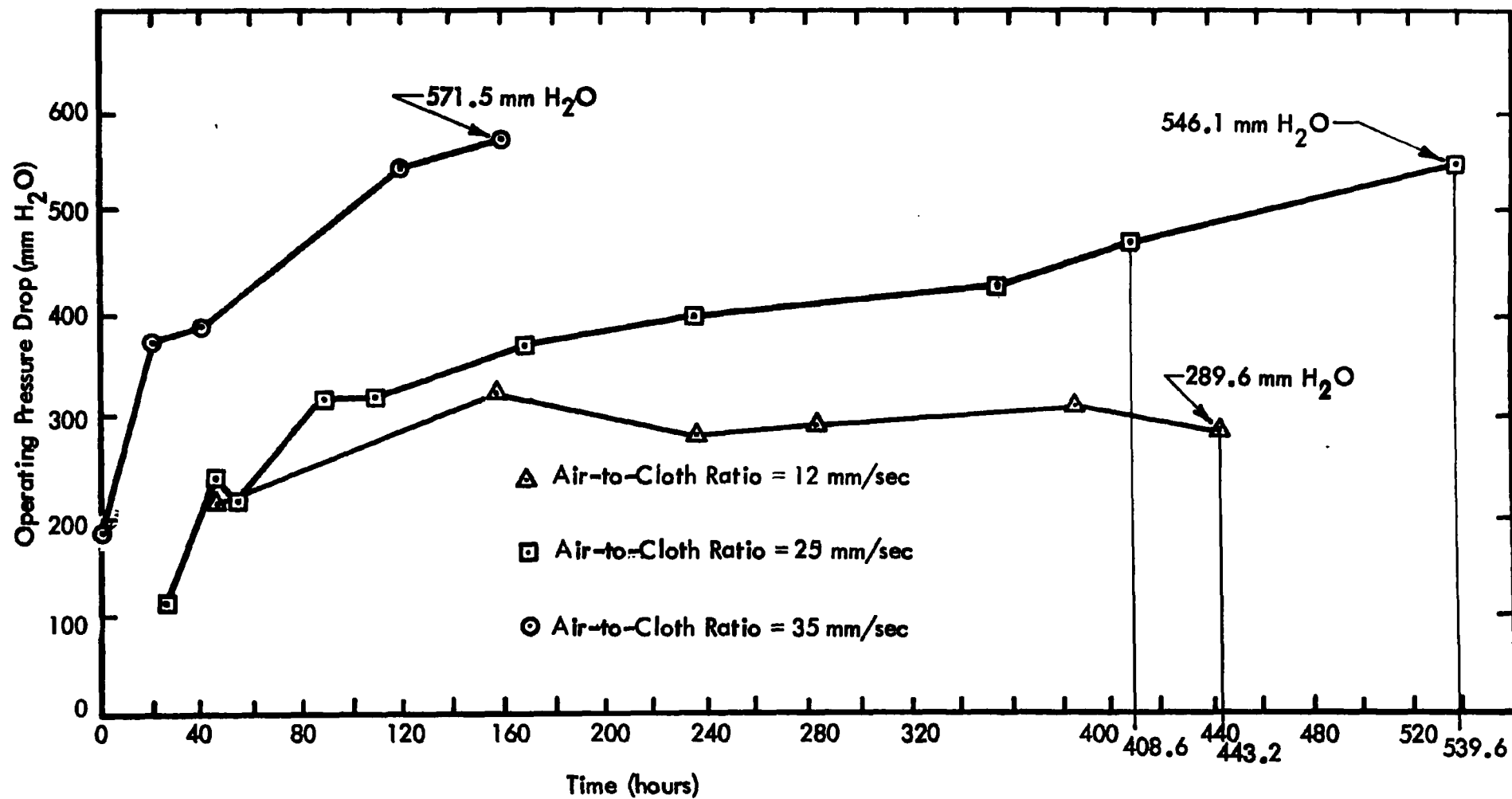


Figure 7-24. Operating Pressure Drop as a Function of Time (Northern Malleable Iron Company)

## 8.0

## ECONOMIC ANALYSIS

To illustrate the cost advantages of the double mat filter in a cartridge configuration, two examples are presented. These examples consist of dust control problems to which four methods of control are applied for cost comparisons. The data for electrostatic precipitation, scrubbers and baghouse filters are taken from "Air Pollution Control Technology and Costs in Seven Selected Areas", EPA-450/3-73-010, December 1973. The cost data for the cartridge filter analysis was obtained from Torit Division Donaldson Company, Inc. and is valid for December 1975. To obtain a conservative estimate, air-to-cloth ratio was held at about 1 for the cartridge filter application and the cost of filter cartridges was estimated to be one and one-half times that of the current cartridges using standard media. Consequently, this cost estimate does not include potential savings from operating at high air-to-cloth ratio.

Note that the four methods of control presented here do not provide equal performance. If submicrometer particles must be controlled, only the barrier filter option is available. Also, in the event that fine particles must be controlled, the double mat filter will provide superior performance over conventional media.

## 8.1

### Dust Control from a Vertical Lime Rock Kiln

The first example selected is dust control from a vertical lime rock kiln (Report EPA-450/3-73-010, December 1973).

The filter removes entrained limestone and lime dust from the exhaust gas of a vertical lime rock kiln. The kiln is fired with natural gas. A portion of the hot exhaust gas from the calcining zone is recirculated for heat recovery. The kiln is fed with 15 to 20 cm sized pieces of high calcium limestone.

The exhaust gas is brought from the kiln exhaust ports to a location 6.1 meters outside of the kiln enclosure by means of a fan. The filter will be located in an area free of space limitations. The fan follows the filter and the fan outlet is 1.5 meters above grade.

Tables 8-1 through 8-8 and Figures 8-1 through 8-9 give cost comparison data on the four methods of dust control from a vertical lime rock kiln.



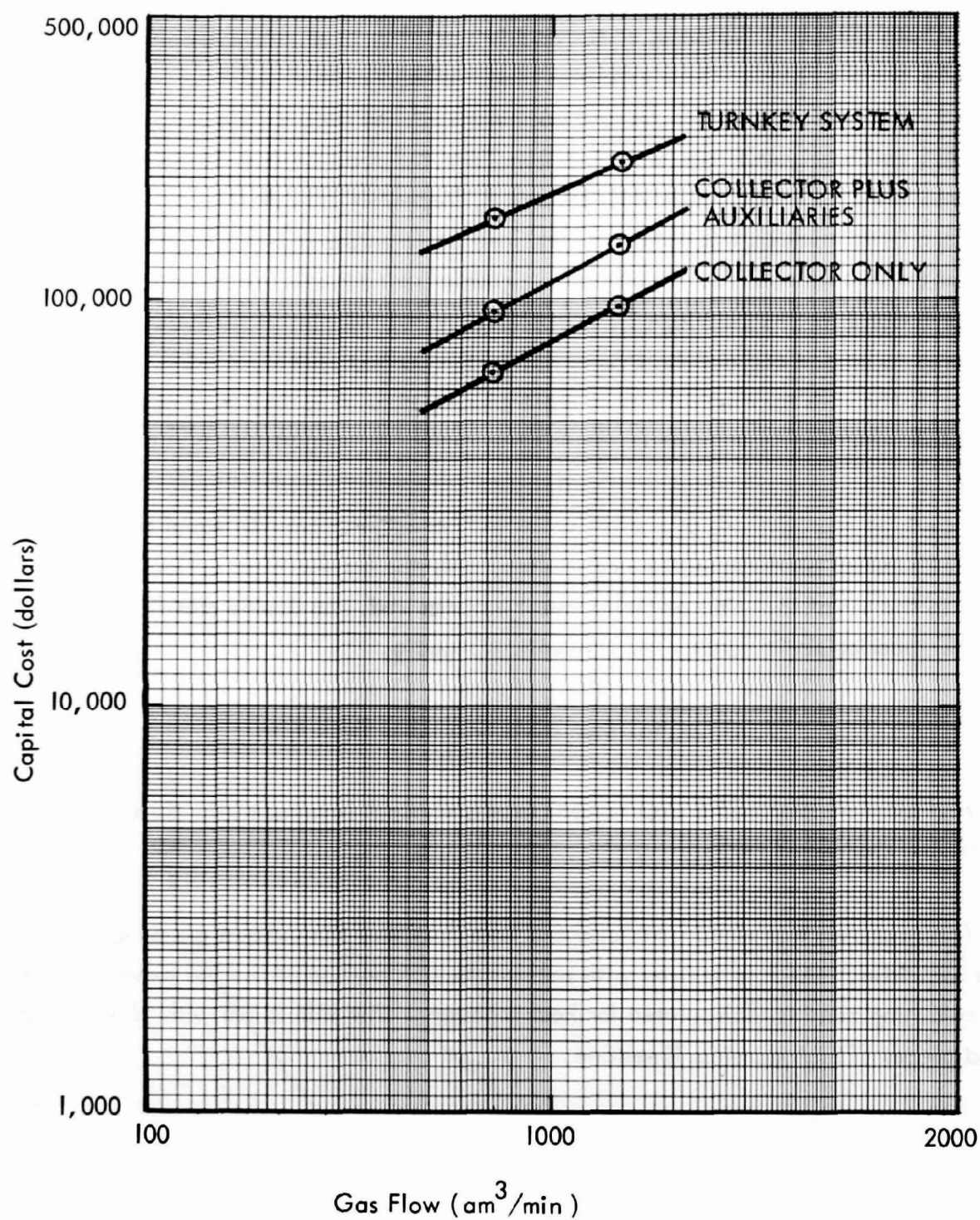


Figure 8-1. Capital Costs for Electrostatic Precipitators for Vertical Lime Rock Kilns (High Efficiency)



Table 8-1. Estimated Capital Cost Data (Costs in Dollars) for Electrostatic Precipitators for Vertical Lime Rock Kilns

	LA Process Wt.		High Efficiency	
	Small	Large	Small	Large
Effluent Gas Flow am <sup>3</sup> /min °C Moisture Content, Vol % Effluent Contaminant Loading gm/am <sup>3</sup> kg/hr			722.08 135 521.03 12 3.02 130.86	1441.3 135 1039.2 12 3.23 278.96
Cleaned Gas Flow am <sup>3</sup> /min °C sm <sup>3</sup> /min Moisture Content, Vol % Cleaned Gas Contaminant Loading gm/am <sup>3</sup> kg/hr Cleaning Efficiency, %			722.08 135 521.03 12 0.023 0.99 99.24	1441.3 135 1039.2 12 0.023 1.98 99.29
(1) Gas Cleaning Device Cost			67,745	95,515
(2) Auxiliaries Cost			25,838	38,225
(a) Fan(s)				
(b) Pump(s)				
(c) Damper(s)				
(d) Conditioning, Equipment				
(e) Dust Disposal Equipment				
(3) Installation Cost				
(a) Engineering				
(b) Foundations & Support Ductwork Stack Electrical Piping Insulation Painting Supervision Startup Performance Test Other			60,060	82,350
(4) Total Cost			153,643	216,090

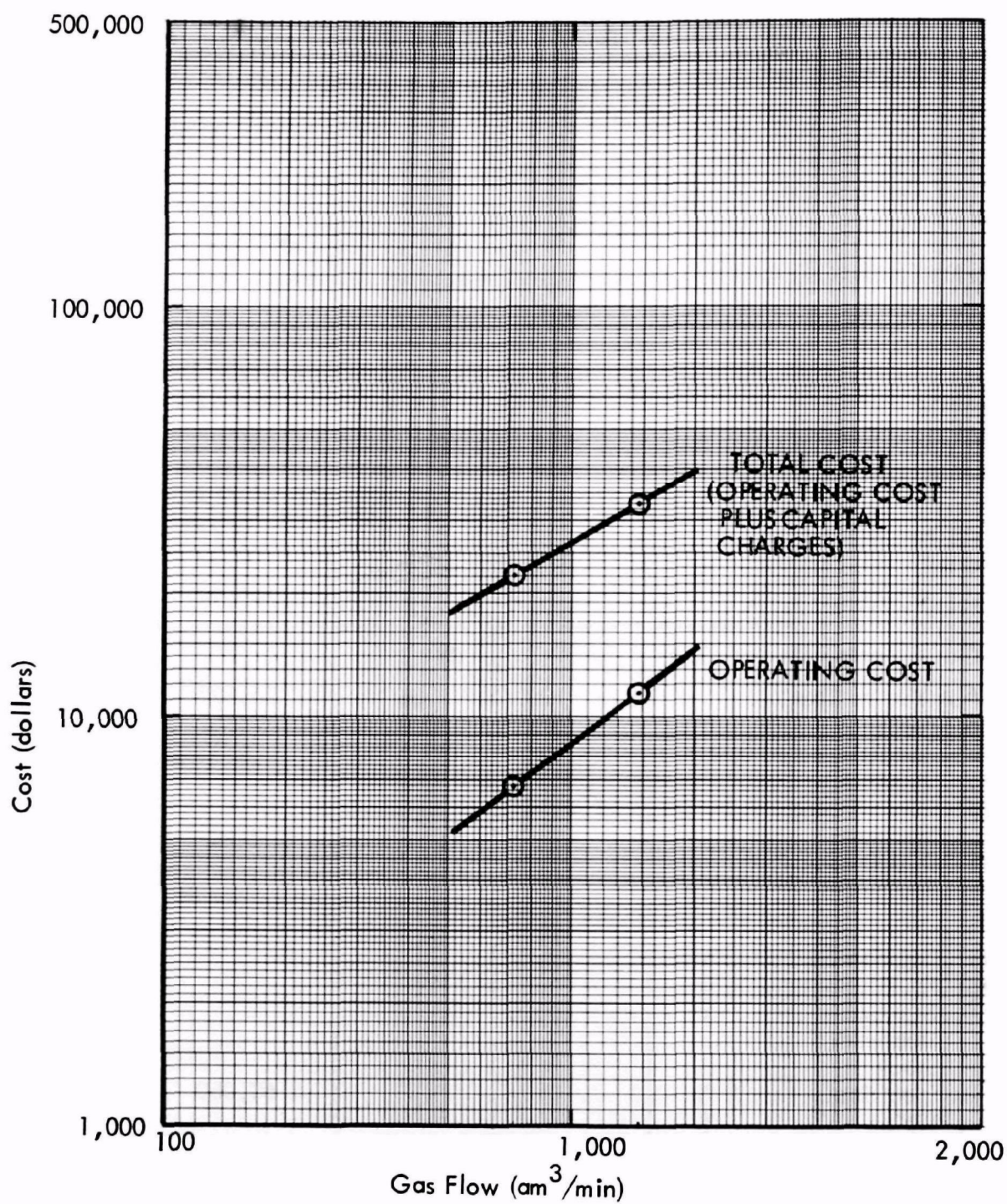


Figure 8-2. Annual Costs for Electrostatic Precipitators for Vertical Lime Rock Kilns (High Efficiency)

Table 8-2. Annual Operating Data (Costs in \$/Yr) for Electrostatic Precipitators for Vertical Lime Rock Kilns

Operating Cost Item	Unit Cost	LA Process Wt.		High Efficiency	
		Small	Large	Small	Large
Operating Factor, Hr/Year					
Operating Labor (if any)					
Operator	\$6/hr			2,000	2,000
Supervisor					
Total Operating Labor				2,000	2,000
Maintenance					
Labor	\$6/hr			1,072	2,139
Materials					
Total Maintenance				1,072	2,139
Replacement Parts				600	1,200
Total Replacement Parts				600	1,200
Utilities					
Electric Power	\$.011/kw-hr			3,036	5,984
Fuel					
Water (Process)					
Water (Cooling)					
Chemicals, Specify					
Total Utilities				3,036	5,984
Total Direct Cost				6,708	11,323
Annualized Capital Charges	10% of Capital			15,364	21,609
Total Annual Cost				22,072	32,932



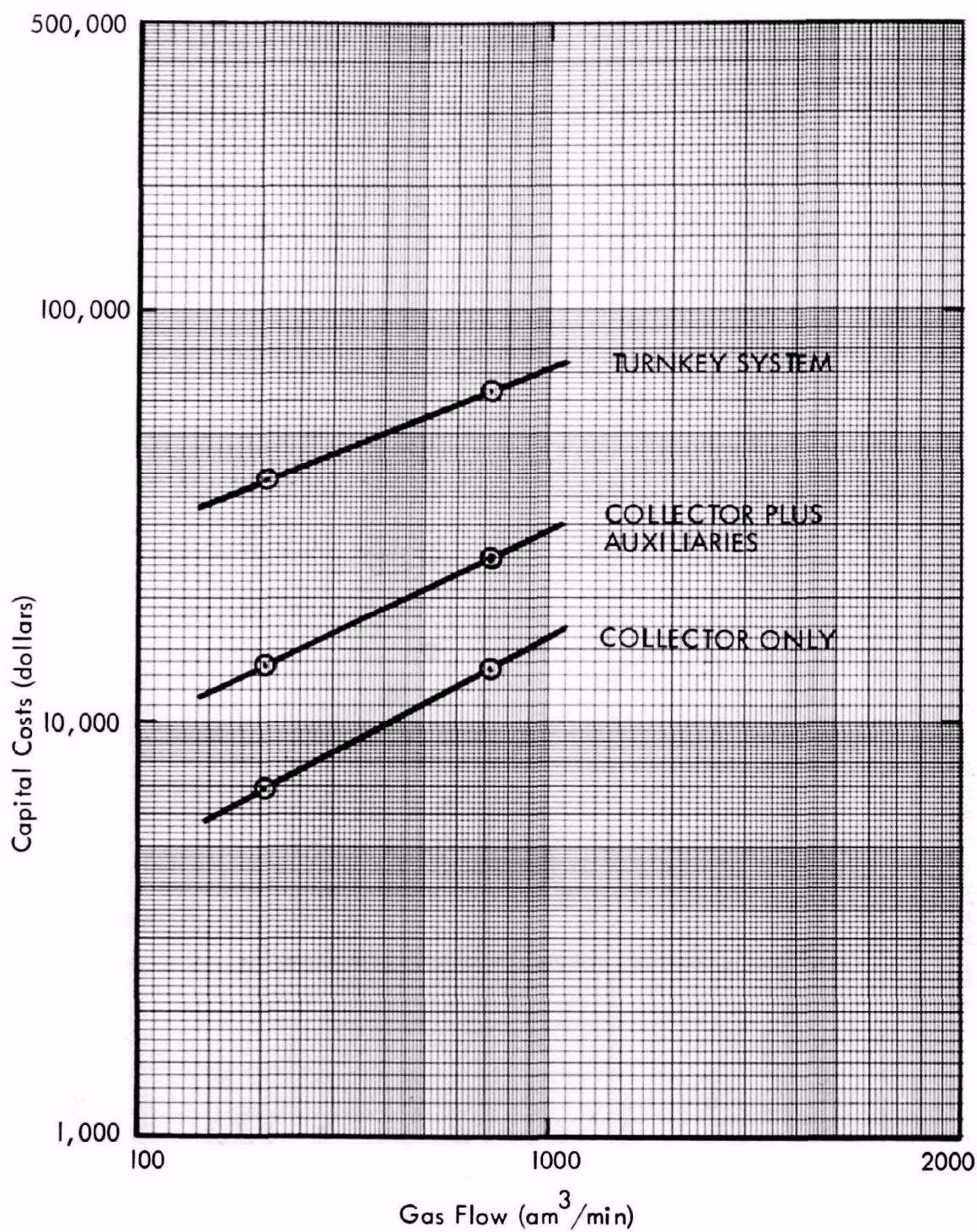


Figure 8-3. Capital Costs for Wet Scrubbers for Vertical Lime Rock Kilns (High Efficiency)

**Table 8-3. Estimated Capital Cost Data (Costs in Dollars) for  
Wet Scrubbers for Vertical Lime Rock Kilns**

	LA Process Wt.		High Efficiency	
	Small	Large	Small	Large
Effluent Gas Flow am <sup>3</sup> /min °C sm <sup>3</sup> /min Moisture Content, Vol % Effluent Contaminant Loading gm/am <sup>3</sup> kg/hr			206.7 135 150.08 12 2.95 36.6	722.08 135 521.03 12 3.02 130.86
Cleaned Gas Flow am <sup>3</sup> /min °C sm <sup>3</sup> /min Moisture Content, Vol % Cleaned Gas Contaminant Loading gm/am <sup>3</sup> kg/hr Cleaning Efficiency, %			184.06 54.4 165.65 15 0.023 0.254 99.31	642.79 54.4 577.66 15 0.023 0.88 99.33
(1) Gas Cleaning Device Cost			6,813	13,357
(2) Auxiliaries Cost			6,559	11,546
(a) Fan(s)				
(b) Pump(s)				
(c) Damper(s)				
(d) Conditioning, Equipment				
(e) Dust Disposal Equipment				
(3) Installation Cost				
(a) Engineering				
(b) Foundations & Support Ductwork Stack Electrical Piping Insulation Painting Supervision Startup Performance Test Other			25,100	38,083
(4) Total Cost			38,472	62,986



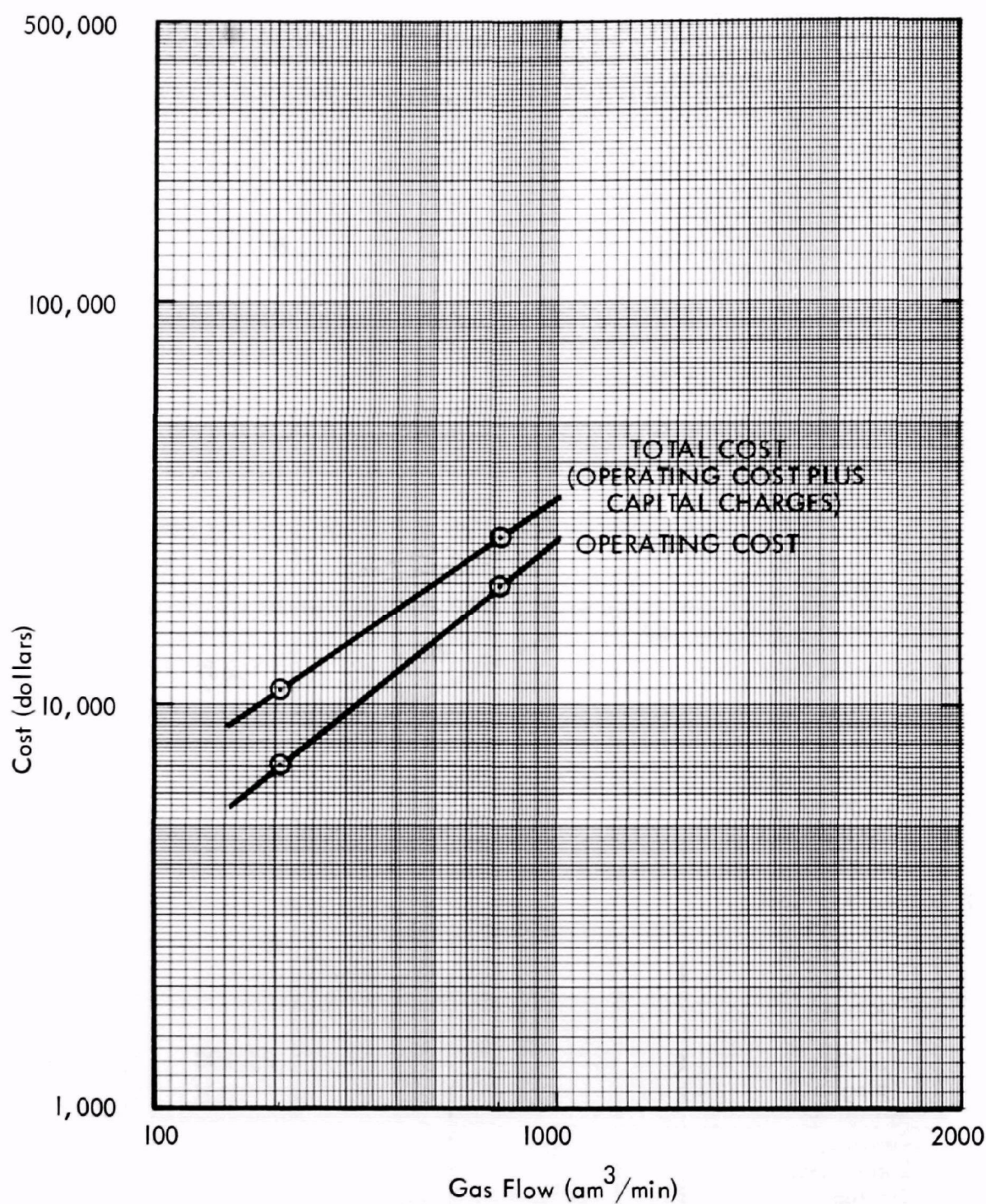


Figure 8-4. Annual Costs for Wet Scrubbers for Vertical Lime Rock Kilns (High Efficiency)

Table 8-4. Annual Operating Cost Data (Costs in \$/Yr) for Wet Scrubbers for Vertical Lime Rock Kilns

Operating Cost Item	Unit Cost	LA Process Wt.		High Efficiency	
		Small	Large	Small	Large
Operating Factor, Hr/Year				8,000	8,000
Operating Labor (if any) Operator Supervisor Total Operating Labor					
Maintenance Labor Materials Total Maintenance	\$6/hr			1,290	2,007
Replacement Parts				727	1,283
Total Replacement Parts				727	1,283
Utilities Electric Power Fuel Water (Process) Water (Cooling) Chemicals, Specify	\$ .011/kw-hr \$ .066/kℓ			4,841 191	15,726 647
Total Utilities				5,032	16,373
Total Direct Cost				7,049	19,663
Annualized Capital Charges	10% of Capital			3,847	6,299
Total Annual Cost				10,896	25,962



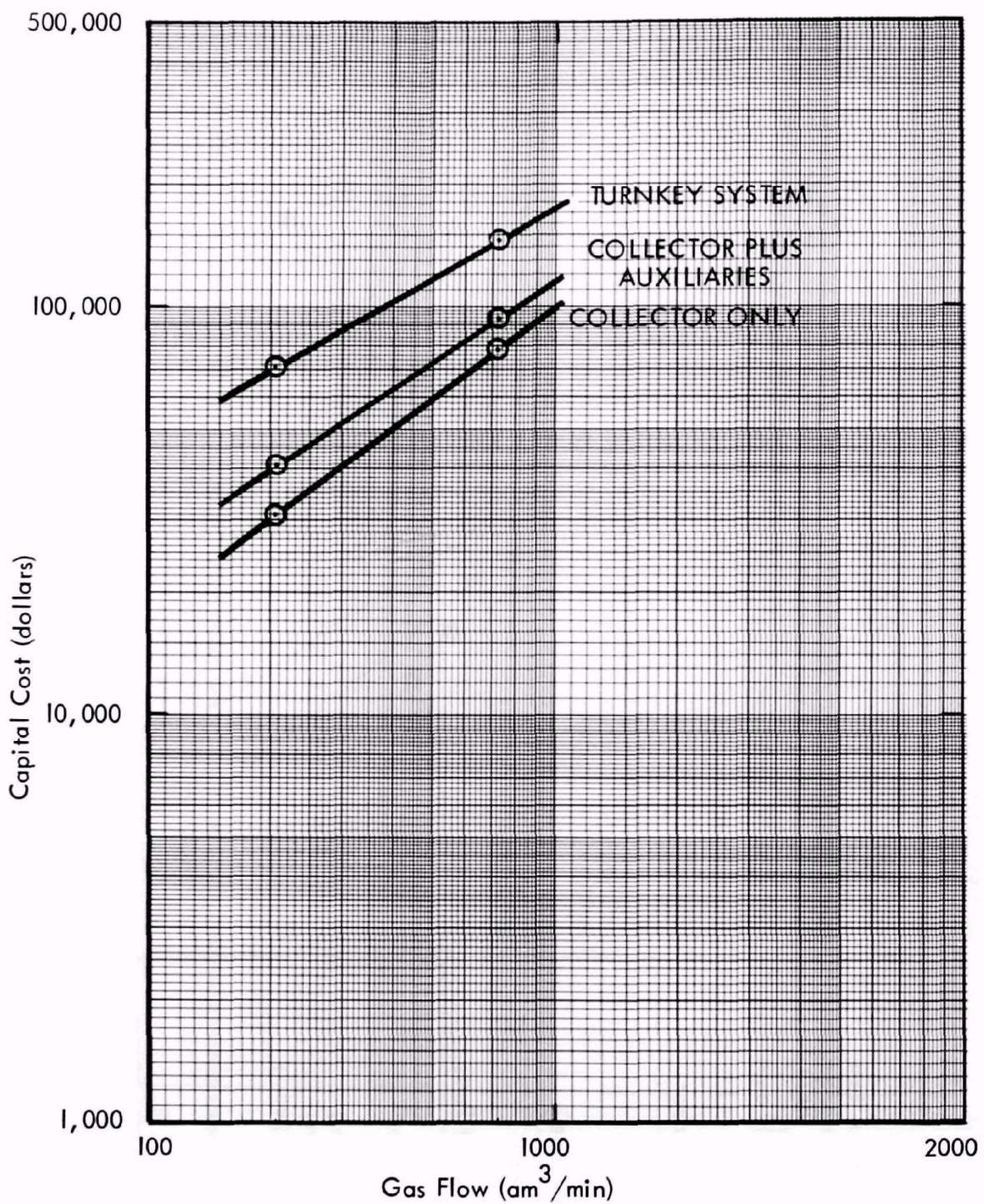


Figure 8-5. Capital Costs for Fabric Filters for Vertical Lime Rock Kilns



**Table 8-5. Estimated Capital Cost Data (Costs in Dollars) for  
Fabric Filters for Vertical Lime Rock Kilns**

	LA Process Wt.		High Efficiency	
	Small	Large	Small	Large
Effluent Gas Flow am <sup>3</sup> /min °C sm <sup>3</sup> /min Moisture Content, Vol % Effluent Contaminant Loading gm/am <sup>3</sup> kg/hr			206.7 135 150.08 12 2.95 36.6	722.08 135 521.03 12 3.02 130.86
Cleaned Gas Flow am <sup>3</sup> /min °C sm <sup>3</sup> /min Moisture Content, Vol % Cleaned Gas Contaminant Loading gm/am <sup>3</sup> kg/hr Cleaning Efficiency, %			206.7 135 150.08 12 .023 .286 99.22	722.08 135 521.03 12 .023 0.99 99.24
(1) Gas Cleaning Device Cost			30,573	78,427
(2) Auxiliaries Cost				
(a) Fan(s)			2,556	6,213
(b) Pump(s)				
(c) Damper(s) Emer.Temp. Temp.Air			2,000	2,000
(d) Conditioning, Equipment				
(e) Dust Disposal Equipment			5,850	5,850
(3) Installation Cost				
(a) Engineering				
(b) Foundations & Support Ductwork Stack *Electrical Piping *Insulation Painting Supervision *Startup Performance Test Other			29,234	52,318
(4) Total Cost			70,213	144,808

\*Not Included:

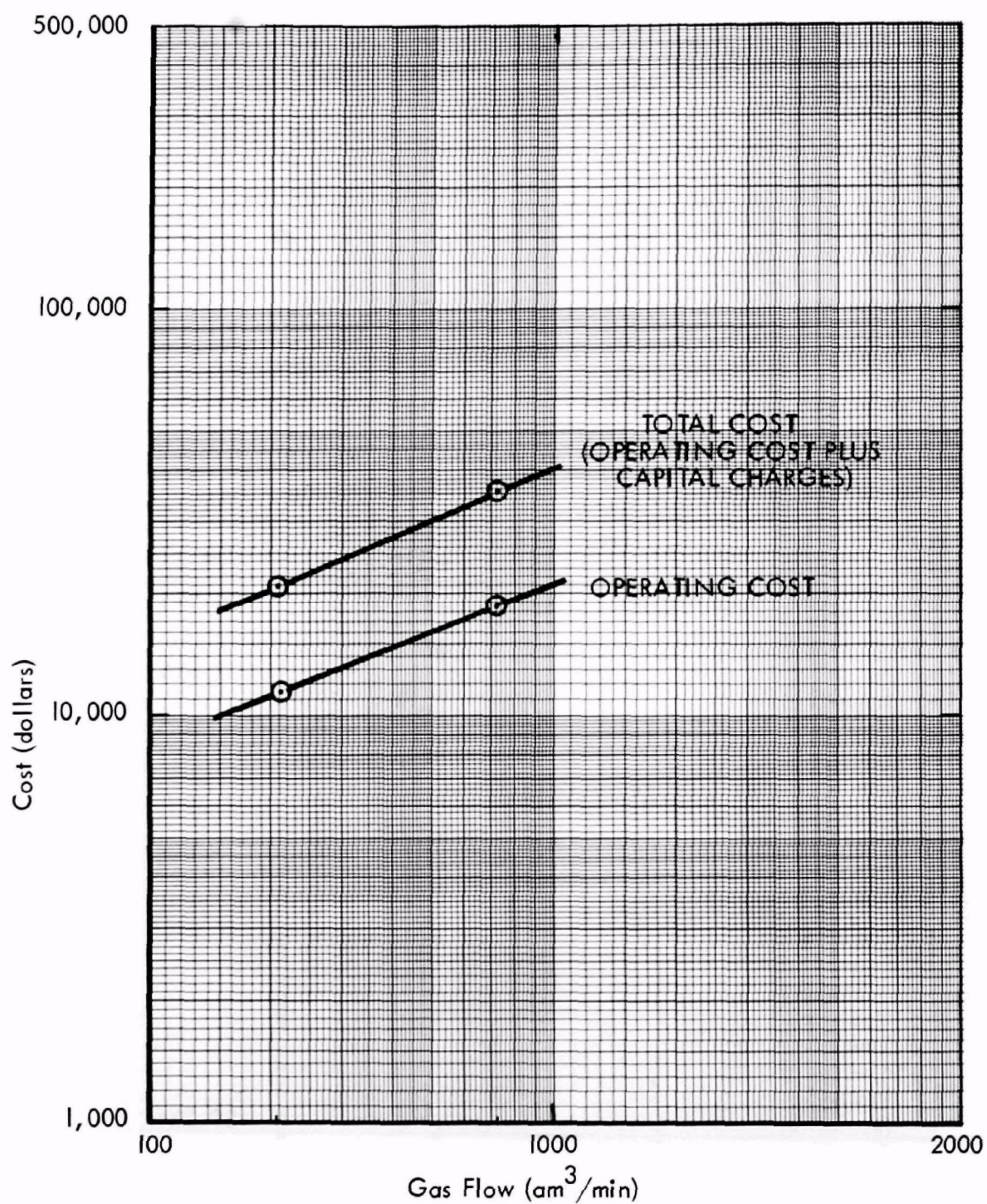


Figure 8-6. Annual Costs for Fabric Filters for Vertical Lime Rock Kilns

Table 8-6. Annual Operating Cost Data (Cost in \$/Yr) for Fabric Filters for Vertical Lime Rock Kilns

Operating Cost Item	Unit Cost	LA Process Wt.		High Efficiency	
		Small	Large	Small	Large
Operating Factor, Hr/Year				8,000	8,000
Operating Labor (if any)					
Operator					
Supervisor					
Total Operating Labor					
Maintenance					
Labor	\$6/hr.			9,000	12,000
Materials				200	600
Total Maintenance				9,200	12,600
Replacement Parts				400	1,400
Total Replacement Parts				400	1,400
Utilities					
Electric Power	\$.011/kw-hr			1,980	6,600
Fuel					
Water (Process)					
Water (Cooling)					
Chemicals, Specify					
Total Utilities				1,980	6,600
Total Direct Cost				11,580	20,600
Annualized Capital Charges	10% of Capital			6,821	14,481
Total Annual Cost				18,401	35,081



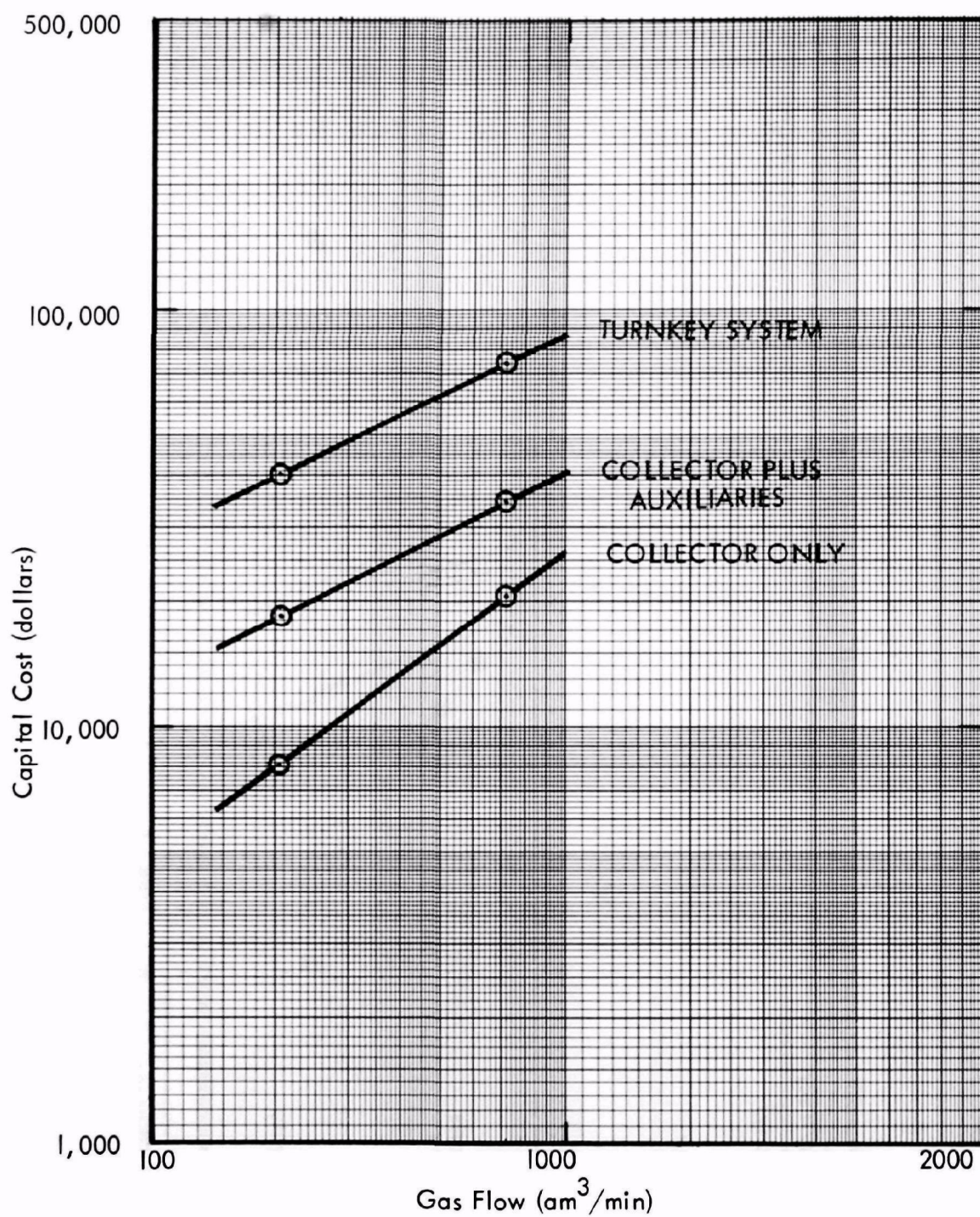


Figure 8-7. Capital Costs for Cartridge Filters for Vertical Lime Rock Kilns

**Table 8-7. Estimated Capital Cost Data (Costs in Dollars) for  
Cartridge Filters for Vertical Lime Rock Kilns**

	LA Process Wt.		High Efficiency	
	Small	Large	Small	Large
Effluent Gas Flow am <sup>3</sup> /min °C sm <sup>3</sup> /min Moisture Content, Vol % Effluent Contaminant Loading gm/am <sup>3</sup> kg/hr			206.7 135 150.08 12 2.95 36.6	722.08 135 521.03 12 3.02 130.86
Cleaned Gas Flow am <sup>3</sup> /min °C sm <sup>3</sup> /min Moisture Content, Vol % Cleaned Gas Contaminant Loading gm/am <sup>3</sup> kg/hr Cleaning Efficiency, %			206.7 135 150.08 12 ≤ .023 ≤ .28 **	722.08 135 521.03 12 ≤ .023 ≤ .99 **
(1) Gas Cleaning Device Cost	8,170	20,530		
(2) Auxiliaries Cost				
(a) Fan(s)			2,556	6,213
(b) Pump(s)				
(c) Damper(s) Emer.Temp. Air			2,000	2,000
(d) Conditioning, Equipment				
(e) Dust Disposal Equipment			5,850	5,850
(3) Installation Cost				
(a) Engineering				
(b) Foundations & Support Ductwork Stack *Electrical Piping *Insulation Painting Supervision *Startup Performance Test Other	21,925	39,238		
(4) Total Cost			40,501	73,830

\*Not Included

\*\*Cartridge Filter Media is 90 % Efficiency on DOP compared to 10% - 20% for Standard Fabric Filters. The "Cleaning Efficiency" should be 99.9% plus.



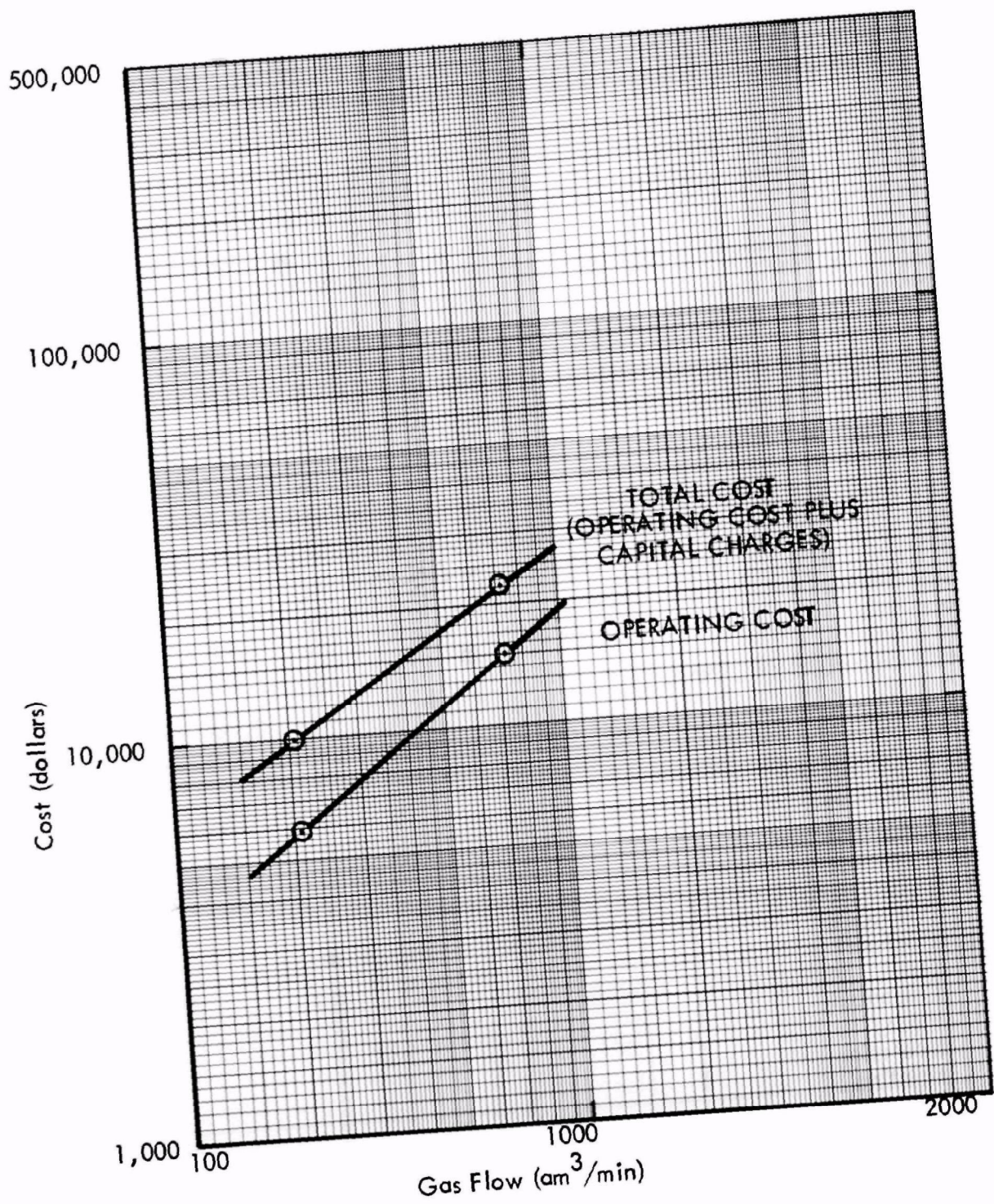


Figure 8-8. Annual Costs for Cartridge Filter for Vertical Lime Rock Kilns

**Table 8-8. Annual Operating Cost Data (Costs in \$/Yr) for Cartridge Filters for Vertical Lime Rock Kilns**

Operating Cost Item	Unit Cost	LA Process Wt.		High Efficiency	
		Small	Large	Small	Large
Operating Factor, Hr/Year				8,000	8,000
Operating Labor (if any)					
Operator					
Supervisor					
Total Operating Labor					
Maintenance					
Labor	\$6/hr			2,400	6,400
Materials					
Total Maintenance				2,400	6,400
Replacement Parts				1,440	1,920
Total Replacement Parts				1,440	1,920
Utilities					
Electric Power	\$.011/kw-hr			1,980	6,600
Fuel					
Water (Process)					
Water (Cooling)					
Chemicals, Specify					
Total Utilities				1,980	6,600
Total Direct Cost				5,820	14,920
Annualized Capital Charges	10% of Capital			4,050	7,383
Total Annual Cost				9,870	22,303



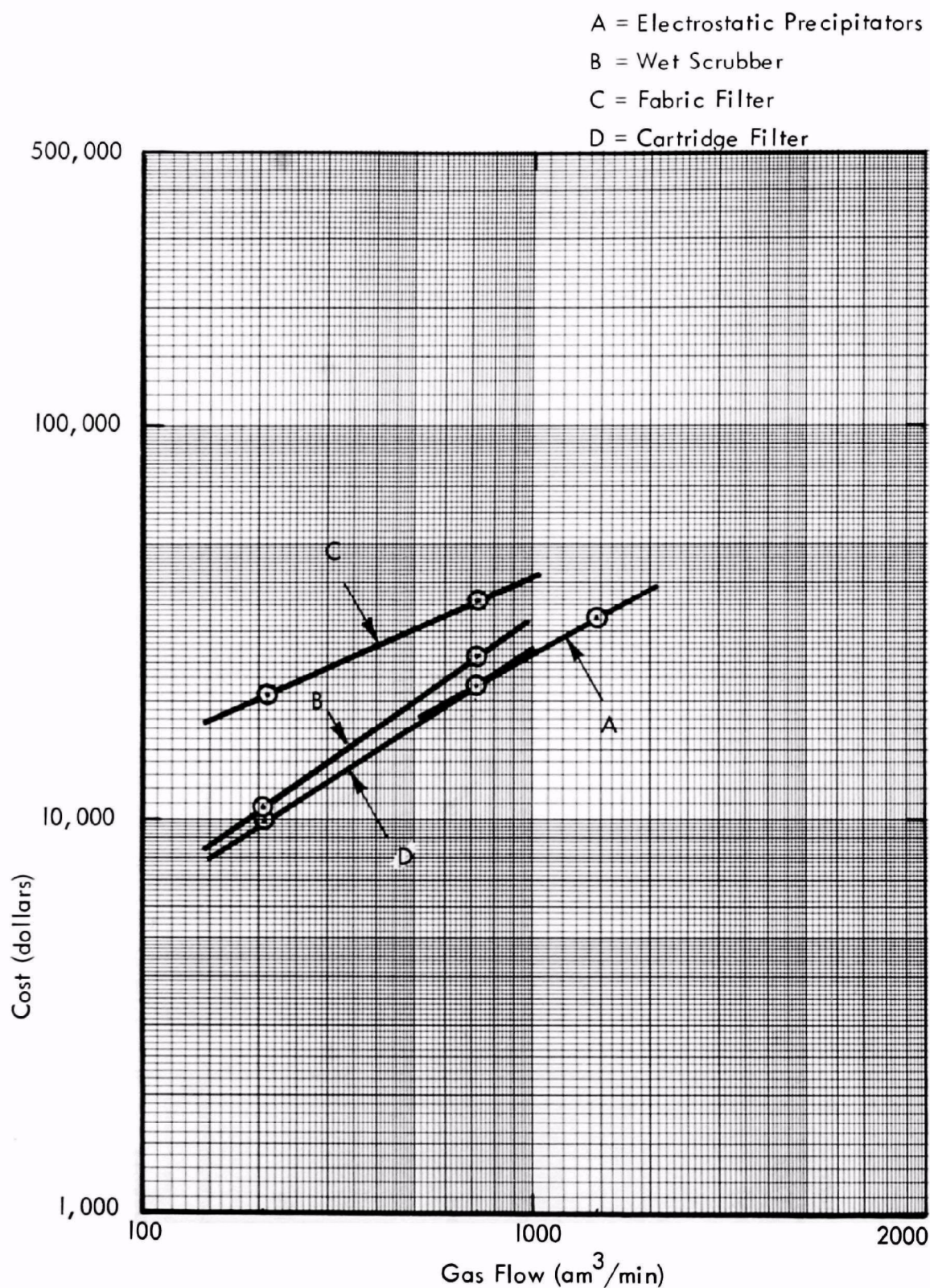


Figure 8-9. Annual Cost Comparison for Electrostatic Precipitators, Wet Scrubbers, Fabric Filters and Cartridge Filters (High Efficiency)

## 8.2

### Particulate Removal From the Exhaust Gas of a Glass-Melting Furnace

The second example selected is a glass-melting furnace (Report EPA-450/3-74-060 December 1974).

A filter removes particulate matter from the exhaust gas of a glass-melting furnace. The furnace is fired with No. 5 fuel oil using 40 percent excess combustion air.

The exhaust gas is to be brought from the furnace exhaust ports to a location 9.1 meters outside of the furnace enclosure by means of a fan. The filter is at ground level in an area beyond the ductwork which is free of space limitations. The fan precedes the filter. The abatement system continuously reduces the furnace outlet loading to the levels specified.

This application requires a filter media which will withstand temperatures up to 260°C. The present cartridge filter media will not meet this requirement; however, for this analysis, we are assuming that a filter media could be developed that would meet the high temperature requirement. Heat recovery could also be employed to reduce the exhaust gas temperature. This would, of course, increase the capital costs; however, the savings could possibly be recovered from use of the energy removed from the exhaust gas.

Tables 8-9 through 8-16 and Figures 8-10 through 8-18 give cost comparison data for this example.

## 8.3

### Conclusion ^

These two examples show that barrier filter units employing cartridge filters are more competitive than standard baghouse units and can easily be shown to be the lowest cost alternative in many cases.

**Table 8-9. Estimated Capital Cost Data (Costs in Dollars) for  
Electrostatic Precipitators for Glass-Melting Furnace**

	Medium Efficiency		High Efficiency	
	Small	Large	Small	Large
Effluent Gas Flow am <sup>3</sup> /min oC sm <sup>3</sup> /min Moisture Content, Vol % Effluent Contaminant Loading gm/am <sup>3</sup> kg/hr			707.9 385 317.15 12 .183 7.66	1699 385 758.89 12 .183 18.37
Cleaned Gas Flow am <sup>3</sup> /min oC sm <sup>3</sup> /min Moisture Content, Vol % Cleaned Gas Contaminant Loading gm/am <sup>3</sup> kg/hr Cleaning Efficiency, %			707.9 385 317.15 12 .023 .97 88	1699 385 758.89 12 .023 2.33 88
(1) Gas Cleaning Device Cost			94,312	152,285
(2) Auxiliaries Cost				
(a) Fan(s)			4,800	6,700
(b) Pump(s)				
(c) Damper(s)			1,309	3,067
(d) Conditioning, Equipment			3,530	4,120
(e) Dust Disposal Equipment			5,066	8,280
Model Study			249,796	339,321
(3) Installation Cost				
(a) Engineering				
(b) Foundations & Support Ductwork Stack Electrical Piping Insulation Painting Supervision Startup Performance Test Other				
(4) Total Cost			358,813	513,773



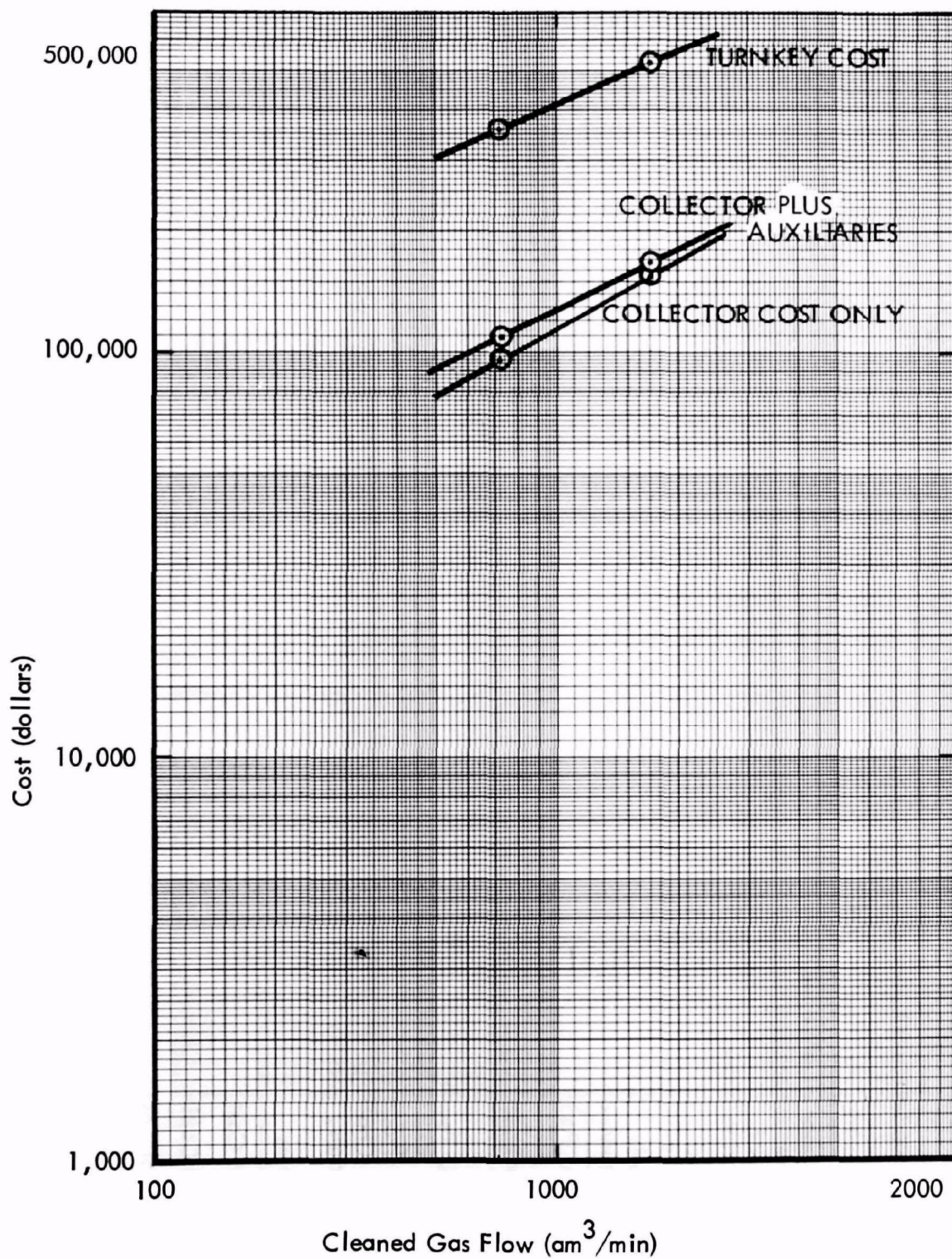


Figure B-10. Capital Cost of Electrostatic Precipitators for Glass-Melting Furnace

Table 8-10. Annual Operating Cost Data (Costs in \$/Yr) for  
Electrostatic Precipitators for Glass-Melting Furnace

Operating Cost Item	Unit Cost	LA Process Wt.		High Efficiency	
		Small	Large	Small	Large
Operating Factor, Hr/Year 8,600					
Operating Labor (if any) Operator Supervisor Total Operating Labor					
Maintenance Labor Materials Total Maintenance	\$6/hr			240 75 315	240 125 365
Replacement Parts Total Replacement Parts				550 550	550 550
Utilities Electric Power Fuel Water (Process) Water (Cooling) Chemicals, Specify Total Utilities	\$.011/kw-hr			6,467     6,467	11,146     11,146
Total Direct Cost Annualized Capital Charges Total Annual Cost	16% of Capital			7,332 57,410 64,742	12,061 82,204 94,265



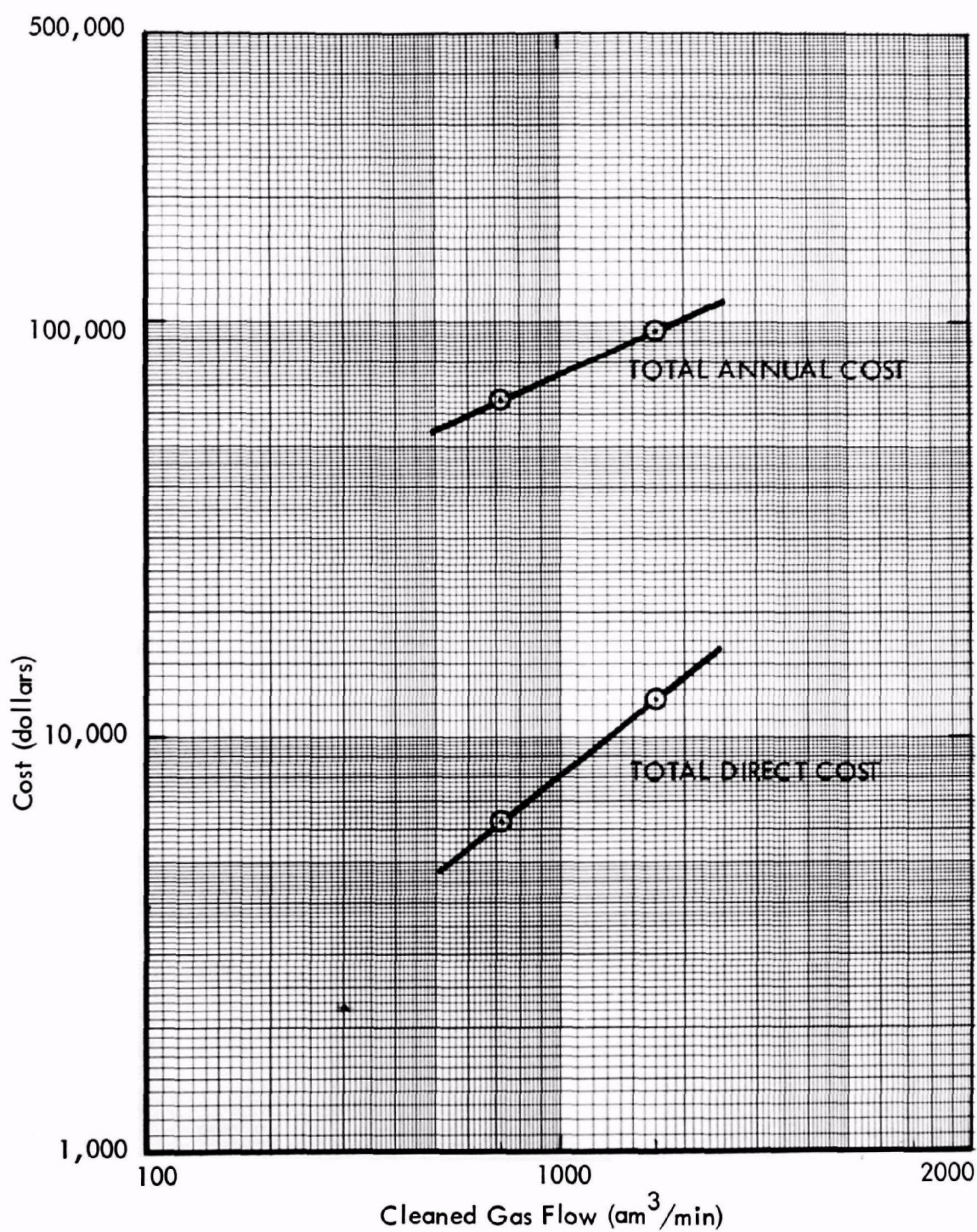


Figure 8-11. Annual Cost of Electrostatic Precipitators for Glass-Melting Furnace



**Table 8-11. Estimated Capital Cost Data (Costs in Dollars) for  
Wet Scrubbers for Glass-Melting Furnace**

	Medium Efficiency		High Efficiency	
	Small	Large	Small	Large
Effluent Gas Flow am <sup>3</sup> /min °C sm <sup>3</sup> /min Moisture Content, Vol % Effluent Contaminant Loading gm/am <sup>3</sup> kg/hr			707.92 385 317.15 12 .183 7.67	1699 385 758.89 12 .183 18.37
Cleaned Gas Flow am <sup>3</sup> /min °C sm <sup>3</sup> /min Moisture Content, Vol % Cleaned Gas Contaminant Loading gm/am <sup>3</sup> kg/hr Cleaning Efficiency, %			483.91 66.7 379.45 26 .023 .603 92	1053.39 66.7 911.80 26 .023 1.45 92
(1) Gas Cleaning Device Cost			13,983	22,418
(2) Auxiliaries Cost				
(a) Fan(s)			37,363	70,455
(b) Pump(s)			1,725	2,698
(c) Damper(s)			175	250
(d) Conditioning, Equipment			17,493	30,493
(e) Dust Disposal Equipment			8,233	8,828
(3) Installation Cost				
(a) Engineering			3,950	3,950
(b) Foundations & Support Ductwork Stack Electrical Piping Insulation Painting Supervision Startup Performance Test Other			62,298	82,518
(4) Total Cost			145,220	221,610

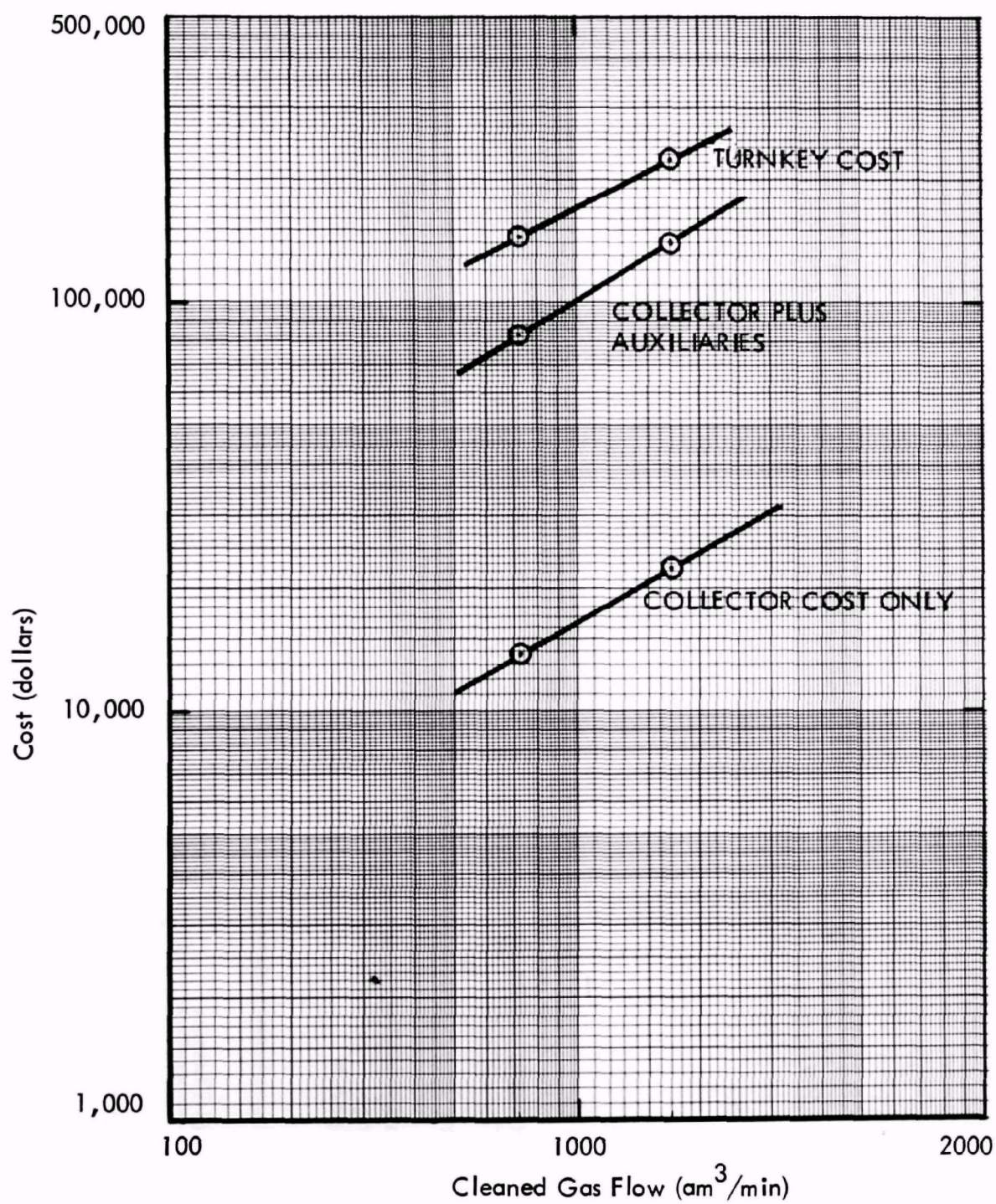


Figure 8-12. Capital Cost of Wet Scrubbers for Glass-Melting Furnace

Table 8-12. Annual Operating Cost Data (Costs in \$/Year) for  
Wet Scrubbers for Glass-Melting Furnace

Operating Cost Item	Unit Cost	Medium Efficiency		High Efficiency	
		Small	Large	Small	Large
Operating Factor, Hr/Year 8,600					
Operating Labor (if any)					
Operator	\$6/hr			6,300	6,300
Supervisor	\$8/hr			1,600	1,600
Total Operating Labor				7,900	7,900
Maintenance					
Labor	\$6/hr			1,950	1,950
Materials				750	875
Total Maintenance				2,700	2,825
Replacement Parts				1,250	2,375
Total Replacement Parts				1,250	2,375
Utilities					
Electric Power	\$.011/kw-hr			17,683	42,834
Fuel					
Water (Process)	\$.066/kℓ			1,506	3,264
Water (Cooling)	\$.0132/kℓ			353	844
Chemicals, Specify					
Total Utilities				19,542	46,942
Total Direct Cost				31,392	60,042
Annualized Capital Charges	16% of Capital			23,235	35,458
Total Annual Cost				54,627	95,500



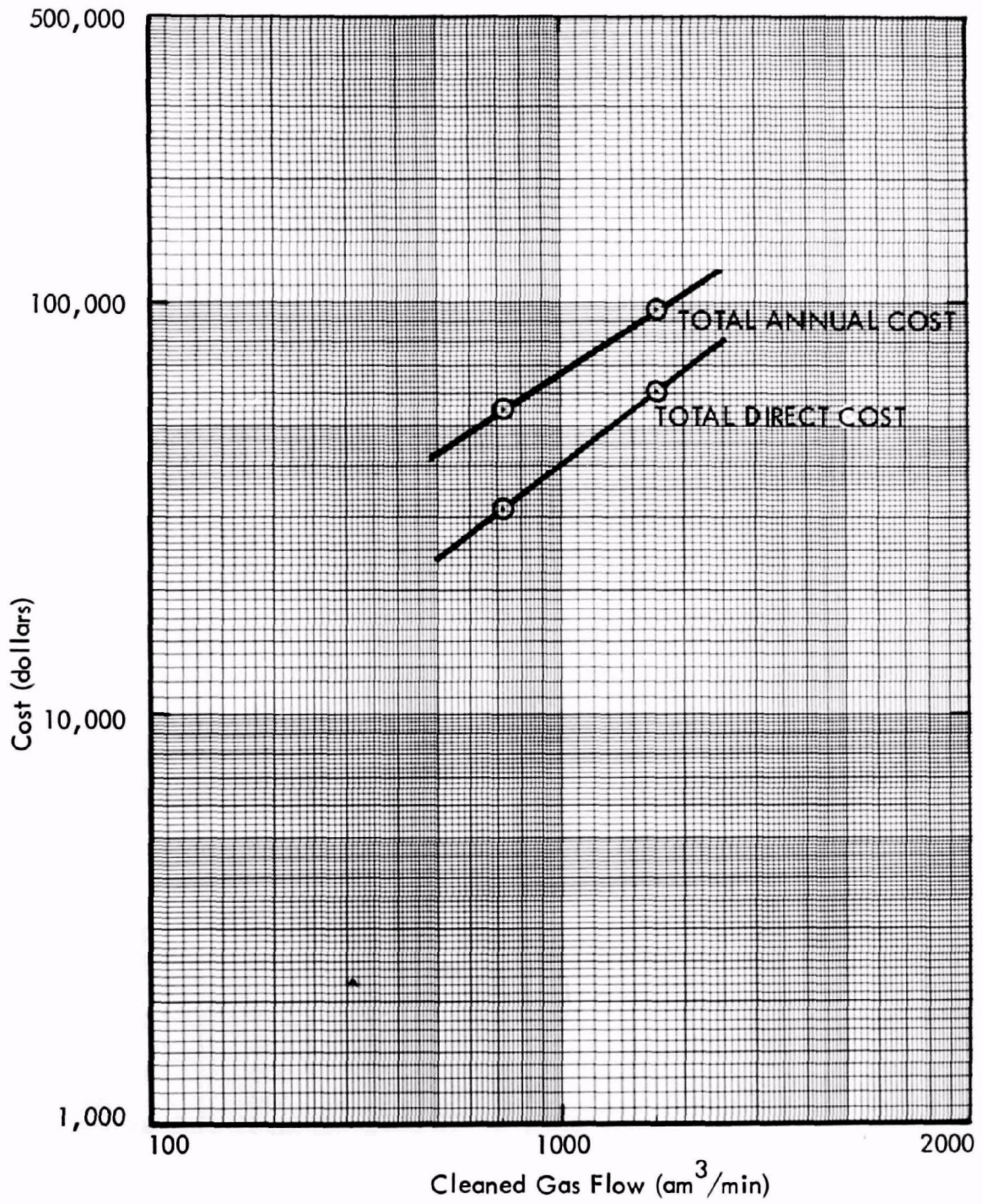


Figure 8-13. Annual Cost of Wet Scrubbers for Glass-Melting Furnace

**Table 8-13. Estimated Capital Cost Data (Costs in Dollars)  
for Fabric Filters for Glass-Melting Furnace**

	Medium Efficiency		High Efficiency	
	Small	Large	Small	Large
Effluent Gas Flow am <sup>3</sup> /min °C sm <sup>3</sup> /min Moisture Content, Vol % Effluent Contaminant Loading gm/am <sup>3</sup> kg/hr			707.92 385 317.15 12 .229 7.67	1699 385 758.89 12 .229 18.37
Cleaned Gas Flow am <sup>3</sup> /min °C sm <sup>3</sup> /min Moisture Content, Vol % Cleaned Gas Contaminant Loading gm/am <sup>3</sup> kg/hr Cleaning Efficiency, %			529.53 218.3 312.15 12 .023 .726 91	1267.18 218.3 758.89 12 .023 1.74 91
(1) Gas Cleaning Device Cost			78,871	147,338
(2) Auxiliaries Cost				
(a) Fan(s)			7,673	15,730
(b) Pump(s)				
(c) Damper(s)			8,823	11,744
(d) Conditioning, Equipment			21,871	47,432
(e) Dust Disposal Equipment			3,619	4,563
(3) Installation Cost				
(a) Engineering			17,838	22,450
(b) Foundations & Support			10,000	17,250
Ductwork			8,229	12,696
Stack			2,090	3,120
Electrical			7,500	10,000
Piping			500	850
Insulation			27,375	45,638
Painting			*	*
Supervision			7,830	11,515
Startup			1,060	1,560
Performance Test			3,000	4,000
Other			57,911	112,983
(4) Total Cost			264,190	468,949

\*Included in (1) above



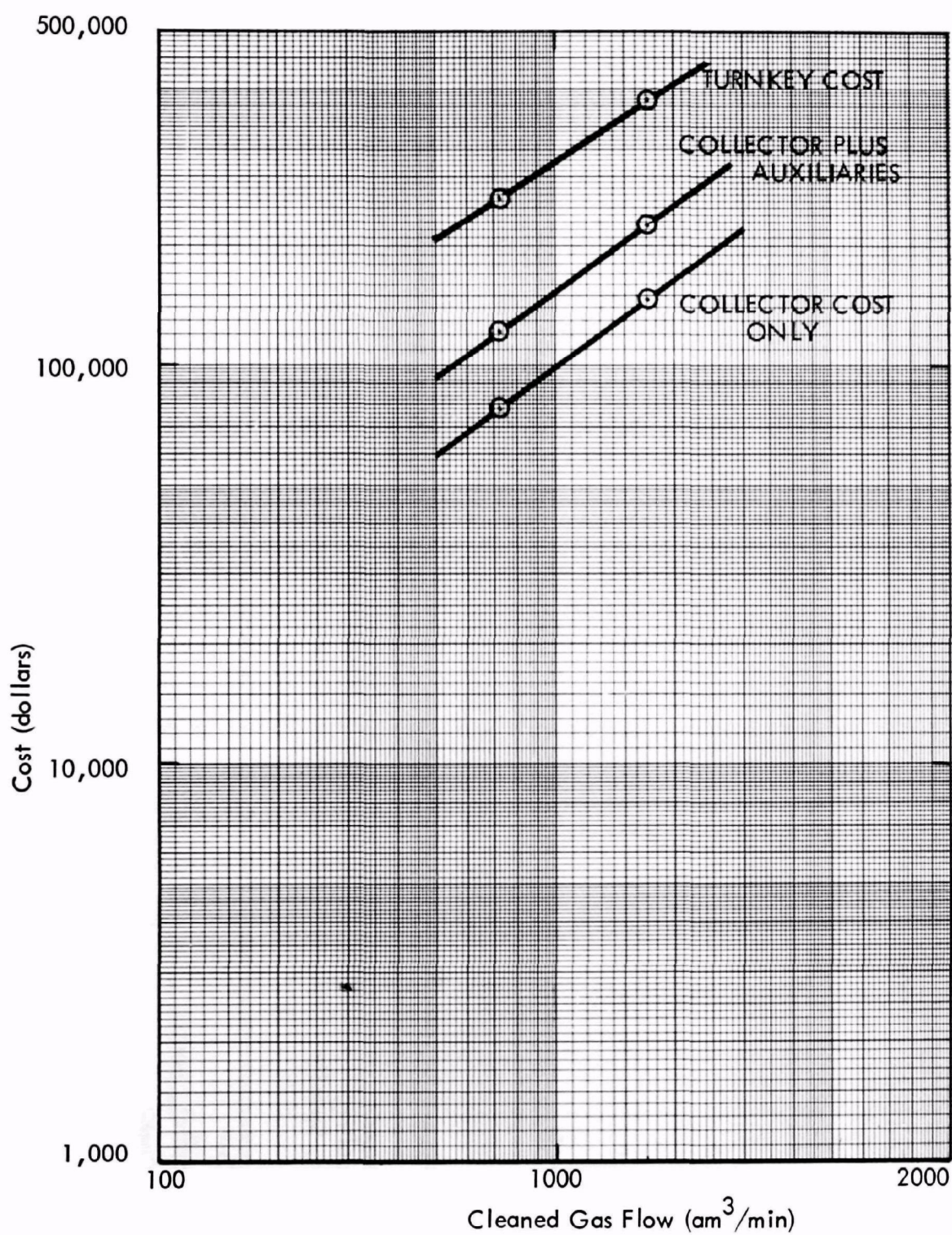


Figure 8-14 . Capital Cost of Fabric Filters for Glass-Melting Furnace



Table 8-14. Annual Operating Cost Data (Costs in \$/Year) for Fabric Filters for Glass-Melting Furnace

Operating Cost Item	Unit Cost	Medium Efficiency		High Efficiency	
		Small	Large	Small	Large
Operating Factor, Hr/Year 8,600					
Operating Labor (if any)					
Operator	\$6/hr.			2,681	3,984
Supervisor	\$8/hr.			835	922
Total Operating Labor				3,516	4,906
Maintenance					
Labor	\$6/hr			1,679	2,674
Materials & Replacement Parts				11,773	22,108
Total				13,452	24,782
Utilities					
Electric Power	\$0.011/kw-hr			16,763	30,739
Fuel					
Water (Process)					
Water (Cooling)					
Chemicals, Specify					
Total Utilities				16,763	30,739
Total Direct Cost				33,731	60,427
Annualized Capital Charges	16% of Capital			42,270	75,032
Total Annual Cost				76,001	135,459

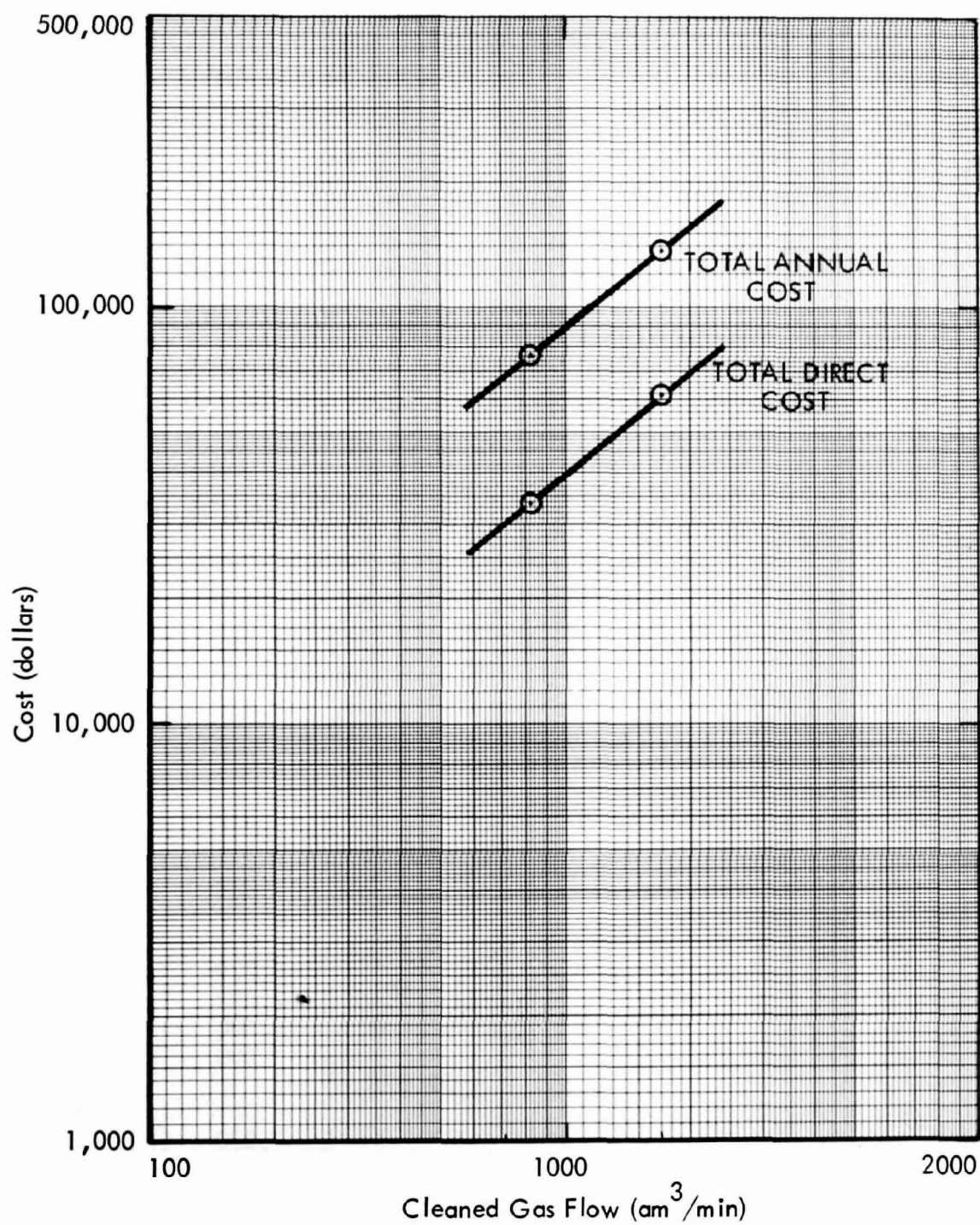


Figure 8-15. Annual Cost of Fabric Filters for Glass-Melting Furnace

**Table 8-15. Estimated Capital Cost Data (Costs in Dollars) for  
Cartridge Filters for Glass-Melting Furnace**

	Medium Efficiency		High Efficiency	
	Small	Large	Small	Large
Effluent Gas Flow am <sup>3</sup> /min °C sm <sup>3</sup> /min Moisture Content, Vol % Effluent Contaminant Loading gm/am <sup>3</sup> kg/hr			707.92 385 317.15 12 .229 7.67	1699 385 758.89 12 .229 18.37
Cleaned Gas Flow am <sup>3</sup> /min °C sm <sup>3</sup> /min Moisture Content, Vol % Cleaned Gas Contaminant Loading gm/am <sup>3</sup> kg/hr Cleaning Efficiency, %			529.53 218.3 317.15 12 ≤.023 ≤.726 **	1267.18 218.3 758.89 12 ≤.023 ≤1.74 **
(1) Gas Cleaning Device Cost	20,530	51,325		
(2) Auxiliaries Cost				
(a) Fan(s)			7,673	15,730
(b) Pump(s)				
(c) Damper(s)			8,823	11,744
(d) Conditioning, Equipment			21,871	47,432
(e) Dust Disposal Equipment			3,619	4,563
(3) Installation Cost				
(a) Engineering			17,838	22,450
(b) Foundations & Support Ductwork Stack Electrical Piping Insulation Painting Supervision Startup Performance Test Other	5,000	8,625	8,229 2,090 7,500 500 * 7,830 1,060 3,000	12,696 3,120 10,000 850 * 11,515 1,560 4,000
(4) Total Cost	172,678	313,170		

\*Included in (1) above

\*\*Cartridge Filter Media is 90 % Efficiency on DOP compared to 10% - 20% for Standard Fabric Filters. The "Cleaning Efficiency" should be 99.9% plus.



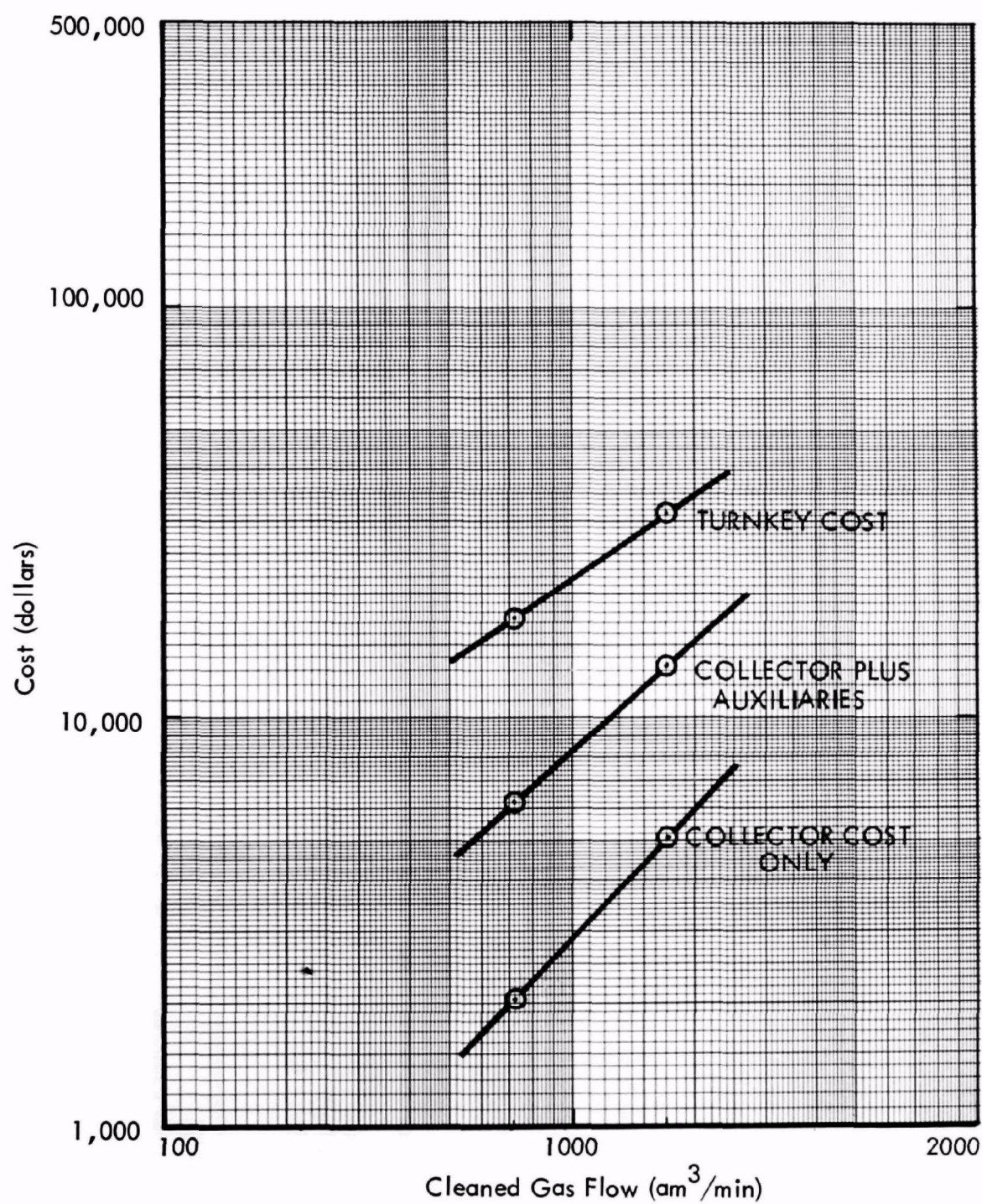


Figure 8-16. Capital Cost of Cartridge Filters for Glass-Melting Furnace

**Table 8-16. Annual Operating Cost Data (Costs in \$/Year) for Cartridge Filter  
for Glass-Melting Furnace**

Operating Cost Item	Unit Cost	Medium Efficiency		High Efficiency	
		Small	Large	Small	Large
Operating Factor, Hr/Year 8,600					
Operating Labor (if any)					
Operator	\$6/hr			2,681	3,984
Supervisor	\$8/hr			835	922
Total Operating Labor				3,516	4,906
Maintenance					
Labor	\$6/hr			1,679	2,674
Materials & Replacement					
Parts		3,840	9,600		
Total		5,519	12,274		
Utilities					
Electric Power	\$ .011/kw-hr			16,763	30,739
Fuel					
Water (Process)					
Water (Cooling)					
Chemicals, Specify					
Total Utilities				16,763	30,739
Total Direct Cost		25,798	47,919		
Annualized Capital Charges	16% of Capital	27,628	50,107		
Total Annual Cost		53,426	98,026		



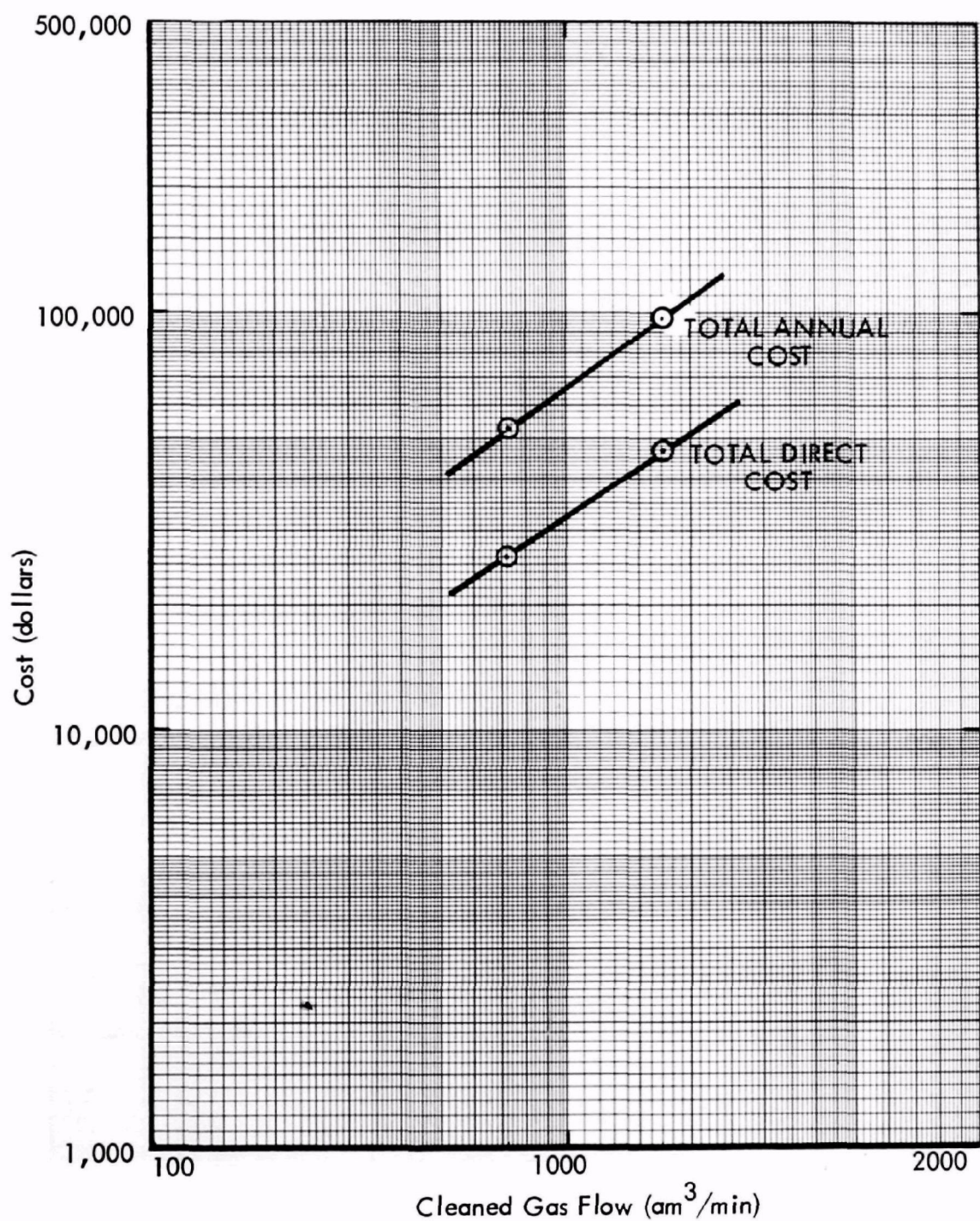


Figure 8-17. Annual Cost of Cartridge Filters for Glass-Melting Furnace



- A = Electrostatic Precipitators
- B = Wet Scrubbers
- C = Fabric Filters
- D = Cartridge Filters

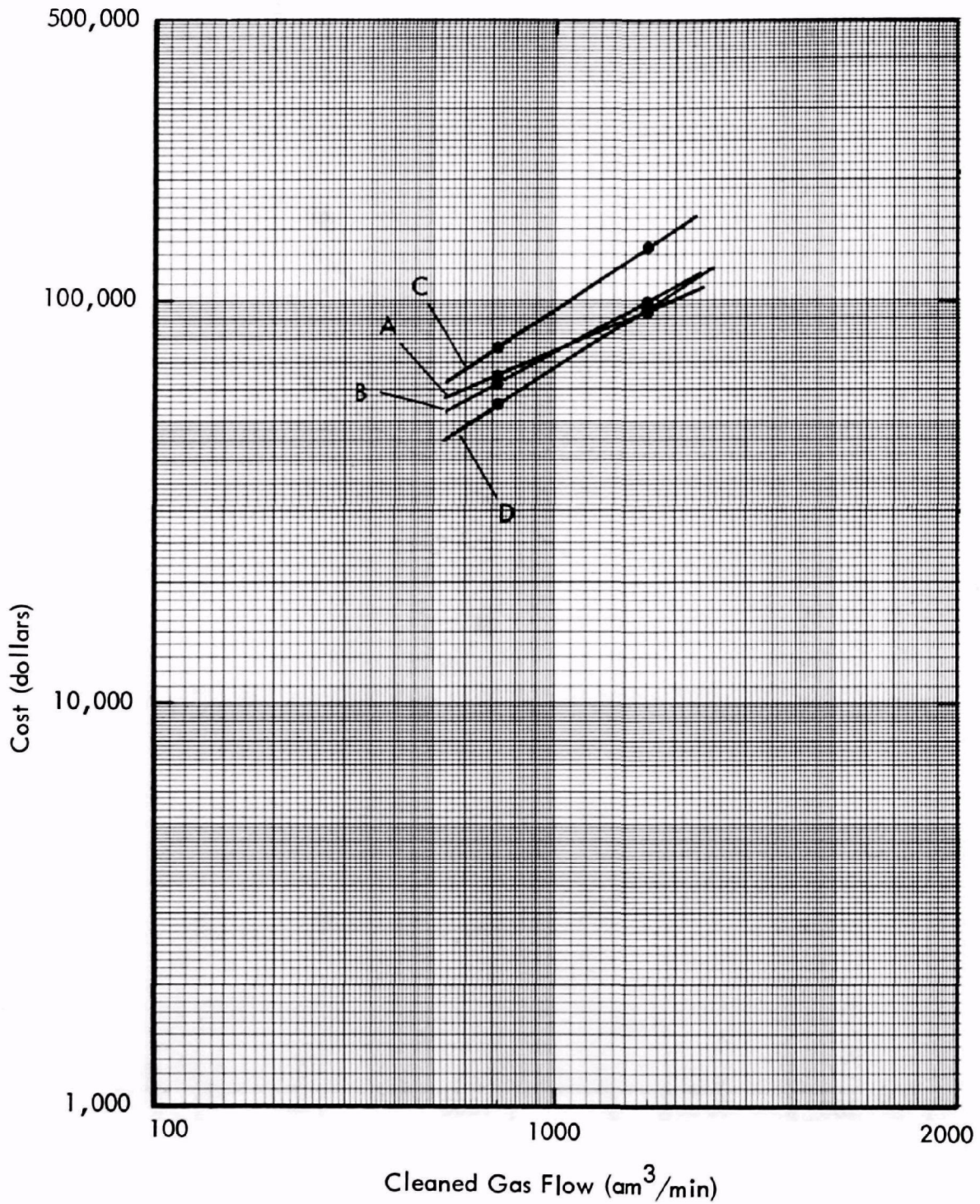


Figure 8-18. Annual Cost Comparison for Electrostatic Precipitators, Wet Scrubbers, Fabric Filters and Cartridge Filters for Glass-Melting Furnace

Air-to-Cloth Ratio - Amount of air volume in ratio to area of cloth in filter.

Basis Weight - Weight per unit area of the filter bed.

Double Mat Filter - Combination of a porous backing medium with a filtration layer of fine fibers.

Efficiency - Weight collected upstream divided by the weight collected upstream plus the weight collected on the downstream absolute.

Filter Bed - Mat of fibers designed to allow the passage of gas but to collect particles entrained in the gas.

Fine Particle - Particle less than  $3\ \mu\text{m}$  in diameter.

Overall Dust Loading - Weight of dust collected on the sample plus the weight of dust collected upstream of the sample expressed as weight per unit area.

Residual Dust Loading - Weight per unit area of dust remaining on the media sample.

Scrim - Durable fabric, usually used for added strength.

Turnkey System - Includes design, all labor and materials, equipment fabrication, erection and start-up.

Calvert, Seymour, et al, Scrubber Handbook, Volume 1, A.P.T., Inc., P.O. Box 71, Riverside, California (1972).

Hardison, L.C., Air Pollution Control Technology and Costs in Seven Selected Areas, EPA-450/3-73-010, pp 481-559 (1973).

Steenberg, L.R., Air Pollution Control Technology and Costs: Seven Selected Emission Sources, EPA-450/3-74-060, pp 99-140 (1974).

Yeh, Hsu-Chi, and Liu, Benjamin Y.H., "Aerosol Filtration by Fibrous Filters - I. Theoretical", Aerosol Science, Vol 5, pp 191-204 (1974)

## CONVERSION FACTORS

As required by the contract, metric units are used throughout this report. For English units, the following conversion factors are provided:

To Convert	Multiply by	To Obtain
Basis weight ( $\text{gm}/\text{m}^2$ )	(0.029467)	oz/yd <sup>2</sup>
Permeability ( $\text{m}^3/\text{min}/\text{m}^2$ @ 12.7 mm H <sub>2</sub> O)	(3.2808)	cfm/ft <sup>2</sup> @ $\frac{1}{2}$ in. H <sub>2</sub> O
Pressure (mm H <sub>2</sub> O)	(0.03937)	in. H <sub>2</sub> O
Pressure (Pascal)	( $1.4513 \times 10^{-4}$ )	psi
Velocity (mm/sec)	(0.19685)	ft/min
Newton /50 mm strip	(0.22857)	lbs <sub>f</sub> /2 in. strip
Air-to-Cloth-Ratio (mm/sec)	0.19685	ft/min
Dust Feed Concentration ( $\text{mg}/\text{m}^3$ )	$2.83168 \times 10^{-5}$	gm/ft <sup>3</sup>
Dust Loading ( $\text{gm}/\text{m}^2$ )	0.092903	gm/ft <sup>2</sup>
Meter	3.281	foot
$\text{m}^3/\text{min}$	35.31466	cfm
$\text{gm}/\text{m}^3$	0.436996	gr/ft <sup>3</sup>
kg/hr	2.20462	lb/hr

**TECHNICAL REPORT DATA**  
(Please read Instructions on the reverse before completing)

1. REPORT NO. <b>EPA-600/7-77-140</b>		2.		3. RECIPIENT'S ACCESSION NO.	
4. TITLE AND SUBTITLE <b>Particulate Control with Cleanable Cartridge Filters Using Double-Layer Media</b>				5. REPORT DATE <b>December 1977</b>	
				6. PERFORMING ORGANIZATION CODE	
7. AUTHOR(S) <b>William J. Krisko and Michael A. Shackleton</b>				8. PERFORMING ORGANIZATION REPORT NO. <b>EPA-001</b>	
9. PERFORMING ORGANIZATION NAME AND ADDRESS <b>Donaldson Company, Inc. P.O. Box 1299 Minneapolis, Minnesota 55440</b>				10. PROGRAM ELEMENT NO. <b>1AB012; ROAP 21ADL-029</b>	
				11. CONTRACT/GRANT NO. <b>68-02-1878</b>	
12. SPONSORING AGENCY NAME AND ADDRESS <b>EPA, Office of Research and Development Industrial Environmental Research Laboratory Research Triangle Park, NC 27711</b>				13. TYPE OF REPORT AND PERIOD COVERED <b>Final; 6/75-10/77</b>	
				14. SPONSORING AGENCY CODE <b>EPA/600/13</b>	
15. SUPPLEMENTARY NOTES <b>IERL-RTP project officer is Dennis C. Drehmel, Mail Drop 61, 919/541-2925.</b>					
16. ABSTRACT <b>The report gives results of a detailed assessment of the feasibility of a new concept in fine particle filtration, nonwoven, double-mat, cartridge filters. The filter consists of a fine fiber filtration layer supported by a porous substrate providing physical strength to the resulting filtration media. A theoretical basis for fine particle control with this media is presented. Test results with 0.3 micrometer DOP smoke confirmed that the design objective of 90% collection efficiency was obtainable. Preliminary economic analysis indicates that the cartridge filter will be less costly than the standard baghouse. The saving is a result of the smaller system possible with the pleated cartridge and the potentially higher air-to-cloth ratios with the fine fiber media. The analyses comprised Phase I of the contract. Phase II evaluated the fine particle control characteristics of the media in a pulse-jet cleaning cartridge configuration. Both laboratory and field tests proved the media capable of high dust removal efficiency of fine particles (&lt;3 micrometers) while achieving good pulse-jet cleaning characteristics.</b>					
17. KEY WORDS AND DOCUMENT ANALYSIS					
a. DESCRIPTORS		b. IDENTIFIERS/OPEN ENDED TERMS		c. COSATI Field/Group	
<b>Air Pollution Dust Control Smoke Filtration Emission Nonwoven Fabrics Scrubbers</b>		<b>Kilns Furnaces Electrostatic Precipitation Calcium Oxides</b>		<b>Air Pollution Control Stationary Sources Particulates Fabric Filters Double Mat Filters Cartridge Filters Baghouses</b>	
				<b>13B      13A 21B 07D      13H 07B 11E 13A</b>	
18. DISTRIBUTION STATEMENT <b>Unlimited</b>		19. SECURITY CLASS (This Report) <b>Unclassified</b>		21. NO. OF PAGES <b>189</b>	
		20. SECURITY CLASS (This page) <b>Unclassified</b>		22. PRICE	